



TAMPEREEN TEKNILLINEN YLIOPISTO
TAMPERE UNIVERSITY OF TECHNOLOGY

Vilma Ratia

**Behavior of Martensitic Wear Resistant Steels in
Abrasion and Impact Wear Testing Conditions**



Julkaisu 1342 • Publication 1342

Tampere 2015

Tampereen teknillinen yliopisto. Julkaisu 1342
Tampere University of Technology. Publication 1342

Vilma Ratia

Behavior of Martensitic Wear Resistant Steels in Abrasion and Impact Wear Testing Conditions

Thesis for the degree of Doctor of Science in Technology to be presented with due permission for public examination and criticism in Festia Building, Auditorium Pieni Sali 1, at Tampere University of Technology, on the 6th of November 2015, at 12 noon.

Tampereen teknillinen yliopisto - Tampere University of Technology
Tampere 2015

ISBN 978-952-15-3610-6 (printed)
ISBN 978-952-15-3627-4 (PDF)
ISSN 1459-2045

Abstract

Wear is a complex phenomenon present in both small and large scale in the industry, but also in our everyday life. The ability of a material to resist wear is not an intrinsic mechanical property, as it depends on the tribosystem as a whole, including all the environmental and operational factors. One of the aims of this work is to analyze the wear testing methods used for abrasive, impact, and impact-abrasive wear performance assessment of materials and thus to add to the current understanding of the wear testing in such conditions.

In this work, wear tests with various test devices were conducted on wear resistant martensitic steels. The tests include high-stress abrasive wear tests with crushing pin-on-disc and uniaxial crusher, impact-abrasive tests with impeller-tumbler, and impact tests with single and continuous impact testers. The impeller-tumbler method was analyzed in more detail by examining the effects of sample angle and test duration as well as the effects of testing procedures on the test results. In high-stress wear tests, the amount of wear was determined through mass loss measurements, while in the impact tests measurements of the impact scars were made. The wear surfaces were characterized with optical and electron microscopy, optical profilometry and residual stress measurements. Moreover, the behavior and changes in the subsurface and microstructure of the materials were studied from prepared cross sections with optical and electron microscopy, microhardness measurements and electron backscatter diffraction.

In wear testing, selection of correct parameters is important, as they affect the wear mechanisms present on the sample surfaces. In abrasive wear, abrasive properties and even indirect counterparts have an influence on the forming wear mechanisms, which finally govern the severity of material removal. On the other hand, some similarities in the wear behavior of wear resistant steels in different abrasive contact conditions of sliding, gouging and impacting could be observed: the harder steels presented more scratching, which can be correlated to their lower ability of plastic deformation and higher amount of cutting. To ensure reaching the correct (steady) state of wear, tests should be of adequate duration, as the response of materials to many contact conditions may be nonlinear and reveal certain evolution of microstructures only after longer exposure.

Wear tests enable the comparison of materials in controlled conditions, but close attention on the test procedures must be paid also when conducting seemingly robust wear tests, especially when the differences to be detected are small. As the tests themselves constitute a tribosystem, local changes in the conditions due to the test procedures, such as sample placement, must be properly understood in order to obtain reliable results. Understanding the concept of a tribosystem and the major interdependencies involved is essential for all wear testing methods and proper analysis of the experimental test results.

Preface

This work was primarily carried out at Tampere Wear Center (TWC) at the Department of Materials Science of Tampere University of Technology. A part of the study was carried out at AC²T research GmbH in Wiener Neustadt, Austria, between November 2012 and May 2013.

This research was a part of the Finnish Metals and Engineering Competence Cluster's (FIMECC) Demanding Applications (DEMAPP) program funded by the Finnish Funding Agency for Technology and Innovation (Tekes) and the participating companies. Finnish Foundation for Technology Promotion (TES), The Finnish Science Foundation for Economics and Technology (KAUTE), Emil Aaltonen Foundation, Fund for the Association of Finnish Steel and Metal Producers, Walter Ahlström Foundation and Research Fund of the City of Tampere are also acknowledged for their financial support. During the studies at AC²T research GmbH, this work was partly performed and funded by the Austrian COMET-Program (Project K2 Xtribology, Grant No. 849109), and was carried out within the Excellence Centre of Tribology. SSAB Europe Oy, formerly known as Ruukki Metals Oy, provided materials for the studies. M.Sc. Anu Kempainen and M.Sc. Olli Oja are acknowledged for their patience in arranging the kind of samples I wished for as well as for proofreading.

I wish to express my sincere gratitude to my supervisor Professor Veli-Tapani Kuokkala for his guidance and his genuine enthusiasm about research, which has been an encouraging example. I am deeply thankful to Lic.Tech. Kati Valtonen, whose help I could always rely on and whose firm and understanding encouragement was an invaluable help. Associate professor Minnamari Vippola is thanked for her helpful advices. I also wish to thank the whole staff of the Department of Materials Science and especially Tampere Wear Center for creating such a great working atmosphere – I feel that I am truly lucky to have you as colleagues! Special thanks go to M.Sc. Vuokko Heino, with whom I have experienced many trips, and who has offered me great peer support during the years.

I want to thank Mr. Ari Varttila and Mr. Terho Kaasalainen for using their ingenious skills for constructing devices and the research assistants who have helped me in tests and specimen preparations. Especially I want to thank M.Sc. Leo Janka for his fresh viewpoints.

I am grateful to the personnel of AC²T research GmbH and especially its deputy scientific head, DI Dr. Ewald Badisch, for letting me conduct research at their facilities. Furthermore, I wish to thank M.Sc. Marcela Petrica for her friendship during my time in Austria.

I am most grateful to my family, who has provided endless support for me. I thank my sister Kaisa for all the extracurricular activities, my father Jukka for encouraging discussions, and my mother Tarja for going above and beyond for me, when needed. I wish to thank my friends for showing me life beyond work. Finally, I want to thank my dear Janne for his patience and support.

Tampere, October 2015

Vilma Ratia

Table of contents

Abstract	I
Preface.....	II
Table of contents.....	III
List of original publications.....	V
Author’s contribution.....	VI
List of symbols and abbreviations	VII
1. Introduction	1
1.1 Aim of the work	1
2. Wear and factors affecting it.....	3
2.1 Abrasive wear.....	4
2.1.1 Role of abrasives.....	6
2.1.2 Role of counterparts.....	7
2.2 Impact wear.....	8
2.3 Impact-abrasive wear.....	8
3. Wear testing methods	11
3.1 Abrasive wear.....	13
3.2 Impact wear.....	14
3.3 Impact-abrasive wear.....	14
4. Typical properties of wear resistant steels	17
4.1 Role of steel properties in abrasive, impact-abrasive and impact wear	20
5. Experimental procedures	22
5.1 Materials	22
5.1.1 Wear resistant steels.....	22
5.1.2 S355 structural steel.....	24
5.1.3 Hard metals.....	24
5.1.4 Abrasives	25
5.1.5 Sample preparation	26
5.2 Wear testing	27
5.2.1 Crushing pin-on-disc.....	27

5.2.2	Uniaxial crusher	29
5.2.3	Impeller-tumbler	30
5.2.4	Single impact tester.....	34
5.2.5	High-temperature cyclic impact abrasion tester	35
5.3	Characterization.....	37
5.3.1	Hardness	37
5.3.2	Microscopy	37
5.3.3	Microstructures	38
5.3.4	Residual stresses	38
6.	Results and discussion.....	39
6.1	Effect of test parameters on the impact-abrasion tests with impeller-tumbler	39
6.1.1	Role of the reference sample	39
6.1.2	Test procedure for three simultaneously tested samples	41
6.1.3	Effects of particle size and size distribution	42
6.1.4	Effect of impact angle on impact-abrasion with relatively large particles	43
6.1.5	Effects of test duration	45
6.1.6	Wear of the edges and inner parts of the samples.....	47
6.1.7	Summary of the characteristics of the impeller-tumbler wear tester.....	49
6.2	Effects of counterpart and abrasive type on the high-stress abrasive wear.....	51
6.2.1	Indirect counterpart.....	51
6.2.2	Abrasive type.....	54
6.2.3	Summary	57
6.3	Behavior of wear resistant steels in abrasion and impact wear testing conditions	57
6.3.1	Effect of hardness on wear in abrasive and impacting conditions	57
6.3.2	Abrasive and impact-abrasive wear mechanisms in wear resistant steels.....	59
6.3.3	Sub-surface effects of abrasive, impact and impact-abrasive wear	62
6.3.4	Summary	66
7.	Concluding remarks and suggestions for future work.....	67
	References	69
	Appendix: Original publications.....	87

List of original publications

This thesis is based on the studies presented in detail in the following five publications. In the text, they are referred to as Publications I-V.

- I Vilma Ratia, Kati Valtonen, Anu Kemppainen, Veli-Tapani Kuokkala, High-stress abrasion and impact-abrasion testing of wear resistant steels, *Tribology Online* 8 (2013) 152-161.
- II Vilma Ratia, Kati Valtonen, Veli-Tapani Kuokkala, Impact-abrasion wear of wear resistant steels at perpendicular and tilted angles, *Proceedings of the Institution of Mechanical Engineers Part J: Journal of Engineering Tribology* 227 (2013) 868-877.
- III Vilma Ratia, Ilkka Miettunen, Veli-Tapani Kuokkala, Surface deformation of steels in impact-abrasion: the effect of sample angle and test duration, *Wear* 301 (2013) 94-101.
- IV Vilma Ratia, Vuokko Heino, Kati Valtonen, Minnamari Vippola, Anu Kemppainen, Pekka Siitonen, Veli-Tapani Kuokkala, Effect of abrasive properties on the high-stress three-body abrasion of steels and hard metals, *Finnish Journal of Tribology* 32 (2014) 3-18.
- V Vilma Ratia, Harald Rojacz, Juuso Terva, Kati Valtonen, Ewald Badisch, Veli-Tapani Kuokkala, Effect of multiple impacts on the deformation of wear-resistant steels, *Tribology Letters* 57 (2015) 15, 16 p.

Author's contribution

In publications I-III, Vilma Ratia was the main researcher and author. She planned and organized the experiments, analyzed the wear test results, conducted most of the optical and electron microscopy and wrote the manuscripts. In publications I-V, the supervisor Prof. Veli-Tapani Kuokkala and Lic.Tech. Kati Valtonen gave advises on the experimental parts and commented the manuscripts. M.Sc. Anu Kemppainen commented the manuscripts of publications I-V. In publication III, M.Sc. Ilkka Miettunen conducted the microstructural investigations on the cross sections of the wear test specimens and participated in the writing of the manuscript.

In publication IV, Vilma Ratia was the main author. The planning and organizing of the experiments and microscopy and writing of the manuscript were conducted together with M.Sc. Vuokko Heino. Assoc.Prof. Minnamari Vippola and Lic.Tech. Pekka Siitonen commented the manuscript.

In publication V, Vilma Ratia was the main author and planned, organized and conducted the impact tests and most of the microscopy and residual stress measurements. M.Sc. Juuso Terva conducted the EBSD measurements for the 400HB specimens, helped in analyzing the results and commented the manuscript. Vilma Ratia analyzed the impact test results together with Ing. Harald Rojacz, who also participated in the writing of the manuscript. Dr. Ewald Badisch commented the manuscript. M.Sc. Kauko Östman conducted the EBSD measurements for the 500HB specimen. Dr. Suvi Santa-aho conducted some of the residual stress measurements and guided in conducting them.

List of symbols and abbreviations

ASTM	American Society for Testing and Materials
A%	elongation at fracture
BSE	backscatter electron
CIAT	continuous impact-abrasion tester
DIN	Deutsches Institut für Normung
EBSD	electron backscatter diffraction
FWHM	full width at half maximum
HB	hardness in Brinell scale
HBW _{2.5}	hardness in Brinell scale with tungsten carbide ball and 2.5 kg load
HRB	hardness in Rockwell scale according to method B
HT-CIAT	high-temperature continuous impact-abrasion tester
HV _{load}	hardness in Vickers scale, load being the used load in kilograms
HVPI	high velocity particle impactor
LAC	LCPC abrasion coefficient, abrasiveness
LBC	LCPC breakability coefficient, crushability
LCPC test	Laboratoire Central des Ponts et Chaussées test for abrasiveness
MDL-10	also MLD-10, dynamically loaded abrasive wear tester
ppm	parts per million
Ra	surface roughness values as the arithmetic average of the absolute values of the roughness profile ordinates
ReH	upper yield strength
Rm	ultimate tensile strength
Rp0.2	yield strength (0.2% offset)
Rq	surface roughness value as the root mean square average between the height deviations and the mean surface
RT	room temperature
SE	secondary electron
SEM	scanning electron microscope
SIT	single impact tester
wt%	weight percent
α	alpha
Σ	summation

1. Introduction

Wear of materials is a wide scale challenge present in both everyday life and industry. It changes the surfaces and dimensions of the components, and may lead to failure creating hazards. Wear is a significant problem also in terms of economics, as some estimations present the costs of abrasive wear alone to be several percent of the national gross product [1]. Worn components require replacements, which interrupt processes and thus lead to nonproductive time. Moreover, wear leads to indirect ecological consequences by raising the amount of replaced components. In this sense, materials with better endurance in harsh conditions offer an opportunity for decreasing the amount of material usage. In addition to lowering the number of replaced components, stronger materials enable the use of smaller material thickness, which makes the machines lighter. This makes larger payloads possible, and also in moving unloaded machines, enables smaller fuel consumption.

Heavy wear, induced by harsh environments, leads to rapid material removal. Mining and construction industries are typical fields where high-stress wear is occurring. According to one calculation, one excavator bucket may need 6350 kg of steel replacements during six months only [2]. Another calculation states that the material loss of crushers can be 24 kg per 1000 tons of processed ore [3]. Machine components that are subjected to heavy wear are often made of wear resistant steels, which are harder and higher in strength than the normal structural steels and endure wear better, but on the other hand are rather lightweight in comparison to, for example, cemented carbides and thus economical in fuel consumption. Wear resistant steels can be used in a variety of fields, including agriculture, earth moving, forestry, and mining. Many of these aforementioned environments expose the materials to both scratching and impacting contacts.

In order to develop steels with better resistance to wear in a certain environment, it is important to know which factors are primarily influencing the wear rate and wear mechanisms in specific conditions. This way it can be recognized, which properties need to be focused on and, on the other hand, what kind of conditions are beneficial or detrimental to the materials. Wear is a complex set of phenomena that are affected by many factors ranging from the environment and contact conditions to materials and their combinations. Wear is also affected by many parameters having interdependent effects, which makes studying of these effects challenging. All the same, by gathering knowledge of the wear behavior of steels in controlled conditions with parameters chosen to simulate real situations, we get closer to understanding the essential factors having an effect on wear in demanding conditions.

1.1 Aim of the work

The aim of this work is to gather knowledge of how wear resistant steels behave under abrasive and impacting test conditions, which simulate the real conditions present in mines or construction sites, and to investigate the factors affecting the wear mechanisms in these tests.

This work was conducted within the Wear Resistant Materials and Solutions project of FIMECC DEMAPP program, whose aim was to tackle wear-related problems and to develop novel breakthrough materials for demanding applications in industry. To reach this goal, building a deep understanding of the demanding conditions in the applications and the related physical phenomena was needed. The role of this study was to determine the wear behavior of wear resistant steels, which also includes a thorough analysis of the applied wear testing methods. The wear test results were used in steel development in another part of the project, which concentrated on the processing and characterization of the steels. The research and development of steels with increasingly better wear resistance will continue in a following program.

The research questions of this thesis are the following:

1. Which factors are characteristic for the impeller-tumbler type impact-abrasion wear testing and how they affect the use of this wear testing method?
2. What kind of behavior the wear resistant steels exhibit in abrasive and impacting conditions?

The scientific novelty of this thesis is the careful consideration of the affecting factors in the utilized impeller-tumbler wear testing method. The testing method has been used by many research groups, but its varied procedures have not been discussed in detail in the open literature. In addition, the study includes research on the behavior of wear resistant martensitic steels in high-stress abrasive conditions and puts together and explains the observations of the wear surfaces formed in varying conditions. The structure of the research work is presented in Figure 1.

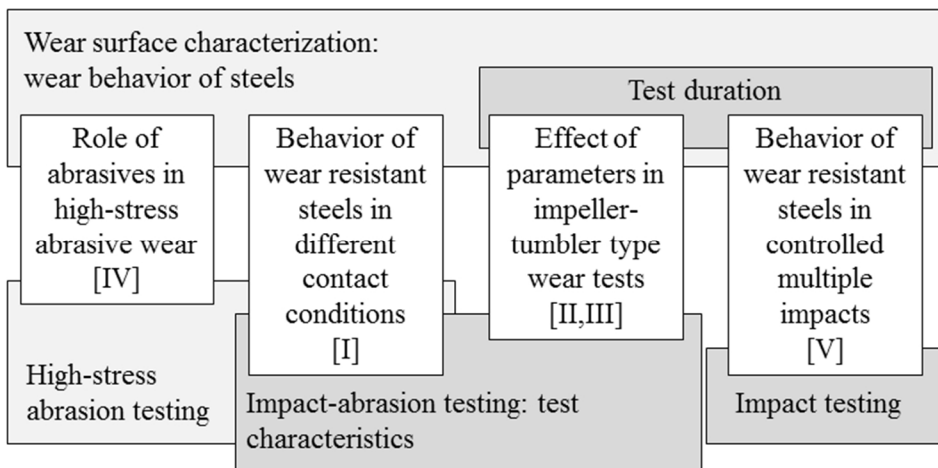


Figure 1. Structure of the thesis work and included publications I-V.

2. Wear and factors affecting it

Wear can be defined as the removal of material from the surface through interaction with another solid body, liquid or gas. As wear is a complex phenomenon, there are several different ways of classifying it into categories. Wear can be divided into subcategories, for example, according to the type of contact, severity of wear [4], relative movement, or wear particle removal mechanism [5]. Generally, adhesion, abrasion, surface fatigue and corrosive wear (or tribochemical reactions) are defined as the main mechanisms [4, 6, 7], but the material removal can happen through several simultaneously working mechanisms. The terminology for describing different conditions and their combinations is vast [5]. Figure 2 presents the key terms related to wear according to Kato and Adachi [4], demonstrating also the complex relations between the wear types and wear modes.

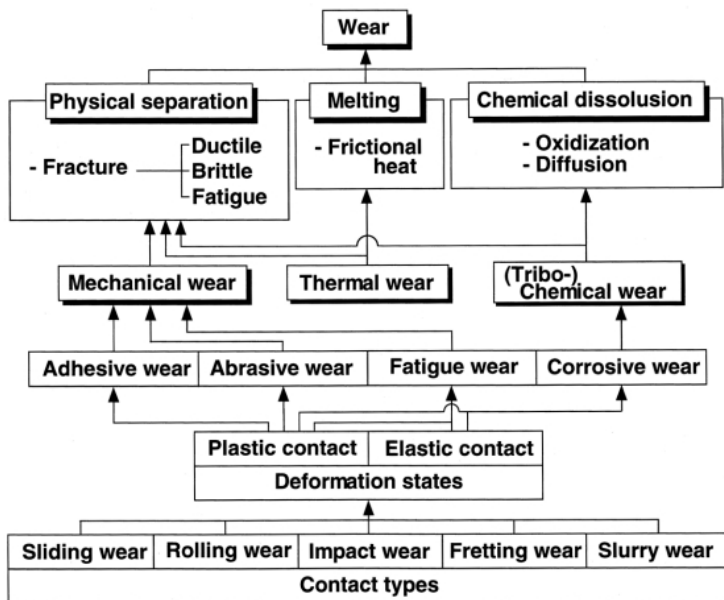


Figure 2. Key terms related to wear according to Kato and Adachi [4].

In this work, abrasive wear, impact wear, and impact-abrasive wear will be taken into closer investigation. Although the term abrasive wear can be thought as a basic mechanism, it can also be a wear type with sliding and rolling contacts. In this work, the term abrasion is intended to cover all interactions occurring between the materials and abrasives in the system.

An essential part in understanding wear is grasping the concept of a wear system, or in more generic terms, of a tribosystem. A tribosystem comprises the materials and the environment in which the system operates [4, 6, 7]. DIN 50320 standard [7] lists the material, counterbody, medium (such as lubricant) and the environment medium (usually air) as parts of the tribosystem. If the medium is thought in a wider concept, it can comprise several different materials, such as foreign abrasive particles and the lubricant. Thus, it may be justified to list also the abrasives or other contaminants as parts of the system.

By the concept of a wear system it is emphasized that the effect of one factor is dependent on the other parts of the system and their interactions. For example, the properties of the counterpart material can affect how the properties of the actual component increase or decrease its relative wear resistance. Thus, when studying the effects of different factors, it is important to take notice of the system as a whole before drawing any conclusions. This is why wear resistance is not an unambiguous property of the material but is closely linked to the entire wear system [8–10].

General factors affecting the wear besides the materials present in the system are the motion, loading, and environmental conditions such as temperature, moisture etc. Factors affecting the wear types investigated in this work the most are presented and discussed in the following subchapters in more detail.

2.1 Abrasive wear

Abrasive wear is considered to be the single most effective wear type in causing economic losses in industry [11]. Abrasive wear is a common cause of failure in machine components of earthmoving and transportation vehicles and excavator buckets. High-stress abrasive wear changes the dimensions of the components and weakens the structures as the material thickness is reduced. In pure abrasion, the correlation between volume loss and sliding distance is often linear, which makes pure abrasive wear perhaps more predictable than some other types of wear [10]. However, this is not to say that the prediction of abrasive wear would not be complex, as the wear system is affected by numerous factors of material properties and environmental effects.

Abrasive wear is removal or displacement of material by hard particles or surface protrusions [12]. When another component with protruding asperities or fixed, partially embedded abrasives scratches the surface directly, the wear type is called two-body abrasive wear. In three-body abrasion, on the other hand, wear is induced by the loose abrasives that are free to slide or roll between the surfaces and into which the counterpart is transferring the load [13]. Figure 3 presents a schematic of two- and three-body abrasion. In this work, the term three-body abrasion is used to describe a situation which initially has three active, clearly separate agents affecting the system, and even during the wear process, a clear majority of them remains in their initial role.

Sometimes the difference between two- and three-body abrasion mechanisms is understood so that two-body abrasion produces scratches and three-body abrasion rolling marks. Some authors prefer the use of terms ‘grooving abrasive wear’ and ‘rolling abrasive wear’ for two- and three-body abrasion, respectively [14]. Furthermore, it is possible to divide three-body abrasion into open and closed situations: in open three-body abrasion, the two surfaces are far apart from each other, while in the closed situation the abrasive particles are trapped between the closely mated surfaces [15]. Even two-body abrasion can be subcategorized to ‘fixed-particle grooving abrasion’ and ‘free-particle grooving abrasion’ [16]. This demonstrates the complexity of

defining the conditions precisely and the breadth of terminology used in describing the phenomena.

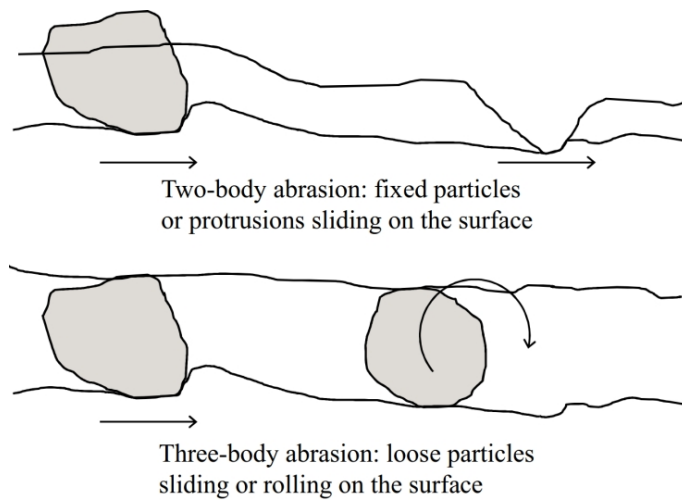


Figure 3. Wear system in a) two-body abrasion and b) three-body abrasion.

The way of classifying abrasion into two- and three-body wear defines the conditions through naming the active bodies participating in the process. However, this kind of oversimplification does not usually appreciate the complexity of real situations, where pure two- or three-body abrasion is rather scarce, and often the two modes occur simultaneously [17]. They can also alternate in the same system, the conditions governing which of the modes is dominant [14]. The division of abrasive processes into two- and three-body situations is more of a description of the initial state than a precise observation of the ongoing process, which is greatly affected by the system in question. For example, the dry sand rubber wheel abrasion test is a three-body abrasion test by its default configuration, but the actual wear occurring in the system can be more towards two-body abrasion, since the sand particles embed in the rubber quite effectively [18]. On the other hand, initially two-body conditions may develop into three-body conditions, if the initially fixed abrasives or existing or forming protrusions are removed from the initial surfaces.

Another classification for specifying the type of abrasive wear is the division to high- and low-stress abrasion. In high-stress abrasion, the load induced into the abrasive is so high that it breaks the abrasive, while in low-stress abrasion the abrasive remains intact [5, 12]. Also a division into mild and severe wear has been used [18–20], as it is often difficult to determine the exact conditions present in the interface.

Overall, a common characteristic for the attempts of classifying the wear processes is its complexity and difficulty. In this work, the abrasive wear occurring through scratching contacts can be characterized to consist mostly of high-stress abrasive wear in a closed situation, which is defined initially as a three-body process. The interaction of the surfaces and abrasives leads to both rolling and sliding, as the particles can be partly embedded into the surfaces.

Abrasive wear can further be divided into micromechanisms, which lead to the final outcome. These are microploughing, microcutting, microfatigue and microcracking [6]. Figure 4 presents these micromechanisms schematically. Another way of categorizing the micromechanisms is to

divide them into cutting, fracture, fatigue by repeated ploughing and grain pull-out [13]. However, grain pull-out is not a generic material removal mechanism, since it can only happen in materials with a grain structure. In another classification, abrasive wear is divided into three different wear modes: cutting, wedge formation and ploughing [21]. In wedge formation, a wedge is formed against the sliding indenter, but some ploughing on the sides of the groove is also occurring.

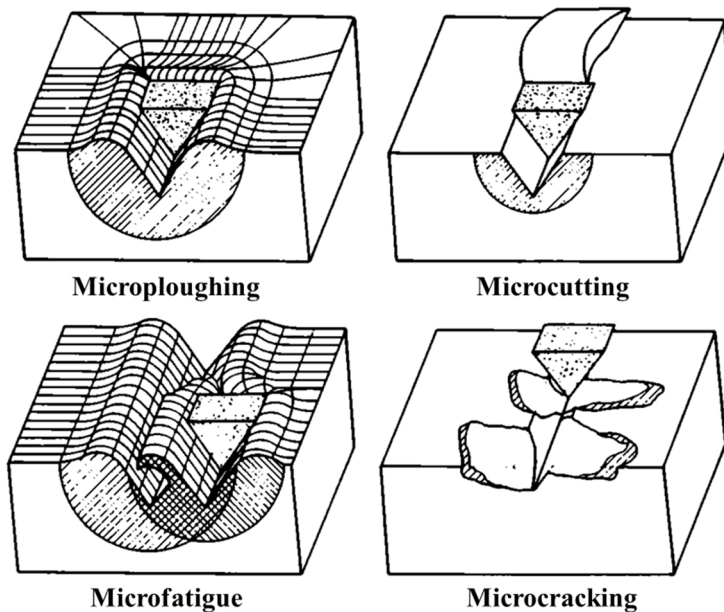


Figure 4. Schematical presentation of the micromechanisms of abrasive wear [6].

In microploughing, no actual removal of material takes place but the material is only displaced to the sides of the scratch. Microcutting, instead, leads to the removal of material, as it is cut away from the surface like a chip. In microfatigue, small pieces of repetitively deformed material become detached from the surface, while in microcracking the material is removed through crack formation and propagation, especially in brittle materials. [6]

2.1.1 Role of abrasives

In abrasive wear, the abrasives are in an essential role in determining the wear process. It is generally accepted that in order for a scratch to form, the hardness of the abrasive has to be at least 1.2 times the hardness of the material to be scratched [22, 23]. Some other abrasive properties affecting wear are the crushability [Publication IV], abrasive size [19, 24–31] and angularity or shape of the abrasives [32–37].

Some of these properties, such as hardness and angularity, have a direct effect on how the abrasive is able to penetrate the material. The attack angle can also determine the more specific wear mechanism: with a low attack angle, the abrasive is more likely to cause ploughing, whereas with a high angle, cutting is more probable [20, 38]. On the other hand, some other properties such as crushability determine the behavior of the abrasive in the system, and thus have a more indirect effect on wear. As an example, an abrasive with high crushability produces a larger quantity of small abrasive particles, which are freshly ground and have high angularity.

Larger abrasives are more blunt and have lower attack angles, thus causing less cutting [30]. If the crushing of particles happens to a large extent, it can mask the effects of abrasive angularity [39]. Moreover, according to Gåhlin and Jacobson [40], if the abrasives are ideally sharp, the size effect does not apply to them.

For relatively small abrasive sizes, it has been found that increasing abrasive size also increases wear. This observation is often called the particle size effect. However, the particle size effect is valid only for small particle sizes, up to 80-150 μm [27, 41, 42], above which the increase in particle size does not increase the damage at the same rate. There are several theories of the reasons for the abrasive size effect. To name some, Misra and Finnie [27] concluded the effect to be caused by the physical size of the abrasive in contrast to the depth of the hardened surface layer. Coronado and Sinatora [30] suggested that the critical size, after which the wear rate changes, is originating from the transition from microcutting with small abrasives to microploughing with larger abrasives, but the occurrence of this phenomenon was dependent on the studied material.

The effect of particle size on abrasive wear is not fully clear in larger scales. For macroscale abrasives of millimeters in size, the size effect remains generally undefined. For particles with a size of several hundreds of micrometers or above, there are findings stating both increased [42] and decreased [43, 44] wear rate with increasing particle size. Elementally, it is a question of the conditions in the tribosystem. For example, if the machine or a wear tester is adjusted in such a way that the abrasives below a certain size can move freely between the surfaces without being loaded, the small particles do not interact with the surface at similar loads as the larger particles.

In tunneling and mining, it is common to define the abrasiveness of the abrasive for making predictions of the service life of the wear parts and for preparing maintenance schedules. Abrasiveness indicates the ability of the rock to cause wear. Abrasiveness can be measured with a number of different procedures, such as thin section analysis [45], Cerchar test [45–53], LCPC test [45, 49, 51–55], Schimazek index test [49, 51], Sievers C-value test [45], Böhme grinding test [45], the brittleness value test, Sievers J-value test, and abrasion value and abrasion value cutter steel test [56]. The LCPC test and Cerchar abrasivity index appear to be the most used tests in Europe recently [45]. The idea behind these tests is quite different: the LCPC test measures the mass loss of a standardized steel block worn with a batch of certain size gravel in impact-abrasive conditions [49, 53, 55, 57], whereas for measuring the Cerchar index a steel pin is sliding against a block of rock [47, 49, 52]. As the methods and the wear mechanisms they produce differ widely, the values obtained by the tests are not comparable. However, some empirical dependence between them has been reported [55].

2.1.2 Role of counterparts

In three-body abrasion, the properties of the counterpart material affect the wear system, thus impacting the wear besides the abrasives. Axén et al. [58] reported that the wear mechanism in abrasive conditions can vary markedly depending on the hardness ratio of the sample material and the counterpart. A softer material (whether it is the sample or the counterpart) is more likely to have abrasives embedded in it, and after that it can work as the abrasive body by sliding and cutting the harder surface. However, the specimen surface and the counterpart are usually able

to become into contact with each other during the test, which adds the question of how the contacts between the surfaces affect the situation, as opposed to the interactions taking place only through abrasives. This would lead to a difference in the active wear mechanism between counterparts of different hardness, and possibly to higher wear rates in the harder sample. In some cases, it could lead to a situation where increased hardness increases wear [59].

2.2 Impact wear

Impact wear happens through the collision of two solid bodies [60]. The actual removal of material can occur by any of the basic wear mechanisms, i.e., adhesion, abrasion, fatigue or corrosion [61]. At times, the term compound impact wear is used for describing impact wear where both impacting and sliding takes place [62].

As for all wear types, there are also several other suggestions for the classification of impact wear into narrower categories. One division is into two-body impact wear and multiple body impact wear, which includes also erosion [63, 64] that some impact wear classifications are excluding [62, 65]. In this work, impact wear is used as a term to describe high-stress wear due to two solid bodies, which both are relatively large (several millimeters) in size.

The severity of impact wear depends on the materials and their elastic and inelastic responses, as well as on the strength and nature of the loading, including the impacting body mass, speed and direction. The effective wear mechanism depends strongly on the surfaces, e.g., the topography and friction between the impacting body and the target material [62]. In the course of the wear process, also the changes occurring on the surface topography, in the material properties and the wear mechanism, as well as in the stress state affect the impact wear [66].

2.3 Impact-abrasive wear

Impact-abrasive wear can be thought as a subcategory of impact wear, as it covers a wide range of contact conditions and media. In this work, these two wear mechanisms are separated, as in [Publication V] the contact occurs without abrasive media and without intended sliding movement, while in [Publications II and III] the abrasive media is an essential part of the wear conditions. Impact-abrasion does not have a definition which would be commonly agreed upon, but it has been used in many scientific articles to describe complex wear in conditions having both impacting and abrasive elements [Publications I-III] [67–84]. In his book chapter about wear testing, Hawk [65] classified impact-abrasion as a wear mode happening through larger abrasives, as opposed to erosion, which usually involves particles in the size range of 10–100 μm .

The range of conditions where impact-abrasive wear can occur is wide. These conditions could be roughly divided into two categories presented in Figure 5:

1. Impact-abrasion with two acting bodies: One body induces both the impacting and abrasive contacts on the material. This can happen in a situation, where a particle is impacting on the surface and continues to slide on it after the impact, the situation remaining essentially between the two acting bodies, i.e., the wear surface and the abrasive. This situation has similarities to erosive wear, but the particle size is larger [65].
2. Impact-abrasion with three acting bodies: The load of the impact and the following sliding movement on the material is induced by an external object. The interface between the external object and the body to be worn contains abrasives, which is causing the abrasive aspect in the conditions [85]. This system comprises three bodies participating in the process: the wear surface, the abrasive, and the counterpart inducing the load.

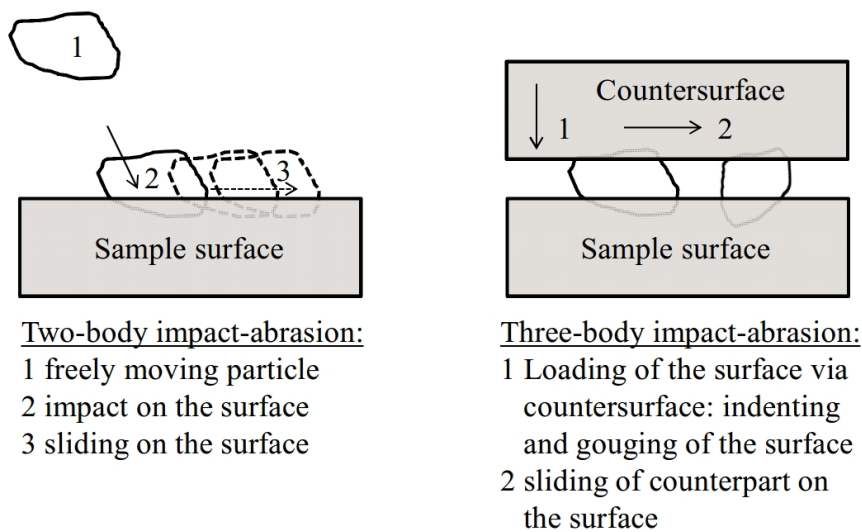


Figure 5. Impact-abrasion with a) two acting bodies and b) three acting bodies.

This work concentrates on the impact-abrasion with two acting bodies, which occurs in impeller-tumbler wear testing (introduced in section 5.2.3). This type of wear is typical in impacting crushers and in rock processing machinery, where the rocks and soil are moved from one machine to another for further handling. Furthermore, also some other wear testing methods used in this work, i.e., crushing pin-on-disc and uniaxial crusher (introduced in sections 5.2.1 and 5.2.2), have characteristics that can be categorized as impact-abrasion with three acting bodies, as the counterbody is pressed against the abrasives cyclically. However, they are referred in this work to as abrasive wear testing methods, since the speed of the impact is very low (less than 1 m/s) and more towards crushing, in contrast to the impact-abrasion contact speed (up to 8 m/s). This classification is rather artificial, as the terminology is not standardized to begin with, but makes the obvious differences between the methods used in this work clearer.

Factors affecting the impact-abrasive wear include those of both impact and abrasive wear, as can be expected. The wear process is essentially affected by the loads and the relative movement of the bodies acting in the system, as well as by the material properties of all the components participating in the process [62, 86]. In the case of impact abrasion conditions with three acting bodies, in addition to the materials of the sample and the counterbody, the material of the abrasive with a set of properties of its own is in an extremely important role, as discussed

in more detail in section 2.1.1. The direction of the contact affects how the sample material behaves under an impact [12], but it can also affect the grazing angle of the abrasive, determining whether the abrasive is more likely to cause cutting or ploughing [38].

If the system is closed and no material is moving in or out of it, the conditions can vary dramatically with time, especially when the rock is being crushed from large chunks to small particles during the process. A rock with a high particle breakage index will comminute during the operation, and thus a part of the energy will be used for the formation of new rock surface and not for causing wear [87]. Moreover, the individual impacting rocks will be smaller, which decreases the impact energy and thus makes the conditions less harsh. This is to say that the properties of the individual parts of the system will have a vital role in how the conditions in the whole system will evolve.

3. Wear testing methods

Wear resistance is not a material property but depends on the entire wear system. This makes wear testing a challenging and necessary task, as it is difficult to predict the behavior of a material based on the results obtained in totally different conditions. To obtain good results that will provide useful information for example for materials selection and material development, the testing conditions must be carefully selected.

A good wear test should simulate the real conditions as closely as possible, but it should also be as well controlled as possible in order to be reliable and repeatable [88]. Usually it is not possible to put both of these requirements fully into practice simultaneously, and thus wear testing is always a compromise between different demands. This often leads to a lack of correlation between the results of laboratory and field tests [89, 90], and reasonable correlation is generally possible to achieve only if the conditions are similar enough [91–93]. Moreover, scaling of the wear results between industrial and laboratory tests can be difficult due to the possible changes in the wear mechanisms in tests of different scales [94].

Wear tests can be categorized according to their degree of reality and control [6, 10], as presented in Figure 6. Field tests have the highest degree of reality but the lowest degree of control. In the field test, real machines are used in real working environments, which makes controlling of the external variables, such as the weather, working grounds, or working procedures quite difficult. In the other end of the test categories are the laboratory model experiments. These are very well controlled tests of highly simplified situations. For example, a scratch test in a controlled atmosphere tells about the behavior of the material under a single scratch in a precise manner. On the other hand, in real life the material is likely to be subjected to several scratches, and perhaps impacts as well. The net result after two overlapping scratches is often not the sum of two single scratches [95] because of factors such as work hardening, orientation differences or changes, surface roughness, and other factors, which change along with the use of the material.

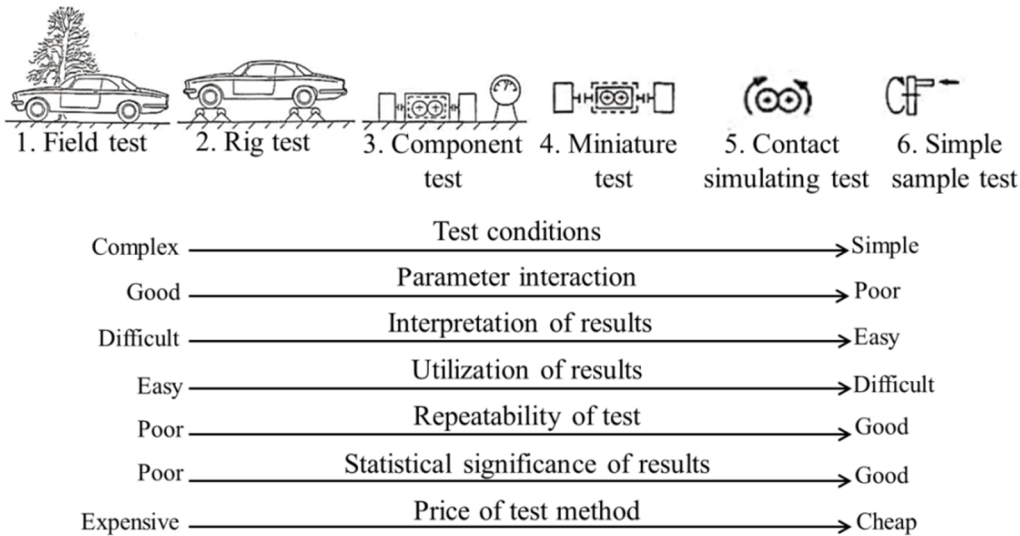


Figure 6. Wear test categories according to their degree of reality and control, modified from [96].

As wear resistance is not a material property, appropriate reference data is needed in order to assess the wear test results. This can be done by using a reference sample, which is made of a material whose properties are well known. If a better material is sought for an application, the reference material can be the material which is used in the component at present. [10] Through the use of a reference material in the field tests, it is possible to analyze the test results more accurately, as the reference samples provide also information about the wear gradients present in the test site [97]. However, it is not possible to attach several samples to the exactly same point, and even a small difference in the positioning may affect the conditions that the samples are experiencing. For example, if the sample plates are attached to a loader bucket, different distances from the edge as well as from the side plate can make a difference. Even if the positions were seemingly identical, the procedures that are dependent on the machine operator may cause differences in the wear conditions of the bucket.

Some general parameters affecting the wear testing are [61, 88]:

- Materials to be tested
- Load
- Environmental conditions (temperature, humidity, atmosphere)
- Surface roughness and material preparation
- Duration of the test and/or recurrence of the contact
- Movement and its speed (vertical/horizontal or both)
- Lubricant and other media present
- Geometry of the contact

3.1 Abrasive wear

In abrasive wear tests, the material to be tested is abraded with either fixed or loose abrasives [10]. Often the wear is measured as the mass loss, so that the sample is weighed before and after the test [98] and, if needed, also during the test. This is a relatively easy means of measuring wear, but when using mass loss measurements, the sample must be able to be removed and reattached accurately and easily for weighing. Mass losses can further be converted into volume losses, when the density of the material is known. Volume loss results enable comparison of the wear of materials with different densities [65]. If the sample cannot be easily removed from the testing device, geometrical measurements can be used [63]. However, in that case the point of measurement must be representative.

Besides the general parameters affecting the wear testing, in abrasive wear tests the counterpart materials and abrasives and their properties are of importance. The counterpart material affects the conditions, since it can affect the movement of the abrasive. [10] Abrasive properties may also be changing during the test, for example, if the abrasive is comminuted during the test [43] and/or it is continuously reused.

Abrasive and erosive wear are perhaps the most standardized wear types for testing. A very popular test is the ASTM G-65 dry sand rubber wheel test [99], in which a block of material is pressed against a rotating rubber wheel and certain type of quartz abrasive is fed into the interface. There are also many variations of the dry sand rubber wheel test: for example, the slurry abrasion test, where the abrasives and a part of the wheel are immersed in a slurry [100], and the dry sand steel wheel test, where the rubber wheel has been replaced with a steel wheel [59, 101]. The steel wheel also enables testing at elevated temperatures through heating of the sample block inductively [102].

Some other abrasive wear tests are the pin-abrasion [103] and pin-on-drum tests [104], which both have initially the two-body abrasion arrangement. The abrasives are fixed onto a paper or cloth, and the pin is pressed against the moving abrasive paper or cloth. All of the abovementioned tests and many other abrasive wear tests [15, 32, 39, 58, 105–107] use rather small size abrasives (up to 500 μm), whereas in real applications abrasive wear can be caused by significantly larger size abrasives. One standard wear test that can be conducted with larger size abrasives is the ASTM G-81 jaw crusher test [108]. In this test, four test plates consisting of two sample plates and two reference plates are worn by crushing 900 kg or 1800 kg of rock.

One test method utilizing larger size abrasives in sliding movement is the crushing pin-on-disc test [43]. In the non-standardized crushing pin-on-disc test, the sample is repeatedly pressed against a loose abrasive bed on the rotating disc. This enables the use of larger size abrasives (up to 10 mm) in the test, the restriction being the distance between the sample holder and the collar holding the abrasives on the disc. During the test, both sliding movement and compression take place as the sample is being pressed down towards the rotating disc. An illustration and a more precise description of the test method are given in section 5.2.1. A comprehensive listing of all abrasive, or any other, wear tests is challenging, since many of the devices such as the crushing pin-on-disc are non-standard and self-built devices.

3.2 Impact wear

In impact wear tests, the sample is repeatedly impacted by another solid body, which can be a larger body or a smaller particle. Impact wear tests help in assessing the impact resistance of materials or coatings in certain conditions. In impact wear tests, like in abrasive wear tests, the wear can be measured through mass or dimension loss, but in some cases it is more practical to measure the time or number of impacts until failure [109]. Crack formation can be detrimental for the performance of the material and lead to a catastrophic failure when the loading is continued. So, even though the material is not yet removed from the surface and the wear is not measurable as mass loss, the component may not be fit for use anymore.

When considering the wear between two larger solid objects and comparing that to abrasive wear, it is obvious that the impact wear is affected by factors that are more towards the contact conditions and their nature. Factors related to the movement of the impacting object [62], such as impact angle, impact velocity, frequency of impacts, and distribution of the impacts on the area are some additional parameters and factors affecting the wear.

In some cases, erosion is also considered as a form of impact wear. There are also some standardized erosion tests, such as the ASTM G73 Test method for liquid impingement erosion using a rotating apparatus, the ASTM G76 Test method for conducting erosion tests by solid particle impingement using gas jets, and the ASTM G134 Test method for erosion of solid materials by cavitating liquid jet [88]. In the erosion tests, the impacting particles are accelerated either with gas, fluid or centrifugal forces. However, this work concentrates more on the heavy forms of wear. Most of the high-stress impact wear tests are non-standardized, such as the high velocity particle impactor (HVPI) [110–114], hammer mill [85, 115], reciprocating hammer [116, 117], ball-on-block [109, 118, 119] and ball dropping test [120, 121]. The hammer mill test can induce impacts on the sample with rotating hammers. The impact energy is typically in the range of 50 J. [115] The ball-on-block test, in turn, induces high energy impacts on samples via a steel ball that is either dropped or shot at the sample repeatedly. [109, 118, 119, 121]

3.3 Impact-abrasive wear

In impact-abrasive wear tests, the samples are simultaneously subjected to both impacting and abrasive conditions. The conditions can be varied, as there are both abrasion and impact parameters that can affect the final outcome of the tests.

As the definition for impact-abrasion is not standardized, neither are the test methods used for testing it. The test methods themselves can be categorized depending whether the load is induced on the sample directly through the abrasive particles (two active bodies in the system) or via an external body (three active bodies in the system), as categorized in section 2.3. In the two-body category, the disintegrator-based impact wear tester [122] and the impeller-tumbler tester, also known as impeller-in-drum [69] or continuous impact abrasion tester (CIAT) [68,

76, 86, 123], can be mentioned. Figure 7 presents the schematics of these test devices. In both of these devices, the gravel is placed loosely inside a drum, in which the samples are rotated. Thus, the samples and rock particles contact with each other at a rather high speed and the rock is comminuted.

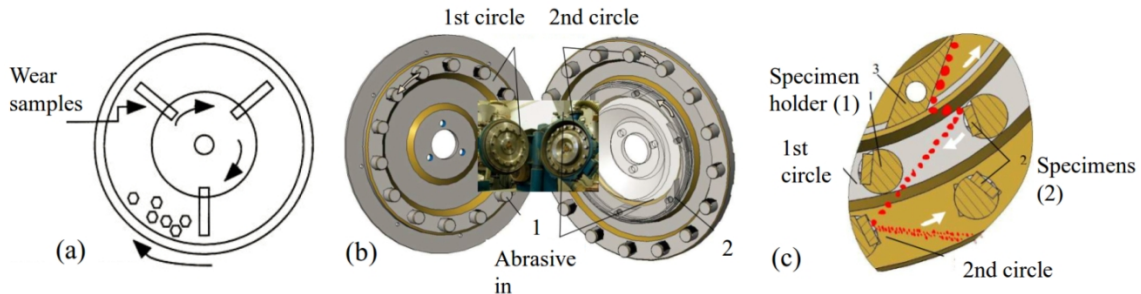


Figure 7. Schematics of a) impeller-tumbler [69], b) disintegrator-based impact wear test device and c) a close-up of the disintegrator-based impact wear test device's specimen section [122].

Inside this type of machines, the flow of the abrasives is affecting the conditions inducing the wear, and therefore the placement of the samples is very important: they must be placed so that the samples have as similar conditions as possible, unless specifically sought otherwise. For good results, as even small differences in the sample holders can lead to an unpredicted outcome, it is best if the tests are conducted so that each sample is rotated through all of the sample holders during the test to even out the test conditions. If several sample holders are available, it is easy to include a reference sample in each test to make sure that the conditions are comparable.

The impeller-tumbler type device was originally designed for comparing the abrasive wear caused by different ores and other materials [124], and certain metal samples were used as indicators for this tendency. Impeller-tumbler devices enable the easy change of abrasives and the use of several types and sizes of them. This can be very beneficial when assessing the performance of a material in a situation where it is subject to several different types and sizes of abrasives. However, during the test the abrasive cannot be changed unless the device is stopped and the used abrasive removed and replaced with fresh abrasive.

In an impact-abrasion test with three acting bodies, the process is divided into two separate phases of impact and abrasion. First, the impact occurs on the sample, induced by another object with abrasives at the interface. In the second phase, the sample and the counterpart move in relation to each other, making the conditions abrasive. Some devices used for this type of impact-abrasive wear testing are MLD-10 (or in some references MDL-10 [70, 125]) and high-temperature cyclic impact abrasion tester (HT-CIAT) [67, 81, 102, 126–130]. Figure 8 presents the schematics of these devices. MLD-10/MDL-10 has been used by many research groups [70, 83, 125, 131–134]. In this device, the sample is dropped onto a moving abrasive counterpart. In HT-CIAT, a plunger with either a flat or ball end is dropped onto a block. The sample can be the plunger, the block, or both. In this method, the abrasive is fed into the interface constantly, which means that the abrasive is always fresh and its size does not change during the test.

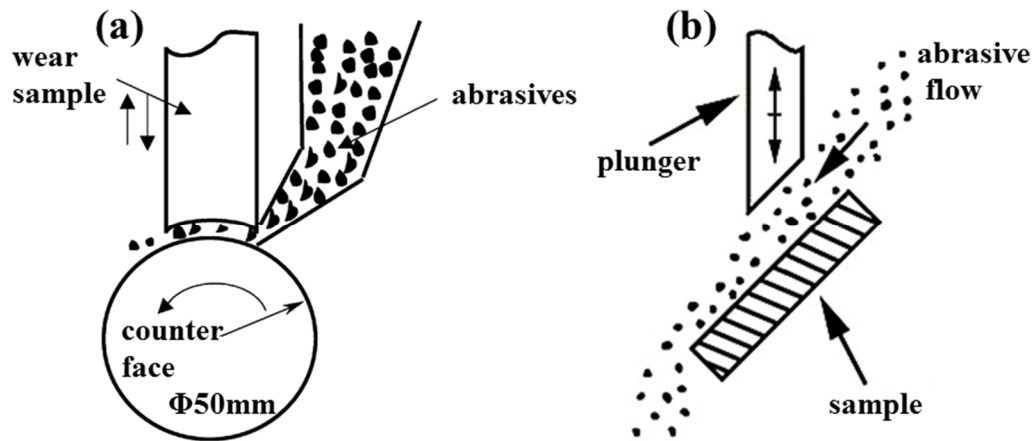


Figure 8. Schematics of a) MDL-10 [125] and b) HT-CIAT test devices [129].

In both types of impact-abrasive wear tests, the abrasive particle size tends to be larger than in the standardized abrasive wear tests, of course depending on the test method. For MLD-10/MDL-10, the use of abrasive sizes between 0.8 and 5 mm [83, 125, 132–134] have been reported. For the HT-CIAT, the corresponding size range is 0.4-0.9 mm [67, 81, 102, 128, 129]. For impeller-tumbler, the reported sizes range from fine grit (<1 mm) [68] to 30 mm [Publications I-III] [68, 69, 76, 78, 84, 86, 91, 104, 123, 127, 135–137], the emphasis usually being on the larger particle size. For comparison, the usual particle size in the standardized dry sand rubber wheel abrasive tests is only 212-300 μm [99].

4. Typical properties of wear resistant steels

As already noted, wear resistance is not a material property but depends highly on the conditions. However, the term wear resistant steel is widely used for marketing purposes, and the steels in this commercial category usually have similarities among their group. The term wear resistant steel also has several subcategories, describing more precisely the properties of the materials. When structural steels can have the strength in their name indexing, wear resistant steels are categorized by their hardness, such as 400HB, 500HB and 600HB grade steels. This is most likely to result from the connection between hardness and abrasion wear resistance at a general level [64]. The purpose of this section is not to list exhaustively all alloying effects and processing parameters, but to give a concise overview on how the materials used in this work relate to other commercially available wear resistant steels.

The compositions and manufacturing processes of wear resistant steels may vary markedly between the steelmakers. Furthermore, the plate or strip thickness also affects alloying [138, 139] and thus the steel properties since with increased plate thickness, more alloying is needed to ensure the through hardening of the plate [140]. Table 1 presents the compositions of some commercial 400HB steels, as reported by the steelmakers. The numbers represent typical maximum values and are thus approximate. However, already based on these numbers it can be suggested that the alloying elements vary a lot between the different nominally similar commercial grades. This has also been reported in a study comparing several commercial wear resistant steel grades by Ojala et al. [141], where the compositions of steels were analyzed with optical emission spectrometer.

The effects of alloying elements on the wear behavior of materials arise from their effect on the processing behavior and thus microstructure of the steels, such as hardenability [141–143], autotempering [144] and work hardening [70, 141]. A wear resistant alloy should contain a sufficient amount of carbon, boron and combined nickel and molybdenum, since the nickel-molybdenum combination was found to have a larger effect on the hardenability than neither of these elements alone [141]. Also Bhakat et al. [145] reported the importance of boron, or alternatively chromium, addition in the alloy for reaching the appropriate hardness during quenching. The alloying, however, can enhance the resistance against one wear mechanism while decreasing the resistance against some other. Ren and Zhu [146] reported that wear due to delamination decreased when the total content of the substitutional alloying elements was decreased but, on the other hand, the quasi-nanometer wear mechanisms were promoted.

Many of the wear resistant steel grades are delivered in the quenched [138, 147–152] or quenched and tempered [153–160] state. Different types of processing, such as quenching and partitioning [161–165], have also been developed to obtain the desired microstructures.

Table 1. Compositions of some 400HB steels as reported by the steelmakers [138, 151, 154, 155, 159, 166, 167].

Trade name	C max %	Si max %	Mn max %	P max %	S max %	Cr max %	Ni max %	Mo max %	B max %	Other max %
Hardox 400 [138]	0.15	0.7	1.6	0.025	0.01	0.5	0.25	0.25	0.004	
Raex 400 [166]	0.23	0.8	1.7	0.025	0.015	1.5	1	0.5	0.005	
Xar 400 [155]	0.2	0.8	1.5	0.025	0.01	1	0	0.5	0.005	
Brinar 400 [159]	0.18	0.5	2	0.015	0.005	1.55	0	0.6	0.005	Al 0,1
Creusabro 4800 [167]	0.2	0	1.6	0	0.005	1.9	0.2	0.4	0	Ti 0,2
Dillidur 400 [151]	0.2	0.5	1.8	0.025	0.01	1,5*	0,8*	0,5*	0,005*	V 0,08* Nb 0,05*
Abrazo 400 [154]	0.2	0.5	1.6	0.025	0.01	1	1.5	0.7	0.004	V 0,1 Nb 0,06 Cu 0,4
average	0.19	0.54	1.69	0.020	0.009	1.28	0.54	0.49	0.004	
median	0.20	0.50	1.60	0.025	0.010	1.50	0.25	0.50	0.005	
min	0.15	0	1.50	0	0.005	0.50	0	0.25	0	
max	0.23	0.80	2.00	0.025	0.015	1.90	1.50	0.70	0.005	

*used singly or in combination

Table 2 lists some of the mechanical properties for selected wear resistant steels of different hardness grades. The wear resistant steels usually have higher hardness and higher yield and tensile strength than the common structural steel grade S355. The hardness of the 400HB steel is twice as high as that of S355, and its yield strength is approximately three times as high. From Table 2 it can be recognized that there are a few distinct categories of wear resistant steels: the hardness categories of 400HB, 500HB and 600HB, and steels designed for impact conditions. The steels with presumably better resistance against impact type loading, such as Xar HT and Dillidur Impact in Table 2, have lower hardness but larger elongation values. The reported impact toughness values of the steels for impact conditions are not much higher or are in the same range as for the other presented wear resistant steel alloys. This can be explained by the values being minimum values for the steels for impact conditions, while for the other steels typical values are presented.

Table 2. Mechanical properties of wear resistant steels as reported by the steelmakers [138, 151, 153, 155–158, 166, 168, 169].

Trade name	Hardness [HB]	Yield strength $R_{p0.2}$ [N/mm ²]	Tensile strength R_m [N/mm ²]	Elongation A [%]	Notch impact energy J/cm ² -40°C
Domex 355 MC [169]	-	355 (ReH)	430-550	23	27*
Laser 355 MC [168]	-	355 (ReH)	430-530	24	40 (-20°C)*
Dillidur impact [153]	310-370	950 (ReH)	1000	15	30*
Xar HT [157]	310-370	960	1000	14	50*
Raex 400 [166]	360-440	1000	1250	10	30
Xar 400 [155]	370-430	1000	1250	10	50
Dillidur 400 [151]	370-430	800	1200	12	30
Hardox 400 [138]	370-430	1000	1250	10	45
Raex 500 [166]	450-540	1250	1600	8	30
Xar 500 [156]	470-530	1300	1600	9	25 (-20°C)
Xar 600 [158]	550	1700	2000	8	20 (-20°C)

*minimum

The harder steel grades, i.e., the 500HB and 600HB steels, have higher strength but quite similar elongation and impact toughness values compared to the 400HB steels: usually the harder grades have lower nominal elongation and lower impact toughness, but the variance between the trade names in the 400HB hardness class is quite substantial. As an example, the typical impact toughness of 400HB steels ranges from 30 J/cm² to 50 J/cm² at -40°C. Elongation values vary between 10 and 12%. Moreover, the reported yield strength values can vary between 800 and 1000 N/mm². On the whole, the comparison based on the datasheet information is not exact due to the differences in testing methods and presentation of data for products of varying thickness. [138, 151, 155, 156, 158, 166]

Ultimately, the properties and thus the wear performance of the steels depend on the microstructure. There is not only one beneficial microstructure for abrasive or impact wear resistance, but the suitability of a material with a certain microstructure depends on the conditions where it is used. Also in similar conditions the ability of the steel to resist material removal, i.e., wear, can be accomplished with several different microstructures [170]. That being said, many of the wear resistant steels have a martensitic or mostly martensitic microstructure [78, 83, 109, 141, 145, 162, 170–173]. This is because martensite is a very hard microstructure with very high ultimate strength [174], which usually correlates with higher hardness and better abrasive wear resistance. However, a wear resistant steel can consist of, or include, several other phases. For example, the steel can be mostly [78, 170] or partly bainitic [78, 125, 175, 176], and contain ferrite [78, 175], pearlite [78, 132] and/or retained austenite [162, 176, 177]. Figure 9 presents some microstructures found in wear resistant steels.

When looking at the microstructure in more detail, smaller grain size usually correlates with good wear resistance [78, 175]. In addition, the block [178–180], packet [178, 181, 182] and

lath [161, 183] sizes of martensite affect the mechanical properties and thus the wear performance of the materials.

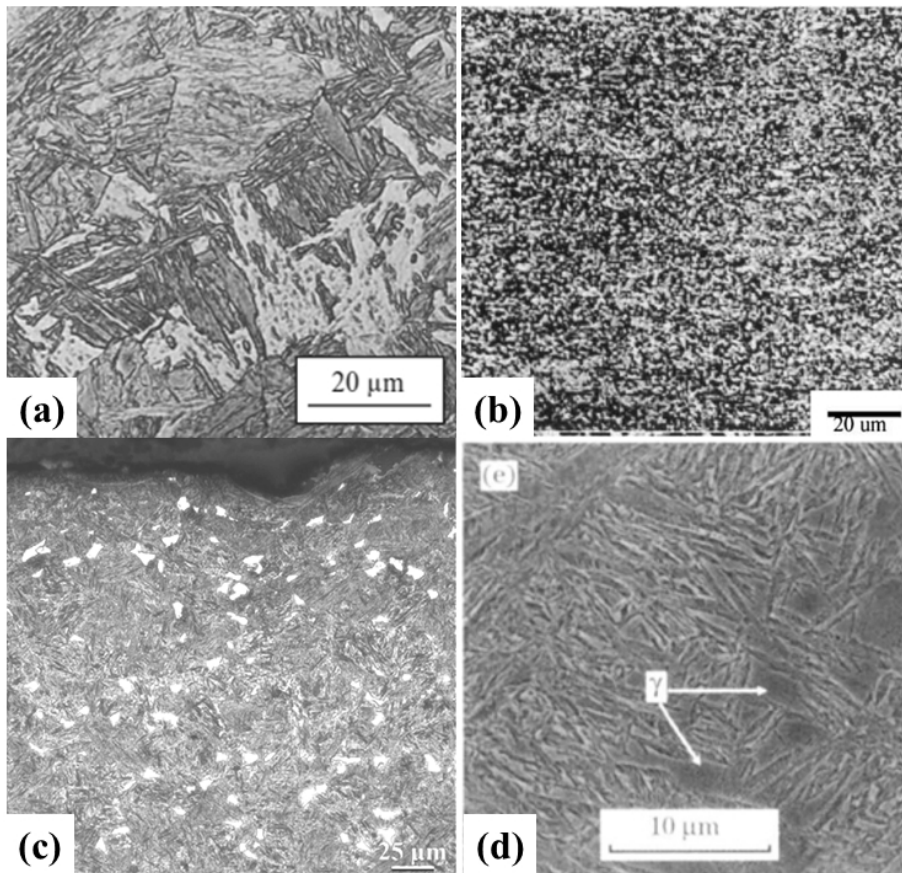


Figure 9. Microstructures of a) martensite [141], b) bainite [78], c) martensite with ferrite islands [Publication III] and d) martensite and bainite with retained austenite (γ) [177].

Wear resistant steels are used in various demanding environments and applications, such as agriculture (ploughs, tillers) [184], wood processing, earth moving and roadbuilding (cutting edges, excavator buckets, tipper bodies) [166, 185], recycling (hammer mills, sieves, shredders) [186] and mining (front loader buckets, hoppers, rail road cars) [187].

4.1 Role of steel properties in abrasive, impact-abrasive and impact wear

In abrasive wear, hardness is an important property in increasing the ability of the steel to resist wear by scratching. The harder the material, the more difficult it is for the abrasive to penetrate into the surface and make a scratch. Another important property, especially when impacts are involved, is toughness of the material. The controversy lies in the fact that in general materials with high hardness tend to have lower impact toughness [188]. Moreover, increased hardness can change the dominant wear mechanism from microploughing to microcutting and further to microcracking, which can cause more material loss [6]. Ideally, the material should have a good

combination of both of these properties, i.e., relatively high hardness and decent toughness. If the loads in the wear system are sufficient to produce work hardening, it often enhances the material's abrasive wear resistance by raising the surface hardness [188]. However, excessive hardening can also lead to brittleness, which can increase the wear rate rapidly [141].

In order to withstand impact and impact-abrasive wear, the material has to be both hard, ductile, and tough enough to accommodate the effects of impacts without catastrophic failure [94]. Adequate hardness is needed for resisting the change of dimensions due to excessive plastic deformation as well as for resisting the formation of a rougher surface. Small grain size usually enhances the toughness while the material can at the same time maintain relatively high hardness, which is probably why smaller grain size has been found to correlate with higher wear resistance [78, 175]. Steels, with various possibilities of different property combinations through the microstructures, are a versatile choice of materials for conditions requiring both hardness and ductility. However, the total usability of the material is a combination of decent cost, easiness of manufacture, weldability, and performance. The material's ability to withstand wear can also be enhanced by design, which utilizes proper understanding of the entire tribosystem and takes into consideration all the effective variables of operation and environment [189].

5. Experimental procedures

This section presents the experimental procedures by introducing the used materials and methods. First, the materials and their typical compositions are presented, including the steels, hard metals and abrasives used in the abrasive wear tests. After that the wear testing methods are presented, along with the description of parameters used in each study. Third, the characterization methods utilized in analyzing the samples are introduced.

5.1 Materials

In this thesis, several wear resistant steels, a structural steel S355, and three hard metals were studied with wear tests. This section presents the test materials, including their compositions. For steels, also typical mechanical properties are introduced. As abrasives are in an essential role in wear tests, the abrasives are presented for their mineral compositions and typical properties.

5.1.1 Wear resistant steels

Three of the four studied steels were commercial grades of different hardness (400-500 HB), and one was a laboratory grade test steel processed at the Materials Science Laboratory of the University of Oulu (650 HB). Table 3 presents the typical compositions and mechanical properties of the steels, and Figure 10 their microstructures. All steels were hot rolled and direct quenched, leading to a mostly martensitic microstructure. The commercial steels contained also a small percentage of retained austenite, while the laboratory test steel contained both retained austenite and ferrite islands.

Table 3. Typical compositions and mechanical properties of the steels studied in this work.

Material	S355	400 HB	450 HB	500 HB	650 HB
Surface hardness* HV [kg/mm ²]	162-190	387-424	468-490	493-532	657-712
Microstructure	ferritic-pearlitic	martensitic with some austenite	martensitic with some austenite	martensitic with some austenite	martensitic with 5% ferrite and 8-12 % austenite
Charpy V impact toughness [J/cm ²]	40 J, -20°C	30 J, -40°C	30J, -40°C	30 J, -40°C	7 J, 20°C
C [%]	0.12	0.25	0.26	0.3	0.468
Si [%]	0.03	0.8	0.8	0.8	0.534
Mn [%]	1.5	1.7	1.7	1.7	0.732
P [%]	0.02	0.025	0.025	0.025	0.006
S [%]	0.015	0.015	0.015	0.015	5-10 ppm
Cr [%]	-	1.5	1	1	0.215
Ni [%]	-	1	1	1	0.064
Mo [%]	-	0.5	0.5	0.5	0.027
B [%]	-	0.005	0.005	0.005	0.001
Al [%]	0.015*	-	-	-	1.65

* Typical surface hardness presents the range of macrohardness in the materials used in Publications I-V. The hardness measurement method was HBW_{2.5}, HV₃ (typically for S355) or HV₁₀. The values have been converted to HV scale for consistency.

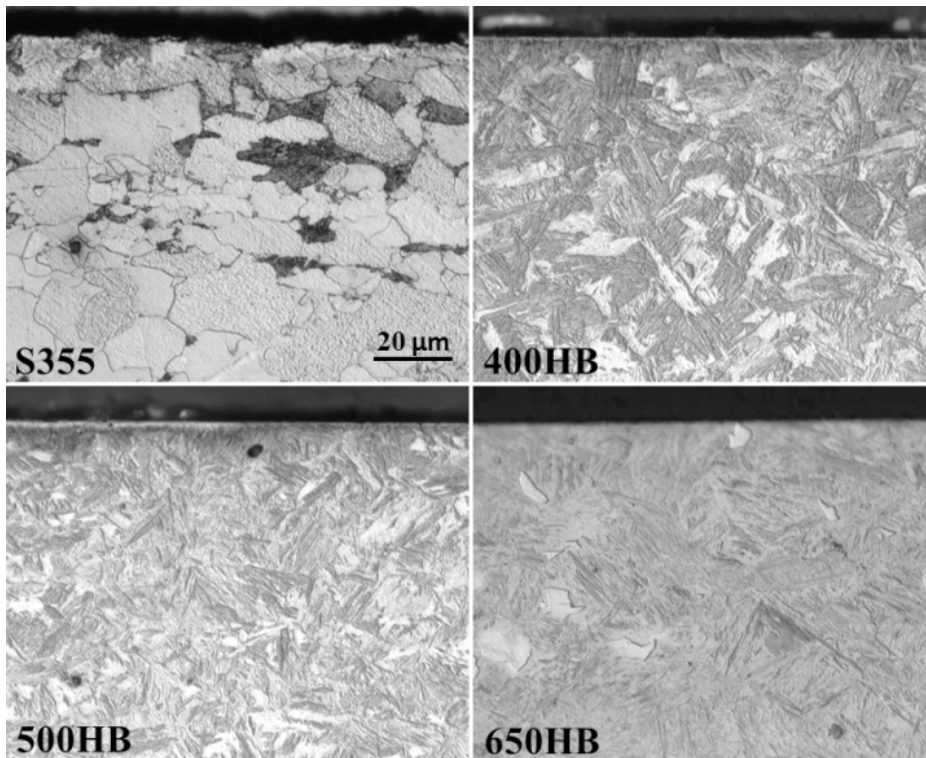


Figure 10. Microstructures of the studied steels [Publication V].

The hardness variations in the commercial wear resistant steels studied in this work were approximately 10-20 HV₁₀ [kg/mm²]. The laboratory test steel, on the other hand, showed somewhat higher hardness variations, the hardness ranging from approximately 650 to 720 HV₁₀ [kg/mm²]. This difference is originating from the laboratory rolling process: although the alloying and processing remain nominally constant, the process is not as standardized as in an automated manufacturing line, and parts of the material may have been subjected to slightly different cooling conditions, for example in the edge parts of the laboratory rolled plate compared to the middle part of the plate.

5.1.2 S355 structural steel

As noted earlier, it is difficult to determine the absolute wear performance of a material in certain conditions without a proper reference data of a material that is commonly used. Therefore, the structural steel S355 was used for comparison purposes, as it is one of the most commonly used steel grades for constructions and machines. Its mechanical properties are also standardized, some of them being shown in Table 2. The main difference between S355 and the wear resistant steels is in their strength and hardness. The strength of S355 is sufficient for many construction purposes, but heavy wear conditions set much higher demands on the materials to be used.

The structural steel used in this work was processed by hot rolling, and its microstructure is distinctly different from the rest of the studied steels. Figure 10 presents also the ferritic-pearlitic microstructure of S355.

5.1.3 Hard metals

Hard metals are composed of hard carbides as the reinforcement of the softer matrix material, such as cobalt, which binds the carbides into a composite. Hard metals are, as the name suggests, very hard and thus can be more wear resistant compared to steels [Publication IV]. However, they are more difficult to manufacture and handle because of their high hardness. Moreover, as the carbides are extremely hard, they are also brittle, although the addition of the binder material raises the overall toughness of the composite material [190]. Hard metals have a high density [191], which makes also the manufactured components quite heavy. In applications where weight is of importance, it may be reasonable to use hard metals only in parts of the machines that are subjected to the heaviest wear rather than as complete machine components. For example, a hard metal can be used as drill buttons [192]. The hard metals studied in this work and their properties are presented in Table 4. The hardness variation was approximately ±10 HV₁₀ [kg/mm²]. The average carbide size of the tested materials was 2.5 μm.

Table 4. The studied hard metals and their properties.

Material	Hardness HV ₁₀ [kg/mm ²]	Density [g/mm ³]	Composition [wt.-%]	
			WC	Co
WC-26Co	870	13.02	74	26
WC-20Co	1050	13.44	80	20
WC-15Co	1260	13.99	85	15

5.1.4 Abrasives

In abrasive wear testing, the abrasive material is in a key role. In this work, most of the testing was conducted with granite excavated from Sorila quarry. In addition, quartzite, tonalite and gneiss were used. Table 5 presents the properties of the abrasives. With natural abrasives, it must be remembered that the values can fluctuate locally quite much, and the presented properties should be regarded only as nominal values. The overall hardness values have been estimated by measuring the average hardness of each mineral phase, and based on the percentage composition of each of these phases the average hardness of the rock type was calculated. The variation in hardness within a mineral phase could be up to approximately 60 HV₁ [kg/mm²].

Table 5. Nominal abrasive properties.

Rock species	Granite	Quartzite	Tonalite	Gneiss
Quarry	Sorila, Tampere	Nilsjä, Haluna	Koskenkylä	Lakalaiva, Tampere
Density [kg/m ³]	2674	2600	2660	2747
Uniaxial compressive strength [MPa]	194	90	308	64
Hardness HV ₁ [kg/mm ²]	800	1200	960	700
Quartz content [wt%]	25	98	40	24
Abrasiveness [g/t]	1920	1840	1460	1430
Crushability [%]	34	74	18	37
Nominal minerals [%]	plagioclase (45) quartz (25) orthoclase (13) biotite (10) amphibole (5)	quartz (98) sericite hematite	quartz (40) plagioclase (40) biotite (17) amphibole (3)	plagioclase (36) biotite (25) quartz (24) orthoclase (7) amphibole (5) garnet(3)

The abrasiveness and crushability values of the rocks were determined using the LCPC test, which is described in the French standard NF P18-579. The tests were conducted at the Metso Minerals Rock Laboratory in Tampere. The LCPC test gives the LCPC abrasion coefficient (LAC) and the LCPC breakability coefficient (LBC) values. In the LCPC test, a standardized steel block with 60-75 HRB hardness (corresponding to approximately 108-136 HV) is rotated in a 500 g batch of 4-6.3 mm rock in a container for five minutes [51, 52]. After that, the abrasiveness value (LAC) is determined from the mass loss of the steel block and the crushability value (LBC) from the rock sieving results using the following equations [57]:

$$LAC = \frac{m_0 - m}{M} \quad (1)$$

$$LBC = \frac{M_{1.6} \cdot 100}{M} \quad (2)$$

where m_0 and m are the steel block's mass before and after the test, respectively. M is the mass of the abrasive (500 g, that is, 0.0005 t) and $M_{1.6}$ is the mass of the sieved <1.6 mm fraction of the abrasives after the test.

5.1.5 Sample preparation

The steel wear test samples were prepared by cutting the sample pieces from steel strips or plates by flame cutting (the actual samples were taken from a distance where the material was not affected by the heat) or water cutting. Depending on the thickness of the material, 0.5-2 mm of the test surface was machined off of all samples in order to remove any decarburized layers. The rolling direction of the steel was considered by cutting the samples lengthwise in the rolling direction for the impeller-tumbler tests. In the other test methods (i.e., crushing pin-on-disc, SIT and HT-CIAT), the rolling direction was irrelevant since the direction of loading on the samples was either perpendicular to the surface or the sample can rotate around its axis, causing the direction to change arbitrarily during the test. However, in the case of the experimental laboratory steel 650HB, the direction of the samples may vary between the samples due to the small amount of the available material.

The initial surface roughness (Ra) of the machined samples was typically 0.3-0.6 μm . Within a certain test series, all surfaces were prepared in a similar manner to ensure comparability of the results. In two test series, the surfaces were further prepared by grinding and/or polishing. In the test series for determining the edge wear of impeller-tumbler samples, a part of the samples was slightly ground for fitting purposes, the initial surface roughness (Ra) being less than 2 μm . The polished impact test samples generally had the initial surface roughness (Ra) of less than 0.1 μm .

The tests with SIT and HT-CIAT, as well as most of the impeller-tumbler tests, were conducted on samples with machined or ground surfaces. In these tests, the initial behavior was compared with the results obtained from longer tests. The tests with the crushing pin-on-disc were always conducted on samples worn for a running-in period. Moreover, the tests with uniaxial crusher and impeller-tumbler presented in Publication I were conducted on samples worn for a running-in period to make the results between the different methods more comparable.

The hard metal wear test samples were ground and not machined before wear testing. Moreover, the hard metal samples were always subjected to a running-in phase before the actual tests in the crushing pin-on-disc.

For examining the initial and deformed microstructures, cross sections are needed. In this work, the cross sections were prepared with basic metallographic procedures. The samples were cut with a sectioning machine and, if needed, mounted in hot or cold resin mount. After this, they

were ground with SiC abrasive papers and polished with 3 and 1 μm diamond paste and cloths. In the case of electron backscatter diffraction (EBSD) samples, the samples were further polished with colloidal silica of 40 nm particle size. To reveal the steel microstructures, nital was used. The etching time depended on the sample, being approximately 2-10 seconds. Nital is good for revealing the martensitic and ferritic-pearlitic structures. However, the downside is its inability to reveal austenite [193].

5.2 Wear testing

To study the abrasive and impact wear behavior of the materials introduced in section 5.1, wear tests were conducted with several different methods presented in the following section along with the parameters used in the tests. For the determination of the abrasive wear resistance of the test materials, crushing pin-on-disc and uniaxial crusher were used. The impeller-tumbler, in turn, was used as an impact-abrasive wear tester. Finally, the single impact tester and the (high-temperature) continuous impact abrasion tester were used for determining the impact behavior of materials included in this work.

5.2.1 Crushing pin-on-disc

The crushing pin-on-disc testing method [43] is based on the common pin-on-disc principle (ASTM G99 [194]), where a pin is pressed against a rotating disc. Figure 11 presents a schematic illustration of the device, and Table 6 and Table 7 show the test parameters used in this work. As opposed to the standard pin-on-disc, in the crushing pin-on-disc there is loose abrasive between the pin and the disc. The pin and the disc are not in direct contact with each other during the test, and thus the test is purely abrasive. The normal wear mechanism in the crushing pin-on-disc is three-body abrasion, but also two-body abrasion is possible if the abrasive particles become embedded in the counterpart surface. The direction of the sample is not fixed but it can rotate around its own axis freely. This causes the scratches to be in arbitrary directions on the surface of the sample. The samples were subjected to a running-in period of 15 or 20 minutes prior to the actual test.

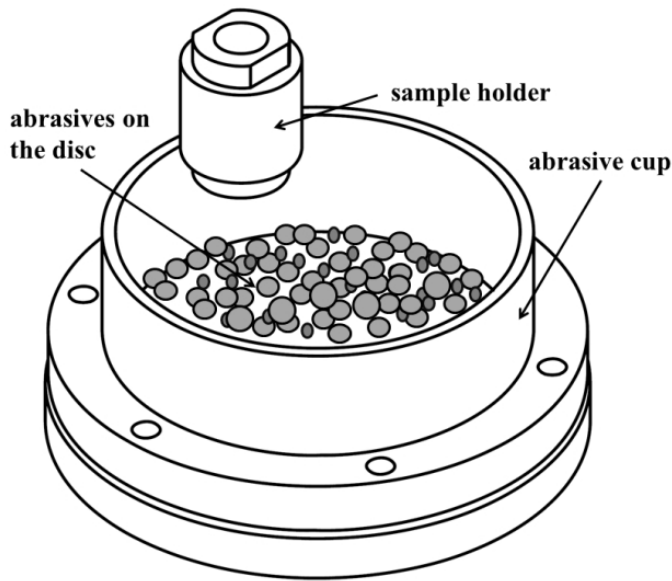


Figure 11. Schematic picture of the crushing pin-on-disc wear testing device [Publication I].

Table 6. Test parameters of the crushing pin-on-disc.

Test time	30 minutes, of which 20 minutes contact time
Sliding distance	approximately 120 m during the test
Abrasive size	2-10 mm, typically according to Table 8
Normal force	up to 500 N
Sample size	cylinder with 36 mm diameter, sample thickness 5-35 mm (wear area 1000 mm ²)
Disc size	160 mm in diameter thickness 5-15 mm
Rotating speed min ⁻¹	28±1

Table 7. Test parameters used in the test series of this work.

Parameter	Publication I	Publication IV
Contact time [min]	20	20
Abrasive size [mm]	see Table 8	2-10
Normal force [N]	200	240
Disc material	Similar material	S355 (steels) WR6 (hard metals)

The gravel between the pin and the disc is replenished by cyclically pressing the pin against the abrasive rotating with the disc for five seconds and then lifting it up for 2.5-5 seconds. The gravel is held on the disc with a collar. Because the gravel is loose in the cup, varying sizes of gravel can be used. This is important since many test devices relying on the sliding abrasion contact, such as the dry sand rubber wheel, feed the abrasive through a nozzle, which restricts

the size of the used abrasive to be rather small. This, again, does not necessarily correlate too well with the real conditions that the device is trying to simulate. In this work, all steels were tested with a specific gravel size distribution consisting of precise amounts of several narrower subsizes, as presented in Table 8. This distribution was used since it was found to cause more aggressive wear than a single size distribution [43].

Table 8. Size distribution of the gravel used in crushing pin-on-disc tests.

Size distribution	Amount
8-10 mm	50 g
6.3-8 mm	150 g
4-6.3 mm	250 g
2-4 mm	50 g
Σ	500 g

The contact type that this testing method induces on the sample is abrasive: during the pressing of the sample, it resembles momentarily gouging, after which the contact turns into a sliding motion. This sliding motion could simulate, for example, unloading of gravel from a tipper body or mineral crushing in a cone crusher. Wear is determined as a mass loss, which can be further converted to a volume loss.

5.2.2 Uniaxial crusher

The uniaxial crusher [195] is a device, which crushes gravel with high force between two surfaces by pressing them towards each other in the vertical uniaxial direction. Figure 12 presents the device and its crushing section. The device consists of a pneumatic motor, a cup to hold the abrasive, a supply tube, an abrasive reservoir and feeding system, and a tilting system. A certain amount of abrasive is taken with the feeding system from the abrasive reservoir and transported through the supply tube to the cup, where the gravel is crushed. After crushing, the cup is tilted and the used abrasive is poured away, after which it is replaced through the tube with another batch of abrasive. This way the abrasive is always fresh in each crush cycle. The crushing is done by pressing the sample downwards by the hydraulic motor.

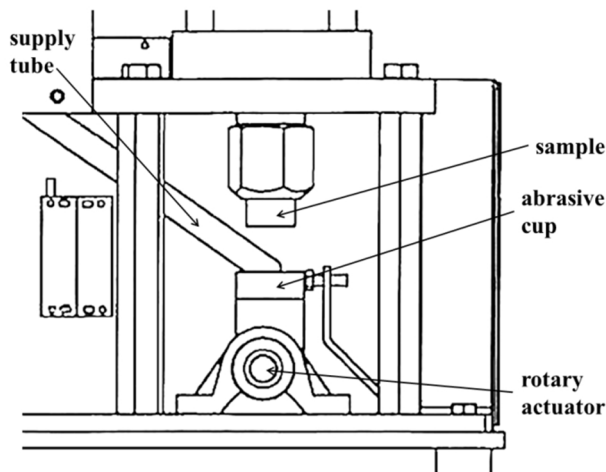


Figure 12. *The uniaxial crusher [Publication I].*

In the uniaxial crusher, the sample is subjected to gouging abrasion. There is no relative movement between the sample and the counterpart, but some short scratches can be found in the wear surface. This is because the abrasive particles are able to move short distances relative to each other as they are being crushed. This method simulates for example a cone crusher or a jaw crusher, but it also simulates the situation where a large pile of gravel is loaded on top of a material, such as in the transportation phase of the earthmoving process. The parameters used in the uniaxial crusher are presented in Table 9. The amount of wear is determined as the mass loss after every 100 crushing cycles.

Table 9. *Test parameters of the uniaxial crusher.*

Parameter	Typical range	Publication I
Sample size	Cylinder with the diameter of 36 mm (wear area 1000 mm ²), thickness 5-35 mm	36 mm cylinder, thickness 5-6 mm
Abrasive size [mm]	4-6.3 mm	4-6.3 mm
Normal force [kN]	up to 86 kN	53 kN
Test duration [cycles]	100-1000	1000

5.2.3 Impeller-tumbler

The impeller-tumbler is an impact-abrasion wear testing device, which can also be called impeller-in-drum or CIAT (continuous impact-abrasion tester). This type of device was first developed for studying the abrasiveness of ores [124], but it can naturally be used for testing metals and other materials for their wear behavior in impact-abrasive conditions.

The impeller-tumbler consists of an impeller part, where one or several samples are attached to a sample holder as impeller blades. The impeller rotates inside a drum, which is filled with gravel or other abrasives. The drum is rotating in the same direction as the impellers in order to

keep the abrasives moving and flowing. The drum is sealed with a lid to keep the gravel inside it.

Often the shafts of the impeller and the tumbler are concentric, but in the impeller-tumbler design at Tampere Wear Center the impeller and the tumbler are separate, working with separate motors and can thus be moved apart, which makes mounting of the samples easier. Figure 13 shows a schematic picture of this separate-motor type impeller-tumbler construction, and Table 10 presents the parameters of the device. Table 11 presents the specific parameter settings used in the tests included in this work.

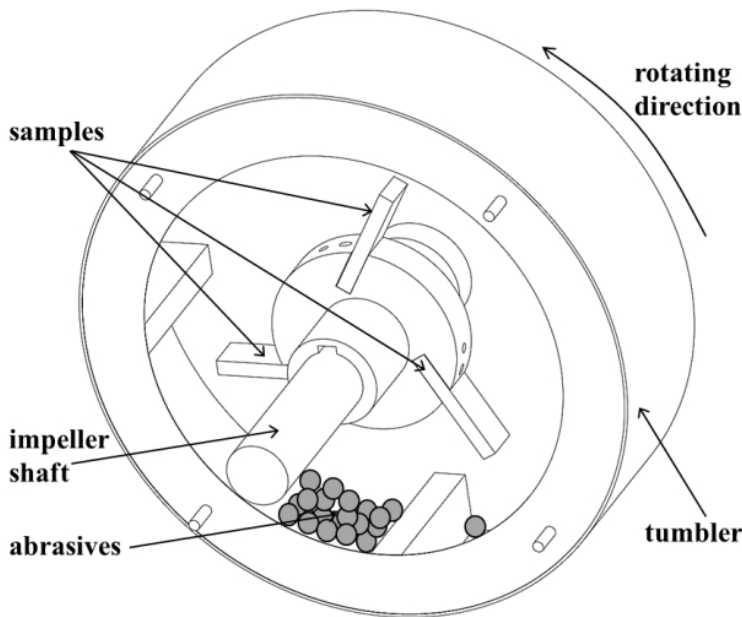


Figure 13. A schematic picture of the impeller-tumbler device [Publication III].

Table 10. Test parameters of the impeller-tumbler at Tampere Wear Center.

Sample size	75 x 25 x (4-12) mm, of which main wear area 1200 mm ²
Rotational speed of impeller	700 min ⁻¹
Rotational speed of tumbler	30 min ⁻¹
Abrasive size	8-10 mm or 10-12.5 mm
Abrasive mass	900 g/15 min
Reference material	400HB wear resistant steel
Diameter of the tumbler	350 mm
Test duration	45, 60, 270 or 360 min
Abrasive	Granite (Sorila quarry, Finland)
Sample angle	30, 60 or 90°
Impact energy	up to 70 mJ
Maximum contact speed	8 m/s (tip of the sample at 30° and 90°)
Average contact speed	7.1 m/s (30°), 6.1 m/s (60°), 6.2 m/s (90°)

Table 11. Test parameters used in the different impeller-tumbler tests included in this work.

Parameter	Publication I	Publication II	Publication III	Edge wear
Sample size [mm]	75 x 25 x 5	75 x 25 x 10	75 x 25 x 10	75 x 25 x 4-5 (68 x 18 x 4-5)
Abrasive size [mm]	10-12.5	8-10 10-12.5	8-10	10-12.5
Abrasive mass [g/15 min]	900	900	900	900
Run-in period (first 15 min excluded)	Yes	No	No	No
Test duration [min]	60	60 360	60 360	45 270
Sample angle [°]	60	60 90	60 90	30 90
Reference in fixed slot/ circulating	Fixed	Fixed	Fixed	Circulating

The amount of wear is determined as the mass loss of the sample. The test can be conducted with either one or several samples being tested simultaneously. If only one sample is used, the wear is heavier on it. This is because more gravel particles come into contact with the single sample since there are no other samples for the particles to collide with and the gravel comminutes slower. In the case of three samples, a comparison of several materials in the same conditions can be done, and the use of a reference sample is possible. This not only provides reliable comparison data for the materials but also helps in assessing the quality of the results. If natural stone is used as abrasive, it may have fluctuations in its properties, despite having been mined from the same quarry and having a quite narrow size distribution. By using a reference sample, for which a typical result is known, it is possible to detect if the used abrasive batch was somehow different from the other batches. The size distribution and shape of the abrasive particles also change as the test proceeds, which usually decreases their ability to cause wear. To minimize this effect, the abrasive is changed every 15 minutes.

In the impeller-tumbler device, there are several sample holder slots available for simultaneous testing of multiple samples. Although the slots are constructed to be identical, some small differences may exist. To minimize the effect of these differences, the samples are usually rotated in a way that each sample is in each slot for an equal time. So when the abrasive is changed every 15 minutes, also the placement of the samples in the slots is changed to ensure even wear.

The impact conditions can be changed by using different sample holders having varying sample angles. The term ‘sample angle’ is used in this case, as the abrasives move freely inside the tumbler and their exact impact angle on the surface cannot be determined. By changing the angle of the samples, the dominating impact angle can also be changed. Figure 14 presents schematic drawings of the used sample angles. The samples protrude 50 mm from the sample

holders for all materials, corresponding to a 50 x 25 mm main wear area. The average sample speeds are presented in Table 10, and they vary a little bit. For the 60° and 90° sample holders, the aim was to obtain a similar average speed. For the 30° and 90° sample holders, the aim was a similar speed at the sample tips.

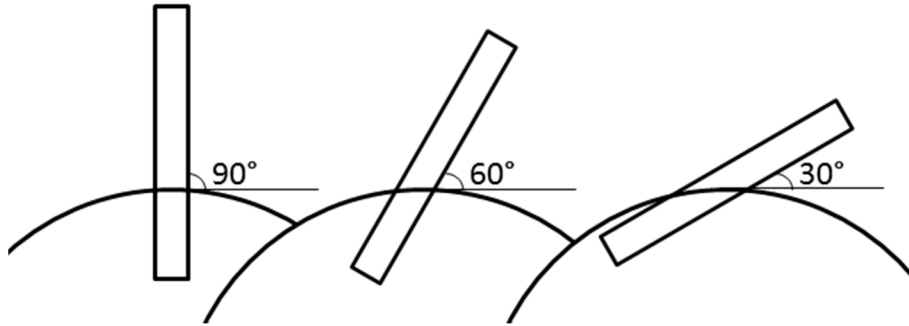


Figure 14. Schematic illustration of the used sample angles in the impeller-tumbler.

In the impeller-tumbler, the samples are subjected to both impacts and abrasion: impacting takes place when the abrasive particle first makes contact with the sample, and abrasion as the particle slides on the forward moving sample. Sundström et al. [78] determined that in their impeller-tumbler device the ratio between impact and abrasion was approximately 100/1, which would then be a rather impact-dominated system.

In the impeller-tumbler method, one characteristic factor is the concentration of wear in the edge areas. This means that the method can be used to simulate wear in different high-wear discontinuity spots, such as tail plates, bucket edges, conveyors, and naturally impactor plants. The edges of components are subject to impacts by dropping particles or shoving of the bucket into the soil, creating an impact on the material. As the particle moves further on the surface or the bucket is pushed further into the ground, the material is subjected to abrasion. In the inner part of the sample, wear resembles mostly impacting conditions, such as during loading of the tipper body or a silo. To study the magnitude of this effect, tightly fitted two-piece samples with separate inner and edge parts were prepared. This method was previously used by Terva et al. [196] for crushing pin-on-disc samples. Figure 15 presents a schematic picture of this sample type for the impeller-tumbler.

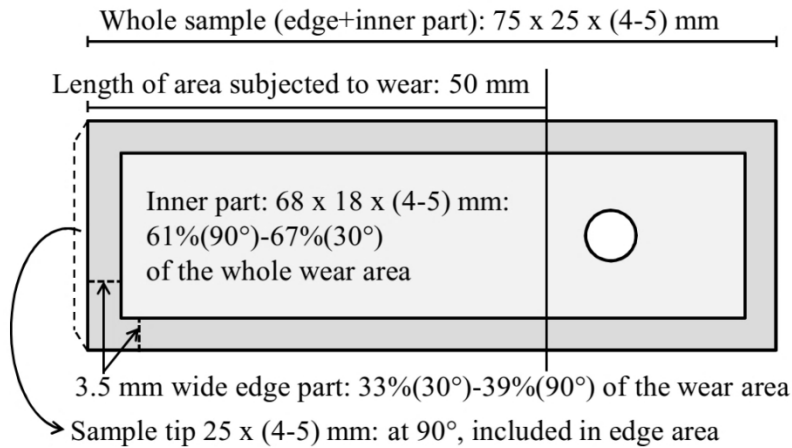


Figure 15. Schematic illustration of the impeller-tumbler sample for studying edge wear.

5.2.4 Single impact tester

The single impact tester (SIT) [127, 129, 197, 198] has been designed at AC²T research GmbH. It is designed to make single impacts on the sample by dropping a defined mass from a defined height. The impact energy can be varied by changing the impact mass and height. With different mass-height combinations it is also possible to vary the momentum of the impact. Figure 16 presents the SIT device. The device consists of a sledge, which accommodates the impacting mass, rails to guide the impact to an exact point, and the sample holder platform.

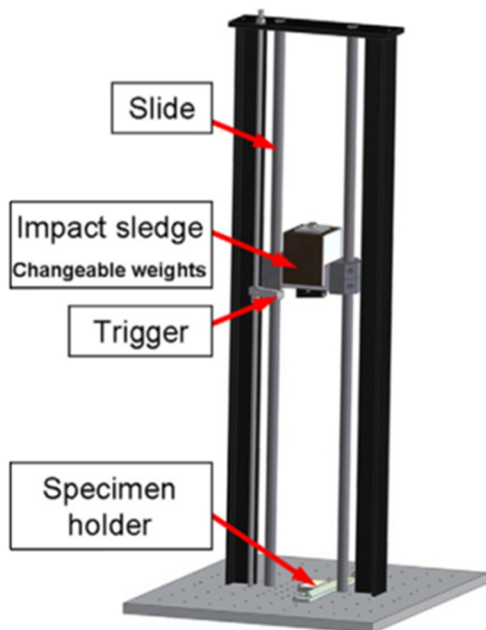


Figure 16. SIT device [198].

The SIT device enables studying of controlled impacts. The available parameter ranges and the parameters used in this work are presented in Table 12. The impact conditions can be studied by characterizing the impact marks produced using certain parameter values. Moreover, the

movement of the impact sledge can be monitored. This means that the bounce back of the impactor can be observed, which tells about the material properties, in the same manner as the Leeb hardness tester [199].

Table 12. Test parameters of SIT.

Parameter	Available range	Publication V
Impact energy [J]	1-100	1- 3
Impactor mass [kg]	0.1-10	1.5- 3.1
Dropping height [mm]	0-300	32-228
Impact momentum [Ns]	1-8	2.46-2.56
Impacting head	6/9/13 mm ball angled impactor	6 mm WC ball
Impact direction	Normal	Normal
Temperature	RT Induction heating up to 800°C	RT

The sample holder platform enables the use of samples of various sizes, as long as they can be attached to the platform. In this work, the samples had a size of 74 x 22 x 5 mm. With induction heaters, there is a possibility to conduct tests at elevated temperatures on materials that can be induction heated, i.e., on electrically conducting materials.

SIT produces impacts on the sample in the normal direction. It is a good method for determining the impact properties of materials more precisely in controlled conditions, the degree of control of the method being higher than the degree of reality.

5.2.5 High-temperature cyclic impact abrasion tester

The high-temperature impact abrasion tester (HT-CIAT) [67, 81, 102, 126–129] was also designed and used at AC²T research GmbH. The device can be used at elevated temperatures due to the chamber where the impacting section is located. In this work, however, all tests were conducted at room temperature. Figure 17 presents a picture of the device. This device subjects the sample to multiple successive impacts. The impacts are induced with an impactor, which is automatically lifted and dropped. A test can include thousands of impacts. The frequency of the impacts can also be changed.

Also in this device the impact energy can be altered by changing the mass of the impacting head and the dropping height. The impactor can be a 6-mm ball or a flat pin. Also the angle of the impact can be changed by tilting the sample: it can be either normal to the impacting direction, or at a 45° angle to it.

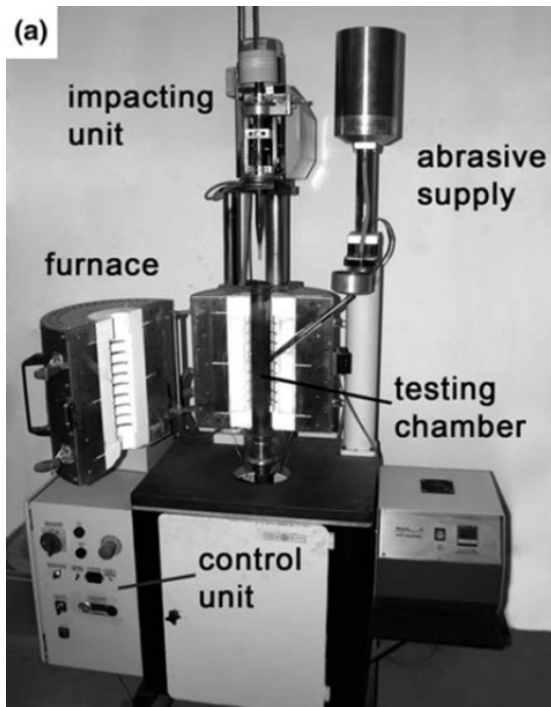


Figure 17. HT-CIAT wear testing device [129].

The device can be used to produce only impacts, as in this work, but it enables the addition of abrasives in the interface as well. The abrasive is added to the pin-sample or ball-sample interface. The flow of the abrasive is adjustable, but the most suitable size of abrasive is 0.4-0.9 mm in order the device to work smoothly. The available parameters and the parameters used in this work are listed in Table 13.

Table 13. Available and used testing parameters of the HT-CIAT device.

Parameter	Typical range	Publication V
Impact energy	0.2-0.8 J	1 J
Impacting head	Pin or 6-mm ball	6 mm WC ball
Sample angle	45° or 90°	90°
Sample size	Approximately 20 x 20 mm	20 x 22 mm
Abrasive size	0.4-0.9 mm	none
Impacting head mass	1-3 kg	3 kg
Impacting frequency	1.1-2 Hz	0.9 Hz
Operating temperature	RT-750°C	RT
Test duration	7 200 impacts	10-1000 impacts

Wear of the sample can be determined through the mass loss (especially in the case of using the abrasives), or by examining the sample microscopically. The volume loss can be determined with optical profilometry, if the actual material removal is so small that there is only little mass loss. HT-CIAT can induce impact or impact-abrasion wear on the materials. In the case of impact-abrasion, the wear process consists of two phases: first the pin or ball hits the sample,

after which it slides on the surface. This can be seen in the wear scars on the samples that have been tested with abrasives.

5.3 Characterization

Mass or volume loss measurements give insight into the scale of the wear phenomena taking place during the test, but it is essential that the reasons behind the observed behavior are recognized. In two samples with similar (numerical) amounts of wear, the wear mechanisms can be distinctly different. Depending on the scale of the active wear processes, these aspects can be examined with microscopy and mechanical testing. In the following section, the methods used in this work are briefly introduced.

5.3.1 Hardness

Hardness is an essential value to know prior to testing, as it often is the single most important property affecting the wear behavior of the material. Struers A-330 was used for macrohardness testing of the materials.

Wear induces more or less deformation on the surface, which can cause work hardening. Work hardening, on the other hand, alters the mechanical properties of the materials and thus can affect their wear performance. The degree of work hardening can be determined for example by microhardness testing. Microhardness testing is conducted with small weights, which means that it is also possible to determine the hardness of smaller volumes, such as of areas close to the surface. There are two ways of conducting hardness measurements after the wear testing: measurements on the surface, or measurements from metallographically prepared cross sections. As the wear scars often are rough, their hardness is rather difficult to measure. On the other hand, from the cross sections it is not possible to get the values from the exact surface, but the depth of the work hardening can be determined. For microhardness measurements conducted in this work, Matsuzawa microhardness tester was used. Depending on the desired resolution, weights of 10, 25 or 50 g were used. With 10 g, the measurement point is the smallest, enabling the detection of differences also in a small area. On the other hand, if the microstructure of the material is not homogeneous, the different phases can affect the results and the measurements are more susceptible to errors, making also the scatter of the results larger.

5.3.2 Microscopy

With optical microscopy, the key wear areas can be examined in more detail. Especially stereo optical microscopes are useful tools, since they enable the inspection of the area in a larger depth. In this work, Leica stereo microscope was used for the optical inspections of the wear surfaces.

Scanning electron microscope (SEM) is an essential tool for studying the wear surfaces. It has good depth-of-field and it enables the distinction between different elements. Both of these capabilities are needed as the wear surfaces are often rough and contain remnants of abrasives

or counterparts. It is important to be able to determine, which part of the surface is the original surface to see how it has behaved without mixing it with the remnants from other materials. In this work, Philips XL30 and Zeiss Ultraplus were used for examining the wear surfaces. Secondary electron (SE) images reveal better the topography of the areas, while backscatter electron (BSE) images show the difference in elements, enabling to distinguish between the abrasives and the steel in the surface. The wear surfaces were prepared for SEM by ultrasonic cleaning in ethanol and by a thin gold coating to prevent the non-conductive abrasive remnants from charging. Optical profilometry was used to study the topography of the surfaces. Veeco Wyko NT1100 was used for the surface roughness measurements, and Alicona InfiniteFocus G5 was occasionally used for observing the surfaces.

5.3.3 Microstructures

Optical microscopy was also used for examining the microstructural cross sections. Optical microscopy can be used for inspecting larger areas of the microstructure, for example, when determining the depth of microstructural changes. Nikon MA metallographic microscope was used for the cross sectional optical investigations. In some cases, also the exact size of microhardness indentations was determined with this method.

The smaller details in the microstructure were examined with SEM. Philips XL30 scanning electron microscope was used for investigating the microstructures. For the parts of microstructural investigations conducted at University of Oulu, also Zeiss Ultra Plus field emission gun scanning electron microscope was used.

As wear alters the material on the surface and possibly causes changes in its microstructure, it is interesting to map these changes by determining the orientations of the microstructure and their changes. This can be done with EBSD, where information of the crystal orientations is gathered into a map. HKL Premium-F Channel EBSD system with ultrafast Nordlys F400 detector attached to Zeiss Ultraplus ultra high resolution field emission SEM was used as the measurement system.

5.3.4 Residual stresses

There are always stresses inside the material, due to the manufacture, machining of the surface, and naturally due to the loads that the material is subjected to. It is known that compressive stresses increase the wear resistance of materials, and Garbar [200] has even found a better correlation of wear resistance with compressive residual stresses than with hardness. Moreover, the full width at half maximum (FWHM) values of the X-ray diffraction peaks can indicate changes in the material. In this work, the residual stresses and FWHM values were determined with Xstress 3000 using CrK α -radiation with 1 mm collimator at 30 kV acceleration voltage.

6. Results and discussion

In the following three subsections, the results of this work are summarized, analyzed and discussed. The first subsection presents the effects of test parameters on the impeller-tumbler wear tests and analyzes the tests as a complete tribosystem. The second subsection presents the effects of abrasive type and counterpart on abrasive wear. The last subsection summarizes and discusses the behavior of materials in impact and abrasion wear testing conditions.

6.1 Effect of test parameters on the impact-abrasion tests with impeller-tumbler

This section presents the results and discussion of the effects of various parameters on impact-abrasion wear testing of steels. First the procedures and use of a reference material are discussed, followed by observations on the effects of sample angle, test duration, and changes in the sample geometry in the course of testing. In the end of the section, a summary of the benefits and disadvantages of the impeller-tumbler type wear tester are presented.

6.1.1 Role of the reference sample [Publications I-III]

The use of a reference material in the wear tests conducted with natural abrasives is important for ensuring the reliability of the test results. Ideally, assuming that all other test parameters remain the same, the use of a reference sample enables detection of the possible differences in the abrasive batches used in the tests. Another important function of the reference sample is to serve as a monitor of the condition and proper functioning of the test equipment [99]. The reference material should be selected such that its properties and, in particular, wear behavior are well known in the test method in question. The microstructure of the reference material should also be relatively homogeneous to produce predictable and consistent wear behavior. In the current tests, 400HB wear resistant steel was chosen as the reference material due to its sufficient hardness but still non-brittle, i.e., ductile wear behavior.

The reference material data can be used in two different ways: to exclude tests with evident anomalies from the results, or as reference data to which the results of the actual test samples are directly compared. The latter is usually done by calculating the mass loss of the sample in relation to the mass loss of the reference sample (in this work referred to as ‘relative mass loss’) [Publications I-III]. In impeller-tumbler, the use of the direct comparison method requires understanding of the entire system and its interdependencies. The interdependence between the samples can be demonstrated for example by the effect of different geometries of the samples included in the test. If, for example, one sample in an impeller-tumbler test is slightly shorter than the other ones, the other samples will be exposed to a higher amount of impacts, which is seen not only as a lower mass loss of the shorter sample but also as a higher mass loss of the other samples. An interdependence such as this could become an important issue when using the direct comparison method, because the calculated weight loss ratios will be skewed in one way

or another. This, again, emphasizes the importance of careful preparation of all samples despite the seemingly robust nature of the impeller-tumbler test method. Also the location of the samples relative to each other can be important, which will be discussed in more details in section 6.1.2.

Figure 18 presents two examples of the use of a reference sample in impeller-tumbler tests, where the specimens were weighed and the abrasive replaced with a new batch every 15 minutes. The reference mass losses are shown with a solid line, while the results of the two actual samples in the tests are shown with dotted lines. In general, the mass losses of the samples and the reference follow quite similar up and down trends in the 15 minute intervals, indicating that there are some evident differences between the individual abrasive batches, some causing less and some more wear than an ‘average’ batch.

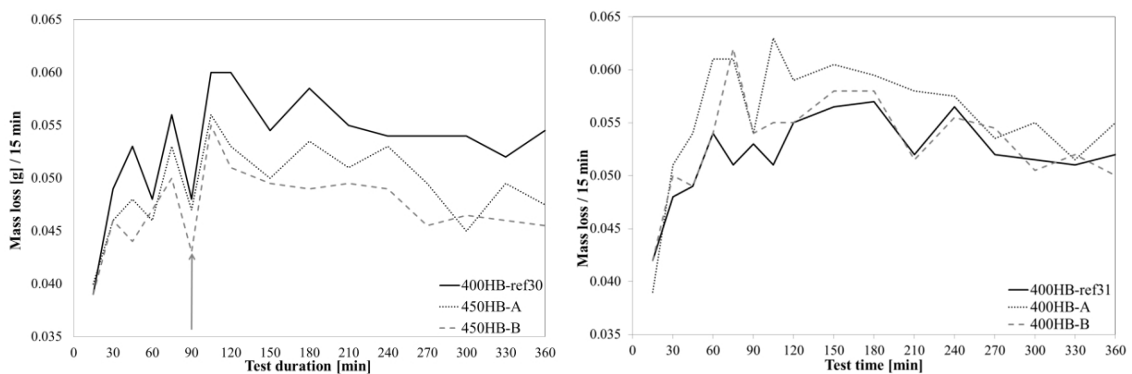


Figure 18. Mass loss results from two impeller-tumbler wear tests with a reference sample (black line) and two actual samples. The sample angle in the tests was 60° . The arrow points to the similar trends between the samples. The tests were conducted with granite abrasive.

The difference between the abrasive batches is not the only thing affecting the fluctuations in the mass loss between the measurement intervals. For example, uneven material removal from the sample can happen because of prolonged material build-up by plastic deformation and the following sudden detachment of larger chunks of material. Also sample slot position, sample geometry changes through rounding of the edges, sudden burr removal, and abrasive embedment into the wear surface can lead to notable variations in the observed wear rate.

Figure 19 presents both the mass loss and relative mass loss results for S355, 400HB and 500HB steels tested with two different abrasive size distributions to demonstrate how the relative mass loss works. It can be seen that the relative mass loss (columns) for each material depends on the conditions. Thus, the direct comparison of the sample mass loss with the reference sample does not reveal the exact (absolute) difference between the tested materials but is limited to the conditions of the tests in question. However, when assessing the conditions of the impeller-tumbler test and the used abrasive batch, the use of a reference sample is almost mandatory, especially if the wear behavior of the material to be tested or the properties and behavior of the abrasive to be used are yet unknown. Overall, the relative wear is more of a tool to determine how the different conditions affect the relative performance of the studied materials.

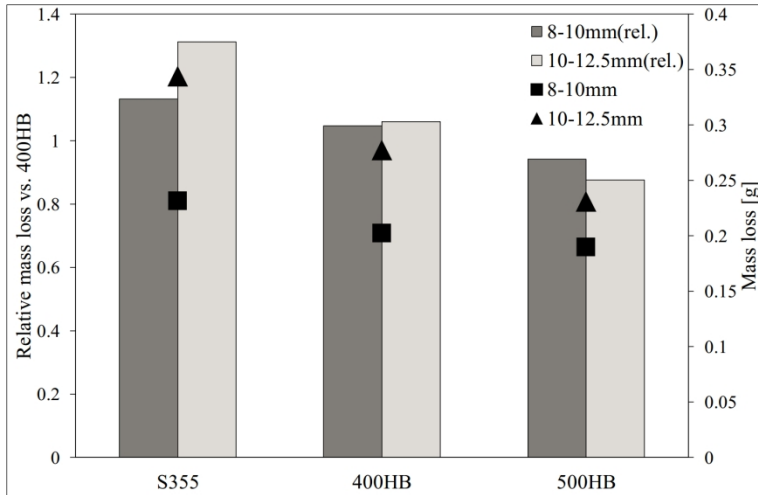


Figure 19. Relative (columns) and absolute mass loss results (points) of impeller-tumbler samples tested with 8-10 mm and 10-12.5 mm granite abrasives for 60 minutes at 60° sample angle.

In this work, the direct comparison method with a reference sample has been used to enable comparison of the wear test results obtained by several different testing methods [Publication I] and to facilitate the determination of the effects of different sample angles in the impact-abrasion tests [Publications II-III].

6.1.2 Test procedure for three simultaneously tested samples

The impeller-tumbler device used in this work enables three samples to be tested simultaneously, as is the case also in some other similar type devices presented in the literature [68, 69, 78]. The use of three samples gives the possibility to include a reference sample in every test and also to test two samples simultaneously in the same conditions. However, the tribosystem becomes a bit more complex with multiple samples, as the samples affect the wear of the other samples, as discussed earlier in 6.1.1.

Use of three samples in a test means that the samples are attached in three separate sample slots, which can have some minor differences between them, affecting the results. To minimize the effect of the possible slot differences, samples must be tested in each slot for an equivalent amount of time. The sample circulation can be done using two different procedures:

- The reference sample is kept in a fixed slot and the two actual samples alternate between the two other slots: this procedure enables determination of the differences between abrasive batches, since the conditions of the reference sample remain the same in all test intervals. On the downside, there is a small difference originating from the different slots used for the reference sample and the actual samples. This procedure has been used in the publications of this work [Publications I-III].
- The reference sample and the actual samples circulate in all slots: this procedure evens out the conditions for all samples during the test, including the reference sample. In this way, comparison between the materials, including the reference, is more straightforward. The relative order of the samples remains the same during the test,

which means that the effects of possible sample disparity on the wear of the other samples are more concentrated on the trailing sample. This procedure has been used in the edge wear tests of this work.

6.1.3 Effects of particle size and size distribution [Publication II]

Badisch et al. [68] concluded that in general higher impact energy of the particles leads to higher wear in an impeller-tumbler test. However, they also reported that if the increase in the impact energy led to the breakage of the particles, it could in some cases also lower the wear rate. As the behavior of Sorila granite used in the tests of this work was not previously studied in impeller-tumbler conditions, a comparison of the mass losses caused by two different granite particle sizes was conducted.

Figure 19 presents the impeller-tumbler results for S355, 400HB and 500HB steels with two size distributions (8-10 mm and 10-12.5 mm) of granite abrasive. Figure 20 presents the mass loss results for the 400HB steel with the same two abrasive sizes together with the results from the tests with a predetermined number of particles to observe the role of particle count.

The mass of the abrasives was 900 g in both cases, making only the size and number of the particles vary in the tests. The smaller size abrasive batch contained 750-800 particles, while the larger size batch contained only 400-450 particles. Thus even if the particle size difference is seemingly small, the difference in the mass and impact energy of the individual particles can be considerable.

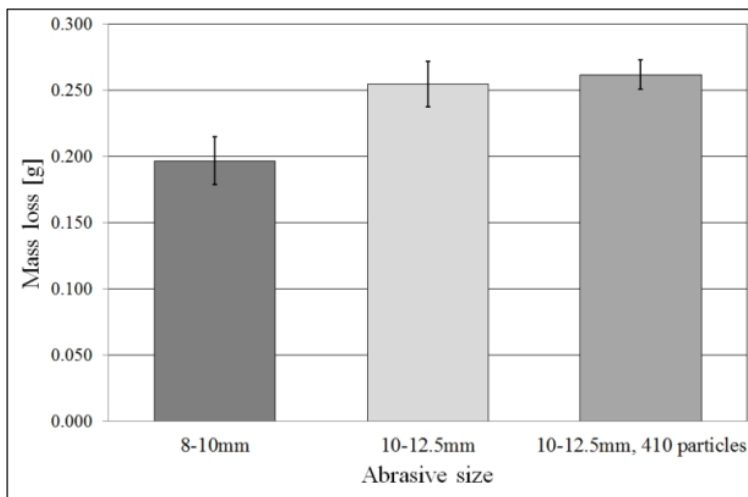


Figure 20. Mass loss results for the 400HB impeller-tumbler reference samples with 8-10 mm and 10-12.5 mm granite abrasives tested at a 60° sample angle for 60 minutes [Publication II].

The results in Figure 19 and 20 show that the abrasive size has a clear effect on the amount of wear, 10-12.5 mm particles causing approximately 30% more mass loss in the 400HB steel than the 8-10 mm particles. The harsher conditions induced by the larger particles are also indicated by the slightly higher Rq surface roughness values of the samples worn with larger abrasives.

When comparing the standard deviations between the tests conducted with 400-450 particles and exactly 410 particles, the observed deviations were 7% and 4%, respectively. Moreover, the results of six out of the eight tests conducted with 410 particles fit within a standard deviation of 1% [Publication II], which can be considered a very good result. Thus, in addition to demonstrating the effect of abrasive size, the results suggest that the width of the size distribution affects the observed scatter in the results.

6.1.4 Effect of impact angle on impact-abrasion with relatively large particles [Publications II-III]

The impact angle is known to cause a difference in the wear behavior in both erosion and impact-abrasion, but many of the published studies on its effect have been conducted with sub-millimeter size particles or at high speeds [66, 201–205], which do not correlate with all real conditions. For impeller-tumbler tests, the sample angle is often not reported [68, 69, 78], or the comparison remains rather limited [206].

In impeller-tumbler tests, changing of the contact angle is possible by using sample holders that place the samples at different angles [Publications II-III]. This angle is called the ‘sample angle’ to avoid the misinterpretation of it being equal to the exact impact angle: while a large part of the abrasives impact the sample approximately at the designated angle, the abrasives move freely inside the tumbler and have interactions with each other, changing their path of flight and thus the impact angle on the sample. For these tests, the 60° and 90° sample angles were chosen since the hitting angle of dropped gravel on a horizontally placed platform is likely to be closer to 60-90° than to lower angles.

In the impeller-tumbler tribosystem, the change of the sample holder leads to the change of several parameters at the same time. Thus it is not possible to compare the mass losses caused by the different sample angles directly. The results are presented as relative wear, showing how the different conditions affect the relative performance of the materials. The parameters changing with the sample holder are:

- Sample angle: the angle at which the sample is tangentially positioned in relation to the rotational axis (see Figure 14).
- Average speed of the sample: with larger sample angles, the sample extends to a wider range of rotational speeds (see Table 10). Thus, it is not possible to keep both the sample tip speed and the average speed similar for the different sample angles.
- Movement of the abrasives inside the tumbler: samples at higher sample angles interfere more with the movement of the abrasives inside the tumbler due to their longer radial extension in comparison with the smaller sample angle samples (see Figure 14)
- Active wear areas: the impeller-tumbler samples wear mainly on the largest surface facing the impacts, and the contacts on the other areas (sample sides, tip area and reverse side) are much fewer. However, positioning of the samples at a different angle can alter the susceptibility of the different areas to impacts.

Figure 21 presents the relative mass losses of S355 and three wear resistant steels with approximately 395-712 HV₁₀ [kg/mm²] hardness at 60° and 90° sample angles for two test

durations. Comparison of the 60° and 90° results reveals that the 90° results are typically slightly higher for both softer and harder materials. Overall, the difference in the results between the sample angles in the present tests was small, only of the order of a few percent, when also the scatter of the method is in the similar range.

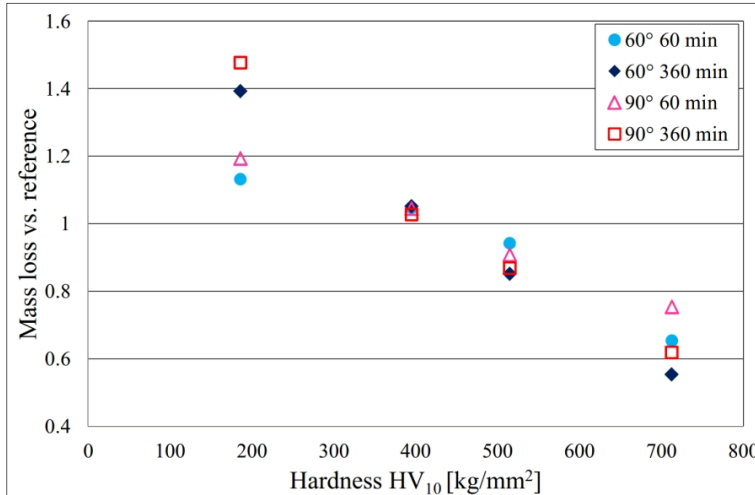


Figure 21. Relative mass loss results for impeller-tumbler samples tested at 60° and 90° sample angles with test durations of 60 and 360 minutes, using the 8-10 mm granite abrasive particle size [Publication III].

The 60° and 90° sample angles produce only slightly different main wear surfaces. In the sample tip, however, the wear surfaces of the 60° and 90° samples are markedly different, as shown in Figure 22. In the 60° sample, the tip has only quite few impact marks, while the 90° sample is severely scratched throughout the area. The 90° sample has an additional wear area in the sample tip, where the conditions are distinctly different from those of the main wear area. On the 90° sample tip, the abrasives move mostly by a sliding motion, whereas the main wear area is mostly subjected to impacting contacts. The conditions in the 90° sample tip area may emphasize more the scratch resistance of the material, and thus may explain the relatively higher wear of both the softest S355 and the hardest 650HB samples, i.e., S355 is too soft to resist the scratching and 650HB has less ductility and is therefore more susceptible to efficient material removal by cutting than the other wear resistant steels.

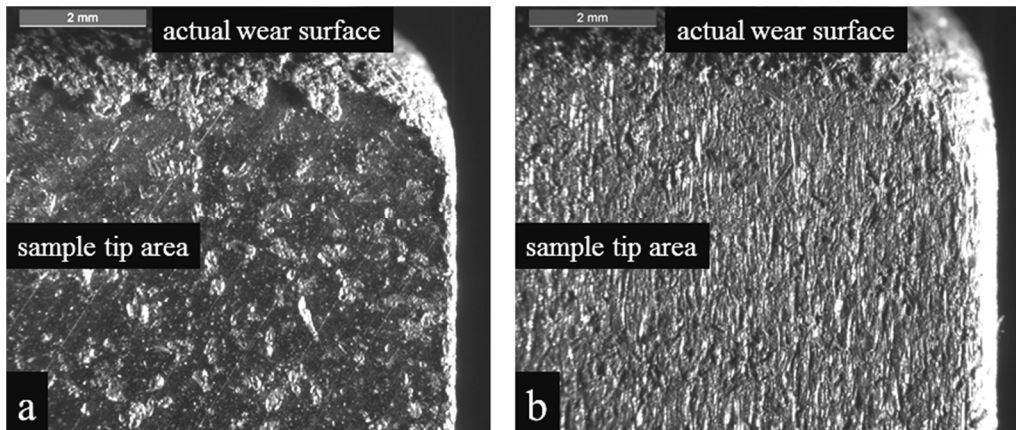


Figure 22. Tip areas of 400HB impeller-tumbler samples tested for 360 minutes at a) 60° and b) 90° sample angles [Publication III].

6.1.5 Effects of test duration [Publications II-III]

Wear leading to failure can be a rather long process. In wear testing, the wear process is usually considerably accelerated, preferably in a manner that keeps the wear mechanisms and wear phenomena as similar as possible with those in the intended real application. The duration of the test, however, can affect the test results through a change in the conditions and the wear mechanisms:

- **Sample geometry:** the dimensions of the sample may be affected by the wear test, changing the active wear area. Moreover, in the case of edge rounding, the local impact angles in the rounded edges become different from the original ones.
- **Change of surface:** the worn surface interacts differently with the abrasives than the original surface, which is why the running-in periods are sometimes used in wear testing to reach the steady-state wear phase. The surface properties can change during the test as a result of embedded abrasives, increasing surface roughness, work hardening rate, etc.
- **Degradation of abrasive:** if the test is conducted with a batch of degrading abrasive, the wear is higher with fresh abrasives than with the already rounded or smaller, broken abrasives in the later stages of the test. The problem of decreasing wear during the test can be remedied to some extent by changing the abrasives at certain time intervals so that the wear remains at a high level throughout the test.

For an impeller-tumbler wear test, a typical test duration is one hour or less [68, 78, 84, 86, 91, 104, 127, 135], but also tests with the duration of five [69, 85] and six [Publication II-III] hours have been used. To observe how the mass loss of the steel samples progresses during the test, Figure 23 presents the mass losses of the studied steels for every 15 minute period in a 360 minute impeller-tumbler test. Generally the wear increases markedly after the first 15 minute period up to about 60 minutes of total testing time. In the very beginning of the test, the break-in takes place: the intact surface of the sample is scratched and indented, some abrasives are embedded into the surface, and the sample geometry becomes more rounded. Some fluctuations between the 15 minute intervals still remain throughout the test due to the differences in the

sample slots, abrasive batches, and removal of burrs, as discussed in 6.1.1. For the wear resistant steels, the wear rate slightly decreases towards the end of the 360 minute test. A similar result was reported by Wilson and Hawk [69], according to whom the wear rate during the first hour exceeded the steady state wear rate obtained from a five hour impeller-tumbler test on average by 14%.

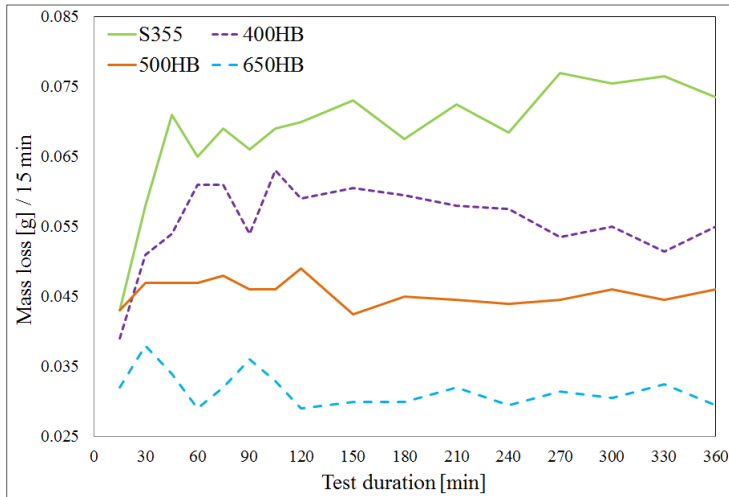


Figure 23. Mass loss results for every 15 minute period during 360 minute impeller-tumbler tests with 60° sample angle. The tests were conducted with granite abrasive.

The relative wear performance of materials may differ in short and long term exposures, as shown in Figure 21. To view how the relative wear performance of the studied steels develops with the test duration, Figure 24 presents their impeller-tumbler results for 360 minute tests. In this graph, the total mass loss of the sample has been normalized by the total mass loss of the reference sample at each measurement point. After the first 60 minutes, the relative mass losses generally begin to stabilize on a certain level, but the differences between the materials tend to grow as the test progresses. Moreover, it appears that the most reliable results concerning steady state wear can be obtained from the data between 120 and 360 minutes.

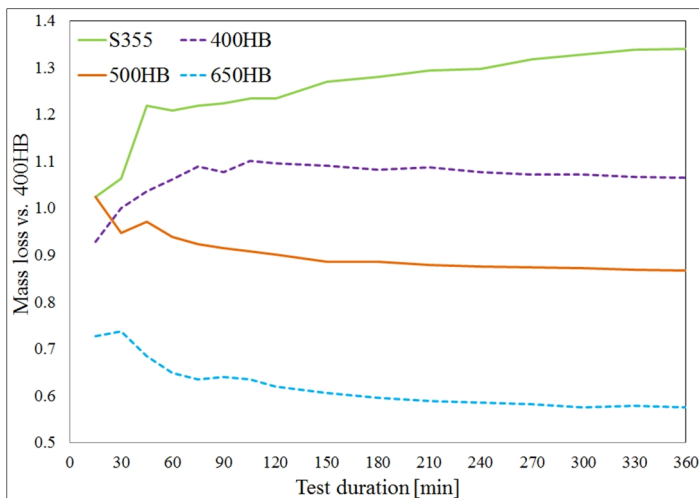


Figure 24. Progress of the relative mass loss during 360 minute impeller-tumbler tests at 60° sample angle with granite abrasive.

Figure 25 presents the main wear surfaces of 400HB samples tested for 60 and 360 minutes. The surfaces of both samples look surprisingly similar, but in a closer look the sample tested for a longer duration appears slightly more heavily worn in comparison to the 60 minute sample, although this observation is not always evident. The 400HB wear surface tested for a longer time has larger formations on its surface, as seen in the leftmost images of Figure 25. It also has larger amount of debris, which can be seen in the 3D optical profilometer images, and slightly higher surface roughness values [Publication III]. The wear mechanism itself does not seem to have been drastically changed between the 60 and 360 minutes of testing. In both cases, removal of the material is occurring due to surface fatigue by repeating impacting of the particles and occasional cutting and ploughing of the abrasives sliding on the surface.

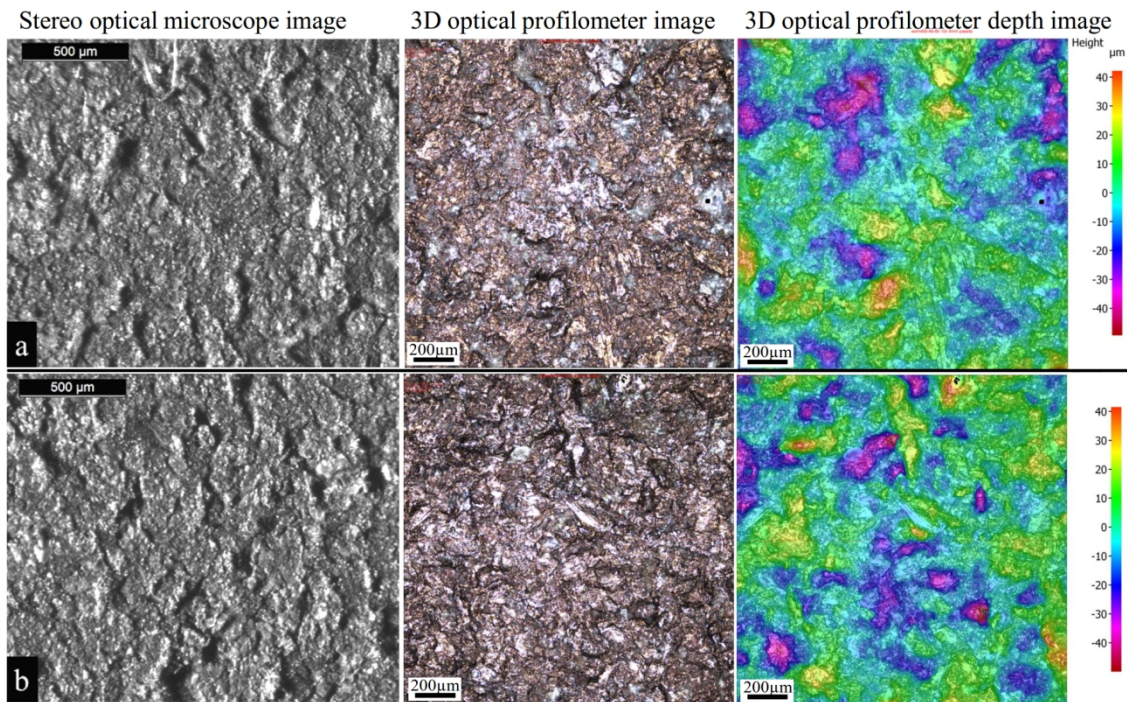


Figure 25. Wear surfaces of the 400HB steel tested at 90° angle for a) 60 minutes and b) 360 minutes in stereo optical and 3D optical profilometer images [partly Publication III]. Note the different scale bars.

6.1.6 Wear of the edges and inner parts of the samples [unpublished]

Impeller-tumbler is a wear testing method where wear takes place mainly in the edges of the samples, which in general manifests itself as rounding of the specimens [Publications II-III] [69, 136]. Nevertheless, the exact role of the edge wear for this test method has not been determined in the published literature. To study this effect, closely fitted two-piece samples with separate edge and inner parts were manufactured (see Figure 15). After the initial weighing done separately for both parts, the sample was tested so that the parts were put together, making the combined sample a normal-size impeller-tumbler sample. After the test, the pieces were taken apart and measured separately again to determine the edge and inner part wear. The sample angles were chosen to represent on one hand the extreme situation of 90°, and on the other hand

a very different situation at the other end of the sample angle range, i.e., 30°, as smaller angles are commonly known to be more severe for ductile materials than the high angles.

The share of the edge part mass loss of the total mass loss of the combined sample was approximately 82% for the 30° samples and 94% for the 90° samples in a 45 minute test. The percentages were similar for both the S355 structural steel and the 400HB wear resistant steel. In a 270 minute test conducted on the 400HB steel, the edge wear percentages of the total mass losses were 66% and 82% for the 30° and 90° sample angles, respectively. This means that the dominance of the edge wear was not as high in longer exposures as it was in the shorter tests. The lower edge concentration of wear in the longer tests could be expected, as the samples undergo the largest changes in their geometry in the beginning of the tests. However, considering that the edge part area is only 33-39% of the whole wear area, the dominance of the mass loss happening in the edge part of the sample is evident in both short and long tests. For the 90° wear samples, also the area of the tip was included in the calculations, as it was found to wear severely at this sample angle in [Publication III].

Table 14 presents the wear rates (mass loss per area per time) of the short tests for S355 and 400HB steels at both selected sample angles. The table also presents the ratio between the edge and inner part wear rates, showing how much more severe the wear rate in the edges is compared with the wear rate in the planar area of the inner part of the sample. The two applied sample angles also result in a significant difference in the edge wear ratio: the samples tested at 90° show much more edge wear in comparison to the inner part wear. However, also at 30° the dominance of edge wear is marked, as the edge wear rate is 9-11 times as high as the inner part wear rate. Thus it can be concluded that even at smaller angles the impeller-tumbler wear testing method is very edge concentrated.

Table 14. Wear rates of the full sample and the edge and inner parts separately for S355 and 400HB at 30° and 90° sample angles in 45 minute tests. The edge/inner rate represents the average of the ratio in each individual sample.

Material and sample angle	Full sample wear rate [g/m ² ·h]	Edge part [g/m ² ·h]	Inner part [g/m ² ·h]	Edge/inner rate
S355 / 30°	380±40	940±160	100±30	11±6
400HB / 30°	290±20	710±40	80±20	9±2
S355 / 90°	280±20	660±40	30±10	20±5
400HB / 90°	260±4	640±10	20±4	31±6

If the test is continued for a longer duration, as presented in Table 15, the wear rate of the edge part is reduced while the wear rate of the inner part is increased. The decrease of edge wear rate is explained by the changes in the sample geometry and easier particle flow on the sample as the edges become severely rounded during the test. The increase in the wear rate of the inner part, in turn, is probably due to a change in the surface properties of the sample during the wear process. In [Publication III] the planar surface in the middle of the sample was found to wear largely by plastic deformation, which will result in material removal by the subsequent impacts.

At the later stages, the surface is more deformed and therefore more susceptible to material removal.

Table 15. Wear rates of the 400HB steel at 30° and 90° sample angles in 270 minute tests.

Material	Full sample wear rate [g/m²·h]	Edge part [g/m²·h]	Inner part [g/m²·h]	Edge/inner rate
400HB / 30°	310	620	160	4
400HB / 90°	230	500	70	7

Although the two parts of the sample were very closely fitted, in most of the cases the two pieces did not remain perfectly aligned throughout the entire test. The nonalignment led some edge areas of the inner parts to become exposed to wear and, on the other hand, especially in the longer tests, some edge part areas could have become covered by the deformed material of the inner part. The aforementioned nonalignment issues are likely to lead to slightly higher wear of the inner part and lower wear of the edge part compared to the ideal situation of alignment. However, it can be safely stated that the edge effect is a major factor in the impeller-tumbler wear testing method at least to an extent shown in Table 14 and Table 15, and probably even more so. Removing and separating of the inner and edge parts of the samples could also remove some chips from the interface area, although special attention was paid to keep the samples as intact as possible. The chip removal during sample measurements can, however, be one reason for the relatively large standard deviations of the results shown in Table 14. Nevertheless, the trends discussed above are very clear.

If the differences in the conditions between the inner and edge parts are analyzed further, it can be observed that the positioning of the sample parts creates a situation where the average impact speed of the particles is higher for the edge part. The difference in the speed of the inner and edge parts is in the range of a few percent (3-6%), but its effect is more difficult to determine since the inner and edge parts of the material undergo varying amounts of impacts.

The current results clearly reveal the extent of edge concentration of wear in the impeller-tumbler wear testing method applied in this study. For determining more closely the differences in the wear between the inner and edge parts in a situation where both parts would be exposed to similar conditions, a couple of alterations to the testing could be made. The use of a sample where the tip part is shielded and only the sides are exposed to wear would enable the same speeds equally for the inner and edge parts. Moreover, in this specific case, the use of only one sample could be beneficial for exposing the inner part more to impacts as well.

6.1.7 Summary of the characteristics of the impeller-tumbler wear tester

Wear tests are always a compromise between controllability and aspiration for the simulation of the real conditions. The impeller-tumbler has some special characteristics as a wear testing method. Many of the factors cannot be deemed purely beneficial or disadvantageous, but they cause certain restrictions or create certain possibilities. Despite the robust appearance of the test, careful controlling of the parameters and samples is imperative in order to obtain reliable

results, especially if the differences between the materials to be characterized are small. In the following, factors characteristic for the impeller-tumbler in the testing of steels are listed regarding the general usability of the device and the overall notions of the testing method.

Usability:

- Easily changed parameters: parameters such as sample angle, rotational speeds and abrasives can be varied easily. Both natural and industrial abrasives of various sizes and size distributions can be used, since the abrasives are loose in the test.
- Abrasive usage: requires rather large amounts (several kilograms) of abrasives in longer tests to maintain the wear at a high level, if the abrasives are degrading during the test.
- Duration of the tests: if very good results are wanted, a test with two samples and a reference will take 180 minutes or longer, excluding the change of abrasives, sample attachment and mass loss measurements.
- Active operating time during testing: the abrasive may have to be replaced every 15 minutes in order to keep the conditions harsh, if the abrasive's ability to produce wear decreases during the test.
- Operational hazards: like many wear testers, the noise and dust levels are high and personal protective equipment is needed when conducting the tests.
- A relatively care-free test method: the device does not have to be monitored all the time.

Impeller-tumbler as a test method:

- Popularity: for a non-standard test, impeller-tumbler (also known as impeller-in-drum and continuous impact-abrasion tester) is rather widespread.
- Consistency and scatter: carefully conducted impeller-tumbler tests produce fairly consistent results. In the current work, the standard deviation was 3-9% [Publications I-III]. Wilson and Hawk [69] reported a typical variance to be less than 10% for duplicate samples.
- Comparability of results: three slots enable including a reference material in all tests and testing of two materials in the same impact-abrasive conditions. The use of reference samples in tests with natural abrasives aids in determining the reliability of the results.
- Consistency of conditions inside the tribosystem: Speed of impact varies across the wear surface and the wear areas of the samples are worn at different contact speeds depending on their distance from the rotational axis, which must be considered when making microscopic investigations.
- Edge concentrated wear: the test method is extremely edge concentrated, which must be considered when using it for determining the wear properties for certain applications.
- Sensitivity to parameter variations: for example, even a relatively small change in the abrasive particle size can bring out of material properties differently, which suggests that especially in the testing for critical applications the parameters have to be monitored very closely.

- Sample geometry: the whole end of the sample without shielding exposed to wear leads to changes in the sample geometry during the test and makes the method more time-dependent.
- Test duration: shorter tests are easier and cheaper to conduct, but they are more susceptible to, for example, sudden burr removal affecting the mass loss, whereas the longer tests describe better the steady-state wear of the material in such conditions. Moreover, unexpected long-term phenomena or changes in the material behavior cannot necessarily be foreseen in shorter tests.
- Interdependence of parameters: the conditions in impeller-tumbler are rather susceptible to changes in the other parameters. For example, a change in the sample angle also affects the contact speed range and the wear area. The 90° test angle samples have two distinctly different wear areas: a main wear area exposed to impacts and a cutting wear area in the tip of the sample.

6.2 Effects of counterpart and abrasive type on the high-stress abrasive wear

The following section presents the results and discusses and summarizes the main findings of the wear tests conducted in three-body abrasive conditions using the crushing pin-on-disc method. In this section, the effects of the counterpart and abrasive type are discussed in more details.

6.2.1 Indirect counterpart [Publications I,IV]

The effect of the counterpart on abrasive wear can be substantial, since the properties of the counterpart affect the tribosystem dynamics. Axén et al. [58] reported that a softer counterpart can embed the abrasives partially and thus cause more aggressive wear through two-body abrasion on the harder sample. However, the specimen surface and the counterpart are usually able to become into contact with each other during the test, which adds the question of how the contacts between the surfaces affect the situation, as opposed to the interactions taking place only through the abrasives. In the following, the situation where the counterparts are not in contact with each other, i.e., indirect counterparts, is discussed.

Figure 26 presents the crushing pin-on-disc mass loss results for the S355, 400HB and 500HB steels tested with S355 counterparts and with counterparts similar to the sample, which lead to different pin/disc hardness ratios. When comparing wear systems with steel as the material of both the sample and the counterpart, the hardness ratio is perhaps the simplest number to be used for the evaluation of the degree of difference between the materials. The ratio is close to unity when the counterpart and the sample are of the same or a similar material, and higher for the harder pins.

Figure 26 shows that the mass losses are slightly higher for the samples tested with the softer S355 counterpart than for the samples tested with a similar counterpart. In other words, the mass

losses with higher pin/disc hardness ratios are relatively larger, which agrees with the results of Terva et al. [43]. A part of the S355 counterpart tests was conducted with a higher force (240 N). In these tests, the mass loss is significantly higher due to the higher load [31], but probably also at least to some extent due to the softer counterpart.

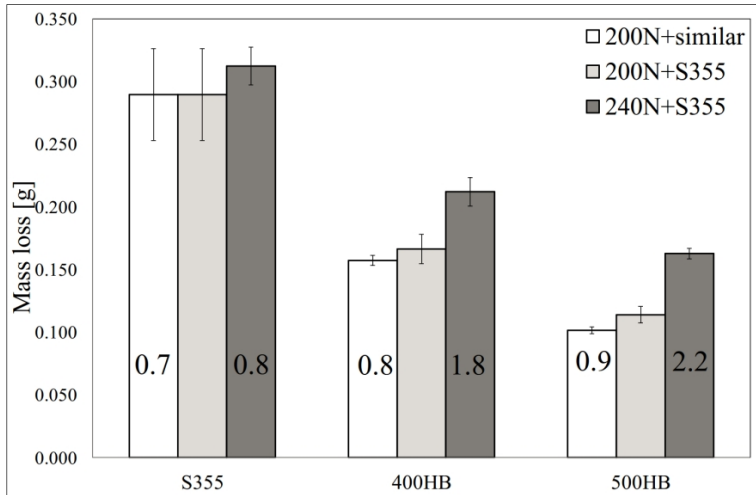


Figure 26. Crushing pin-on-disc mass loss results for pins and discs of similar hardness and for pins tested with S355 discs. The abrasive used in the tests was granite. The values in each column present the pin/disc hardness ratio of the tested sample/counterpart combination.

The disc influences the wear occurring in the crushing pin-on-disc tests. Figure 27 presents the mass losses of S355 discs in tests with different pin materials using several different abrasive types. It can be seen that with all used abrasive types the overall disc mass loss decreases when the pin material is harder than the disc, which agrees with the findings of Terva et al. [43]. This difference further supports the general observation that the hardness ratio of the materials plays an important role in the wear in various tribosystems, even when the two materials are not in direct contact with each other.

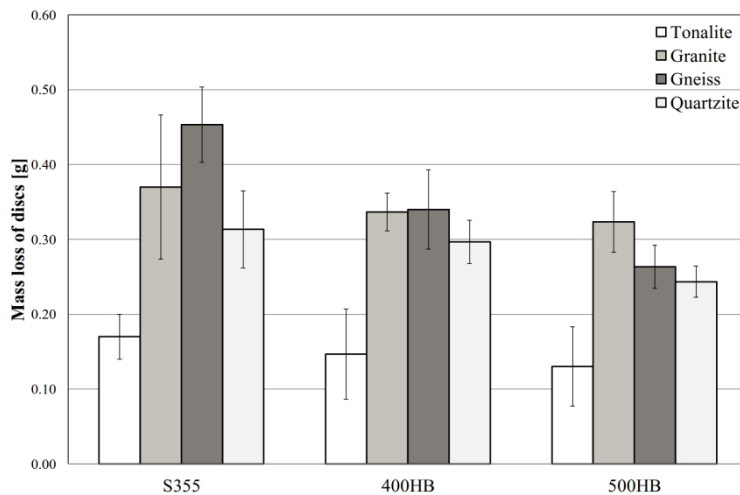


Figure 27. Mass losses of the S355 discs in the crushing pin-on-disc tests with different pin materials and tonalite, granite, gneiss and quartzite as abrasives.

To observe the changes in the wear mechanisms due to the different conditions, Figure 28 presents stereo microscope images of the 500HB pin surfaces tested at different pin/disc hardness ratios. With a higher pin/disc hardness ratio, the amount, width and length of the scratches in the wear surfaces seem to have increased. The increased amount of scratches suggests that the conditions are more favorable for the abrasives to become fixed into the counterpart, as in general during a scratch formation the abrasive in a fixed counterpart position slides on the sample surface. Evidently the abrasives can more easily become fixed into softer counterparts and result in more scratching and less rolling on the surface, which has been reported also by other authors [15, 43]. Also Fang et al. [207] reported that harder materials experience more cutting in three-body abrasion, when the counterpart remains the same for all tests (pure iron), which correlates well with the current results.

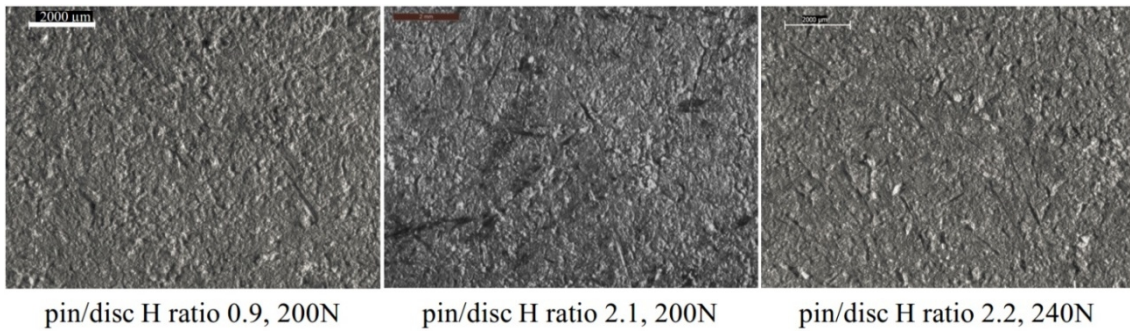


Figure 28. Stereo microscope images of worn crushing pin-on-disc 500HB pin samples tested in different pin/disc ratio conditions using two different normal forces.

Figure 29 presents a closer look at the 500HB pin wear surfaces in the form of SE and BSE images, which reveal the wear surface and the presence of abrasive remnants in more detail. The images confirm that the surfaces with the higher pin/disc hardness ratio appear to have experienced more cutting than the surfaces with the lower pin/disc hardness ratio. The higher amount of cutting can also be seen as the lower amount of embedded abrasives, which appear as dark in the BSE image.

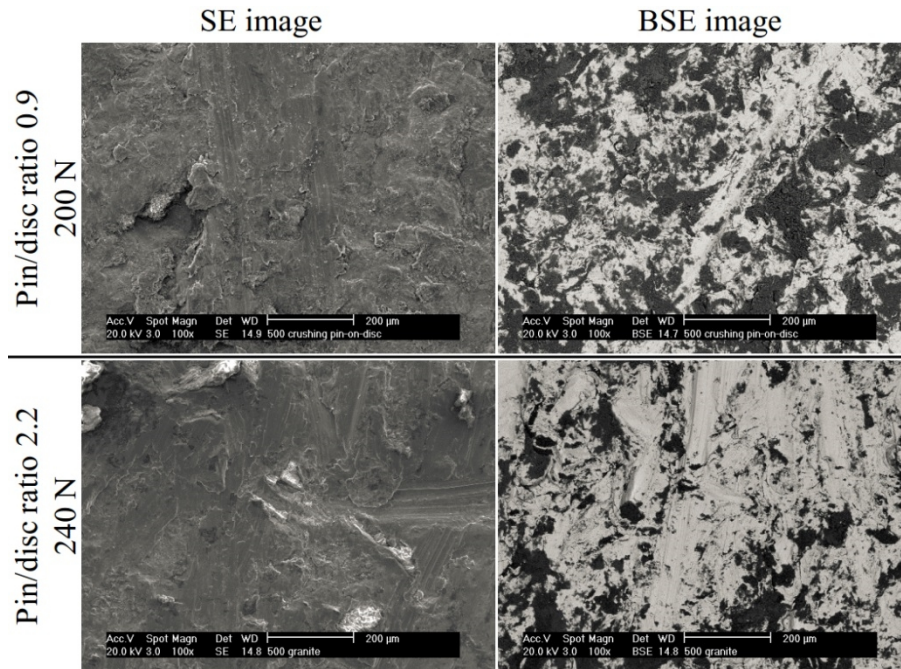


Figure 29. SE and BSE images of the 500HB pin surface.

6.2.2 Abrasive type [Publication IV]

The properties of the abrasives play an important role in abrasive wear. Figure 30 presents the volume loss results for the studied steels and hard metals tested with the crushing pin-on-disc method with four different rock abrasives. Figure 30 demonstrates two important points: different abrasives cause the materials to wear at different rates, and the severity of wear caused by a certain abrasive is not similar for all materials. For example, granite causes the most severe wear in steels, while the volume loss caused by tonalite in the same materials can be even 20-40% lower. For the differences in the severity of rock types on the wear of different materials, quartzite provides a good example: it causes distinctly higher volume loss in hard metals, while in steels the wear rate caused by quartzite is low when compared to the other abrasives. Even within steels there is clear variation in the relative severity of quartzite in causing wear.

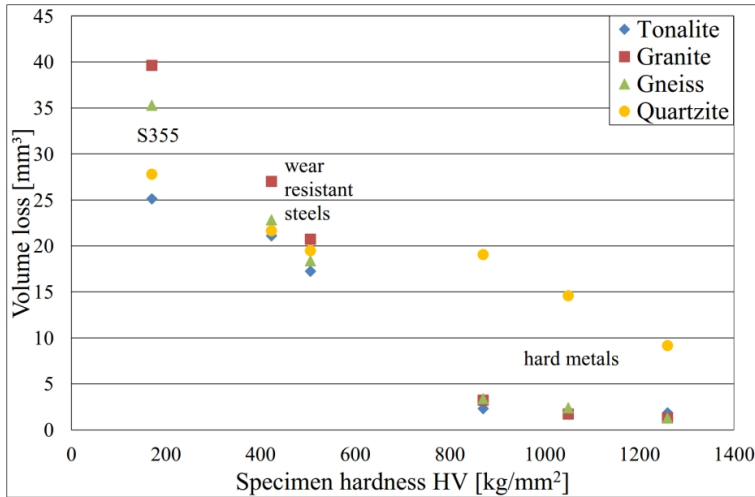


Figure 30. Volume loss results of the crushing pin-on-disc tests on steels and hard metals abraded with tonalite, granite, gneiss and quartzite.

The characteristics of the wear mechanisms caused by different abrasive types can be quite well explained by the abrasive properties presented in Table 5. Figure 31 presents SEM images of the worn surfaces of 500HB samples tested with four different abrasives. The surface tested with quartzite (Figure 31c) has shorter and less well-defined scratches in comparison to the surfaces abraded by the other abrasives. The short appearance of the scratches in the sample tested with quartzite can be linked to the high crushability of quartzite in comparison to the other abrasive types used in this the study: as the quartzite particle does not remain intact for long before it is crushed, it shortens the scratches.

Granite (Figure 31b), on the other hand, has produced rather narrow scratches but with cutting characteristics. Granite caused the highest wear in steels, and when the material is removed by cutting, the mass losses are higher than in the case where mainly ploughing occurs. Granite also has quite high uniaxial compressive strength, which may enable the abrasive particles to maintain their shape better and produce cutting wear. Gneiss (Figure 31a), with lower uniaxial compressive strength and with crushability values in the same range with granite, produces a scratchy surface but closer to the characteristics of the sample tested with quartzite. [Publication IV]

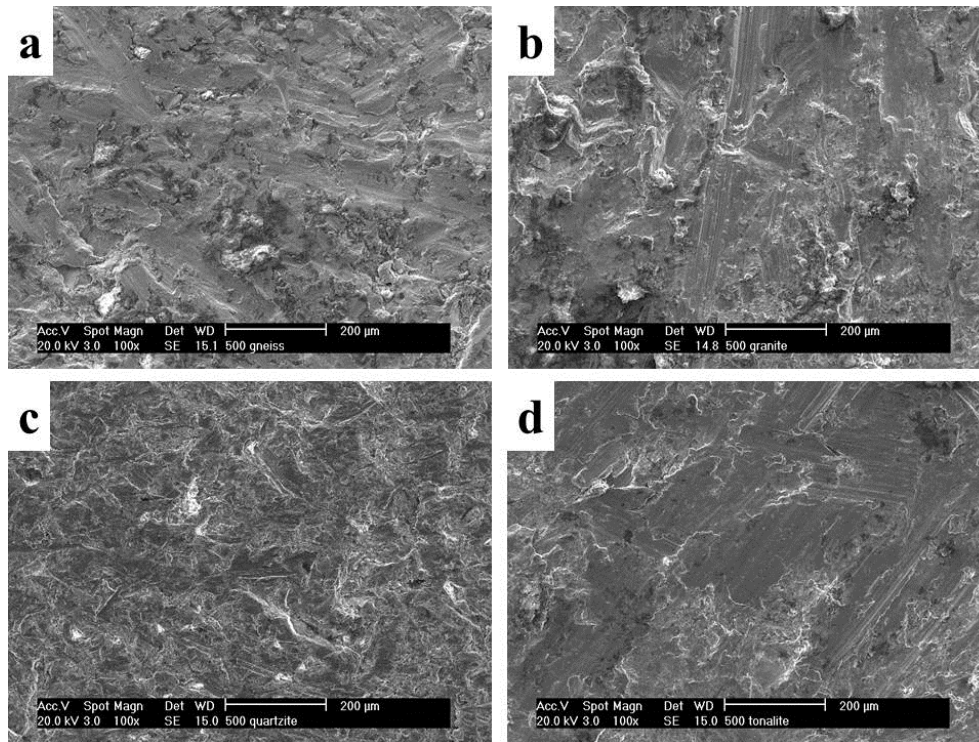


Figure 31. Wear surfaces of 500HB crushing pin-on-disc pin samples worn with a) gneiss, b) granite, c) quartzite and d) tonalite.

Tonalite (Figure 31d), in turn, produces wide and long scratches, which have a shallow general appearance. The longer and wider scratches can be explained by the lower crushability of tonalite and its high compressive strength, which enable the abrasive particles to stay intact longer. [Publication IV]

In the case of hard metals, the abrasive properties together with the microstructure of the worn material offer an explanation for the much higher wear caused by quartzite in comparison with the other abrasives. The high crushability of quartzite and thus its ability to produce small, hard and angular particles combined with the high hardness is the reason why quartzite can be detrimental for hard metals, even when their ability to resist scratching and wear against other abrasives is very good. The macroscale properties of hard metals are a combination of their hard carbide and softer binder phases, but locally the properties vary markedly, depending on the phase. If the abrasive particles are so small that they can reach the matrix between the hard carbides, they can wear the matrix more easily, as is the case in [Publication IV]. Wear of the matrix leads to a situation where the matrix is no longer able to support the carbides [208, 209], which can be pulled out from the matrix or more easily broken provided that the force is sufficient.

While the characteristics of the wear mechanisms correlate with certain abrasive properties, no simple correlation between the amount and mechanisms of wear in steels and the studied abrasive properties could be found. The analysis of the wear behavior of the studied materials in the crushing pin-on-disc tests did not reveal any general dependencies on abrasiveness, uniaxial compressive strength, or quartz content [Publication IV]. The observation of abrasiveness having little correlation with the abrasive wear results in [Publication IV] is quite interesting.

However, abrasiveness is a factor, for which there are several different definitions and procedures for determining it, as mentioned in section 2.1.1. The lack of correlation between the abrasiveness and the wear results emphasizes the fact that the abrasiveness indices and coefficients must be used with caution, keeping in mind the conditions that the tested sample of metal or other material is aimed for. Such conditions can also include, for example, moisture, abrasive grain size, and soil pressure [210].

6.2.3 Summary

- The counterpart can affect the wear of the specimen in terms of mass loss and wear mechanisms, even when the material and its counterpart are not in direct contact with each other. This is because the conditions in the wear system may change, which is a factor that should not be overlooked in wear testing.
- The properties of abrasives can govern the wear mechanisms and thus the amount of wear. However, the effects of abrasive properties on wear depend also strongly on the type of the wearing material. For example, higher crushability can promote wear due to the microstructure of the hard metals, which contains phases of very different hardness.

6.3 Behavior of wear resistant steels in abrasion and impact wear testing conditions

In the following section, the behavior of wear resistant steels in different abrasion and impact abrasion conditions is discussed first from the viewpoint of hardness and then regarding the wear mechanisms on the surface. After that, the changes occurring beneath the surface are discussed, mainly in impacting conditions.

6.3.1 Effect of hardness on wear in abrasive and impacting conditions [Publication I]

Hardness is often regarded as the governing factor in the wear performance of materials, and as a general trend this seems to hold true also for the current samples. Figure 32 presents the relative mass loss results for S355 and the studied wear resistant steels in relation to the result of the 400HB steel in several different wear testing conditions. The normalization by the 400HB reference results is intended to make the values better comparable between the different methods. The harder steels clearly perform better in all test conditions, both abrasive and impacting, meaning that they suffer less mass loss and thus possess higher wear resistance in these conditions. The effect of ultimate tensile strength on wear was similar to that of the effect of hardness, as could be expected due to the usually quite linear correspondence between hardness and tensile strength. The higher elongation or ductility values, in turn, corresponded with higher mass losses in the wear tests.

When comparing the relative mass loss results presented in Figure 32 between the different methods, i.e., crushing pin-on-disc, uniaxial crusher and impeller-tumbler, it is evident that the

increase in hardness increases the wear resistance of the studied materials slightly differently in the applied conditions. For example, while the mass loss of S355 is more than twice that of the 400HB wear resistant steel in gouging-type abrasion induced by uniaxial crusher, in impact-abrasion the difference in the mass loss between S355 and 400HB steels is only about 30%. For impeller-tumbler, quite small differences in the wear rates between the alloys of different hardness have been reported previously by other authors [69, 84], and some authors stated hardly any correlation to exist between the material hardness and mass loss [91, 104].

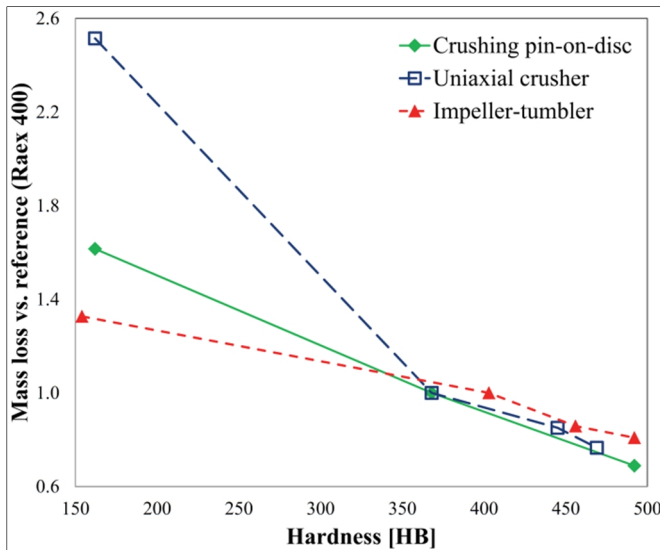


Figure 32. Relative mass loss results from crushing pin-on-disc, uniaxial crusher and impeller-tumbler wear tests with granite abrasive [Publication I].

If one wants to compare the overall severity of wear caused by the different methods used for abrasive testing, comparison of the wear rate is quite useful. In this case, the wear rate is calculated as the mass loss of the sample per wear area per test duration. Figure 33 presents the wear rates for the results presented in Figure 32. Figure 33 reveals that in general the uniaxial crusher produces the highest wear rate of the used testing devices, while the impeller-tumbler samples have worn the least. That being said, it must be considered that the wear conditions vary along the impeller-tumbler samples, as the impact speeds of the abrasive particles are higher at the sample tips. In the crushing pin-on-disc and uniaxial crusher methods, the load induced by the gravel is similar throughout the sample surface.

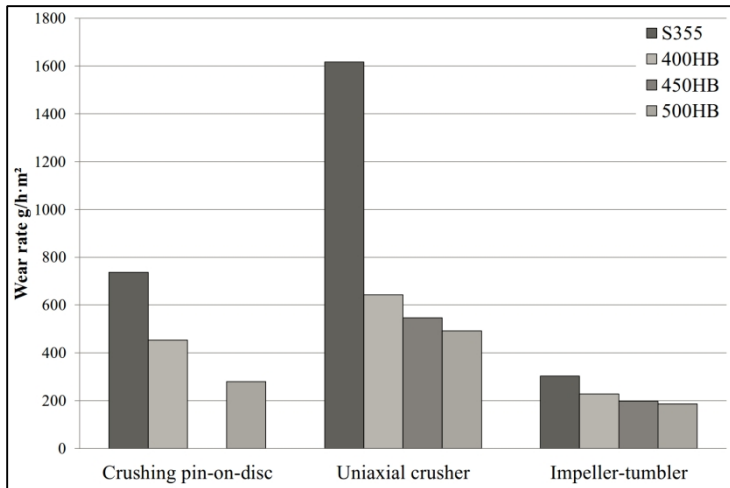


Figure 33. Wear rates of steels tested with three abrasive wear testing methods using granite as abrasive.

6.3.2 Abrasive and impact-abrasive wear mechanisms in wear resistant steels [Publications I-V]

Wear induced by the crushing pin-on-disc [Publications I,IV], uniaxial crusher [Publication I] and impeller-tumbler [Publications I-III] is defined as high-stress abrasive wear. The surfaces undergo high amounts of plastic deformation, which results in uneven surfaces. Moreover, all of the surfaces become embedded with abrasive fragments, which indicates the high-stress nature of these methods. As the contact conditions are all abrasive but different in terms of particle movement, the resulting wear surfaces are described first separately and then compared to each other.

Figure 34 presents the wear surfaces of the crushing pin-on-disc samples tested with a counterpart made of a similar material. The surfaces of the wear resistant steels show signs of both sliding and rolling, i.e., scratches by ploughing and cutting, and indentation marks, which suggest that the abrasive particle has also rolled between the two surfaces. When comparing the wear resistant steels with each other, the harder materials seem to contain more scratches but less plastic deformation. When including also S355 in the comparison, the difference becomes even more evident, as S355 shows mostly plastic deformation but fewer scratches: the number of detectable scratches was approximately half of that in the hard 500HB steel [Publication I].

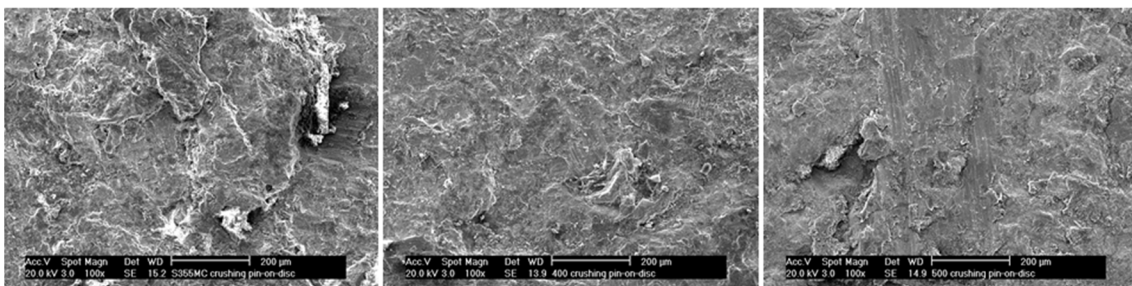


Figure 34. Crushing pin-on-disc wear surfaces of S355, 400HB and 500HB steels tested with granite abrasive.

Axén et al. [58] studied the wear mechanisms in three-body abrasion systems with equal and varying hardness between the samples and the counterpart. They concluded that with material pairs of equal hardness, the particles can roll, indent on both surfaces or indent alternating between the surfaces, as occurred in the wear surfaces of [Publication I]. Axén et al. [58] also reported that in self-mated steel pairs, the amount of grooving and rolling is approximately equal, and that the self-mated aluminum contains the most distinct grooves. They did not, however, elaborate the wear surface differences between softer and harder self-mated steel pairs to be directly compared with the current results.

Fang et al. [211] studied the movement patterns of individual abrasive particles in three-body abrasion and concluded that the maximum friction coefficient value was higher for rolling than for sliding particles. This may explain why there is a higher amount of scratches on the harder surfaces: in a material, which has high hardness and thus is able to resist the penetration, the particle slides than rolls more easily. Also Nahvi et al. [16] reported that sliding is favored with materials of higher hardness and in systems with higher loads. Another suggestion is that as the material does not yield as easily in either the sample or the counterpart, the particle is not able to roll but rather slides on the surfaces [Publication I].

The uniaxial crusher samples had a more gouging-type surface after the tests when compared to the crushing pin-on-disc samples. The surface contained larger and smaller indentation marks and exhibited signs of heavy plastic deformation. There were also scratches which, however, were quite short. These scratches had been produced by the relative movement of the abrasive particles in the abrasive bed when the bed was being crushed. In these tests, there was no sideways movement between the sample and the counterpart. When looking more closely at the scratches, they were more well-defined in the harder wear resistant steels [Publication I].

The impeller-tumbler samples wore largely due to microfatigue, as the subsequent impacting caused the previously deformed material to become removed from the surface. Similar observations have been made by Sundström et al. [78] and Wilson and Hawk [69]. Figure 35 presents SEM images of the wear surfaces of the impeller-tumbler tested samples. The images of the samples with hardness ranging from 186 HV₃ [kg/mm²] (S355) to 712 HV₁₀ [kg/mm²] (wear resistant steels 400-650HB) were taken with both SE and BSE modes of SEM. The SE mode images show that the wear particle formation is moving more towards chip formation as the materials become harder. This observation can be explained with the mechanical properties of the steels: in the harder steels, the ductility is lower, which leads to easier chip formation. The BSE mode images reveal that there is a distinct difference in the amount of embedded abrasives on the surfaces. The softer steels contain significantly higher amounts of embedded abrasives, which are also covering larger continuous areas. [Publications I-III]

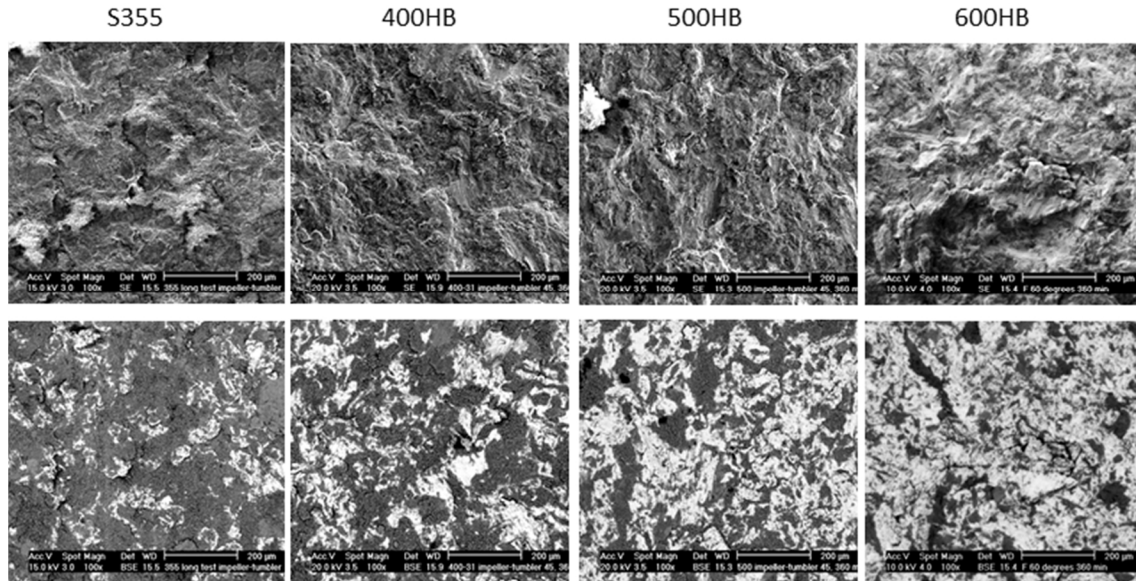


Figure 35. SEM images of the wear surfaces of impeller-tumbler samples in SE-mode (above) and BSE-mode (below). Abrasives are seen as dark gray in the BSE images.

To summarize the similarities between the surfaces produced by the different wear testing methods with the abrasives used in [Publications I-IV], the hardness of the material clearly correlates with the amount of scratches detected on the sample surfaces. The main reason for this is the lower ductility and limited plastic deformation of harder materials, incapable of covering the previous scratches, and the tendency to cutting instead of ploughing of the material. The differences in the wear surfaces between the materials are observable not only in the samples, which have been tested for a longer duration, but already after the first contacts with the abrasives. Figure 36 presents images of single impacts that have occurred in an impeller-tumbler test, which show that in S355 the abrasives are more easily embedded into the surface. Moreover, the higher degree of plastic deformation can be observed as deeper dents in softer materials compared to harder materials having shallower wear scars.

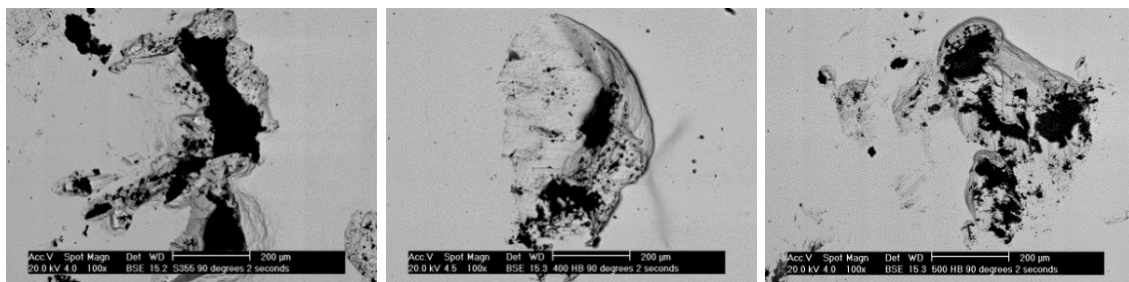


Figure 36. SEM images of single impacts occurred in the impeller-tumbler tests on S355, 400HB and 500HB steels [modified from Publication II].

In the tests with impacting contacts and no abrasive component, the size of the initial impact scars is determined by the mechanical properties of the material under impact. In the first impact, hardness governs the penetration of the impactor into the material. However, the size of the scar after several impacts is also affected by the mechanism of material removal at the site of the impact. Figure 37 shows how the 400HB steel (left hand side) has a distinctly different

appearance compared to the harder 500HB and 650HB steels after impacts. The individual impacts are more visible in 400HB than in the other steels after 10 impacts, and after 1000 impacts there is a seemingly detached layer on the crater of the 400HB steel. Lindroos et al. [112] reported the material removal to occur through adhesion and fracture in a multiple impact test with similar ball and sample materials. The softer materials tend to adhere [4] to the WC impactor more easily. The attachment of sample material onto the impactor can also further accelerate material removal from the sample, as materials have a higher tendency to adhesion with a similar material [4]. A situation of similar materials arises when a layer of the tested steel is adhered to the WC ball and is further impacted on the steel surface. At times the adhered material also detaches from the ball surface and gets reattached onto the crater. [Publication V]

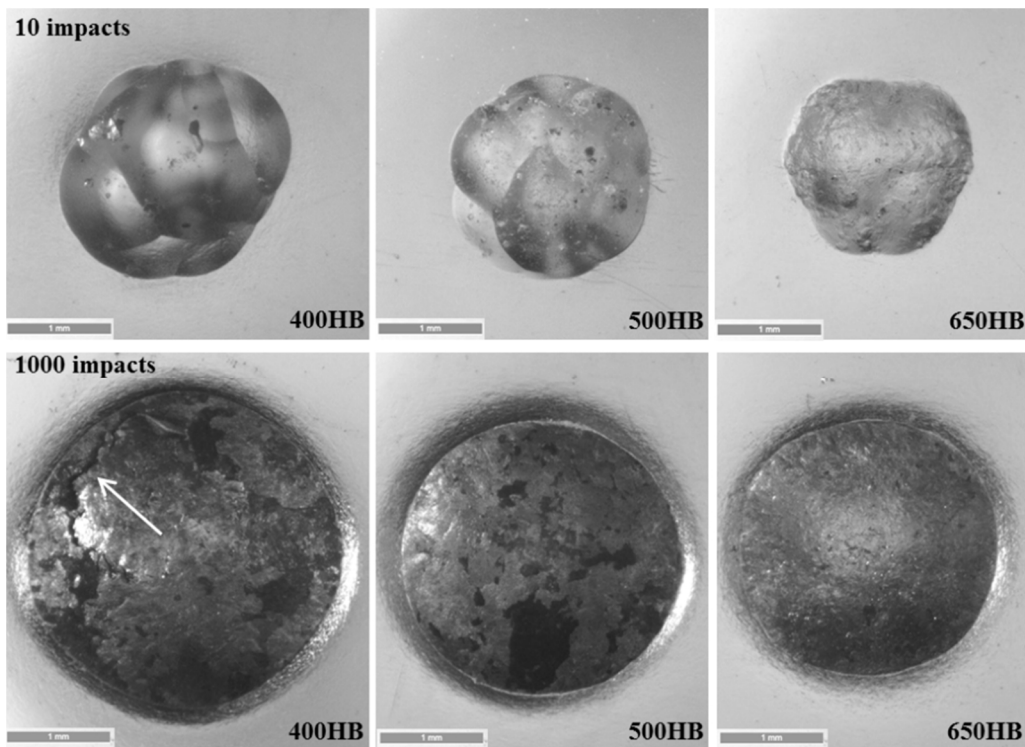


Figure 37. Impact marks on 400HB, 500HB, and 650 HB samples after 10 and 1000 impacts. Arrow points to the partially detached area. [Publication V]

6.3.3 Sub-surface effects of abrasive, impact and impact-abrasive wear [Publications I-V]

Surface observations and profilometry cannot reveal information about the work hardening taking place in and below the surface layer and the extent of abrasive particle embedment, especially if the embedded abrasives are covered with deformed material. Therefore, wear surface cross section examinations were used to complete the wear mechanism studies. Figure 38 presents cross section images of the 500HB steel tested with the three different abrasive testing methods. The images show that abrasive particles or dust embedment is present in all methods, although its scale varies expectedly: in the uniaxial crusher sample tested with high forces, the penetration depth of the embedded abrasives is the highest [Publication I]. Figure 38

also shows how the embedded abrasives may be partly or fully covered by the plastically deformed material of the sample.

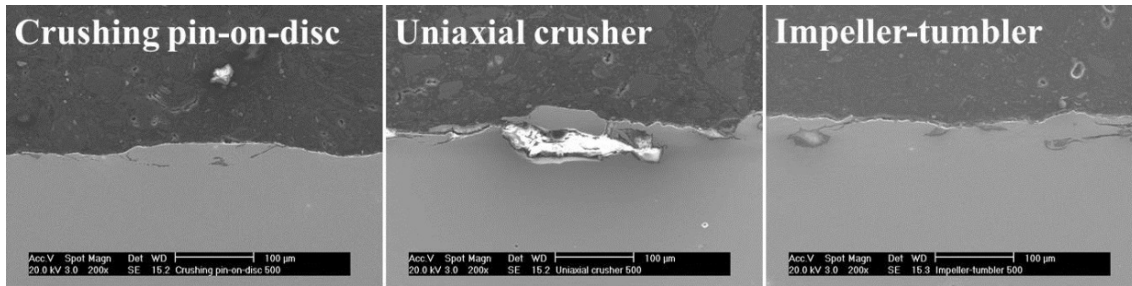


Figure 38. Cross section images of 500HB samples after wear tests with crushing pin-on-disc, uniaxial crusher and impeller-tumbler.

When comparing the behavior between the studied steels, the role of ductility in the wear mechanism becomes evident. Figure 39 presents the cross sections of S355 and wear resistant steels after impeller-tumbler testing, supporting the observations already made on the surface in 6.3.2: in the softer steels, the formations on the surface extend deeper and the degree of abrasive embedment is higher. The embedded abrasives may work in two different ways: they raise the overall hardness of the surface region but, on the other hand, the lip that has possibly formed over the abrasive particle has only a thin layer of material to support it, which may lead to the removal of relatively large chunks of material at once. In impact-abrasion with abrasives added in the process, the properties of the abrasives can affect the depth of the mechanically mixed layer formed by the steel and the embedded abrasives [86].

Impacting conditions can cause quite unpredictable wear effects. To demonstrate how multi-hour impact-abrasive exposure can affect the microstructures, Figure 40 shows deformed microstructures found in the steels after impeller-tumbler testing for 360 minutes. The deformation depths in the harder steels were much lower than in the softer steels, but the appearance of the areas very close to the surface had similarities in all materials. The tribolayer consists of mechanically fibered substructures, which are oriented in wavy patterns following the topography of the surface. In S355, the pearlite lamellae have flattened in wavy patterns, and in the martensitic wear resistant steels the martensite laths are following the topographical shapes very close to the surface. The laboratory steel 650HB contained ferrite in the martensitic matrix, leading to more deformation inside the ferrite grains but also in the martensite in the proximity of the ferrite. On the other hand, the 650HB steel seems to undergo deformation only in the areas very close to the surface.

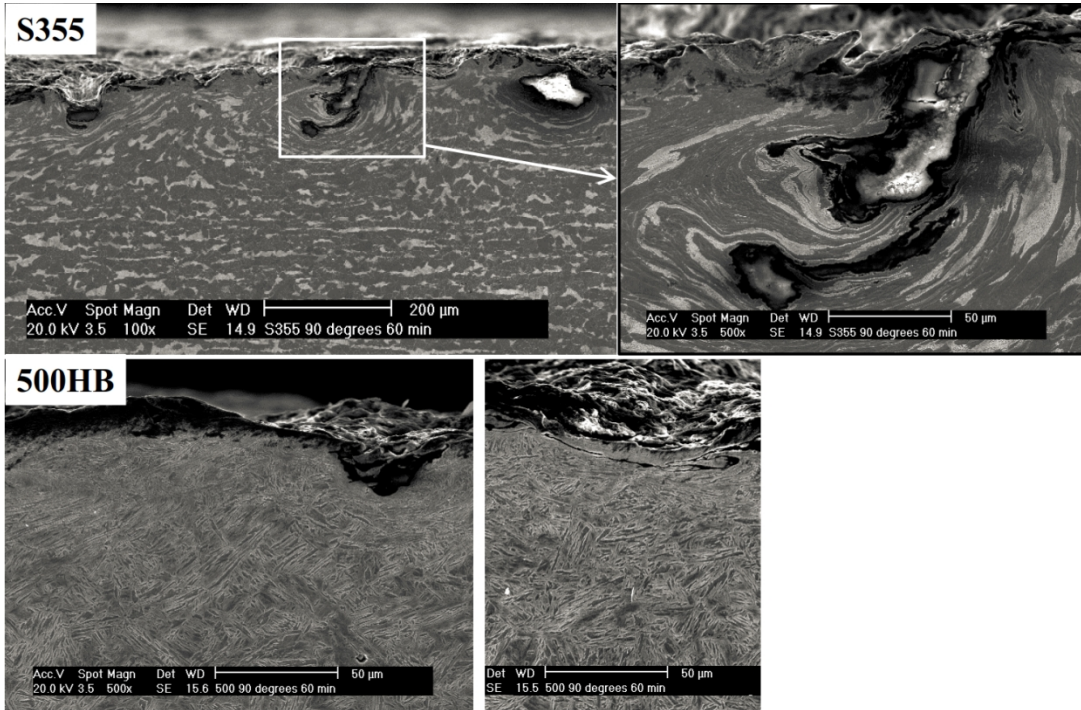


Figure 39. Cross section images of S355 and 500HB samples tested in the impeller-tumbler at 90° sample angle for 60 minutes.

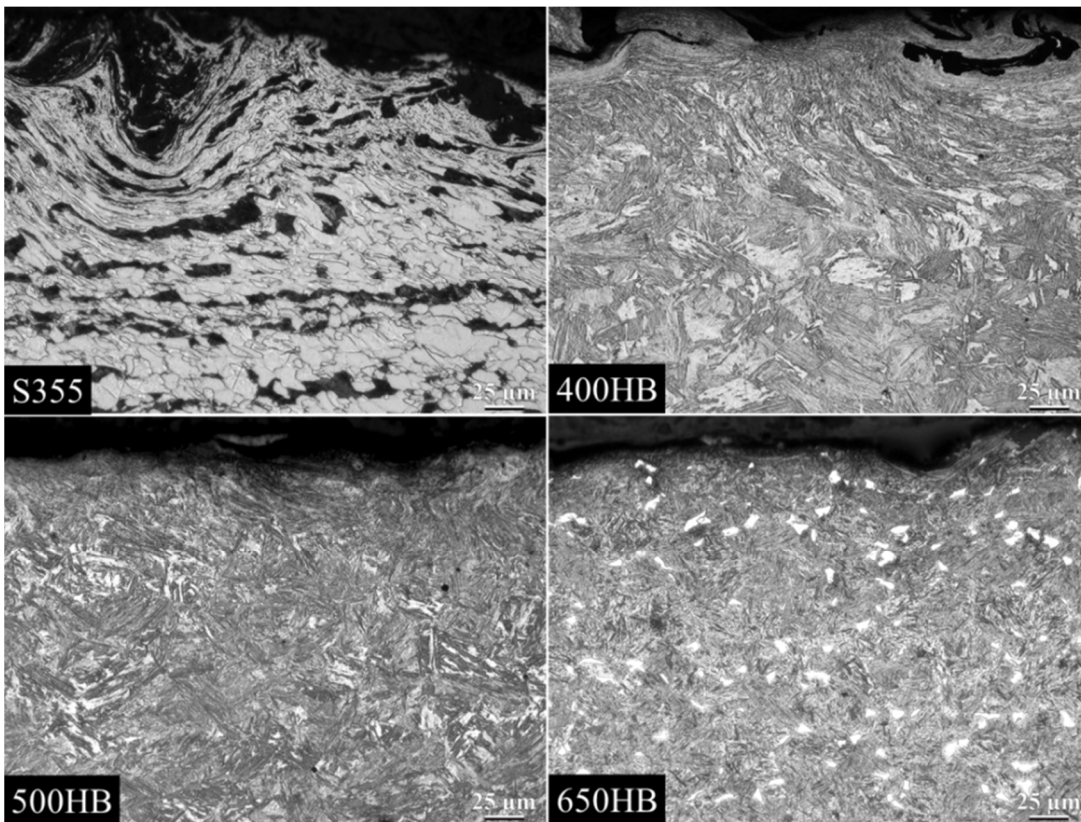


Figure 40. Microstructures of steels after impeller-tumbler tests at 90° sample angle for 360 minutes [modified from Publication III].

As seen in Figure 40, the microstructure of the material can change during the wear process. The stresses cause reactions in the material, causing deformation, which can lead to work hardening and alteration of substructures, such as refinement and alignment of the grain structure. Thus the material with certain properties in the beginning of the test or wear process can have distinctly different properties after being subjected to stresses. To show the changes occurring in more controlled, purely impacting conditions, Figure 41 presents the cross sections of samples impacted for 1000 times. In Figure 41, especially the S355, 400HB and 500HB samples show that the microstructure close to the surface is very different from the microstructure deeper in the material. The softer steels are affected much deeper than the harder wear resistant steels, and especially S355 shows signs of detaching and reattaching of material layers on the surface.

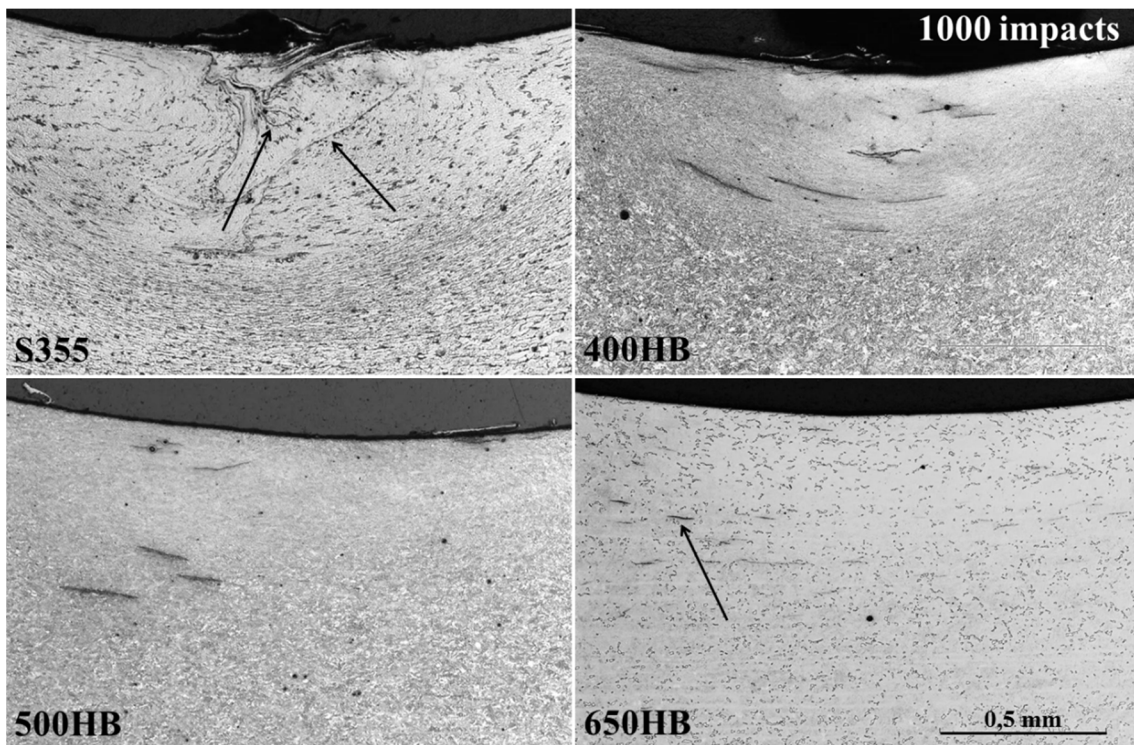


Figure 41. Cross sections of impact marks after 1000 impacts by HT-CIAT [Publication V]. The arrows point to the cracks in the region.

To further study the nature of the structural changes in the heavily deformed 400HB steel, EBSD measurements were conducted on the wear surface after selected numbers of impacts. Even though there are some changes in the microstructures observable already after ten impacts, they may not yet be so evident [Publication V]. After prolonged exposure to impacts, the effects become more visible. Figure 42 presents pole figures of a 400HB sample at the initial state and after 10 and 1000 impacts, and of a 500HB sample after 1000 impacts. The pole figures show that the grain structures are initially rather randomly oriented, and also remain so after ten impacts, but after 1000 impacts the formation of a favorable orientation of $\langle 111 \rangle$ is clear. In the compression of bcc metals, the developing textures are commonly of type $\langle 111 \rangle$ or $\langle 100 \rangle$ [212]. The changes in the (preferred) orientation and increase of the dislocation density lead to a

clear hardening of the material, which affects also the wear behavior of the material [Publication V].

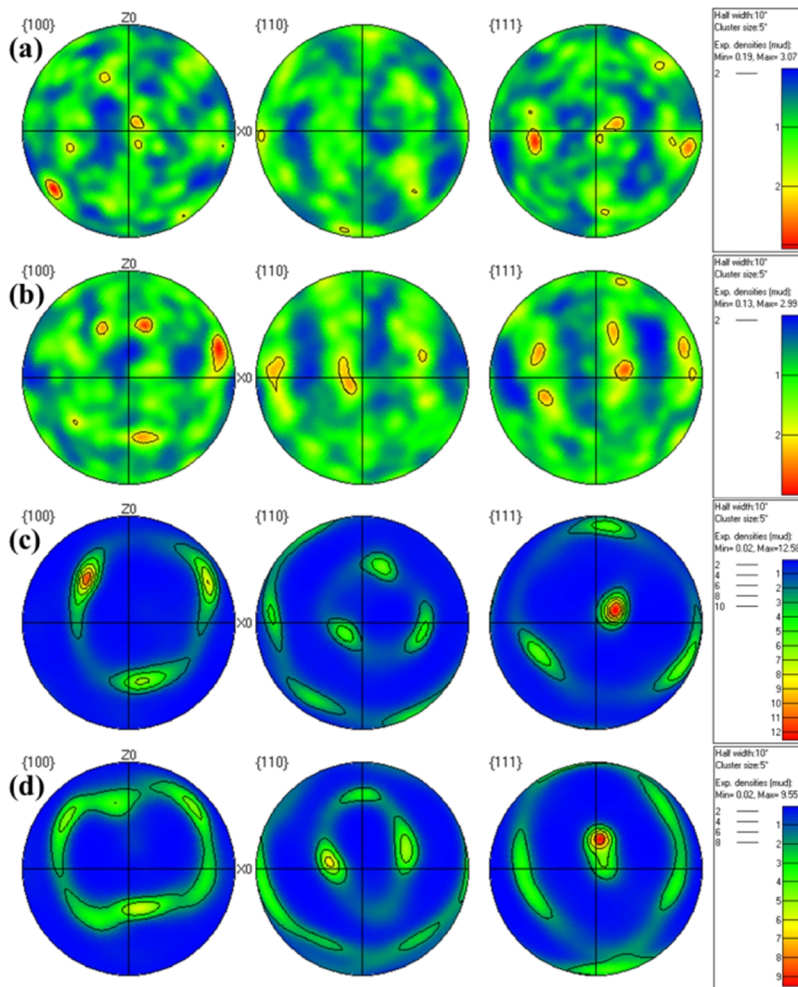


Figure 42. $\{100\}$, $\{110\}$ and $\{111\}$ pole figures of a 400HB sample at a) initial state, b) after 10 impacts, c) after 1000 impacts and d) a 500HB sample after 1000 impacts [Publication V].

6.3.4 Summary

To summarize the findings presented in the previous sections, the following conclusions can be made:

- In all high-stress abrasion tests with three acting bodies, the harder materials undergo more cutting independent of the prevailing contact type, i.e., impact, gouging or scratching.
- The material properties can change substantially during the wear process and lead to unforeseen behavior especially during extended exposures. This further emphasizes the use of adequate test durations in the determination of the material's wear behavior, especially in applications which involve heavy loads.

7. Concluding remarks and suggestions for future work

The use of more durable materials can save significant amounts of time and expenses by decreasing the down time due to maintenance. The performance of materials can of course be tested in the field, but since the conditions in the in-service tests can vary markedly, a more cost efficient way to estimate or pre-evaluate the material performance in controlled conditions is laboratory wear testing. In laboratory wear testing, however, it is important to realize the restrictions of the testing method and the interdependencies between the test parameters, the wear mechanisms, and the obtained results.

In this study, the parameters of the impeller-tumbler test were analyzed and the testing device was evaluated as an impact-abrasive wear testing method using natural gravel as abrasive. The effects of several parameters and the testing procedures were discussed in detail. It can be concluded that in order to obtain reliable results, attention must be paid to both the test procedure and the test parameters, such as the abrasive size distribution, which can have a surprisingly large effect on the outcome of the tests by emphasizing the material properties differently. Determining of the exact range of the effective impact angles caused by the different sample angles with theoretical calculations or simulations remains an interesting subject of study for the future. As a method, the impeller-tumbler causes very edge concentrated wear, as the wear rate in the edge areas can be an order of magnitude higher than the wear rate in the inner areas of the sample. Moreover, to obtain representative wear surfaces for further examinations, it is important to conduct tests with adequate duration. Overall, for the needs of applications where edge wear has an important role, the impeller-tumbler method is capable of producing consistent wear test results when used with a reference sample and careful parameter monitoring.

In sliding scratching conditions, the abrasive type and even the indirect counterpart can affect the formation and behavior of the tribosystem. For example, a softer counterpart can promote cutting wear in the sample through partial embedment of the abrasives in the counterpart. In addition, the abrasive with the highest hardness, i.e., quartzite, was found to cause less wear in the studied steels than the softer ones. This is because also the other properties of the materials involved in the abrasive and impacting wear tests, such as the crushability of the abrasive, are clearly equally important and can affect the behavior of the entire tribosystem quite drastically.

Despite the differences in the abrasive contact conditions in the abrasive and impact wear tests of wear resistant steels, the wear mechanisms were found to have many similarities: the harder steels contained more visible scratches due to their lower plasticity, and they also contained less embedded abrasives. As expected, the role of hardness was depending on the contact conditions, but also on the duration of the test. The importance of sufficient test duration was further highlighted by the results of the impact tests, where the microstructure of the steel could transform or change unexpectedly, leading to significantly different properties in comparison to the initial microstructure.

Wear resistance is not a material property but depends on the conditions of the tribosystem. Therefore there is no simple and straightforward way of determining the behavior of materials

in wear prone conditions. Furthermore, wear is an extremely complex phenomenon, and understanding and resolving it requires persistent research in several kinds of conditions. The wear processes have to be assessed considering the contact conditions, including all materials in question and how they behave in the system. Moreover, characterization of the tribosystem associated with a particular wear testing method is essential in order to prevent from being driven to wrong conclusions. This work concentrated primarily on assessing the high-stress wear testing in impacting and abrasive conditions from the viewpoint of steels. In the future, it will be important to verify more closely what kind of in-service conditions the wear tests considered in this work are exactly simulating. For this, more precise data from different types of field tests will also be needed.

References

- [1] J. H. Tylczak, “Abrasive wear,” in *ASM Handbook Volume 18. Friction, Lubrication, and Wear Technology*, USA: ASM International, 1992, pp. 184–190.
- [2] J. A. Hawk and R. D. Wilson, “Tribology of earthmoving, mining, and minerals processing,” in *Modern Tribology Handbook*, B. Bhushan, Ed. Boca Raton: CRC Press, 2001, pp. 1–40.
- [3] A. D. Sarkar, *Friction and Wear*. Bristol: Academic Press, 1980.
- [4] K. Kato and K. Adachi, “Wear Mechanisms,” in *Modern Tribology Handbook*, B. Bhushan, Ed. Boca Raton: CRC Press, 2001, pp. 1–28.
- [5] M. B. Peterson, “Classification of wear processes,” in *Wear Control Handbook*, M. B. Peterson and W. O. Winer, Eds. New York: The American Society of Mechanical Engineers, 1980, pp. 9–15.
- [6] K.-H. Zum Gahr, *Microstructure and Wear of Materials*, vol. 10. Amsterdam: Elsevier, 1987.
- [7] “DIN 50320 Verschleiß - Begriffe, Systemanalyse von Verschleißvorgängen, Gliederung des Verschleißgebietes,” in *DIN-Taschenbuch 198*, Berlin: Deutsches Institut für Normung, Beuth Verlag GmbH, 1991, pp. 199–206.
- [8] P. J. Blau, “Fifty years of research of metals,” *Tribology International*, vol. 30, no. 5, pp. 321–331, 1997.
- [9] K. Kato and K. Adachi, “Metals and ceramics,” in *Modern Tribology Handbook*, B. Bhushan, Ed. Boca Raton: CRC Press, 2001, pp. 1–15.
- [10] N. Axén, S. Hogmark, and S. Jacobson, “Friction and wear measurement techniques,” in *Modern Tribology Handbook*, no. 1987, B. Bhushan, Ed. Boca Raton: CRC Press, 2001, pp. 1–18.
- [11] D. Scott, “Wear,” in *Industrial Tribology — The Practical Aspects of Friction, Lubrication and Wear*, vol. 8, M. H. Jones and D. Scott, Eds. Amsterdam: Elsevier B.V., 1983, pp. 12–30.
- [12] I. M. Hutchings, *Tribology - Friction and wear of engineering materials*. Suffolk: Butterworth Heinemann, 1992.
- [13] G. W. Stachowiak and A. W. Batchelor, *Engineering Tribology*, 3rd ed. Burlington: Butterworth-Heinemann, 2006.

- [14] R. I. Trezona, D. N. Allsopp, and I. M. Hutchings, "Transitions between two-body and three-body abrasive wear: influence of test conditions in the microscale abrasive wear test," *Wear*, vol. 225–229, pp. 205–214, 1999.
- [15] R. Dwyer-Joyce, R. Sayles, and E. Ioannides, "An investigation into the mechanisms of closed three-body abrasive wear," *Wear*, vol. 175, pp. 133–142, 1994.
- [16] S. M. Nahvi, P. H. Shipway, and D. G. McCartney, "Particle motion and modes of wear in the dry sand–rubber wheel abrasion test," *Wear*, vol. 267, pp. 2083–2091, 2009.
- [17] M. Mosleh, E. A. Gharahbagh, and J. Rostami, "Effects of relative hardness and moisture on tool wear in soil excavation operations," *Wear*, vol. 302, no. 1–2, pp. 1555–1559, 2013.
- [18] J. D. Gates, "Two-body and three-body abrasion: A critical discussion," *Wear*, vol. 214, pp. 139–146, 1998.
- [19] G. Pintaude, F. G. Bernardes, M. M. Santos, A. Sinatora, and E. Albertin, "Mild and severe wear of steels and cast irons in sliding abrasion," *Wear*, vol. 267, pp. 19–25, 2009.
- [20] J. A. Williams, "Wear modelling: analytical, computational and mapping: a continuum mechanics approach," *Wear*, vol. 225–229, pp. 1–17, 1999.
- [21] K. Hokkirigawa and K. Kato, "An experimental and theoretical investigation of ploughing, cutting and wedge formation during abrasive wear," *Tribology International*, vol. 21, pp. 51–57, 1988.
- [22] I. M. Hutchings, "Abrasion processes in wear and manufacturing," *Proceedings of the Institution of Mechanical Engineers, Part J: Journal of Engineering Tribology*, vol. 216, pp. 55–62, 2002.
- [23] A. A. Torrance, "An explanation of the hardness differential needed for abrasion," *Wear*, vol. 68, pp. 263–266, 1981.
- [24] G. Pintaude, D. K. Tanaka, and A. Sinatora, "The effects of abrasive particle size on the sliding friction coefficient of steel using a spiral pin-on-disk apparatus," *Wear*, vol. 255, pp. 55–59, 2003.
- [25] M. Woldman, E. Van Der Heide, T. Tinga, and M. A. Masen, "The influence of abrasive body dimensions on single asperity wear," *Wear*, vol. 301, pp. 76–81, 2013.
- [26] J. J. Coronado and A. Sinatora, "Effect of abrasive size on wear of metallic materials and its relationship with microchips morphology and wear micromechanisms: Part 1," *Wear*, vol. 271, pp. 1794–1803, 2011.

- [27] A. Misra and I. Finnie, "On the size effect in abrasive and erosive wear," *Wear*, vol. 65, pp. 359–373, 1981.
- [28] I. Sevim and I. B. Eryurek, "Effect of abrasive particle size on wear resistance in steels," *Materials & Design*, vol. 27, pp. 173–181, 2006.
- [29] A. A. Torrance, "The effect of grit size and asperity blunting on abrasive wear," *Wear*, vol. 253, pp. 813–819, 2002.
- [30] J. J. Coronado and A. Sinatora, "Effect of abrasive size on wear of metallic materials and its relationship with microchips morphology and wear micromechanisms: Part 2," *Wear*, vol. 271, pp. 1804–1812, 2011.
- [31] D. V. De Pellegrin, A. A. Torrance, and E. Haran, "Wear mechanisms and scale effects in two-body abrasion," *Wear*, vol. 266, pp. 13–20, 2009.
- [32] G. B. Stachowiak and G. W. Stachowiak, "Wear mechanisms in ball-cratering tests with large abrasive particles," *Wear*, vol. 256, pp. 600–607, 2004.
- [33] G. B. Stachowiak, G. W. Stachowiak, and J. M. Brandt, "Ball-cratering abrasion tests with large abrasive particles," *Tribology International*, vol. 39, pp. 1–11, 2006.
- [34] G. B. Stachowiak and G. W. Stachowiak, "The effects of particle characteristics on three-body abrasive wear," *Wear*, vol. 249, pp. 201–207, 2001.
- [35] D. A. Kelly and I. M. Hutchings, "A new method for measurement of particle abrasivity," *Wear*, vol. 250, pp. 76–80, 2001.
- [36] M. G. Hamblin and G. W. Stachowiak, "A multi-scale measure of particle abrasivity," *Wear*, vol. 185, pp. 225–233, 1995.
- [37] M. G. Hamblin and G. W. Stachowiak, "Characterisation of surface abrasivity and its relation to two-body abrasive wear," *Wear*, vol. 206, pp. 69–75, 1997.
- [38] K. Kato, "Abrasive wear of metals," *Tribology International*, vol. 30, pp. 333–338, 1997.
- [39] N. B. Dube and I. M. Hutchings, "Influence of particle fracture in the high-stress and low-stress abrasive wear of steel," *Wear*, vol. 233–235, pp. 246–256, 1999.
- [40] R. Gåhlin and S. Jacobson, "The particle size effect in abrasion studied by controlled abrasive surfaces," *Wear*, vol. 224, pp. 118–125, 1999.
- [41] D. V De Pellegrin and G. W. Stachowiak, "Assessing the role of particle shape and scale in abrasion using 'sharpness analysis,'" *Wear*, vol. 253, pp. 1026–1034, 2002.

- [42] T. Chandrasekaran and Kishore, “Grinding abrasive wear and associated particle size effect,” *Materials Science and Technology*, vol. 8, pp. 722–728, 1992.
- [43] J. Terva, T. Teeri, V.-T. Kuokkala, P. Siitonen, and J. Liimatainen, “Abrasive wear of steel against gravel with different rock–steel combinations,” *Wear*, vol. 267, pp. 1821–1831, 2009.
- [44] G. Pintaude, A. P. P. Tschiptschin, D. K. K. Tanaka, and A. Sinatora, “The particle size effect on abrasive wear of high-chromium white cast iron mill balls,” *Wear*, vol. 250, pp. 66–70, 2001.
- [45] K. Thuro and H. Käsling, “Classification of the abrasiveness of soil and rock,” *Geomechanik und Tunnelbau*, vol. 2, pp. 179–188, 2009.
- [46] M. Alber, “Stress dependency of the Cerchar abrasivity index (CAI) and its effects on wear of selected rock cutting tools,” *Tunnelling and Underground Space Technology*, vol. 23, pp. 351–359, 2008.
- [47] R. Plinninger, H. Käsling, K. Thuro, and G. Spaun, “Testing conditions and geomechanical properties influencing the CERCHAR abrasiveness index (CAI) value,” *International Journal of Rock Mechanics and Mining Sciences*, vol. 40, pp. 259–263, 2003.
- [48] S. I. Al-Ameen and M. D. Waller, “The influence of rock strength and abrasive mineral content on the Cerchar Abrasive Index,” *Engineering Geology*, vol. 36, pp. 293–301, 1994.
- [49] R. Fowell and M. A. Bakar, “A review of the Cerchar and LCPC rock abrasivity measurement methods,” in *11th Congress of the International Society for Rock Mechanics*, 2007, pp. 155–160.
- [50] O. Yaralı, E. Yaşar, G. Bacak, and P. G. Ranjith, “A study of rock abrasivity and tool wear in Coal Measures Rocks,” *International Journal of Coal Geology*, vol. 74, pp. 53–66, 2008.
- [51] R. J. Plinninger and U. Restner, “Abrasiveness Testing, Quo Vadis? – A Commented Overview of Abrasiveness Testing Methods,” *Geomechanik und Tunnelbau*, vol. 1, pp. 61–70, 2008.
- [52] H. Käsling and K. Thuro, “Determining abrasivity of rock and soil in the laboratory,” *Geologically Active*, pp. 1973–1980, 2010.
- [53] M. Köhler, U. Maidl, and L. Martak, “Abrasiveness and tool wear in shield tunnelling in soil / Abrasivität und Werkzeugverschleiß beim Schildvortrieb im Lockergestein,” *Geomechanics and Tunnelling*, vol. 4, no. 1, pp. 36–54, Feb. 2011.

- [54] P. D. Jakobsen, A. Bruland, and F. Dahl, “Review and assessment of the NTNU/SINTEF Soil Abrasion Test (SATTM) for determination of abrasiveness of soil and soft ground,” *Tunnelling and Underground Space Technology*, vol. 37, pp. 107–114, 2013.
- [55] K. Thuro, J. Singer, H. Käsling, and M. Bauer, “Determining Abrasivity with the LCPC Test,” in *Rock Mechanics - Meeting Society’s Challenges and Demands: Proceedings of the 1st Canada-US Rock Mechanics Symposium, Vancouver, 2007*, pp. 827–834.
- [56] F. Dahl, A. Bruland, P. D. Jakobsen, B. Nilsen, and E. Grøv, “Classifications of properties influencing the drillability of rocks, based on the NTNU/SINTEF test method,” *Tunnelling and Underground Space Technology*, vol. 28, pp. 150–158, 2012.
- [57] H. Käsling and K. Thuro, “Determining rock abrasivity in the laboratory,” in *Proceedings of European Rock Mechanics Symposium EUROCK 2010*, 2010, pp. 1–4.
- [58] N. Axén, S. Jacobson, and S. Hogmark, “Influence of hardness of the counterbody in three-body abrasive wear—an overlooked hardness effect,” *Tribology International*, vol. 27, pp. 233–241, 1994.
- [59] G. J. Gore and J. D. Gates, “Effect of hardness on three very different forms of wear,” *Wear*, vol. 203–204, pp. 544–563, 1997.
- [60] “G40-13 Standard terminology related to wear and erosion,” ASTM International, 2013, pp. 1–9.
- [61] H. Czichos, *Tribology - a systems approach to the science and technology of friction, lubrication and wear*. Amsterdam: Elsevier Scientific Publishing Company, 1978.
- [62] P. A. Engel, “Impact Wear,” in *ASM Handbook Volume 18. Friction, Lubrication, and Wear Technology*, vol. 18, ASM International, 1992, pp. 263–270.
- [63] P. J. Blau, “Wear Testing,” in *Metals Handbook*, 2nd ed., J. R. Davis, Ed. USA: ASM International, 1998, pp. 1342–1347.
- [64] K. Holmberg and A. Laukkanen, “Wear Models,” in *Handbook of Lubrication and Tribology, Volume II: Theory and Design*, 2nd ed., R. W. Bruce, Ed. Boca Raton: CRC Press, 2012, pp. 1–22.
- [65] J. Hawk, “Abrasive Wear Testing,” in *ASM Handbook, Volume 8: Mechanical Testing and Evaluation*, vol. 8, H. Kuhn and D. Medlin, Eds. Materials Park, OH: ASM International, 2000, pp. 325–337.
- [66] P. A. Engel, *Impact Wear of Material*, vol. 2. Amsterdam: Elsevier Scientific Publishing Company, 1978.

- [67] S. Sarkar, E. Badisch, R. Mitra, and M. Roy, "Impact Abrasive Wear Response of Carbon/Carbon Composites at Elevated Temperatures," *Tribology Letters*, vol. 37, pp. 445–451, 2009.
- [68] E. Badisch, M. Kirchgaßner, and F. Franek, "Continuous impact/abrasion testing: influence of testing parameters on wear behaviour," *Proceedings of the Institution of Mechanical Engineers, Part J: Journal of Engineering Tribology*, vol. 223, pp. 741–750, 2009.
- [69] R. D. Wilson and J. A. Hawk, "Impeller Wear Impact-Abrasive Wear Test," *Wear*, vol. 225–229, pp. 1248–1257, 1999.
- [70] J. Tianfu and Z. Fucheng, "The work-hardening behavior of medium manganese steel under impact abrasive wear condition," *Materials Letters*, vol. 31, pp. 275–279, 1997.
- [71] M. Qian and W. Chaochang, "Impact-abrasion behavior of low alloy white cast irons," *Wear*, vol. 209, pp. 308–315, 1997.
- [72] Y. Geller, L. Pavlova, and G. Sorokin, "Impact-abrasive wear of nitrided tool steels," *Metal Science and Heat Treatment*, vol. 14, no. 1, pp. 48–52, 1972.
- [73] N. Kitaigora, "Impact-abrasion wear resistance of high-chromium cast iron," *Metal Science and Heat Treatment*, vol. 17, no. 5, pp. 417–420, 1975.
- [74] O. Komarov, V. Ivashkin, and N. Urbanovich, "Mechanism of surface layer hardening in impact-abrasive wear of high-chromium cast iron," *Metal Science and Heat Treatment*, vol. 32, no. 4, pp. 278–280, 1990.
- [75] G. Sorokin, L. Bobrova, and B. Matveevskii, "Effect of electroslog remelting on the impact-abrasive wear resistance of steel D7KhFN," *Metal Science and Heat Treatment*, vol. 21, no. 3, pp. 234–236, 1979.
- [76] E. Badisch, S. Ilo, and R. Polak, "Multivariable Modeling of Impact-Abrasion Wear Rates in Metal Matrix-Carbide Composite Materials," *Tribology Letters*, vol. 36, pp. 55–62, 2009.
- [77] X. Deng, Z. Wang, Y. Tian, T. Fu, and G. Wang, "An investigation of mechanical property and three-body impact abrasive wear behavior of a 0.27% C dual phase steel," *Materials & Design*, vol. 49, pp. 220–225, 2013.
- [78] A. Sundström, J. Rendón, and M. Olsson, "Wear behaviour of some low alloyed steels under combined impact/abrasion contact conditions," *Wear*, vol. 250, pp. 744–754, 2001.
- [79] H. Wang, Q. Zhang, and H. Shao, "Behaviours of austenite under impact abrasion," *Acta Metallurgica Sinica (English edition)*, vol. 4, no. 1, pp. 37–42, 1991.

- [80] M. Fiset, G. Huard, M. Grenier, C. Jacob, and G. Comeau, “Three-body impact-abrasion laboratory testing for grinding ball materials,” *Wear*, vol. 217, pp. 271–275, 1998.
- [81] E. Badisch, H. Winkelmann, and F. Franek, “High-temperature cyclic impact abrasion testing: wear behaviour of single and multiphase materials up to 750 °C,” *Estonian Journal of Engineering*, vol. 15, no. 4, pp. 359–366, 2009.
- [82] D. Kennedy and M. Hashmi, “Test rig design and experimental results of coated systems under impact abrasion conditions,” *Surface and Coatings Technology*, vol. 86–87, pp. 493–497, 1996.
- [83] X. Deng, Z. Wang, Y. Han, H. Zhao, and G. Wang, “Microstructure and Abrasive Wear Behavior of Medium Carbon Low Alloy Martensitic Abrasion Resistant Steel,” *Journal of Iron and Steel Research, International*, vol. 21, pp. 98–103, 2014.
- [84] J. Rendón and M. Olsson, “Abrasive wear resistance of some commercial abrasion resistant steels evaluated by laboratory test methods,” *Wear*, vol. 267, pp. 2055–2061, 2009.
- [85] K. Osara, *Characterization of Abrasion, Impact-Abrasion and Impact Wear of Selected Materials*, Doctoral T. Tampere: Tampere University of Technology, 2001.
- [86] M. Petrica, M. Painsi, E. Badisch, and T. Peinsitt, “Wear Mechanisms on Martensitic Steels Generated by Different Rock Types in Two-Body Conditions,” *Tribology Letters*, vol. 53, pp. 607–616, 2014.
- [87] M. Petrica, C. Katsich, E. Badisch, and F. Kremsner, “Study of abrasive wear phenomena in dry and slurry 3-body conditions,” *Tribology International*, vol. 64, pp. 196–203, 2013.
- [88] “G190-06 Standard Guide for Developing and Selecting Wear Tests,” ASTM International, 2007, pp. 1–5.
- [89] C. I. Walker and P. Robbie, “Comparison of some laboratory wear tests and field wear in slurry pumps,” *Wear*, vol. 302, pp. 1026–1034, 2013.
- [90] K. M. Mashloosh and T. S. Eyre, “Abrasive wear and its application to digger teeth,” *Tribology International*, vol. 18, pp. 259–266, 1985.
- [91] J. H. Tylczak, J. A. Hawk, and R. D. Wilson, “A comparison of laboratory abrasion and field wear results,” *Wear*, vol. 225–229, pp. 1059–1069, 1999.
- [92] J. E. Fernández, R. Vijande, R. Tucho, J. Rodríguez, and A. Martín, “Materials selection to excavator teeth in mining industry,” *Wear*, vol. 250, pp. 11–18, 2001.

- [93] C. Spero, D. J. Hargreaves, R. K. Kirkcaldie, and H. J. Flitt, "Review of test methods for abrasive wear in ore grinding," *Wear*, vol. 146, pp. 389–408, 1991.
- [94] C. Aldrich, "Consumption of steel grinding media in mills – A review," *Minerals Engineering*, vol. 49, pp. 77–91, 2013.
- [95] M. Lindroos, K. Valtonen, A. Kemppainen, A. Laukkanen, K. Holmberg, and V.-T. Kuokkala, "Wear behavior and work hardening of high strength steels in high stress abrasion," *Wear*, vol. 322–323, pp. 32–40, 2015.
- [96] K. Holmberg, "Tribological accelerated testing," *Tribologia - Finnish Journal of Tribology*, vol. 9, no. 3–4, pp. 13–35, 1990.
- [97] R. Blickensderfer, "Design criteria and correction factors for field wear testing," *Wear*, vol. 122, pp. 165–182, 1988.
- [98] M. J. Neale and M. Gee, Eds., "Appendix B: Recommended detailed test procedures for the various tests," in *A Guide to Wear Problems and Testing for Industry*, Suffolk: William Andrew Publishing, 2001, pp. 123–138.
- [99] "G65-04 Standard Test Method for Measuring Abrasion Using the Dry Sand / Rubber Wheel Apparatus," ASTM International, 2010, pp. 1–12.
- [100] "G105-89 (Reapproved 1997) Standard Test Method for Conducting Wet Sand/Rubber Wheel Abrasion Tests," in *Annual book of ASTM standards*, vol. 03.02, 2001.
- [101] P. Hosseini and P. Radziszewski, "Combined study of wear and abrasive fragmentation using Steel Wheel Abrasion Test," *Wear*, vol. 271, pp. 689–696, 2011.
- [102] M. Varga, H. Rojacz, H. Winkelmann, H. Mayer, and E. Badisch, "Wear reducing effects and temperature dependence of tribolayer formation in harsh environment," *Tribology International*, vol. 65, pp. 190–199, 2013.
- [103] "G132-96 Standard test method for pin abrasion testing," in *Annual book of ASTM standards*, ASTM International, 2001, pp. 553–560.
- [104] J. A. Hawk, R. D. Wilson, J. H. Tylczak, and Ö. N. Doğan, "Laboratory abrasive wear tests: investigation of test methods and alloy correlation," *Wear*, vol. 225–229, pp. 1031–1042, 1999.
- [105] R. Nilsson, F. Svahn, and U. Olofsson, "Relating contact conditions to abrasive wear," *Wear*, vol. 261, pp. 74–78, 2006.
- [106] M. S. Bingley and S. Schnee, "A study of the mechanisms of abrasive wear for ductile metals under wet and dry three-body conditions," *Wear*, vol. 258, pp. 50–61, 2005.

- [107] L. Fang, X. Kong, and Q. Zhou, "A wear tester capable of monitoring and evaluating the movement pattern of abrasive particles in three-body abrasion," *Wear*, vol. 159, pp. 115–120, 1992.
- [108] "G81-97a Standard test method for jaw crusher gouging abrasion test," in *Annual book of ASTM standards*, ASTM International, 1997, pp. 354–359.
- [109] G. I. Laird, "Repetitive-and single-blow impact testing of wear-resistant alloys," *Journal of Testing and Evaluation*, vol. 23, no. 5, pp. 333–340, 1995.
- [110] E. Sarlin, M. Apostol, M. Lindroos, V.-T. Kuokkala, J. Vuorinen, T. Lepistö, and M. Vippola, "Impact properties of novel corrosion resistant hybrid structures," *Composite Structures*, vol. 108, pp. 886–893, 2014.
- [111] E. Sarlin, M. Lindroos, M. Apostol, V.-T. Kuokkala, J. Vuorinen, T. Lepistö, and M. Vippola, "The effect of test parameters on the impact resistance of a stainless steel/rubber/composite hybrid structure," *Composite Structures*, vol. 113, pp. 469–475, 2014.
- [112] M. Lindroos, V. Ratia, M. Apostol, K. Valtonen, A. Laukkanen, W. Molnar, K. Holmberg, and V.-T. Kuokkala, "The effect of impact conditions on the wear and deformation behavior of wear resistant steels," *Wear*, vol. 328–329, pp. 197–205, 2015.
- [113] W. Molnar, S. Nugent, M. Lindroos, M. Apostol, and M. Varga, "Ballistic and numerical simulation of impacting goods on conveyor belt rubber," *Polymer Testing*, vol. 42, pp. 1–7, 2015.
- [114] M. Lindroos, M. Apostol, V.-T. Kuokkala, A. Laukkanen, K. Valtonen, K. Holmberg, and O. Oja, "Experimental study on the behavior of wear resistant steels under high velocity single particle impacts," *International Journal of Impact Engineering*, vol. 78, pp. 114–127, 2015.
- [115] K. Osara and T. Tiainen, "Three-body impact wear study on conventional and new P/M + HIPed wear resistant materials," *Wear*, vol. 250, pp. 785–794, 2001.
- [116] T. Slatter, R. Lewis, and A. H. Jones, "The influence of induction hardening on the impact wear resistance of compacted graphite iron (CGI)," *Wear*, vol. 270, pp. 302–311, 2011.
- [117] T. Slatter, R. Lewis, and A. H. Jones, "The influence of cryogenic processing on wear on the impact wear resistance of low carbon steel and lamellar graphite cast iron," *Wear*, vol. 271, pp. 1481–1489, 2011.
- [118] R. Blickensderfer and B. L. Forkner, "Bureau of Mines Report of Investigations 8794: A Ball-on-Block Impact-Spalling Wear Test and Results on Several Iron Alloys." United States Department of the Interior, pp. 1–18, 1983.

- [119] J.-M. Kivinen, V.-M. Järvenpää, and J. Montonen, “A new experimental ball-on-block impact-spalling wear test environment,” in *Proceedings of 13th Nordic Symposium on Tribology Nordtrib 2008*, 2008, pp. 1–9.
- [120] B. Zhang, W. Shen, Y. Liu, X. Tang, and Y. Wang, “Microstructures of surface white layer and internal white adiabatic shear band,” *Wear*, vol. 211, pp. 164–168, 1997.
- [121] Y. Yang, H.-S. Fang, Y. Zheng, Z. Yang, and Z.-L. Jiang, “The failure models induced by white layers during impact wear,” *Wear*, vol. 185, pp. 17–22, 1995.
- [122] R. Tarbe, *Abrasive Impact Wear: Tester, Wear and Grindability Studies*, Doctoral T. Tallinn: TUT Press, 2009.
- [123] M. Petrica, E. Badisch, and T. Peinsitt, “Abrasive wear mechanisms and their relation to rock properties,” *Wear*, vol. 308, pp. 86–94, 2013.
- [124] F. C. Bond, “Lab equipment and tests help predict metal consumption in crushing and grinding units,” *Engineering & Mining Journal*, vol. 165, no. 6, pp. 169–172, 1964.
- [125] Z. Xu, “Capability of nodular eutectic and austenite–bainite polyphase structure to resist impact abrasive wear,” *Wear*, vol. 253, pp. 597–603, 2002.
- [126] H. Winkelmann, E. Badisch, M. Varga, and H. Danninger, “Wear Mechanisms at High Temperatures. Part 3: Changes of the Wear Mechanism in the Continuous Impact Abrasion Test with Increasing Testing Temperature,” *Tribology Letters*, vol. 37, pp. 419–429, 2009.
- [127] F. Franek, M. Kirchgaßner, and E. Badisch, “Advanced Methods for Characterisation of Abrasion / Erosion Resistance of Wear Protection Materials,” *FME Transactions*, vol. 37, pp. 61–70, 2009.
- [128] E. Badisch, C. Katsich, H. Winkelmann, F. Franek, and M. Roy, “Wear behaviour of hardfaced Fe-Cr-C alloy and austenitic steel under 2-body and 3-body conditions at elevated temperature,” *Tribology International*, vol. 43, pp. 1234–1244, 2010.
- [129] H. Winkelmann, E. Badisch, M. Kirchgaßner, and H. Danninger, “Wear mechanisms at high temperatures. Part 1: Wear mechanisms of different Fe-based alloys at elevated temperatures,” *Tribology Letters*, vol. 34, pp. 155–166, 2009.
- [130] H. Winkelmann, M. Varga, E. Badisch, and H. Danninger, “Wear Mechanisms at High Temperatures: Part 2: Temperature Effect on Wear Mechanisms in the Erosion Test,” *Tribology Letters*, vol. 34, pp. 167–175, 2009.
- [131] K. Wang, X.-D. Du, K.-T. Youn, Y. Hayashi, C. G. Lee, and B. H. Koo, “Effect of impact energy on the impact-wear properties of low carbon high manganese alloy steels

- in corrosive conditions,” *Metals and Materials International*, vol. 14, no. 6, pp. 689–693, 2008.
- [132] H. Fu, D. Zou, Z. Jiang, J. Yang, J. Wang, and J. Xing, “A Study of Boron-Bearing Wear-Resistant Alloy Steel Liner,” *Materials and Manufacturing Processes*, vol. 23, no. 5, pp. 469–474, 2008.
- [133] Y. Ma, X. Li, C. Wang, and L. Lu, “Microstructure and Impact Wear Resistance of TiN Reinforced High Manganese Steel Matrix,” *Journal of Iron and Steel Research, International*, vol. 19, no. 7, pp. 60–65, 2012.
- [134] Z. He, Q. Jiang, S. Fu, and J. Xie, “Improved work-hardening ability and wear resistance of austenitic manganese steel under non-severe impact-loading conditions,” *Wear*, vol. 120, pp. 305–319, 1987.
- [135] M. Kirchgaßner, E. Badisch, and F. Franek, “Behaviour of iron-based hardfacing alloys under abrasion and impact,” *Wear*, vol. 265, pp. 772–779, 2008.
- [136] E. Badisch and M. Kirchgaßner, “Influence of welding parameters on microstructure and wear behaviour of a typical NiCrBSi hardfacing alloy reinforced with tungsten carbide,” *Surface and Coatings Technology*, vol. 202, pp. 6016–6022, 2008.
- [137] E. Badisch, M. Kirchgaßner, R. Polak, and F. Franek, “The comparison of wear properties of different Fe- based hardfacing alloys in four kinds of testing methods,” *Tribotest*, vol. 14, pp. 225–233, 2008.
- [138] “Hardox 400 Wear resistant plate,” *Data sheet*, 2011. [Online]. Available: <http://www.ssab.com/en/Products--Services/Products--Solutions/Products/Hardox/Hardox-400/>. [Accessed: 13-Feb-2014].
- [139] N. Ishikawa, K. Ueda, S. Mitao, Y. Murota, and T. Sakiyama, “High-Performance Abrasion-Resistant Steel Plates with Excellent Low-Temperature Toughness,” in *2011 International Symposium on the Recent Developments in Plate Steels*, 2011, pp. 81–92.
- [140] D. J. Naylor and W. T. Cook, “Heat Treated Engineering Steels,” in *Materials Science and Technology*, 2006.
- [141] N. Ojala, K. Valtonen, V. Heino, M. Kallio, J. Aaltonen, P. Siitonen, and V.-T. Kuokkala, “Effects of composition and microstructure on the abrasive wear performance of quenched wear resistant steels,” *Wear*, vol. 317, pp. 225–232, 2014.
- [142] A. K. Bhakat, A. K. Mishra, N. S. Mishra, and S. Jha, “Metallurgical life cycle assessment through prediction of wear for agricultural grade steel,” *Wear*, vol. 257, pp. 338–346, 2004.

- [143] K. Luo and B. Bai, "Microstructure, mechanical properties and high stress abrasive wear behavior of air-cooled MnCrB cast steels," *Materials & Design*, vol. 31, pp. 2510–2516, 2010.
- [144] H. Matsuda, R. Mizuno, Y. Funakawa, K. Seto, S. Matsuoka, and Y. Tanaka, "Effects of auto-tempering behaviour of martensite on mechanical properties of ultra high strength steel sheets," *Journal of Alloys and Compounds*, vol. 577, pp. S661–S667, 2013.
- [145] A. K. Bhakat, A. K. Mishra, and N. S. Mishra, "Characterization of wear and metallurgical properties for development of agricultural grade steel suitable in specific soil conditions," *Wear*, vol. 263, pp. 228–233, 2007.
- [146] X. Ren and J. Zhu, "The effect of substitutional alloying elements on the impact wear rate of medium carbon steels related to delamination and quasi-nanometer wear mechanisms," *Materials Science and Engineering: A*, vol. 528, pp. 7020–7023, 2011.
- [147] "Hardox Extreme Abrasion resistant plate," *Data sheet*, 2013. [Online]. Available: <http://www.ssab.com/en/Products--Services/Products--Solutions/Products/Hardox/Hardox-Extreme/>. [Accessed: 13-Feb-2014].
- [148] "Hardox 500," *Data sheet*, 2013. [Online]. Available: <http://www.ssab.com/en/Products--Services/Products--Solutions/Products/Hardox/Hardox-500/>. [Accessed: 17-Feb-2014].
- [149] "Hardox 600," *Data sheet*, 2013. [Online]. Available: <http://www.ssab.com/en/Products--Services/Products--Solutions/Products/Hardox/Hardox-600/>. [Accessed: 13-Feb-2014].
- [150] "Hardox HiTuf," *Data sheet*, 2013. [Online]. Available: <http://www.ssab.com/en/Products--Services/Products--Solutions/Products/Hardox/Hardox-HiTuf/>. [Accessed: 13-Feb-2014].
- [151] "Dillidur 400 V Water quenched wear resistant steel," *Data sheet*, 2010. [Online]. Available: http://www.dillinger.de/imperia/md/content/dillinger/produkte/marke/dillidur400v_03_2010_e.pdf. [Accessed: 17-Feb-2014].
- [152] "Dillidur 500 V Water quenched wear resistant steel," *Data sheet*, 2010. [Online]. Available: https://www.dillinger.de/imperia/md/content/dillinger/produkte/marke/dillidur500v_03_2010_e.pdf. [Accessed: 17-Feb-2014].
- [153] "Dillidur Impact Water quenched wear resistant steel," *Data sheet*, 2010. [Online]. Available: https://www.dillinger.de/imperia/md/content/dillinger/produkte/marke/dillidur_impact_12_2010_e.pdf. [Accessed: 17-Feb-2014].

- [154] “Abrazo® technical guide: Wear resistant roller quenched steel,” *Data sheet*, 2012. [Online]. Available: [http://www.tatasteeleurope.com/file_source/StaticFiles/Sectors/Lifting_and_Excavating/Abrazo technical guide_V3_low.pdf](http://www.tatasteeleurope.com/file_source/StaticFiles/Sectors/Lifting_and_Excavating/Abrazo%20technical%20guide_V3_low.pdf). [Accessed: 13-Feb-2014].
- [155] “Wear-resistant special structural steel XAR 400,” *Data sheet*, 2013. [Online]. Available: http://grobblech.thyssenkrupp-steel-europe.com/documents/1976/XAR_400_%28WB_703%29_englisch.pdf. [Accessed: 19-Feb-2014].
- [156] “Wear-resistant special structural steel XAR 500,” *Data sheet*, 2012. [Online]. Available: http://grobblech.thyssenkrupp-steel-europe.com/documents/1935/XAR_500_%28WB704%29_englisch.pdf. [Accessed: 17-Feb-2014].
- [157] “Wear-resistant special structural steel XAR HT,” *Data sheet*, 2013. [Online]. Available: http://grobblech.thyssenkrupp-steel-europe.com/documents/1980/XAR_HT_%28WB712%29_englisch.pdf. [Accessed: 17-Feb-2014].
- [158] “Wear-resistant special structural steel XAR 600,” *Data sheet*, 2012. [Online]. Available: [http://grobblech.thyssenkrupp-steel-europe.com/documents/1936/XAR_600_\(WB705_englisch.pdf](http://grobblech.thyssenkrupp-steel-europe.com/documents/1936/XAR_600_(WB705_englisch.pdf). [Accessed: 17-Feb-2014].
- [159] “Verschleißfeste Stähle – BRINAR® 400 / Abrasion Resistant Steels – BRINAR ® 400,” *Data sheet*, 2012. [Online]. Available: http://www.ilsenburger-grobblech.de/MDB/Download/Material_Specification_Sheets/Abrasion_resistant_steel/Abrasion_Resistant_Steels_BRINAR400.pdf. [Accessed: 17-Feb-2014].
- [160] “Verschleißfeste Stähle – BRINAR® 500 / Abrasion Resistant Steels – BRINAR ® 500,” *Data sheet*, 2012. [Online]. Available: http://www.ilsenburger-grobblech.de/fileadmin/mediadb/ilg/produkte/werkstoffblaetter/Abrasion_Resistant_Steels_BRINAR500.pdf. [Accessed: 17-Feb-2014].
- [161] T. Y. Hsu (Xu Zuyao), X. J. Jin, and Y. H. Rong, “Strengthening and toughening mechanisms of quenching–partitioning–tempering (Q–P–T) steels,” *Journal of Alloys and Compounds*, vol. 577, pp. S568–S571, 2013.
- [162] C. Y. Wang, J. Shi, W. Q. Cao, and H. Dong, “Characterization of microstructure obtained by quenching and partitioning process in low alloy martensitic steel,” *Materials Science and Engineering: A*, vol. 527, pp. 3442–3449, 2010.

- [163] S. G. Liu, S. S. Dong, F. Yang, L. Li, B. Hu, F. H. Xiao, Q. Chen, and H. S. Liu, "Application of quenching–partitioning–tempering process and modification to a newly designed ultrahigh carbon steel," *Materials & Design*, vol. 56, pp. 37–43, 2014.
- [164] G. Gao, H. Zhang, Z. Tan, W. Liu, and B. Bai, "A carbide-free bainite/martensite/austenite triplex steel with enhanced mechanical properties treated by a novel quenching–partitioning–tempering process," *Materials Science and Engineering: A*, vol. 559, pp. 165–169, 2013.
- [165] M. Somani, D. Porter, L. Karjalainen, and K. Devesh, "Evaluation of DQ&P Processing Route for the Development of Ultra-high Strength Tough Ductile Steels," *International Journal of Metallurgical Engineering*, vol. 2, no. 2, pp. 154–160, 2013.
- [166] "Raex® wear-resistant steel." Rautaruukki Corporation, pp. 1–7, 2013.
- [167] "Creusabro 4800 datasheet." Sandvik, pp. 1–2, 2013.
- [168] "Ruukki Laser structural steel." Rautaruukki Corporation, pp. 1–5, 2014.
- [169] "Domex 355 MC Hot rolled, high strength, cold forming steel datasheet." SSAB EMEA AB, Borlänge, pp. 1–2, 2011.
- [170] S. Das Bakshi, P. H. H. Shipway, and H. K. D. H. Bhadeshia, "Three-body abrasive wear of fine pearlite , nanostructured bainite and martensite," *Wear*, vol. 308, pp. 46–53, 2013.
- [171] V. G. Efremenko, K. Shimizu, T. Noguchi, A. V. Efremenko, and Y. G. Chabak, "Impact–abrasive–corrosion wear of Fe-based alloys: Influence of microstructure and chemical composition upon wear resistance," *Wear*, vol. 305, pp. 155–165, 2013.
- [172] Y. Cao, Z. Wang, J. Kang, D. Wu, and G. Wang, "Effects of Tempering Temperature and Mo/Ni on Microstructures and Properties of Lath Martensitic Wear-Resistant Steels," *Journal of Iron and Steel Research, International*, vol. 20, pp. 70–75, 2013.
- [173] W. Dudziński, Ł. Konat, and G. Pękalski, "Structural and strength characteristics of wear-resistant martensitic steels," *Archives of Foundry Engineering*, vol. 8, no. 2, pp. 21–26, 2008.
- [174] G. Krauss, "Martensite in steel: strength and structure," *Materials Science and Engineering: A*, vol. 273–275, pp. 40–57, 1999.
- [175] X. Xu, W. Xu, F. H. Ederveen, and S. Van Der Zwaag, "Design of low hardness abrasion resistant steels," *Wear*, vol. 301, pp. 89–93, 2013.

- [176] R. Zhou, Y. Jiang, D. Lu, R. Zhou, and Z. Li, "Development and characterization of a wear resistant bainite/martensite ductile iron by combination of alloying and a controlled cooling heat-treatment," *Wear*, vol. 250, pp. 529–534, 2001.
- [177] M. H. Shaeri, H. Saghafian, and S. G. Shabestari, "Effects of Austempering and Martempering Processes on Amount of Retained Austenite in Cr-Mo Steels (FMU-226) Used in Mill Liner," *Journal of Iron and Steel Research, International*, vol. 17, no. 2, pp. 53–58, 2010.
- [178] P. Shanthraj and M. A. Zikry, "Optimal microstructures for martensitic steels," *Journal of Materials Research*, vol. 27, pp. 1598–1611, 2012.
- [179] S. Morito, H. Yoshida, T. Maki, and X. Huang, "Effect of block size on the strength of lath martensite in low carbon steels," *Materials Science and Engineering: A*, vol. 438–440, pp. 237–240, 2006.
- [180] J. W. Morris, C. Kinney, K. Pytlewski, and Y. Adachi, "Microstructure and cleavage in lath martensitic steels," *Science and Technology of Advanced Materials*, vol. 14, p. 014208 (9pp.), 2013.
- [181] M. R. Green, W. M. Rainforth, M. F. Frolish, and J. H. Beynon, "The effect of microstructure and composition on the rolling contact fatigue behaviour of cast bainitic steels," *Wear*, vol. 263, pp. 756–765, 2007.
- [182] L. Rancel, M. Gómez, S. F. Medina, and I. Gutierrez, "Measurement of bainite packet size and its influence on cleavage fracture in a medium carbon bainitic steel," *Materials Science and Engineering: A*, vol. 530, pp. 21–27, 2011.
- [183] K. Zhu, O. Bouaziz, C. Oberbillig, and M. Huang, "An approach to define the effective lath size controlling yield strength of bainite," *Materials Science and Engineering: A*, vol. 527, pp. 6614–6619, 2010.
- [184] "Helti High degree of agricultural machinery," *Product reference brochure*, 2013. [Online]. Available: <http://www.ruukki.com/References/Agriculture-and-forestry/Helti--High-degree-of-agricultural-machinery-->. [Accessed: 09-Apr-2015].
- [185] "Hardox on site - Roadbuilding," *Product brochure*, 2009. [Online]. Available: http://www.ssab.com/Global/Hardox/Brochures/en/030_Hardox_on_site_roadbuilding_UK.pdf. [Accessed: 09-Apr-2015].
- [186] "Hardox on site - Recycling," *Product brochure*, 2011. [Online]. Available: http://www.ssab.com/Global/Hardox/Brochures/en/119_Hardox_on_site_recycling_UK.pdf. [Accessed: 09-Apr-2015].

- [187] “Hardox on site - Underground mine,” *Product brochure*, 2009. [Online]. Available: http://www.ssab.com/Global/Hardox/Brochures/en/032_Hardox_on_site_underground_mine_UK.pdf. [Accessed: 09-Apr-2015].
- [188] K.-H. Zum Gahr, “Wear by hard particles,” *Tribology International*, vol. 31, pp. 587–596, 1998.
- [189] M. B. Peterson, “Design considerations for effective wear control,” in *Wear Control Handbook*, M. B. Peterson and W. O. Winer, Eds. New York: The American Society of Mechanical Engineers, 1980, pp. 413–473.
- [190] W. D. J. Callister, *Materials science and engineering - an introduction*, 6th ed. USA: John Wiley & Sons, Inc., 2003.
- [191] U. Beste, *On the Nature of Cemented Carbide Wear in Rock Drilling*, Doctoral T. Uppsala: Uppsala University, 2004.
- [192] U. Beste, S. Jacobson, and S. Hogmark, “Rock penetration into cemented carbide drill buttons during rock drilling,” *Wear*, vol. 264, pp. 1142–1151, 2008.
- [193] A. O. Benschoter, “Carbon and alloy steels: metallographic techniques and microstructures,” in *ASM Handbook vol. 9: Metallography and microstructures*, ASM International, 1998, pp. 273–357.
- [194] “G99-95a (Reapproved 2000) Standard test method for wear testing with a pin-on-disk apparatus,” in *Annual book of ASTM standards 3.02*, ASTM International, 2001, pp. 417–422.
- [195] V. Heino, M. Kaipainen, P. Siitonen, V. Ratia, and K. Rissa, “Compressive Crushing of Granite with Wear-Resistant Materials,” in *Proceedings of the 14th Nordic Symposium on Tribology, Nordtrib 2010*, 2010, pp. 1–8.
- [196] J. Terva, V.-T. Kuokkala, and P. Kivikytö-Reponen, “The Edge Effect of Specimens in Abrasive Wear Testing,” *Finnish Journal of Tribology*, vol. 31, no. 3–4, pp. 27–35, 2012.
- [197] H. Rojacz, M. Hutterer, and H. Winkelmann, “High temperature single impact studies on material deformation and fracture behaviour of metal matrix composites and steels,” *Materials Science and Engineering: A*, vol. 562, pp. 39–45, 2013.
- [198] H. Rojacz, G. Mozdzen, H. Winkelmann, and G. Modzen, “Deformation and strain hardening of different steels in impact dominated systems,” *Materials Characterization*, vol. 90, pp. 151–163, 2014.

- [199] “ASTM E 448-82 (Reapproved 1997) Standard practice for scleroscopic hardness testing of metallic materials,” in *Annual book of ASTM standards*, vol. 03.01, Baltimore: ASTM, 2001, pp. 491–495.
- [200] I. I. Garbar, “Correlation between abrasive wear resistance and changes in structure and residual stresses of steels,” *Tribology Letters*, vol. 5, pp. 223–229, 1998.
- [201] G. Sheldon, “Similarities and differences in the erosion behavior of materials,” *Journal of Basic Engineering*, vol. 92, no. 3, pp. 619–626, 1970.
- [202] R. Veinthal, *Characterization and modelling of erosion wear of powder composite materials and coatings*, Doctoral T. Tallinn: Tallinn University of Technology, 2005.
- [203] M. Vite-Torres, J. R. Laguna-Camacho, R. E. Baldenebro-Castillo, E. a. Gallardo-Hernández, E. E. Vera-Cárdenas, and J. Vite-Torres, “Study of solid particle erosion on AISI 420 stainless steel using angular silicon carbide and steel round grit particles,” *Wear*, vol. 301, pp. 383–389, 2013.
- [204] Y. I. Oka, H. Olmogi, T. Hosokawa, and M. Matsumura, “The impact angle dependence of erosion damage caused by solid particle impact,” *Wear*, vol. 203–204, pp. 573–579, 1997.
- [205] Y. I. Oka and K. Nagahashi, “Measurements of plastic strain around indentations caused by the impact of round and angular particles, and the origin of erosion,” *Wear*, vol. 254, pp. 1267–1275, 2003.
- [206] P. Geiderer, *Testing of combined impact-abrasion wear*, Masters th. Wiener Neustadt: University of Applied Sciences Wiener Neustadt, 2005.
- [207] L. Fang, Q. Zhou, and Y. Li, “An explanation of the relation between wear and material hardness in three-body abrasion,” *Wear*, vol. 151, pp. 313–321, 1991.
- [208] G.-C. Ji, C.-J. Li, Y.-Y. Wang, and W.-Y. Li, “Microstructural characterization and abrasive wear performance of HVOF sprayed Cr₃C₂-NiCr coating,” *Surface and Coatings Technology*, vol. 200, pp. 6749–6757, 2006.
- [209] I. Konyashin and B. Ries, “Wear damage of cemented carbides with different combinations of WC mean grain size and Co content. Part II: Laboratory performance tests on rock cutting and drilling,” *International Journal of Refractory Metals and Hard Materials*, vol. 45, pp. 230–237, 2014.
- [210] E. A. Gharahbagh, J. Rostami, and A. M. Palomino, “New soil abrasion testing method for soft ground tunneling applications,” *Tunnelling and Underground Space Technology*, vol. 26, pp. 604–613, 2011.

- [211] L. Fang, X. L. Kong, J. Y. Su, and Q. D. Zhou, "Movement patterns of abrasive particles in three- body abrasion," *Wear*, vol. 162–164, no. B, pp. 782–789, 1993.
- [212] O. Engler and V. Randle, "Evaluation and representation of macrotexture data," in *Introduction to Texture Analysis*, 2nd ed., no. Chapter 9, Boca Raton: CRC Press, 2010, pp. 123–172.

APPENDIX: ORIGINAL PUBLICATIONS

Publication I

Vilma Ratia, Kati Valtonen, Anu Kemppainen and Veli-Tapani Kuokkala

High-stress abrasion and impact-abrasion testing of wear resistant steels

Tribology Online 8 (2013) 152-161

<http://doi.org/10.2474/trol.8.152>

© 2013 Japanese Society of Tribologists
Reprinted with permission

Article

High-Stress Abrasion and Impact-Abrasion Testing of Wear Resistant Steels

Vilma Ratia^{1)*}, Kati Valtonen¹⁾, Anu Kemppainen²⁾ and Veli-Tapani Kuokkala¹⁾

¹⁾Tampere University of Technology, Department of Materials Science, Tampere Wear Center
P.O.Box 589, 33101 Tampere, Finland

²⁾Ruukki Metals Inc.

P.O.Box 93, 92101 Raahe, Finland

*Corresponding author: vilma.ratia@tut.fi

(Manuscript received 10 March 2012; accepted 15 January 2013; published 15 February 2013)
(Presented at Technical Session in the International Tribology Conference Hiroshima 2011)

Energy can be saved by enhancing the service life of machinery and by designing lighter units. These design changes enable, for example, lower fuel consumption and larger payloads. The implementation of this kind of solutions, however, requires development of better wear resistant materials. In this study, the wear resistance of a structural steel and three grades of wear resistant steel was evaluated with granite abrasive in tests simulating the conditions in heavy machinery in mining and transportation. Two high-stress abrasion and one impact-abrasion wear testing methods were used. In all tests, higher hardness led to decreased mass loss, but in impact-abrasion the hardness dependence was smaller than in the heavy abrasion tests. This may, however, at least partly result from deformation of softer materials over the sample edges, which is not shown as mass loss. Wear surfaces of structural steel samples exhibited the highest degree of plastic deformation due to their lower hardness and higher ductility compared to the wear resistant steels. On the other hand, in harder materials the scratches were more visible, indicating a change in wear mechanism. Both differences and similarities in the behavior and wear mechanisms of the selected steels were observed in the applied conditions.

Keywords: abrasion, hardness, impact, steel, wear

1. Introduction

Severe conditions in earthmoving and mining cause heavy wear in equipment used in the field. For example, it has been estimated that 6350 kg of steel is used for replacements per excavation bucket in just six months [1]. In the development towards less energy consumption, besides reducing the use of materials, energy can be saved by enhancing the service life of machinery and by designing lighter units. Lighter units enable less fuel consumption and larger payloads. However, the implementation of these solutions requires the use of more durable materials.

The suitability of materials for a certain application can be assessed by field and laboratory testing. Laboratory testing enables controlled conditions and lower costs. In laboratory tests, however, the testing conditions need to be simplified in order to create a well controlled system. Wear testing is often conducted by using industrial abrasives of a narrow size distribution for better control of the abrasive properties. On the other

hand, to simulate the real conditions properly, also testing with natural abrasives is important.

In applications such as earthmoving and mining machinery, the gravel and minerals generate heavy abrasion and impact wear. Moreover, the material can be subjected to several different kinds of conditions during its service. Loading, unloading and transportation all cause slightly different conditions to the tipper body, as the movement of the abrasive relative to the material surface and the applied load vary. Thus, more than one type of testing with various conditions and parameters is needed to assess the wear properties of the materials. In this work, the wear of selected steel grades was studied using natural granite as an abrasive in three different test procedures to simulate the severe conditions in these kinds of applications. Two high-stress abrasion and one high-stress impact-abrasion methods were used.

One of the classifications of abrasive wear is the division into high-stress abrasion and low-stress abrasion. In high-stress abrasion, the stress in the wear area is sufficient to cause crushing of the abrasive. In low-stress

abrasion, the abrasives remain intact. [2] In all testing methods used in this study, crushing of the abrasives occurs. Thus, based on this classification, they all are high-stress abrasion testing methods.

In earlier studies [3-5], similar impact-abrasion wear testing equipment has been used in addition to, for example, dry sand rubber wheel or pin-on-disc testing. However, the particle size used in the latter mentioned abrasive testing methods has been typically much smaller than the one used in impact-abrasion testing, i.e., 40-300 μm compared to 1.6-25 mm.

Rendón and Olsson [3] compared the results of impeller-tumbler and pin-on-disc with abrasive paper. 12-20 mm quartzite gravel was used in the impeller-tumbler tests and SiC paper of mesh 320 in the pin-on-disc tests. The authors observed clear differences in the resulting wear surfaces and formed tribolayers under the surface: the impeller-tumbler produced a thicker tribolayer with embedded abrasives whereas the samples tested with the pin-on-disc did not have any embedded abrasives. However, in those tests, the abrasive for testing the impact-abrasive and the abrasive wear was not similar and the difference in the grain size was substantial. Moreover, the abrasives in the abrasive wear method were fixed to a paper, causing mainly two-body abrasive wear. Considering mining and transportation applications, the abrasive material is usually loose.

The low and high impact loading impeller-tumbler tests of four hardfacing alloys were compared to standard ASTM G65 rubber wheel test and single impact test results by Badisch et al. [4]. They used 212-300 μm Ottawa silica sand for the ASTM G65 tests and 1.6-2.2 mm silica sand or 5-10 mm corundum for the low and high impact loading tests in impeller-tumbler, respectively. It was found that the performance of the materials in those tests strongly depended on the microstructure. However, although impact, impact-abrasive and abrasive conditions were covered in the testing, the abrasive was different in all methods and thus the significant difference in abrasive properties also had an effect on the results.

Tylczak et al. [5] tested several steel types in the field and in multiple laboratory tests. They used pin-on-drum testing with approximately 100 μm garnet as the abrasive,

ASTM G65 rubber wheel testing with 200-300 μm rounded silica, jaw crusher test with 25.4 mm quartzite, and impeller-tumbler with 19-25 mm quartzite. Increased hardness reduced the wear of the materials with a linear correlation in the abrasive pin-on-drum and ASTM G65 tests. However, the gouging abrasion in jaw crusher and impact-abrasion in impeller-tumbler caused different wear behavior and the correlation between hardness and wear resistance was negligible. This extensive study with several testing methods produced variable wear environments, but there was a notable difference between the used abrasive sizes.

In real-life applications, the used abrasive media causes both impacts and abrasion. Thus, it is important to use comparable abrasives when testing several wear modes with different tests. In the present study, the abrasive was natural stone granite in all testing methods. The particle sizes in the abrasive and impact-abrasive tests were on average 5-6 mm and 11 mm, respectively, so they were close to each other. To correlate to the real life applications, the testing methods were selected to simulate the steps of a transportation process: loading, transportation and unloading. The impact-abrasive impeller-tumbler method simulates loading, where the gravel falls onto the tipper body with abrasion resistant steel plates. Crushing abrasion by the uniaxial crusher method simulates the compaction and transportation of the heavy loads. The unloading, where the load slides on the floor plates of the tipper body, is simulated by the crushing pin-on-disc, in which the samples are subjected to heavy abrasive conditions between a pin and a rotating disc. The study aims to present differences and similarities in the behavior and wear mechanisms of the selected steel grades in versatile heavy abrasion conditions, which are typical for earth moving and mining processes. The results assist the material selection in these applications.

2. Experimental methods

This Chapter presents the tested steels and the abrasive. In addition, the used wear testing methods are introduced together with the analyzing equipment used to determine the mass losses and to characterize the wear surfaces after the tests.

Table 1 Surface hardness and typical mechanical properties of the test materials

Material	Hardness [HB]			Tensile strength R_m [N/mm ²]	Elongation A5 [%]
	Crushing pin-on-disc	Uniaxial crusher	Impeller- tumbler		
S355	162	162	154	430-530	24
Raex 400	368	368	403	1250	10
Raex 450	-	445	456	1450	8
Raex 500	492	469	492	1600	8

Table 2 Parameters of the applied testing methods

Method	Wear type	Motion	Force	Abrasive size
Crushing pin-on-disc	High-stress abrasion	crushing sliding	200 N	2-10 mm
Uniaxial crusher	High-stress abrasion	crushing	53 kN	4-6.3 mm
Impeller-tumbler	High-stress impact-abrasion	impact sliding	N/A	10-12.5 mm

2.1. Materials

The materials studied in this work were a structural steel (S355) and three martensitic wear resistant steels (Raex) manufactured by Ruukki Metals, Inc. Table 1 presents the Brinell hardness values and typical tensile strengths and elongation values of the test materials. The hardness of the same steel grades used in different tests varied, because they were from different batches.

Granite was the abrasive used in all tests, but its size distribution varied slightly with the test method. To minimize the effect of natural variation in the properties of the rock material, the abrasives were all from a single batch from Sorila quarry in Finland. Table 2 presents the size distributions used for different testing methods. The abrasive size distributions were chosen to cause the most severe wear conditions within the limits of the testing devices. The abrasive was crushed and angular in shape.

2.2. Methods

The materials were tested using two high-stress abrasive and one high-stress impact-abrasive wear testing method. The equipment was designed and constructed at the Tampere Wear Center. The differences between the methods are the motion of the sample

surface and the applied force. In the crushing pin-on-disc method, the sample is subjected to both crushing and sliding, whereas in the uniaxial crushing method the motion is uniaxial and there is no sliding movement between the sample and the counterpart. In the current tests, the applied force was substantially higher in the uniaxial crusher, approximately 265 times that in the crushing pin-on-disc. In the impeller-tumbler method, the sample is subjected to both impacts and sliding of loose abrasives. Table 2 presents the characteristic parameters of each testing method. All tests were conducted at room temperature.

2.2.1 Crushing pin-on-disc

The crushing pin-on-disc test method [6], which is based on the common pin-on-disc principle, was used to determine the abrasion wear resistance of the test materials. In the crushing pin-on-disc method, loose abrasive is placed between the rotating disc and the pin, which is cyclically pressed against the abrasive. Figure 1 illustrates the crushing pin-on-disc device. The pin and the disc are not in direct contact at any point of the test.

In the current tests, the pin sample was a solid cylinder with a diameter of 36 mm, creating a wear area of 1000 mm². The orientation of the sample pin was not fixed and thus it could rotate around its own axis to cause even wear throughout the sample surface. The diameter of the disc was 160 mm. The used discs were structural steel for the S355 and wear resistant steel for Raex samples. Table 3 presents the hardness of the used discs. The rotating speed of the disc was 28 rpm and the sliding distance of the pin center point during the test

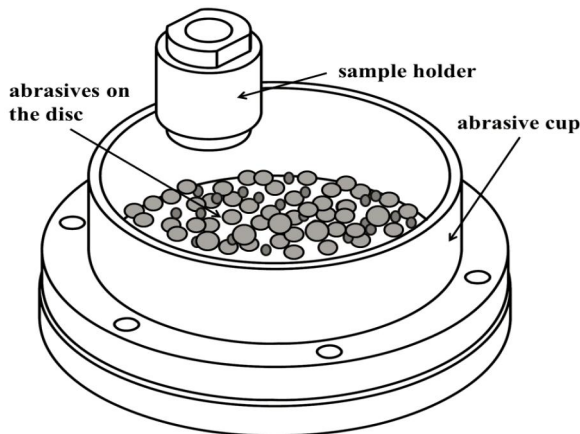


Fig. 1 Crushing pin-on-disc wear test device

Table 3 Hardness of the discs used in crushing pin-on-disc

Disc	Hardness [HB]
S355	205
Raex 400	461
Raex 500	520

Table 4 The abrasive size distribution used in the crushing pin-on-disc testing method

Size distribution [mm]	Mass [g]
2-4	50
4-6.3	250
6.3-8	150
8-10	50
Σ	500

approximately 120 m. The force used in the current tests was 200 N.

Table 4 presents the size distribution of the abrasive mixture used in the tests. This distribution causes efficient wear in the samples in this testing method. The total amount of gravel in one test was 500 g. The abrasive in the cup was not changed during the test, which led to changing testing conditions due to comminution of the abrasive by crushing. However, the abrasive in the pin-rock interface was replenished between each crush by cyclically lifting the pin above the gravel bed. The pin was cyclically pressed down for 5 s and then lifted up for 2.5 s for the abrasive to change in the pin-rock interface due to the rotation of the disc. The duration of the test was 30 minutes, which equals approximately 240 compressions and 20 minutes of contact time. To reach the steady-state wear, the samples were subjected to a 20 minute running-in stage before the actual test. The standard deviation of the results obtained with the crushing pin-on-disc method is on average 7%.

2.2.2 Uniaxial crusher

The uniaxial crusher method [7] was used to evaluate the durability of the test materials under plain compression by the abrasive media. Figure 2 presents the crushing section of the uniaxial crusher device. In the present study, the gravel was crushed between the sample and the tool steel counterpart with hardness of 690 HV in a rubber cup. The movement of the sample is vertical, so the sample and the counterpart do not move in relation to each other. For every compression, the gravel is replaced using an automatic supply tube that fills the cup. A rotary actuator tilts the cup to empty it from the crushed abrasive at the end of each cycle. The used abrasive was granite of the size distribution 4-6.3 mm. This size enabled steady removal and replacement of the abrasive.

The samples were similar to those used in the crushing pin-on-disc tests, having a wear surface of 1000 mm². The used force was 53 kN. The running-in stage included 100 compressions, and the duration of the actual test was 900 compressions. The standard deviation of the results with this method is approximately 15%.

2.2.3 Impeller-tumbler

The impeller-tumbler wear tester was used to measure the impact-abrasion wear resistance of the test

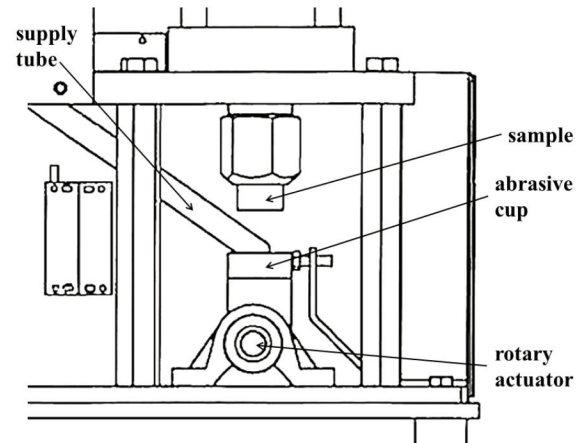


Fig. 2 Crushing section of the uniaxial crusher device

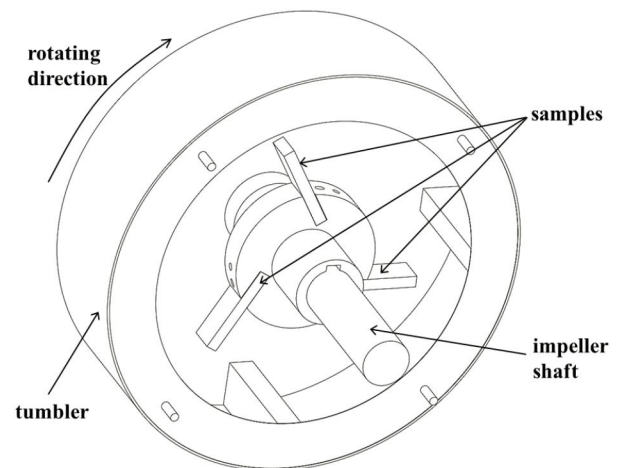


Fig. 3 Impeller-tumbler wear test device

materials. Figure 3 presents a schematic picture of the impeller-tumbler device. The samples act as impeller blades attached to the sample holder, and the tumbler contains the gravel. Both the impeller and the tumbler rotate in the same direction at rotation speeds of 700 rpm and 30 rpm, respectively. During the test, the samples are impacted and scratched by the moving abrasives, which are kept in motion with the tumbler. The diameter of the tumbler is 350 mm.

In the present tests, the sample size was 75 × 25 × 5 mm, of which 1200 mm² constituted the wear surface. The distance from the outer edge of the sample to the center of the sample holder was approximately 105 mm. The samples were attached at a 60° angle to the sample holder perimeter. It must, however, be emphasized that the sample angle in this method is not equal to the abrasive incidence angle, as the abrasive particles are loose and move freely inside the tumbler and thus impact the samples at arbitrary angles.

The duration of each test was 60 minutes. The

samples were weighted and the abrasive was renewed every 15 minutes. The running-in stage was 15 minutes. Three samples were tested simultaneously, one of which was always a Raex 400 reference sample. This enabled accounting for the effects of property variance of the natural abrasives. The samples were circulated in the sample holder slots to exclude the possible effects of the sample positions. The reference sample was kept in the same slot for the whole test to provide steady conditions for it. The mass losses were calculated as an average of the result from three samples in relation to the mass loss of the reference sample. The standard deviation of the results was less than 3%.

The used abrasive was granite of 10-12.5 mm in size. Larger particle size correlates with higher wear rates, which is why a larger abrasive size was used with the impeller-tumbler than with the other methods. The amount of gravel in the tumbler was 900 g. As the abrasive was renewed every 15 minutes, the total amount of abrasive in a 60 minute test was 3600 g. The particle count was approximately 410 in each 900 g gravel batch.

2.2.4 Analyzing methods

The wear rate was determined by measuring the mass loss during the test. The samples were cleaned with pressurized air or ethanol before weighting. The accuracy of the used balance was 0.001 g.

Veeco Wyko NT1100 optical profilometer was used for surface roughness measurements. The measurements were conducted with 5x objective and 0.5 field of view lens. The results were filtered using the median 3 filter.

The Vickers hardness HV0.1 of the worn samples was measured with Matsuzawa MMT-X7 microhardness tester from the cross sections as close to the surface as possible to reveal the possible work hardening of the material. The penetration depth in the wear scars was determined from the cross-sections with Leica DM 2500 M optical microscope. The cross sections from the length of 5 mm were studied and the maximum depth of each distinguishable scar inside the 5 mm region was

measured.

The wear surfaces were characterized with Leica MZ 7.5 zoom stereomicroscope and Philips XL30 scanning electron microscope (SEM). The samples were cleaned in ultrasonic bath and sputtered with a thin layer of gold to avoid charging of the abrasive remnants on the surface.

3. Results

In this Chapter, the wear test results and their correlation to the mechanical properties are presented. Moreover, the characterization of wear surfaces by surface roughness, penetration depth and hardness measurements are presented along with observations made by optical and electron microscopy.

3.1. Wear tests

The wear rate of the samples was determined by mass loss measurements. The effect of the abrasive remnants on the mass loss measurements was minimized by doing a running-in phase to all samples. In this way, the steady state of wear was reached before starting the actual test.

3.1.1 Crushing pin-on-disc

Figure 4 presents the mass loss results for the pins in the crushing pin-on-disc tests. The mass loss of S355 was much higher than that of the wear resistant steels. The difference between the wear resistant steels was evident as well, the mass loss of Raex 500 being approximately 30% lower than the mass loss of Raex 400.

3.1.2 Uniaxial crusher

Figure 5 presents the mass loss results from the uniaxial crusher tests. The mass loss of S355 was more than double compared to the wear resistant steels. On the other hand, the wear resistant steels showed smaller differences between each other than in the crushing pin-on-disc test.

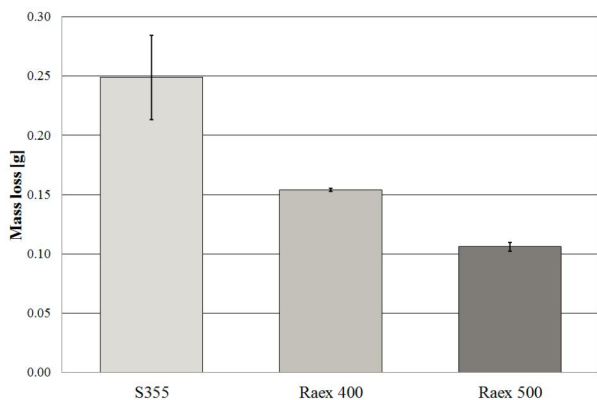


Fig. 4 Crushing pin-on-disc wear test results. The error bars indicate standard deviation

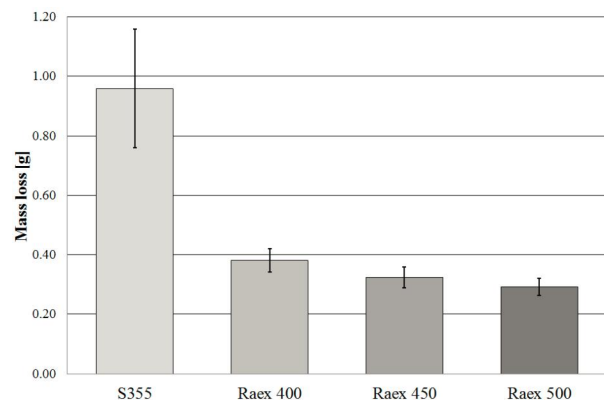


Fig. 5 Uniaxial crusher wear test results. The error bars indicate standard deviation

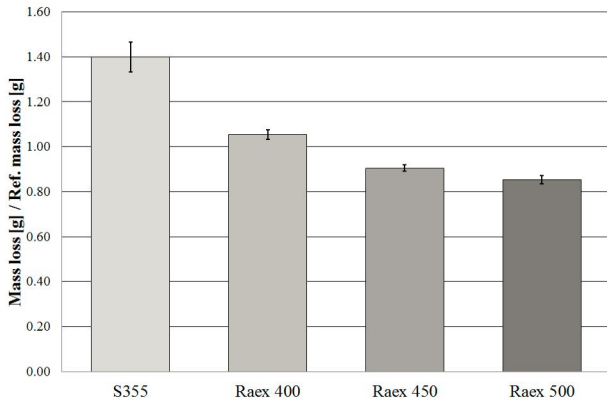


Fig. 6 Impeller-tumbler wear test results. The error bars indicate standard deviation

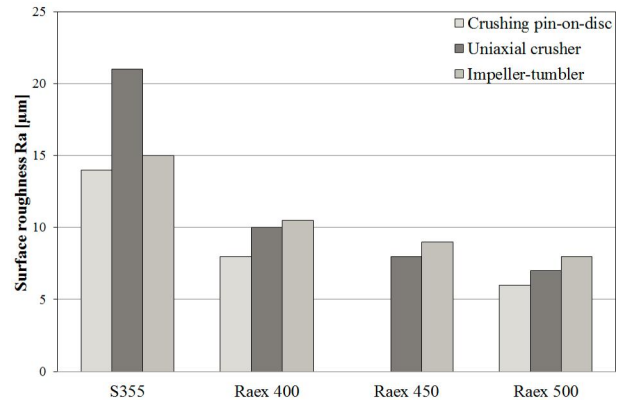


Fig. 8 Ra values for wear tested samples [µm]

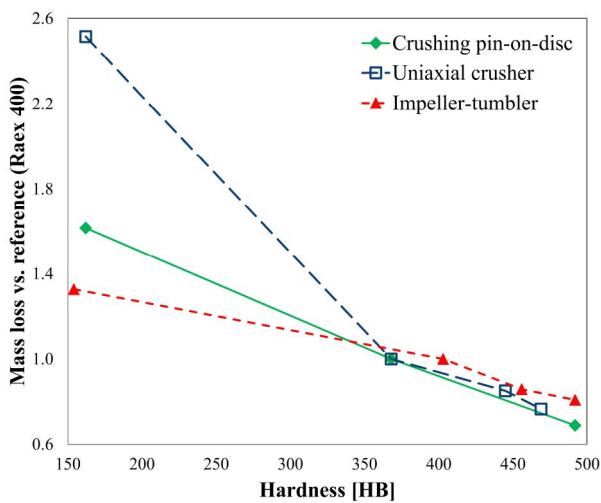


Fig. 7 Results of the wear tests as mass loss vs. material hardness. The mass losses have been normalized by the mass loss of the reference material

3.1.3 Impeller-tumbler

The results of the impeller-tumbler wear tests are presented in Figure 6. The results reveal that the difference between the wear resistant steels and the structural steel is substantially smaller than with other methods used in this study. The difference within the wear resistant steels is similar to that in the uniaxial crusher results.

3.2. Role of mechanical properties

A summary of the wear test results for all test methods in correlation with hardness is presented in Figure 7. To be able to compare the results obtained by different methods and conditions, the results were scaled by the wear rate of the reference material. The used reference material was Raex 400, as it gave reasonably constant results and was thus well suited for a reference material.

In all tests, higher hardness led to lower wear rate, but the strength of this relationship varied. The crushing

pin-on-disc and impeller-tumbler tests produced quite linear curves. For impeller-tumbler results, the correlation of the higher hardness with the reduction of wear was lower than for the other methods. In the uniaxial crusher tests, the difference in the wear rates between the structural steel and wear resistant steels was large. However, in this method the dependence of wear on hardness for the wear resistant steels was much weaker.

The correlation between the wear test results and the ultimate tensile strength was very similar to the correlation between the hardness and wear, which was expected as the tensile strength and hardness usually show a quite linear correspondence. In all methods, higher ultimate tensile strength decreased wear. In impact-abrasion with impeller-tumbler, the dependence was weaker than in the abrasive methods.

Considering the typical elongation or ductility values, higher ductility correlated with higher mass loss results. Again, the strength of the dependence varied with test conditions, abrasive methods producing a stronger correlation than the impact-abrasion method.

3.3. Hardness of the worn surface

The results indicated that work hardening takes place to some extent in all studied steels, but the effect is much smaller in harder steels. In the structural steel, the hardness increased substantially in samples tested with all methods. The increase of hardness in the region down to 50 µm from the surface was 100-160 HV. In wear resistant steels the hardening could not be observed as clearly. In Raex 400, the hardness increased approximately 30-50 HV in the corresponding region. In harder Raex 500, the increase was even smaller. There was no distinct difference observed between the methods.

3.4. Surface roughness measurements

The surface roughness was determined with an optical profilometer. The initial surface roughness of the samples was approximately 0.5 µm. Figure 8 presents the results as an average of five measurements for each

sample. Materials with lower hardness showed in general higher surface roughness values after the tests. In the abrasion tests, the difference between the structural and wear resistant steels was significantly larger than in the impact-abrasion tests. In the high-stress abrasion tests, the surface roughness of the S355 samples was at least 70% higher than that of the wear resistant steels.

3.5. Penetration depths

The deepest individual scars were observed in uniaxial crusher samples, where the deepest scars found in the studied regions were 133 μm for S355 and 71 μm for Raex 500. The uniaxial crusher produced the deepest scars also on average, whereas the crushing pin-on-disc produced the shallowest scars on average. However, the scatter of the measurements was large, as every wear scar is different and therefore the average penetration depth value can be heavily influenced by a few deeper wear scars. When comparing materials, the harder materials had smaller penetration depths both on average and defined by the deepest individual scars within the studied regions.

3.6. Wear surface studies

The wear surfaces of tested samples were characterized using a stereomicroscope and a scanning electron microscope. The stereomicroscope enabled the observation of larger surface formations, while with SEM it was possible to study the wear surfaces in detail. The abrasive remnants were easily distinguished from the steel with a backscatter electron detector (BSE). To provide quantitative information about the amount of abrasive remnants, energy dispersive X-ray spectrometry (EDS) was used.

3.6.1 Crushing pin-on-disc

Both two-body and three-body abrasive wear occurred in all steel samples, and scratches and rolling marks were present on all surfaces. Figure 9 presents a SEM image of a S355 sample with a clear scratch mark on an otherwise evenly deformed wear surface. In the

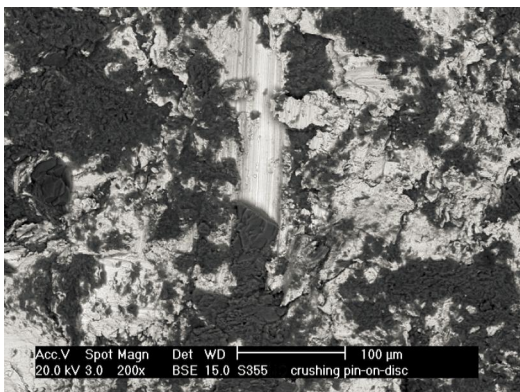


Fig. 9 SEM image of a wear surface of S355 tested with the crushing pin-on-disc (BSE mode)

BSE image, the lighter areas are metal and abrasive remnants are shown as dark.

Signs of both ploughing and cutting were detected on all studied surfaces. The degree of plastic deformation was much higher in the structural steel than in the wear resistant steels, and also the amount of embedded abrasives was much larger. The structural steel had some large burrs on the surface, whereas in the wear resistant steels the formations were more chip-like, smaller and edgier, obviously due to the lower ductility of the material. Signs of severed chips were more visible in harder steels.

The surfaces of wear resistant steels were clearly flatter, as indicated also by the surface roughness measurements. Figure 10 presents shallow scratches on the wear surface of Raex 500. The scratches were more visible in steels with higher hardness. When determining the number of scratches from stereo optical images, the number of detectable scratches was approximately twice as high in Raex 500 as in S355.

3.6.2 Uniaxial crusher

The wear surfaces of the samples tested with the uniaxial crusher revealed indentations, plastic

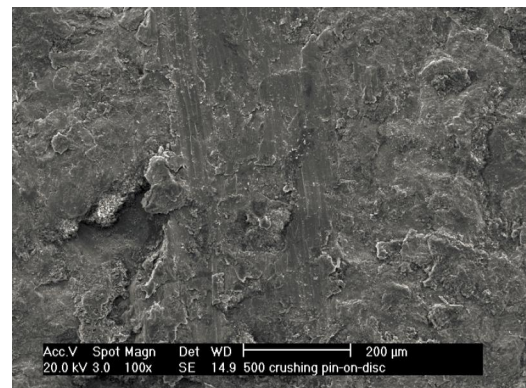


Fig. 10 SEM image of a wear surface of Raex 500 tested with the crushing pin-on-disc

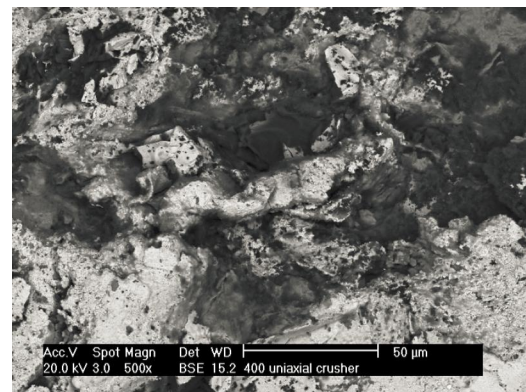


Fig. 11 SEM image of a wear surface of Raex 400 tested with the uniaxial crusher (BSE mode)

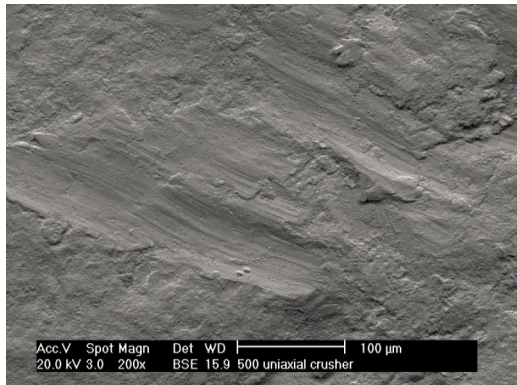


Fig. 12 SEM image of a wear surface of Raex 500 tested with the uniaxial crusher (topographic BSE mode)

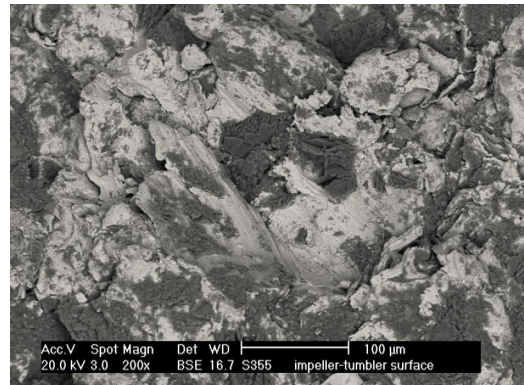


Fig. 15 SEM image of a wear surface of S355 tested with the impeller-tumbler (BSE mode)

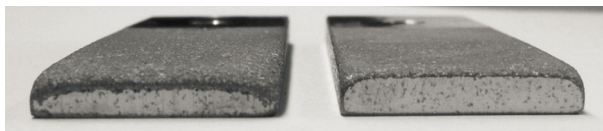


Fig. 13 Impeller-tumbler sample edges of S355 (on the left) and Raex 400 (on the right)

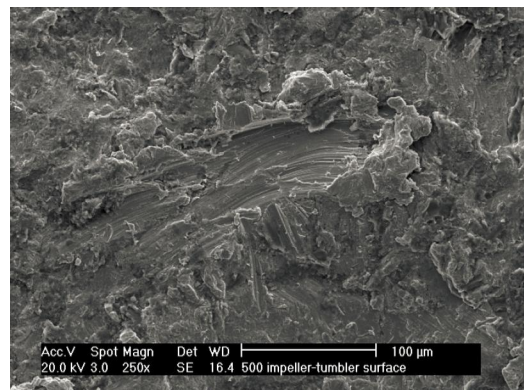


Fig. 16 SEM image of a wear surface of Raex 500 tested with the impeller-tumbler

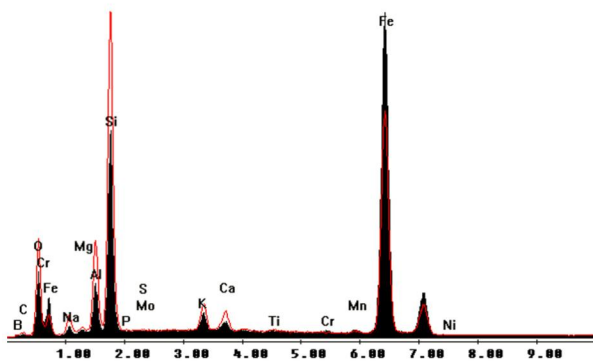


Fig. 14 Comparative EDS spectra from worn surfaces of S355 (red line) and Raex 500 (black graph)

deformation and microscratches. As the rocks in the abrasive bed were crushed, they moved relative to each other and could slide for short distances on the surface of the sample. The structural steel contained more abrasive remnants than the wear resistant steels, but embedded abrasive could be found in all samples. Figure 11 shows dark abrasive remnants on the lighter metal surface of worn Raex 400.

Similarly to the crushing pin-on-disc tests, the structural steel was severely deformed while the harder materials exhibited flatter and smoother surfaces. On the other hand, there were more well-defined short scratches in the harder materials. Figure 12 presents a SEM image of scratches on the surface of Raex 500.

3.6.3 Impeller-tumbler

In the samples tested with the impeller-tumbler, wear was most severe in the sample edges. Figure 13 shows the edges of the structural steel and Raex 400 samples. In both samples the edges are clearly rounded, but in the structural steel the rounding is much heavier and the material has been displaced over the sample's edge as a burr. In the wear resistant steel only slight burring was observed.

When studying the wear surfaces in the center areas of the samples, the structural steel contained more abrasive remnants compared to the wear resistant steels. Figure 14 presents EDS spectra from both S355 and Raex 500 impeller-tumbler wear surfaces. Compared to Raex 500, the analysis from the S355 surface contains considerably more silicon, aluminum and potassium, which are the major elements in granite [8]. This also indicates a larger amount of embedded rock on the S355 surface.

Figure 15 presents a heavily deformed wear surface of S355 with extensive ploughing, wedges and chips. In the wear resistant steels, the chips and wedges were smaller and the degree of deformation was lower. It

seemed that besides scratching, wear has occurred largely by the removal of the formerly deformed areas through the following impacts.

Figure 16 presents a scratch on the wear surface of Raex 500. In general the scratches were more well-defined and the surfaces smoother in the harder materials. When determining the number of scratches from the stereo optical images, the number of detectable scratches was approximately twice as high in Raex 500 as in S355.

4. Discussion

In agreement with the common observation, also in the current tests higher hardness correlated with better wear resistance, but the degree of this relation varied with the applied wear conditions. In general, a harder material resists the penetration of the abrasive through its higher surface hardness and strength, decreasing the wear rate. For samples tested in the impact-abrasion conditions (i.e., the impeller-tumbler tests), the positive effect of hardness was substantially smaller than for the high-stress abrasion methods. Also Rendón et al. [3] and Hawk et al. [9] have reported that in the impeller-tumbler tests the change in the wear rate can be notably small even for relatively large changes in the alloy hardness.

The results of this study, however, could at least partly be connected to edge-concentrated wear. The sample edges were not shielded in any of the applied test types, but in the impeller-tumbler samples the wear of the edges was clearly most severe. One explanation for the relatively low wear rate (as quantified by the mass loss) of the structural steel in the impeller-tumbler tests is the higher ductility that enables the material to deform around the edges by forming a burr without actual removal of the material. In the wear resistant steels only very small burrs could be observed, which suggests that the removal of the material in the edges occurs mostly by cutting and cracking of the deformed edges.

In order to enable the comparison of the abrasion wear resistance of materials in the center areas of the sample, i.e., to exclude the edge effects, the tests should be conducted with shielded edges. Especially in the impeller-tumbler tests, wear at the sample edges possibly dominates the measured mass losses. However, the wear of the edges correlates well with the real wear conditions in the tipper body, where the edge part of the tail plate is subjected to most severe wear.

There were some similarities in the wear surfaces produced by all testing methods. All the studied wear surfaces were plastically deformed and contained abrasive remnants on the surface. The structural steel was always the most heavily deformed and contained most abrasive remnants. On the other hand, the most distinct scratches were found in the harder steels in all methods.

However, the differences in the wear conditions and their effects on the steels' behavior could be easily detected also on the wear surfaces. In the structural steel

samples, wear was most severe in samples tested with the uniaxial crusher, where the relative mass loss, surface roughness and penetration depth values were clearly the highest of all samples. This is a direct result of the much higher forces applied in this test method.

In the impeller-tumbler test, the nature of the contact between the abrasive and the sample is more of an impact than in the other test methods. Sundström et al. [10] have determined the ratio of impact and abrasion to be 100/1 in a similar type test equipment. In the structural steel the material can be more easily deformed and displaced than removed due to its higher ductility compared to wear resistant steels, in which the material seems to be more easily cut away from the surface by impacts. This decreases the effect of hardness on the wear rate.

The crushing pin-on-disc is a three-body abrasion test method, and thus the effect of the counterpart cannot be excluded. Axén et al. [11] stated that the amount of rolling increases as the hardness of the counterpart material increases. In their study, self-mated steel surfaces in three-body abrasion showed about equal amounts of rolling and sliding. In the tests of the present study, the counterpart was slightly harder than the sample, possibly promoting rolling of abrasives on the pin sample. Differences in the behavior of the pin materials could be observed. Based on wear surface examination, the amount of scratching increased as the material hardness increased. Both the surface roughness and penetration depth were the smallest for Raex 500 in this method, suggesting that even when the amount of scratches was higher, they were only shallow and thus did not cause substantial material removal. The similarity of the hardness of the Raex 500 pin and the disc, and thus the higher pin/disc hardness ratio compared to the other tested materials, may have promoted sliding on the Raex 500 pin surface in this method. However, higher amount of scratches was observed also in the Raex 400 pin.

For all methods, harder materials contained more scratches. This was basically for two reasons: in these materials less deformation occurs to cover the previous scratches, and the proportion of sliding is higher than in softer materials. The increased sliding results from the ability of the harder material to resist the penetration of the abrasives. For an angular abrasive to roll, some deformation, either elastic or plastic, must occur in the surface. The harder surface resists this more, thus increasing the propensity to sliding instead of rolling. Gore and Gates [12] reported that increased specimen hardness led to a transition from rolling to sliding of the abrasive particles in three-body abrasive wear, which agrees with the wear scars found in this study. Also Fang et al. [13] observed more scratches in harder materials in their study concentrating on abrasive wear in materials with a wide range of hardness. For impeller-tumbler, a same kind of observation about the scratches, although less defined, was done by Sundström et al. [10].

5. Conclusions

For all materials and test methods used in this study, higher hardness led to decreased mass loss. The strength of this dependence, however, varied depending on the test method and other properties of the materials. Impact-abrasion showed the weakest dependence on hardness, possibly due to the concentration of wear by cutting on the specimen edges. In this case, the higher ductility of the structural steel enabled the material to deform and create burrs over the sample edges without actual loss of material.

In all testing methods, the degree of plastic deformation was the highest in the structural steel, which was the softest material. On the other hand, in harder materials the scratches were more well-defined and visible, indicating a change in the wear mechanism. For an angular abrasive to roll, some kind of deformation must occur in the surface. The harder surface resists this more, increasing the possibility of sliding. The lower degree of plastic deformation was also not sufficient to cover the formed scratches as effectively as in the softer materials.

This study shows that the performance of different steels depends on the conditions of abrasive wear. The used test methods complement each other and provide useful laboratory scale simulations of the wear conditions typical in earth moving and mining.

Acknowledgements

The work has been done within FIMECC Ltd and its DEMAPP program. We gratefully acknowledge the financial support from Tekes and the participating companies.

References

- [1] Hawk, J. A. and Wilson, R. D., "Tribology of Earthmoving, Mining, and Minerals Processing," in *Modern Tribology Handbook*, Vol. 2, Bhushan, B. (ed.), CRC Press, Boca Raton, 2000.
- [2] Zum Gahr, K.-H. (ed.), "Grooving Wear," in *Tribology Series*, Vol. 10, Elsevier, Amsterdam, 1987, p. 132.
- [3] Rendón, J. and Olsson, M., "Abrasive Wear Resistance of Some Commercial Abrasion Resistant Steels Evaluated by Laboratory Test Methods," *Wear*, 267, 11, 2009, 2055-2061.
- [4] Badisch, E., Kirchgaßner, M., Polak, R. and Franek, F., "The Comparison of Wear Properties of Different Fe-Based Hardfacing Alloys in Four Kinds of Testing Methods," *Tribotest*, 14, 4, 2008, 225-233.
- [5] Tylczak, J. H., Hawk, J. A. and Wilson, R. D., "A Comparison of Laboratory Abrasion and Field Wear Results," *Wear*, 225-229, 2, 1999, 1059-1069.
- [6] Terva, J., Teeri, T., Kuokkala, V.-T., Siitonen, P. and Liimatainen, J., "Abrasive Wear of Steel against Gravel with Different Rock-Steel Combinations," *Wear*, 267, 11, 2009, 1821-1831.
- [7] Heino, V., Kaipainen, M., Siitonen, P., Ratia, V., Valtonen, K., Lepistö, T and Kuokkala, V.-T., "Compressive Crushing of Granite with Wear-Resistant Materials," *Finnish Journal of Tribology*, 30, 1-2, 2011, 21-28.
- [8] Silva, B. and Aira, N., Martínez-Cortizas, A., Prieto, B., "Chemical Composition and Origion of Black Patinas on Granite," *Science of the Total Environment*, 408, 1, 2009, 130-137.
- [9] Hawk, J. A., Wilson, R. D., Tylczak, J. H. and Doğan, Ö. N., "Laboratory Abrasive Wear Tests: Investigation of Test Methods and Alloy Correlation," *Wear*, 225-229, 2, 1999, 1031-1042.
- [10] Sundström, A., Rendón, J. and Olsson, M., "Wear Behaviour of Some Low Alloyed Steels under Combined Impact/Abrasion Contact Conditions," *Wear*, 250, 1-12, 2001, 744-754.
- [11] Axén, N., Jacobson, S. and Hogmark, S., "Influence of Hardness of the Counterbody in Three-Body Abrasive Wear – An Overlooked Hardness Effect," *Tribology International*, 27, 4, 1994, 233-241.
- [12] Gore, G. J. and Gates, J. D., "Effect of Hardness on Three Very Different Forms of Wear," *Wear*, 203-204, 1997, 544-563.
- [13] Fang, L., Zhou, Q. D. and Li, Y. J., "An Explanation of the Relation between Wear and Material Hardness in Three-Body Abrasion," *Wear*, 151, 2, 1991, 313-321.

Publication II

Vilma Ratia, Kati Valtonen and Veli-Tapani Kuokkala

Impact-abrasion wear of wear resistant steels at perpendicular and tilted angles

*Proceedings of the Institution of Mechanical Engineers Part J: Journal of Engineering
Tribology 227 (2013) 868-877*

<http://doi.org/10.1177/1350650113487831>

© 2013 Sage Publications Ltd
Reprinted with permission

Impact-abrasion wear of wear-resistant steels at perpendicular and tilted angles

Vilma Ratia, Kati Valtonen and Veli-Tapani Kuokkala

Proc IMechE Part J:
J Engineering Tribology
227(8) 868–877
© IMechE 2013
Reprints and permissions:
sagepub.co.uk/journalsPermissions.nav
DOI: 10.1177/1350650113487831
pij.sagepub.com



Abstract

Earth moving and processing machinery has to withstand heavy wear caused by impacts and scratching by the soil. Especially, the edges are subjected to heavy wear. To simulate these conditions, impeller–tumbler impact-abrasion wear testing equipment was used to determine the wear resistance of four steel grades at perpendicular and tilted sample angles. The angles were selected to simulate the loading conditions. Natural granite rock was used as abrasive. The amount of wear was clearly smaller in the harder materials. The significance of hardness was quite similar at both sample angles in the steady-state wear of wear-resistant steels. On the initial state wear, hardness had a slightly greater effect at the perpendicular angle due to more severe wear in sample edges already at the beginning of the test. Overall, the largest differences in wear were observed in the sample edges. At the perpendicular sample angle, the sample edges were much more rounded. Some small differences were observed in the surface formations due to dissimilar movement of the abrasive. Deformed surfaces and fractured lips indicated that wear occurred mainly by the deformation of material followed by the removal of the deformed areas through impacts. In addition, scratches and dents were observed. It was found that larger sized abrasives caused higher mass loss than abrasives of similar mass but smaller size. Moreover, same amount of abrasive particles in each test reduces the scatter of the results.

Keywords

Wear, testing, abrasion, impact, steel, angle

Date received: 15 October 2012; accepted: 5 April 2013

Introduction

Wear is becoming increasingly important in industrial applications, in particular due to its environmental impact through the reduction of the service life of machinery. Extremely heavy wear takes place in construction and mining, where large amounts of rocks and soil are processed. The earth moving machinery has to withstand heavy wear caused by loading and unloading of rocks and soil onto the tipper body, which subjects it to impact-abrasion wear caused by impacts and scratching by the minerals. Wear-resistant steels are often used as a material for this kind of machinery since it has better durability than mild steels and thus provides longer service life.

The impeller–tumbler wear testing method has been widely used for determining the impact-abrasion wear resistance of materials.^{1–7} The method has been used for studying metals and coatings with natural and industrially manufactured abrasives. Since the method is not standardized, the used parameters vary between researchers and laboratories.

Impact-abrasion has similarities to erosive process,¹ especially when induced by smaller particles, i.e. diameter in the range of 1.6–2.2 mm.² Erosion of steels, including the effect of impact angles, has been

studied by many authors. Zum Gahr⁸ concluded that the effect of the impact angle is influenced by several factors, such as particle size, velocity, and the targeted material.

Sheldon⁹ reported erosion wear test results at 10–90° angles for several different materials, including hardened steel. In their tests, the angle of maximum wear depended on the brittle or ductile behaviour of the material. In brittle behaviour, the amount of wear was almost similar at all tested angles. On the other hand, when the behaviour was predominantly ductile, the impact angle for maximum wear of hardened steel was 20°. The change of behaviour was caused only by changing the particle size from 127 µm (brittle) to 8.75 µm (ductile behaviour), indicating that the particle size has a substantial effect on the behaviour of the material.

Tampere Wear Center, Department of Materials Science, Tampere University of Technology, Finland

Corresponding author:

Vilma Ratia, Tampere Wear Center, Department of Materials Science, Tampere University of Technology, Korkeakoulunkatu 6, PO Box 589, 33101 Tampere, Finland.
Email: vilma.ratia@tut.fi

Although the effect of impact angle is well comprehended in erosion of steels, it has not been widely studied with larger particles in impact-abrasive conditions. The test results obtained with relatively small micron-scale particles do not necessarily correlate with the phenomena induced by gravel particles, which are in different magnitude of size. It could be hypothesized that larger particles cause brittle behaviour by default and thus the effect of angle is very small for them, as in the study of Sheldon.⁹ However, as the impact velocity can also have an effect on the dependence between impact angle and erosion rate,^{8,10} brittle behaviour cannot be assumed to occur for larger particles under all conditions. In the tests by Sheldon,⁹ the particle velocity was approximately 150 m/s. This kind of velocity is not likely to be present, for example, in transportation of gravel.

Badisch et al.² studied the effect of morphology, energy and size of the abrasive particles on the wear of materials in impact-abrasion with impeller-tumbler test. The wear rate of materials was tested with a variety of abrasives: steel grit, quartz abrasive, steel balls and glass balls. According to Badisch et al.,² the impact energy of particles is an essential parameter in this kind of test. However, for each particle size, the abrasive was different in their study. Thus it is possible that the properties of the abrasives also have an effect on the wear they produce.

In this study, four grades of steel were tested in impact-abrasion conditions at perpendicular and tilted sample angles. This provides information on the effect of the sample angle on wear in impact conditions, which is lacking in the current literature for large particles. In construction and mining applications it is not always possible to control the incidence angle, but knowledge of the material behaviour under

various conditions helps in the material selection. The applied sample angles were 90° (perpendicular) and 60° (tilted). Angles of this range are present when gravel or other materials being processed are loaded onto tipper bodies, containers, sieves and conveyor belts. This makes the applied impact conditions of the tests to be common in many process stages. Moreover, the effect of particle size on wear is demonstrated comparing the results obtained with two different relatively large particle sizes of the same abrasive.

Materials and methods

Materials

A structural steel (S355) and three grades of martensitic wear-resistant steel were studied. Table 1 presents the typical mechanical properties and alloy compositions of the tested materials. The hardness values were measured at Tampere University of Technology. The other information is provided by the manufacturer of the commercial steels. 400 HB steel was used as a reference material.

Natural stone granite was used as an abrasive in the tests in order to better simulate the real-life conditions. The local differences in the bedrock cause variations in the properties of the granite gravel even within one quarry. To minimize the variations in the gravel properties, a single batch from Sorila quarry in Finland was used. Before conducting the tests, the gravel was sieved to a size distribution of 8–10 mm or 10–12.5 mm. The amount of abrasive loaded in the impeller-tumbler was 900 g, which was replenished every 15 min to ensure efficient wear throughout the test. The total amount of gravel was 3600 g in the 60-min tests and 21,600 g in the 360-min tests.

Table 1. Typical mechanical properties and alloying compositions (max%) of the tested materials.

Material	S355	400 HB	450 HB	500 HB
Hardness (HV)	186 ± 4	395 ± 14	479 ± 11	515 ± 17
Yield strength $R_{p0.2}$ (N/mm ²)	355 ^a	1000	1200	1250
Tensile strength R_m (N/mm ²)	430–530	1250	1450	1600
Elongation A_5 (%)	24	10	8	8
C (wt%)	0.12	0.25	0.26	0.3
Si (wt%)	0.03	0.8	0.8	0.8
Mn (wt%)	1.5	1.7	1.7	1.7
P (wt%)	0.02	0.025	0.025	0.025
S (wt%)	0.015	0.015	0.015	0.015
Cr (wt%)	–	1.5	1	1
Ni (wt%)	–	1	1	1
Mo (wt%)	–	0.5	0.5	0.5
B (wt%)	–	0.005	0.005	0.005
Al (wt%)	0.015 ^b	–	–	–

^aMinimum yield strength, R_{eH} .

^bmin%

Wear testing method

The wear tests were conducted with an impeller–tumbler device,¹¹ which consists of a sample holder shaft and a tumbler, as shown in Figure 1(a). The samples are attached to the sample holder as impellers, which rotate at a high speed (700 r/min) inside the tumbler filled with gravel. The speed at the sample tip was approximately 8 m/s. The tumbler rotates at a lower speed (30 r/min) in the same direction as the impellers to rotate the abrasive particles during the test. The tumbler is sealed with a lid during the test to contain the gravel.

In the developed device, the impellers and the tumbler are separate, which makes mounting and removing the specimens and changing the test conditions easier. The sample angle, rotating velocities of the impeller and the tumbler, and the amount, size and type of the abrasive can be varied.

Two different sample holders were used in the tests in order to vary the sample angle. Figure 1(b) presents a picture of the mounting of the sample. In the holders, the sample is mounted either at a 60° or a 90° angle with respect to the sample holder perimeter. It must be emphasized that the sample angle is not equal to the abrasive incidence angle. The abrasive particles are loose and thus can move freely inside the tumbler, impacting the surface at several angles that cannot be accurately determined.

The sample size was 75×25×10 mm. The sample area subjected to wear was approximately 1200 mm² for both sample holders. The distance from the outer edge of the sample to the centre of the sample holder was approximately 105 mm for the 60° sample angle and 110 mm for the 90° sample angle.

The amount of wear was determined as the mass loss of the sample. Three samples were tested simultaneously in each test, one sample always being the

reference made of 400 HB steel. The reference sample was in a certain slot during the entire test to account for the differences between gravel loads. Thus, the results from different tests are comparable.

To reduce the possible effect of the slot position in the sample holder, the positioning of the samples was altered after each weighing. In all tests, the samples were in both slots for an equal amount of time. The reference sample was always in the third slot.

Tests of two different durations were conducted: short tests lasting 60 min for the initial state wear and longer 360-min tests for determining the steady-state wear. Table 2 presents the number of the samples and the length of tests conducted with the 60° and 90° sample angles. These tests were conducted with 8–10 mm gravel size. Table 3, in turn, presents the tests conducted with 60° angle for determining the effect of rock size on wear and the effect of particle amount on the scatter of the results.

For intermittent weighing during the test, the samples were cleaned with pressurized air to remove the dust. The accuracy of the balance was 0.001 g. In 60-min tests, the samples were weighed every 15 min. In 360-min tests, the samples were weighed every 15 min during the first 120 min of the test. From 120 min onwards, the samples were weighed only every 30 min. The abrasive was always replenished every 15 min.

To study the initial wear mechanisms at both sample angles, the materials were tested for one rotation of the tumbler only. Thus the duration of the test was just 2 s. To be able to observe the individual wear marks as clearly as possible, the samples were polished with 3 μm diamond paste before the tests. For both angles, a sample set consisting of a structural steel, 400 HB steel and 500 HB steel were tested. The used abrasive was 8–10 mm granite with 757 individual particles.

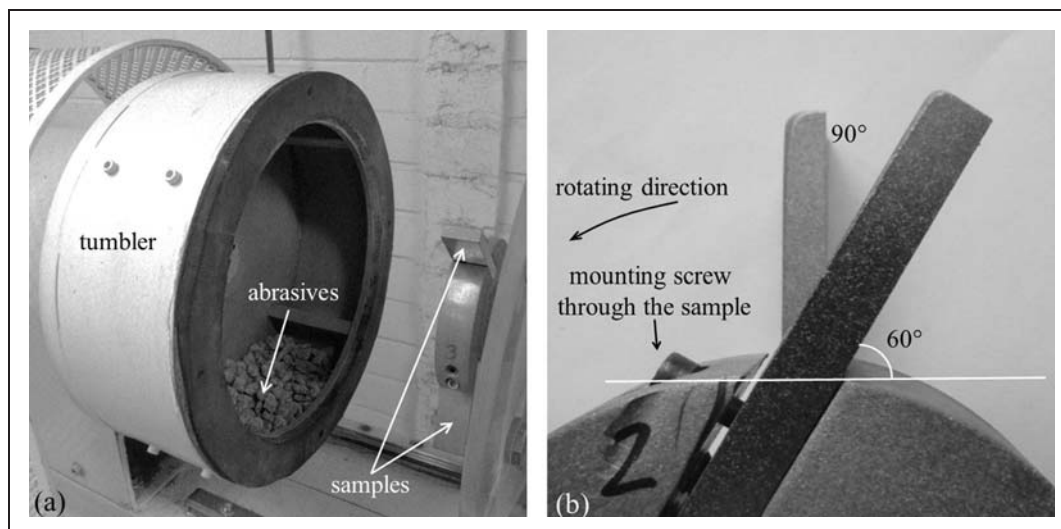


Figure 1. (a) The impeller–tumbler test device and (b) a close-up of mounting of the sample.

Table 2. Number of samples tested for determining the effect of sample angle with 8–10 mm gravel size.

Material	60° sample angle	90° sample angle
S355	3 × 60 min, 1 × 360 min	4 × 60 min, 1 × 360 min
400 HB	3 × 60 min, 1 × 360 min	3 × 60 min, 1 × 360 min
450 HB	3 × 60 min, 1 × 360 min	4 × 60 min, 1 × 360 min
500 HB	3 × 60 min, 1 × 360 min	3 × 60 min, 1 × 360 min

Table 3. Tests conducted for the rock size effect and to determine the scatter of the results.

Granite	Amount of samples	Amount of particles
8–10 mm	9 × 60 min	750–800
10–12.5 mm	3 × 60 min	400–450
10–12.5 mm counted	8 × 60 min	410

Analysing methods

The wear surfaces were examined with Leica MZ 7.5 zoom stereomicroscope and Philips XL 30 scanning electron microscope (SEM). Before the SEM studies, the samples were cleaned with ethanol in ultrasonic bath and sputter coated with a thin layer of gold to avoid charging of the embedded abrasive.

The surface roughness of the samples was measured with Veeco Wyko NT1100 optical profilometer. The used objective lens was 5× and the field of view lens was 0.5, corresponding to the measured area of 2.47 × 1.88 mm. Optical resolution with the used objective was 2.5 μm. The data was processed with a median 3 filter.

The surface hardness measurements were conducted with Duramin-A300 macro hardness tester with a Vickers tip. The used method was HV10 for the wear-resistant steels and HV3 for the structural steel. Each hardness sample was measured five times and the results are averages from two samples.

Results and discussion

Here, the effect of sample angle on the wear is presented and discussed. In addition, the role of particle amount in decreasing the scatter of the results as well as the effect of particle size on wear are discussed. In addition, observations about the wear surfaces are presented and discussed.

Relative mass losses

The results are presented as mass losses of the samples in relation to the mass loss of the 400 HB reference sample in the same test. It shows the performance of the materials in relation to each other, which is essential in material selection. The results give insight into the effect of hardness in different conditions, since in real applications it is often not possible to control the exact angle of incidence. The presented 60-min test results are averages of the results of three or four samples per material.

Table 4 presents the values of the relative wear results. The values of the 400 HB results are not exactly 1.00, as the location of the 400 HB material sample was altered between the sample slots to minimize the effect of slot position, whereas the reference sample was fixed to the same slot throughout the whole test. The standard deviation of all samples was on average less than 4%. The 90° angle results showed slightly smaller scatter than the 60° angle results. The observed scatter agrees quite well with previously reported values, which are typically less than 10%.^{1,3}

Figure 2(a) presents the wear test results of Table 4 as graphs of relative mass loss versus hardness for the 60-min tests at 60° and 90° angles. The trends are the same for both studied angles: as the hardness increases, wear decreases.

As the amount of wear is presented in relation to the reference material, the difference in the mass loss between the two studied angles is in principle not visible and these results represent essentially only the effect of hardness. However, some small differences can be observed. In the 90° tests the dependence of mass loss on hardness is somewhat stronger than in the 60° tests. By examining the samples, it was observed that already in the 60-min tests the 90° samples were more rounded in the edges compared with the 60° samples and therefore wear had been more severe. Wilson and Hawk¹ reported that in their study with similar equipment that the wear of the edges seemed to have a significant effect on wear during the early stages of the test.

Figure 2(b) presents the results from the 360-min tests. The results were determined from the test period of 120–360 min to show only the steady state wear data. The results were quite similar for both tested angles, the difference being only 2–6%. These results show stronger relative wear dependence on the hardness of the material than the 60-min test results. The dependence is quite linear for wear-resistant steels.

Sundström et al.⁴ also reported a linear dependence between abrasive wear and hardness for steels having a similar microstructure but different hardness. In their study, the hardness dependence was linear for both non-martensitic and martensitic steels but the results arranged in separate lines. The same observation can be made from the current results as

Table 4. Values of the relative wear results for 60- and 360-min tests at both sample angles. The relative wear is mass loss of the sample divided by mass loss of the reference sample in the same test.

Material	60° sample angle 0–60 min	90° sample angle 0–60 min	60° sample angle 120–360 min	90° sample angle 120–360 min
S355	1.13 ± 0.13	1.19 ± 0.04	1.39	1.48
400 HB	1.05 ± 0.03	1.04 ± 0.01	1.05	1.03
450 HB	0.95 ± 0.01	0.92 ± 0.01	0.91	0.94
500 HB	0.94 ± 0.05	0.91 ± 0.01	0.85	0.87

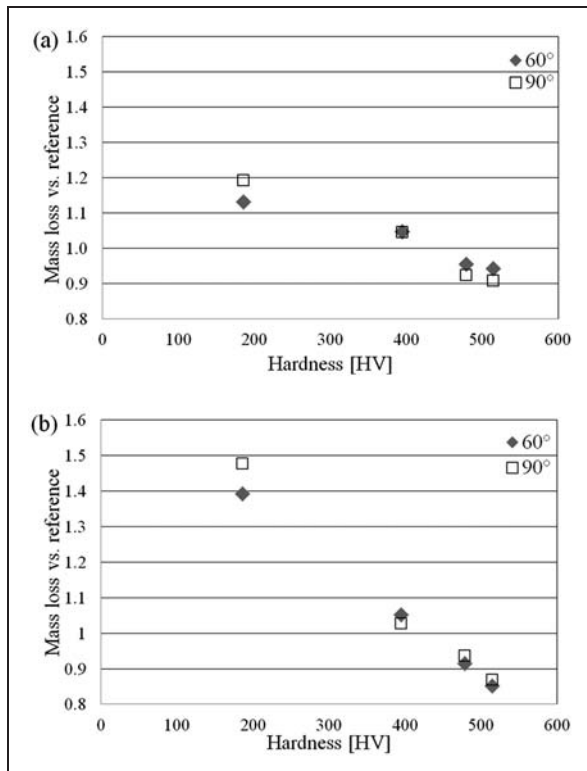


Figure 2. Wear test results of (a) 60- and (b) 360-min tests in relation to sample hardness.

well: wear in martensitic wear-resistant steels (395–515 HV) shows quite linear dependence on hardness.

Figure 3(a) presents the development of mass losses during the test, showing the mass losses of 15-min periods for reference samples. In the 60° tests, the wear rate increased gradually before reaching the steady state in about 120 min, which is why the steady-state data was determined as the mass loss of 120–360 min time period. On the other hand, in the 90° tests, the steady state was reached much sooner, even within 60 min. Thus, as wear in the edges was more severe already in the beginning of the 90° tests, the hardness and strength of the steel assumed a more important role than in the 60° tests.

Figure 3(b) presents a cumulative graph showing the development of mass loss during the 360-min test. The graph is calculated by summing up the results from each measuring period. There are no distinct

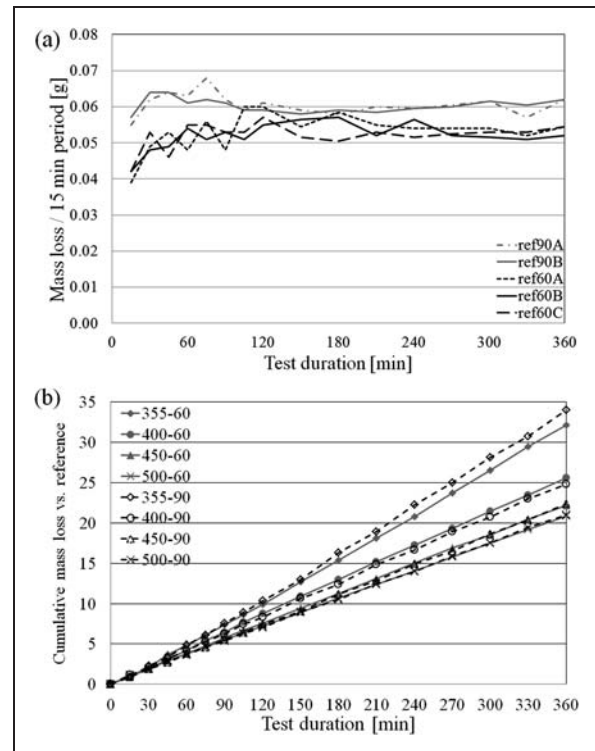


Figure 3. (a) Mass losses during 15-min periods for reference samples and (b) cumulative mass losses of the samples in relation to the reference material in the 360-min tests.

differences between the two different angles regarding these trends. For S355, the wear rate is constantly increasing in relation to the reference material as the test progresses. This can be seen as a steepening slope of the cumulative graph.

One explanation for the increasing wear rate of S355 is the removal of burrs. The burrs develop in the sample edges during the test but are not removed until the edges are worn enough.

Effects of particle size on mass loss and amount of particles on standard deviation

The effect of particle size on the mass loss was determined by comparing the 400 HB reference sample results from the tests conducted with 8–10 mm and 10–12.5 mm rocks, as presented in Table 3. All tests were conducted using the same abrasive mass and 60°

sample angle. Thus only the particle size and amount varied. The particle amount in the 8–10 mm loads was typically 750–800, whereas in the 10–12.5 mm loads, it was 400–450. The size fractions of the abrasives were sieved from the same batch; thus the grain shapes were similar.

Figure 4 presents the mass loss of the reference samples in tests conducted with 8–10 mm and 10–12.5 mm abrasives. The mass loss in the 8–10 mm tests was on average 197 mg with a standard deviation of 9%. For the particle size of 10–12.5 mm, the corresponding values were 255 mg and 7%. It can be concluded that in this type of test, the larger particle size produces more wear.

The effect of particle properties on the wear rate in impact-abrasion has been reported also by Badisch et al.² Their observation was that the higher single particle energy usually led to higher wear rates. This agrees with the results of this study, since particles with larger size and mass have larger energy.

To study the scatter-reducing effect of the predetermined particle amount, a set of eight tests was conducted with 10–12.5 mm abrasive of approximately 410 particles using the 60° sample angle. The standard deviation of the results for the reference material samples with predetermined particle amount was 4%, six of the results falling inside a standard deviation of less than 1%. Thus, the standard deviations in the 60° angle tests are smaller when using the same amount of abrasives instead of the same mass, as shown in Figure 4.

Wear surfaces

Figure 5 presents the surface roughness R_q values of the samples tested for 360 min. The values were measured 5 or 10 mm from the edge. The initial surface roughness was approximately 1 μm . For the 90° samples, the measurements were made at both distances to determine the roughness at a similar distance from

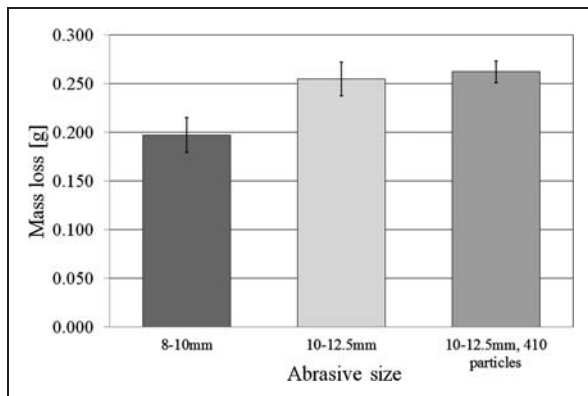


Figure 4. Mass loss of the reference samples with 8–10 mm and 10–12.5 mm abrasives and 10–12.5 mm abrasives with a predetermined particle amount. The sample angle was 60°. The error bars represent the standard deviation.

the sample holder centre as for the 60° samples. The results show only minor differences between the two angles. Softer materials showed higher surface roughness due to the higher plastic deformation.

The impeller–tumbler tests were conducted with edges exposed to wear to provide information on the wear of the edges. In earth moving applications, especially the edge parts, such as the tail plates of the trucks, are subjected to heavy wear. Some mining applications with especially high quantity of edges in impacting conditions are screens, sieves and conveyor belts.

Figure 6 presents the edges of four samples tested at 60° and 90° angles for 360 min. The samples tested at the 90° angle were more rounded than the samples tested at the 60° angle, as can be seen in Figure 6. This difference was visible also in the 60-min samples. In the samples tested at 60° angle, the abrasive particles can probably more easily roll across the sample, causing less wear. The more severe conditions in the sample edge are indicated by the amount of abrasive remnants, which is lower in the 90° samples. The abrasives may not be as easily embedded in the 90° sample edges due to more cutting compared with the 60° samples. The 5 mm longer distance of the 90° sample edge from the centre of the sample holder also subjects the sample edge to slightly higher velocities, what may cause some additional wear.

The S355 samples contained distinct burrs over the edges, as can be seen in Figure 6. The burrs were observed in both 60- and 360-min tests, extending even 1 mm over the sample edge as a result of heavy plastic deformation. The amount of burrs in the wear-resistant steels was substantially smaller due to their lower ductility.

Signs of microcutting and microploughing were visible on the sample surfaces. Also, step-like fractured lip formations were present in all samples. Figure 7(a) presents an SEM image of a step-like formation on the wear surface of 500 HB steel tested for

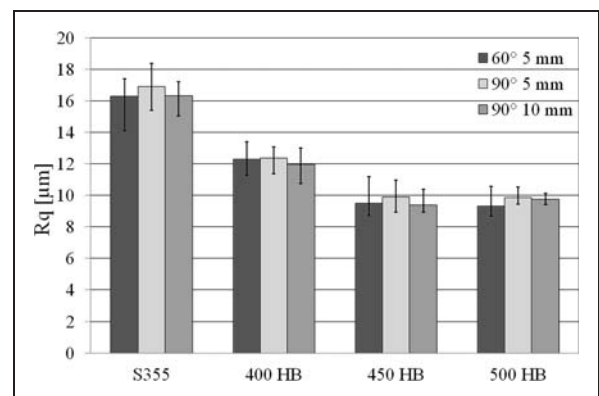


Figure 5. Surface roughness R_q values of materials tested at 60° and 90° angles for 360 min. The error bars show the minimum and maximum values.

360 min. It has probably been formed by the deformation and displacement of thin layers of material, which are removed by subsequent high power impacts. Also, Wilson and Hawk¹ and Sundström et al.⁴ reported that in their tests conducted with a similar method, wear occurred mostly through detachment of deformed material by impacts.

When comparing the wear surfaces of samples tested at 60° and 90° angles, evident similarities and some differences could be observed. All samples showed plastic deformation, dents, lips and abrasive remnants. The amount of dents, however, was slightly higher in the 90° samples. Also the lip formations were wider in these samples compared with the 60° samples. This is probably due to the different movement of the abrasives during the tests: in the 60° samples the abrasives are more likely to roll along the sample surface towards the tip, whereas in the 90° samples, movement also to the sample sides is more probable.

In the studies of Sheldon,⁹ enlarging the particle size caused the erosion behaviour of hardened steel to be predominantly brittle and the erosion rate was similar at all impact angles, whereas in ductile behaviour induced by smaller particles, the 60° and 90° angles had a distinct difference in the wear rate. In the current study, the center areas of wear surfaces of the samples tested at the two angles were quite similar in appearance, indicating that the behaviour of the materials was similar in these conditions. It seems that whereas the movement of the abrasive particles on the samples is slightly different at 60° and 90°

sample angles, the particle size at this impacting velocity is inducing large enough impact energy to produce essentially similar material behaviour.

When comparing the two different types of test materials, the wear surfaces of the S355 samples were more heavily deformed and rougher than those of the wear-resistant steels. The S355 samples also contained more abrasive remnants on the surface compared with the harder materials. Figure 7(b) presents a backscatter electron SEM image of the wear surface of an S355 sample tested for 360 min. The abrasive remnants are shown as dark and metal as light areas.

In wear-resistant steels, the scratches were more clearly defined. Such observations have been made also by Sundström et al.⁴ The harder material resists the penetration of an abrasive particle, enabling it to slide or roll on the surface for longer distances.

In harder materials, the surface formations were more chip-like compared to S355. The formations were also thinner and edgier. This is evidently caused by the higher hardness of the martensitic steels, resisting the penetration and thus leading only to removal of smaller amounts of material. The edginess also results from the lower ductility of the harder steels.

Initial stages of wear

Samples tested only for one rotation of the tumbler were studied in order to obtain information about the

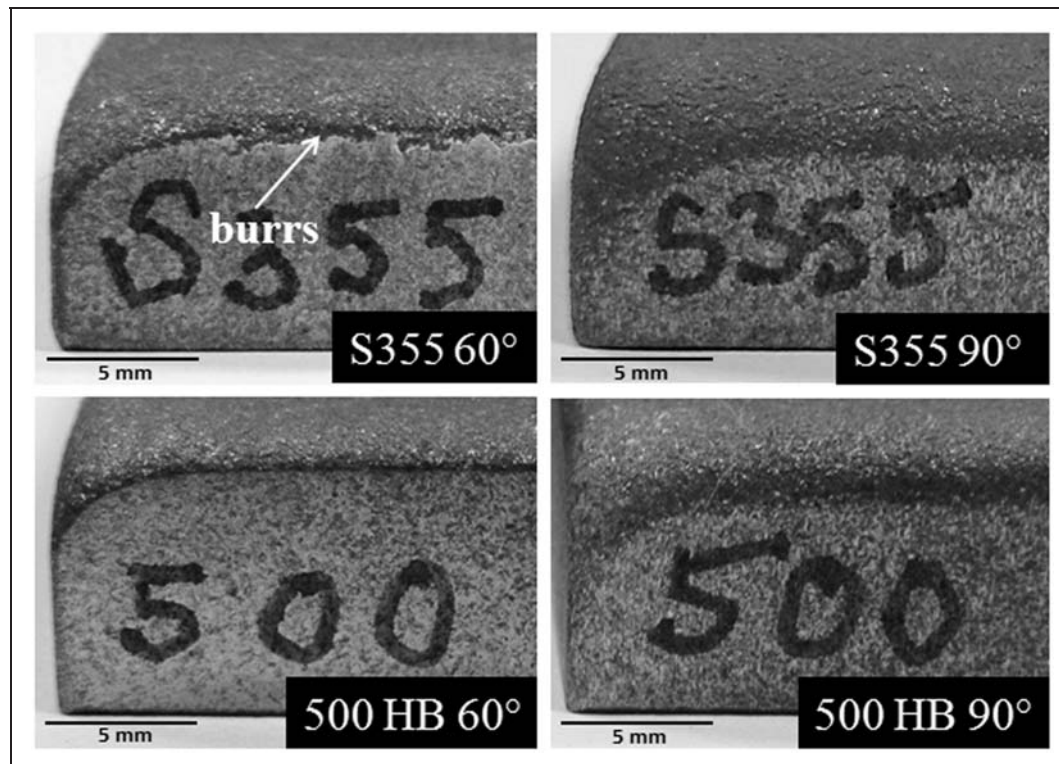


Figure 6. Edges of S355 and 500 HB steel samples tested at 60° and 90° angles.

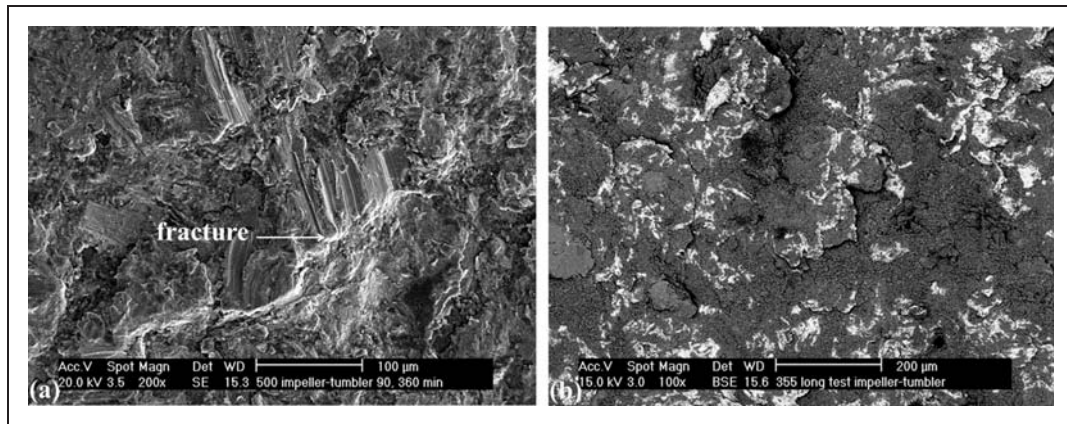


Figure 7. Scanning electron microscope images of wear surfaces with: (a) a step-like formation on the wear surface of 500 HB steel and (b) heavily deformed surface of S355.

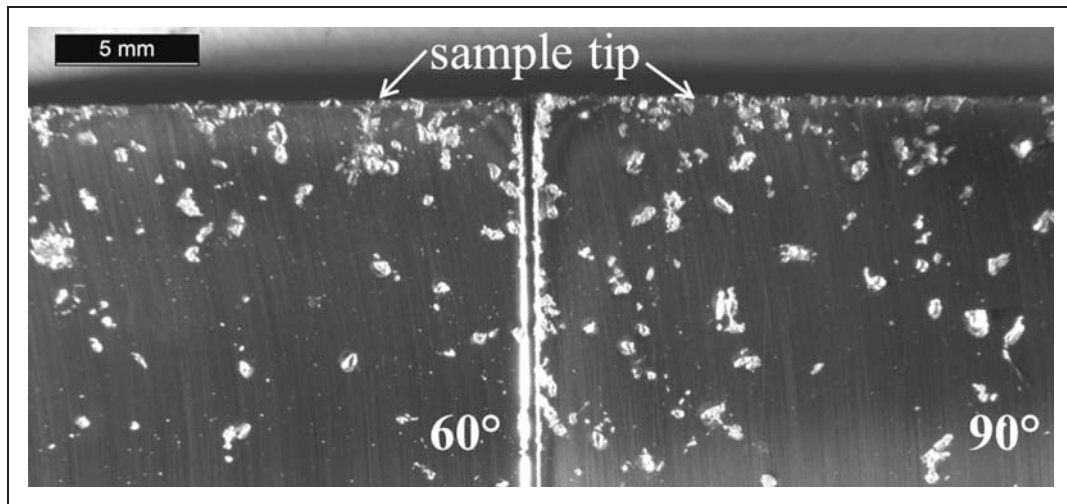


Figure 8. Wear surfaces of S355 samples tested at 60° and 90° angles for 2 s.

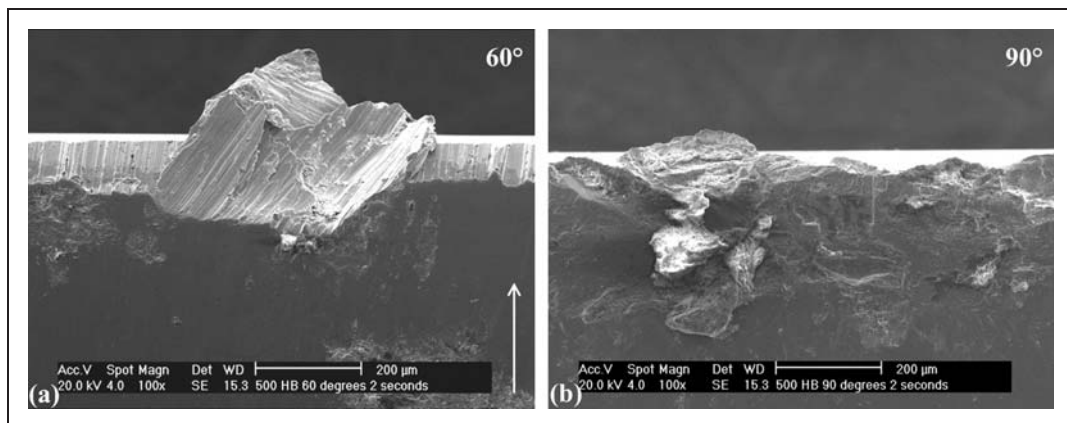


Figure 9. Scanning electron microscope images of single impacts in the edge of a 500 HB steel sample tested at: (a) 60° and (b) 90° angles.

initial stages of wear. As the test duration was only 2 s, no detectable mass loss occurred.

The number of impacts on a sample during one rotation of the tumbler was in the range of 150–220,

of which approximately 90% were within a distance of 20 mm from the sample tip. However, the impacts were unevenly distributed across the specimen face. The 90° samples had experienced slightly more

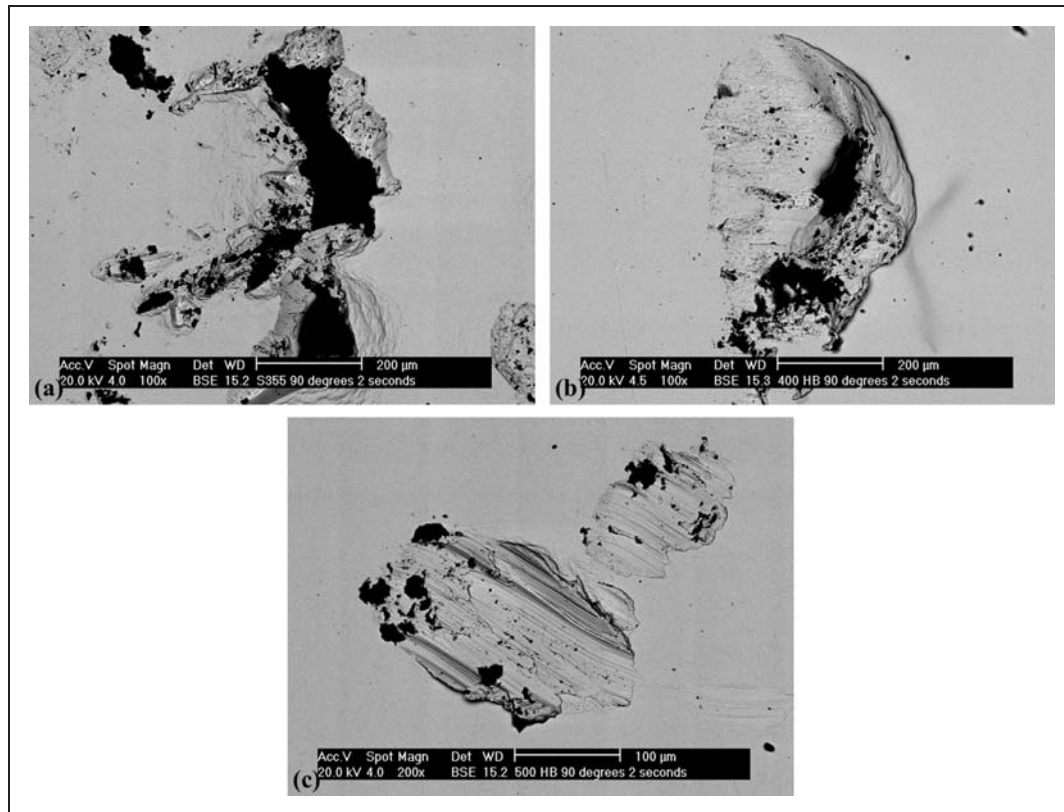


Figure 10. Scanning electron microscope images of single impacts on the polished surface of: (a) S355, (b) 400 HB and (c) 500 HB steels tested at 90° angle for 2 s. The light areas are metal and dark areas are abrasive remnants.

impacts than the 60° samples, possibly due to a bit longer distance of the sample tip from the centre. Moreover, the exact number of the impacts was difficult to determine even from such a short test due to possible multiple impacts in the same area. This was especially challenging in the edges of the samples.

Figure 8 presents the wear surfaces of the S355 samples tested for 2 s. The wear marks were randomly oriented at both testing angles. Some of the marks were even perpendicular compared to the sample movement.

Figure 9 presents impacts in the sample edges of a 500 HB steel tested at 60° and 90° sample angles, showing clearly the difference of the impacts at different angles in the edge area. In the 60° sample, the impact has partly cut material from the edge but for a large part the material has only been deformed over the edge. The direction of the movement of the abrasive towards the tip can also be clearly seen, as indicated by the arrow in Figure 9(a). In the 90° sample, the impact has also led to some deformation over the edge but the marks are shorter and the material seems to be more cut off from the edge. This supports the general conclusion that wear in the edges is both qualitatively and quantitatively different when judged based on edge rounding or burr formation.

The wear mechanisms in the centre area of the sample did not differ distinctly between the two

angles. Between the materials there were, however, some differences. Figure 10 presents backscatter electron SEM images of each material tested for 2 s at 90° angle. There was visible plastic deformation in all steels but in the harder steels, the wear marks were shallower and there seemed to be more cutting caused by the abrasive particles.

Conclusions

- Harder steels have a higher endurance to impact-abrasive wear in the studied hardness range, 180–520 HV. Overall, the significance of hardness is quite similar at both studied sample angles, i.e. 60° and 90° . At 90° , however, hardness has a slightly greater effect on the initial state wear.
- The sample angle has a significant effect on the wear of the sample edges. At 90° , the edges are much more rounded than in the 60° samples.
- In the samples tested with the impeller–tumbler, the main wear mechanisms are the plastic deformation of the material followed by the removal of the deformed areas through impacts. In addition, sliding of the abrasive particles forms scratches on the sample surfaces. The wear mechanisms in center areas of the samples were quite similar at both tested angles.
- Larger abrasive size causes higher mass loss compared with smaller size abrasives of the same total

mass. The scatter of the results decreases when the initial number of abrasive particles in the tests is kept constant.

Funding

The work has been done within FIMECC Ltd and its DEMAPP program. We gratefully acknowledge the financial support from Tekes and the participating companies.

References

1. Wilson RD and Hawk JA. Impeller wear impact-abrasive wear test. *Wear* 1999; 225–229: 1248–1257.
2. Badisch E, Kirchgaßner M and Franek F. Continuous impact/abrasion testing: influence of testing parameters on wear behaviour. *Proc IMechE Part J: J Engineering Tribology* 2009; 223: 741–750.
3. Hawk JA, Wilson RD, Tylczak JH, et al. Laboratory abrasive wear tests: investigation of test methods and alloy correlation. *Wear* 1999; 225–229: 1031–1042.
4. Sundström A, Rendon J and Olsson M. Wear behaviour of some low alloyed steels under combined impact/abrasion contact conditions. *Wear* 2001; 250: 744–754.
5. Kirchgaßner M, Badisch E and Franek F. Behaviour of iron-based hardfacing alloys under abrasion and impact. *Wear* 2008; 265: 772–779.
6. Rendón J and Olsson M. Abrasive wear resistance of some commercial abrasion resistant steels evaluated by laboratory test methods. *Wear* 2009; 267: 2055–2061.
7. Tylczak JH, Hawk JA and Wilson RD. A comparison of laboratory abrasion and field test results. *Wear* 1999; 225–229: 1059–1069.
8. Zum Gahr K-H (ed.) Erosive wear of metals. In: *Microstructure and wear of materials*. Amsterdam, The Netherlands: Elsevier, 1987, pp.535–536.
9. Sheldon GL. Similarities and differences in the erosion behavior of materials. *Trans ASME: J Basic Eng* 1970; 92: 619–626.
10. Castberg TS, Johnsen R and Berget J. Erosion of hard-metals: dependence of WC grain size and distribution, and binder composition. *Wear* 2013; 300: 1–7.
11. Ratia V, Valtonen K, Kemppainen A, et al. High-stress abrasion and impact-abrasion of wear resistant steels. *Tribol Online* 2013; 8: 152–161.

Publication III

Vilma Ratia, Ilkka Miettunen and Veli-Tapani Kuokkala

Surface deformation of steels in impact-abrasion: the effect of sample angle and test duration

Wear 301 (2013) 94-101

<http://doi.org/10.1016/j.wear.2013.01.006>

© 2013 Elsevier B.V.
Reprinted with permission



Surface deformation of steels in impact-abrasion: The effect of sample angle and test duration



Vilma Ratia^{a,*}, Ilkka Miettunen^b, Veli-Tapani Kuokkala^a

^a Tampere University of Technology, Department of Materials Science, Tampere Wear Center, PO Box 589, FI-33101 Tampere, Finland

^b University of Oulu, Centre for Advanced Steels Research, PO Box 4200, FI-90014 Oulu, Finland

ARTICLE INFO

Article history:

Received 31 August 2012

Received in revised form

19 December 2012

Accepted 4 January 2013

Available online 12 January 2013

Keywords:

Wear testing

Abrasion

Impact wear

Steel

Hardness

Surface analysis

ABSTRACT

Wear causes both significant economic and environmental losses by shortening the service life of machinery. Earthmoving machinery is an example of machinery subjected to heavy wear in extreme conditions, where materials suffer from both impacts and scratching by the abrasives. In this work, we have determined the wear surface deformation of four impact-abraded steels to reveal the possible differences between materials and impact conditions. The tested materials include a structural steel and three wear resistant steels with different microstructures. The tests were conducted with impeller-tumbler wear testing equipment. The duration of the tests and the sample angle varied. The longer test duration decreased the relative amount of wear in the harder samples. The sample angle did not have a distinct effect on the wear surfaces in the center areas of the samples. In the edges, however, the larger sample angle caused more wear. Despite some microstructural differences, the correlation between higher hardness and decreased wear was linear in the steady-state wear. The ferrite grains and retained austenite in the martensitic matrix of the 650HB steel had only a small effect on the overall impact-abrasion wear resistance of the material when compared to steels with a fully martensitic microstructure.

© 2013 Elsevier B.V. All rights reserved.

1. Introduction

Wear of materials causes plenty of problems in the industry, such as deterioration of the mechanical strength and dimensional changes of machine components. These lead to additional costs as well as increased environmental burden when the components need to be replaced prematurely. Mining is a branch of industry where heavy wear conditions are common, for example when large amounts of rocks and soil are excavated and moved during the process. This exposes the materials used in the machines such as drills, excavators and transportation equipment to heavy impacts and scratching. The importance of mining and its sustainable and efficient execution is growing, as the natural resources have to be extracted from increasingly challenging locations.

Wear testing can be used as a means to determine the wear resistance of materials in controlled conditions before using them in the field. A widely used method for testing of the impact-abrasion wear properties of materials is the impeller-tumbler method, originally developed for examining the abrasiveness of ores [1]. Impeller-tumblers have been used, for example, to test

the impact-abrasion wear resistance of various steels [2–6] and wearfacing welding alloys [7]. Moreover, the effects of kind and size of different natural and industrial abrasives have been studied [7] along with comparative studies to other laboratory wear testing methods [3,4] and field tests [4]. However, the impeller-tumbler method is not standardized and the parameters used vary.

A typical variable is the test duration, which can range from some tens of minutes [7] to several hours [6,8]. According to Wilson and Hawk [6], who conducted tests with both 1 and 5 h duration, the 1 h tests should be regarded only as indicating the “break in” of the material, whereas 5 h tests give a more realistic wear rate.

The effect of the angle between the sample and the impacting abrasive has not been studied widely, especially not with larger size abrasives. For example, Geiderer [9] has reported that altering the angle results in changes in mass losses. In our previous study [8] it was presented that the effect of steel hardness is similar at 60° and 90° angles, higher hardness decreasing the relative mass loss by the same amount at both angles in steady-state wear.

The aim of this paper is to produce information about the effects of test duration and the sample angle on the wear behavior of selected steels by determining their wear properties in various testing conditions. The better understanding of the wear mechanisms makes the material selection easier for impact-abrasion environment.

* Corresponding author. Tel.: +3584 849 0057; fax: +3583 3115 2330.

E-mail addresses: vilma.ratia@tut.fi (V. Ratia),
ilkka.miettunen@oulu.fi (I. Miettunen),
veli-tapani.kuokkala@tut.fi (V.-T. Kuokkala).

2. Materials and methods

In the following section, the test materials and the methods used for testing and characterizing the wear behavior of these materials are presented.

2.1. Materials

Four steels with different hardness and microstructures were tested. Wear resistant steels have been direct quenched after rolling. Table 1 presents the compositions and some characteristics of the tested steels. One of the materials was a commercial structural steel S355 with ferritic–pearlitic microstructure. The wear resistant steels denoted as 400HB and 500HB are commercial martensitic steels but do not have a standard designation. The 650HB steel is an experimental multiphase-steel with a martensitic microstructure with 5% polygonal ferrite and 10% austenite. The ferrite in the 650HB steel originates from the high aluminum content in the composition. Aluminum is known to raise the A_3 -temperature [10,11]. The wear resistant steels present materials that are used in applications requiring high wear resistance. The structural steel provides a comparison material with more conventional properties.

Natural stone granite from Sorila quarry in Finland was used as abrasive in the tests to simulate conditions in real applications. The shape of the abrasive particles was angular. Before conducting the tests, the gravel was sieved to a size distribution of 8–10 mm.

2.2. Wear testing method

The wear tests were conducted with an impeller–tumbler impact-abrasion wear tester at the Tampere Wear Center. Fig. 1 presents a schematic picture of the device, consisting of an impeller where the samples are acting as blades, and a tumbler containing the gravel. The impeller and the tumbler rotated in the same direction at the rotation speeds of 700 and 30 min^{-1} , respectively. All tests were conducted at room temperature.

Using two different sample holders, the samples were mounted at 60° or 90° sample angle relative to the sample holder tangent, as presented in Fig. 2. The sample angle, however, was not the same as the abrasive incidence angle, because the abrasive particles were loose and could move freely inside the tumbler impacting the sample surface at various angles.

The sample size was 75 × 25 × 10 mm, of which 1200 mm^2 constituted the wear surface. The distance from the sample tip to the center of the sample holder was approximately 105 mm for

60° sample angle and 110 mm for 90° sample angle. The diameter of the tumbler was 350 mm.

Three samples were tested simultaneously in each test, one sample always being a 400HB reference sample. The reference sample was placed in the same sample holder slot during the entire test to account for the differences between gravel loads. The other samples were rotated in the slots after each weighing to exclude the possible effects of the sample position.

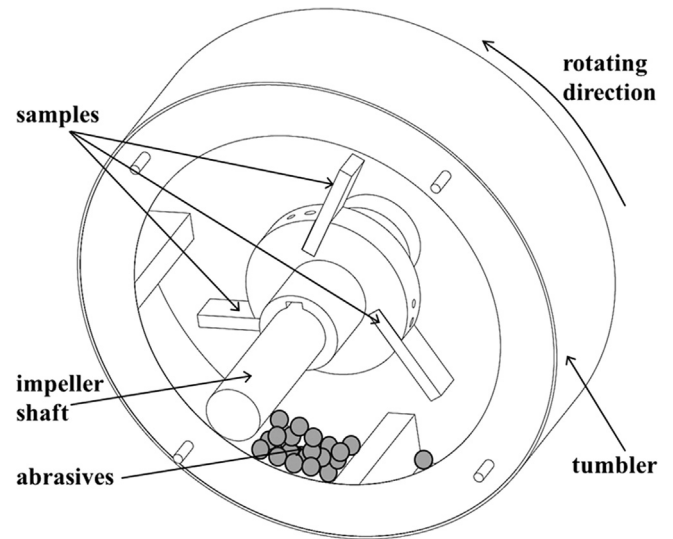


Fig. 1. A schematic picture of the impeller-tumbler wear testing device.

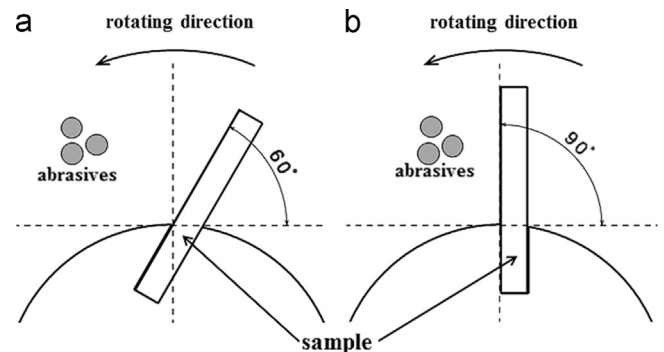


Fig. 2. A schematic picture of the mounting of the samples at (a) 60° and (b) 90° angle.

Table 1

The test materials. The S355, 400HB and 500HB commercial steel compositions are presented as maximum values. The 650HB experimental steel composition has been measured from the batch. In S355 steel, Nb, V, Ti or B may also be used as an alloying element.

Material	S355	400HB	500HB	650HB
Surface hardness [HV]	186	395	515	712
Microstructure	Ferritic–pearlitic	Martensitic with 3% austenite	Martensitic with 4% austenite	Martensitic with 5% ferrite and 10% austenite
Charpy V impact toughness	40 J, –20 °C	20 J, –40 °C	20 J, –30 °C	7 J, 20 °C
C [%]	0.12	0.25	0.3	0.468
Si [%]	0.03	0.8	0.8	0.534
Mn [%]	1.5	1.7	1.7	0.732
P [%]	0.02	0.025	0.025	0.006
S [%]	0.015	0.015	0.015	5–10 ppm
Cr [%]	–	1.5	1	0.215
Ni [%]	–	1	1	0.064
Mo [%]	–	0.5	0.5	0.027
B [%]	–	0.005	0.005	0.001
Al [%]	0.015*	–	–	1.65

* Minimum.

Wear tests with two different durations were conducted. The short tests lasted for 60 min and the longer tests for 360 min. A minimum of three samples of each material were tested for 60 min. For 360 min tests, 1–2 samples of each material were tested. The abrasive gravel was replenished every 15 min to ensure efficient wear conditions throughout the test. One gravel load was 900 g, and the total amount of gravel was 3600 g in 60 min tests and 21,600 g in 360 min tests.

The amount of wear was determined as mass loss by weighing the samples with a scale having the accuracy of 0.001 g. Before weighing, the samples were cleaned with pressurized air to remove the dust. In 60 min tests, the samples were weighed every 15 min. In 360 min tests, the samples were weighed every 15 min during the first 120 min. From 120 min onwards, the samples were weighed only every 30 min.

2.3. Analyzing methods

The HV10 surface hardness of the materials was determined from the unworn surfaces with Duramin-A300 hardness tester. Siemens D5000 X-ray diffractometer was used for determining the amount of retained austenite. The amount of ferrite was determined with point counting method from the etched cross section.

The wear surfaces were analysed by determining their surface roughness and characterizing the wear scars. Moreover, microhardness profiles, penetration depths and microstructural changes were determined from the cross sections of the worn samples. The cross sectional studies were conducted in an area that was at a 5 mm distance from the sample tip.

The wear surfaces and their cross sections were studied with optical and scanning electron microscopes. The wear surfaces were characterized with Leica MZ 7.5 zoom stereomicroscope and cross sections with optical microscope Nikon Eclipse MA 100. Field emission gun scanning electron microscope (FEG-SEM) Zeiss Ultra Plus and Philips XL30 scanning electron microscope (SEM) were used for studying the wear surfaces and determining the microstructural changes in the worn samples. Before SEM studies, the wear surface samples were cleaned in ultrasonic bath with ethanol and sputtered with a thin layer of gold to avoid charging of the abrasive remnants on the surface. The cross sectional samples were mounted, polished and etched with 5% Nital to reveal the microstructures.

The surface roughnesses of the worn samples were measured with Veeco Wyko NT1100 optical profilometer. The measurements were conducted with $5\times$ objective and 0.5 field of view lens and the results were filtered using the median 3 filter. A minimum of five measurements were conducted for each material.

The Vickers hardness HV0.025 of the worn samples were determined with Matsuzawa MMT-X7 microhardness tester. For better precision, the indentations were measured with an optical or scanning electron microscope.

The penetration depths of the wear scars were determined from the cross sections with an optical microscope. The maximum depths of five deepest scars or embedded abrasives inside 1 mm long regions were measured. The cross sections were studied over the total length of 5 mm, and thus the number of the measured depths was 25. The studied area was at a 5–10 mm distance from the sample tip.

3. Results

This section presents the results obtained from wear testing, optical profilometry and hardness measurements. Moreover, the

wear surface examinations and observations made from the cross sectional samples are presented.

3.1. Wear test results

The amount of wear was determined as mass loss during the test. The wear results are presented as mass loss of the sample relative to the mass loss of the 400HB reference sample used in the test in order to account for the possible effect of differences between the gravel loads of natural stone. Consequently, the results do not directly show the differences in the severity of wear between the studied sample angles but reveal the performance of the materials in different conditions. For the 360 min tests, the first 120 min are excluded from the values so that they present only the steady state wear of the materials during 240 min of testing. The standard deviation of the results was on average 3%.

Fig. 3 presents the wear test results. The duration of the test had a distinct effect on wear. The effect of hardness on the reduction of wear was larger in the steady state wear (360 min tests) than in the initial state (60 min tests). When presented in relation to the mass loss of the 400HB reference sample, the wear rate in the harder steels was lower in 360 min test than in 60 min test, whereas for the softest steel S355 the wear rate increased substantially as the duration of the test increased. The difference was for S355 more than 20% at both sample angles.

Fig. 4 presents the mass losses of the 400HB samples in different types of tests. The effect of sample angle can be clearly seen from these values, 90° angle leading to larger mass losses

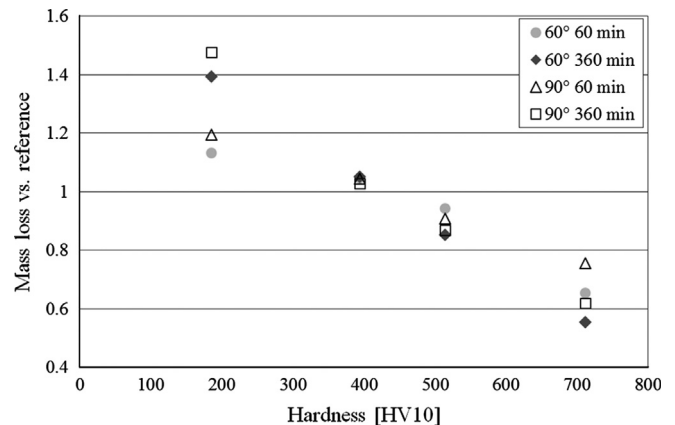


Fig. 3. Wear test results of the impeller-tumbler test in relation to the 400HB reference sample.

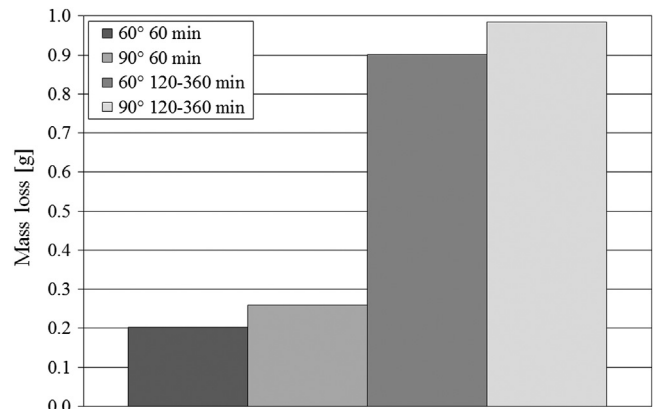


Fig. 4. Mass loss of 400HB samples in the tests.

than the 60° sample angle. This may, however, at least partly be caused by the slightly longer distance of the sample tip from the center of the sample holder, leading to higher speed at the sample tip. Moreover, in the plain mass loss values the possible differences between the gravel loads are not accounted for. Nevertheless, for S355 and 650HB steels also the relative mass losses showed higher values at 90° sample angle.

3.2. Microhardness measurements

In S355, work hardening extended deeper than in the other materials. The hardness immediately next to the surface exceeded 300 HV, which was more than 100 HV higher than the bulk hardness. Even at a distance of 300 μm from the surface the hardness was still over 200 HV.

The surface of the 400HB wear resistant steel was substantially work hardened, and the hardness was over 550 HV at the depth of 20 μm from the surface. Also in the 500HB wear resistant steel the hardness was clearly increased, but the effective depth was less than in the softer wear resistant steel. In the 650HB steel, however, the hardened depth seemed to be slightly larger than in the 500HB steel, which could be related to the behaviour of soft ferrite islands or austenite amongst the hard martensite.

The test duration also seems to have an effect on the work hardening, and in general the samples tested for 360 min showed slightly higher hardness values in the surface compared to the 60 min samples. As regards the effect of the sample angle, it seemed that there was no distinct difference between the angles.

3.3. Optical profilometry

The surface roughness values were measured to obtain a single numerical value that can be used in the comparison of the wear surfaces. The surface roughnesses are presented as R_q values, since R_q is more sensitive to deep valleys and high formations on the surface than R_a . The surface roughness values are shown in Fig. 5. As seen in the figure, the softer materials had a clearly higher surface roughness than the harder materials. Longer test duration produced slightly higher R_q -values, but overall the differences were small. Moreover, there were only small differences between the 60° and 90° angle results. Still, the 90° sample angle produced slightly higher surface roughness in general.

3.4. Penetration depths

The penetration depth was measured as the depth of the scars and embedded abrasives from wear surface. Fig. 6 presents the average

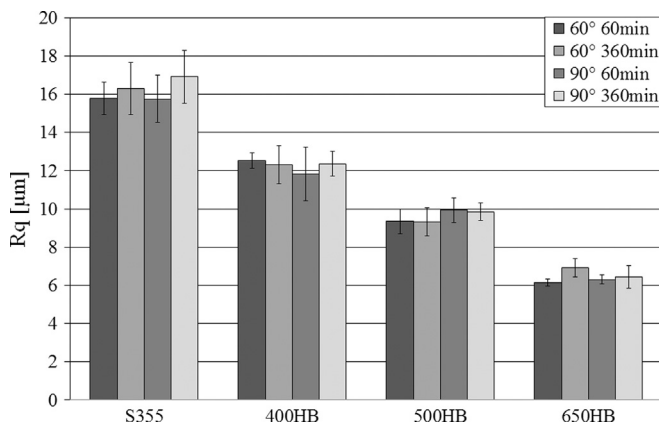


Fig. 5. Average R_q -values for the tested materials. Error bars represent the standard deviation.

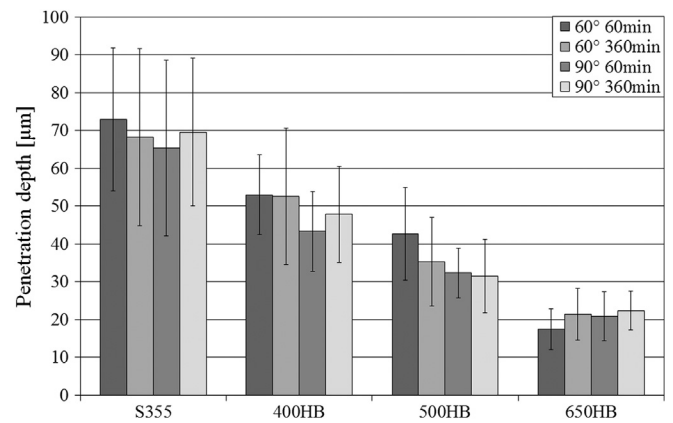


Fig. 6. Average penetration depth values. Error bars represent the standard deviation.

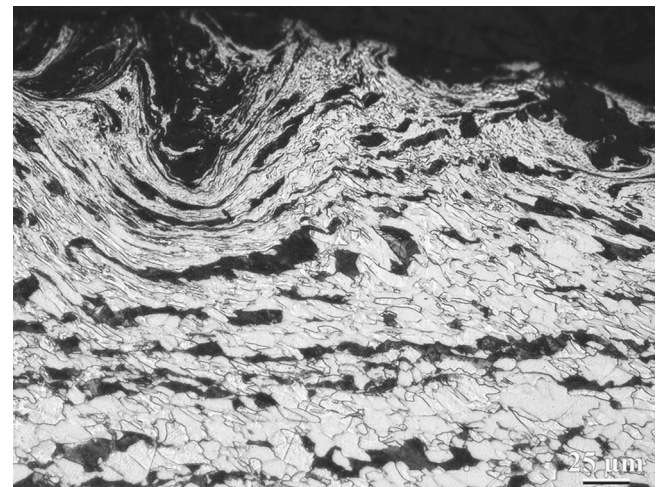


Fig. 7. Micrograph of the wear surface cross section of S355. The white areas are ferrite and dark pearlite.

values obtained from the penetration depth measurements. The large scatter results from the large variation of the depth of individual scratches. As for the surface roughness, harder materials yielded smaller values. In general, the 60° samples had larger penetration depths. This could be associated with more distinct scratches. The test duration did not cause a clear difference.

3.5. Microstructures after wear testing

The samples tested for 360 min at the 90° angle were studied in more detail to map the possible microstructural changes in the materials. The largest deformation depths were observed in S355, which had clearly deformed grains even at the depth of 220 μm . Fig. 7 presents a micrograph of the cross section of the worn surface of S355, showing mechanical fibering and waviness of the deformed grains. Also the lamellae of pearlite had flattened and oriented in a wavy pattern, as seen in Fig. 8.

Figs. 9 and 10 present micrographs of the cross sections of the worn surfaces of 400HB and 500HB steels, respectively. In both martensitic wear resistant steels the grains and martensite laths have been mechanically fibered following the wear surface. Close to the surface, the martensite laths formed again wavy patterns as a result of uneven impacting by individual abrasives. The laths were pushed more closely together in the immediate subsurface, as seen in Fig. 11. In the 360 min test, the observed deformation

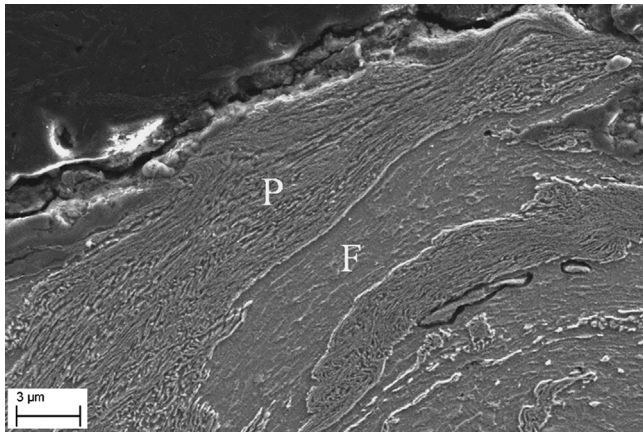


Fig. 8. FEG-SEM image of deformed structure of S355 with ferrite (F) and pearlite (P). Wear surface is at the top of the image.

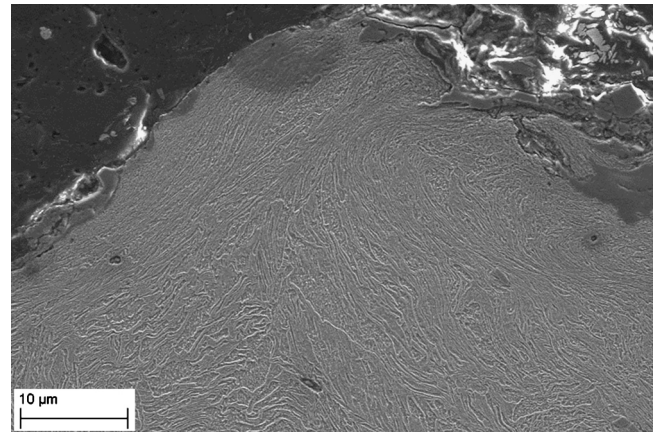


Fig. 11. FEG-SEM image of deformed structure of 500HB steel. Wear surface is at the top of the image.

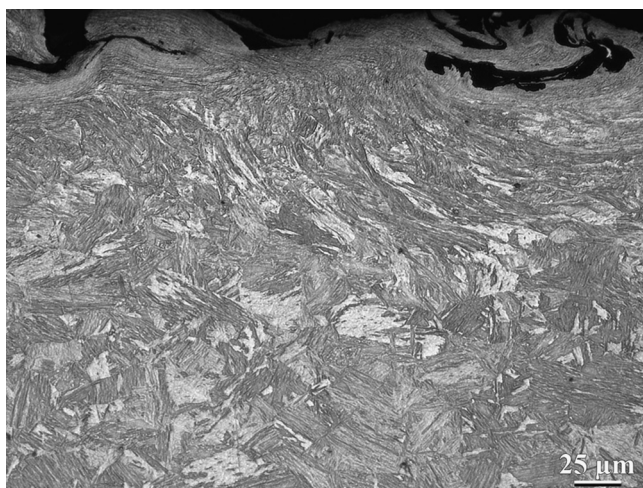


Fig. 9. Micrograph of the wear surface cross section of 400HB steel.

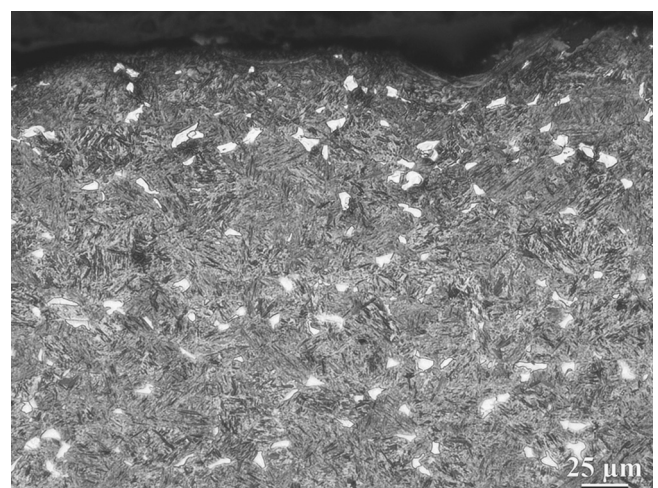


Fig. 12. Micrograph of the wear surface cross section of 650HB steel. The white areas are ferrite.

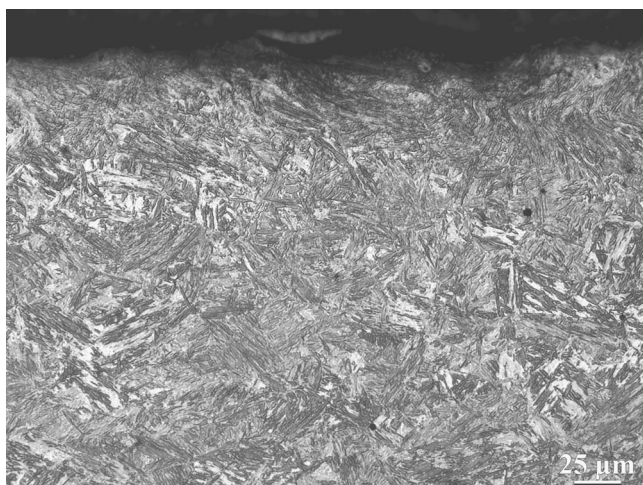


Fig. 10. Micrograph of the wear surface cross section of 500HB steel.

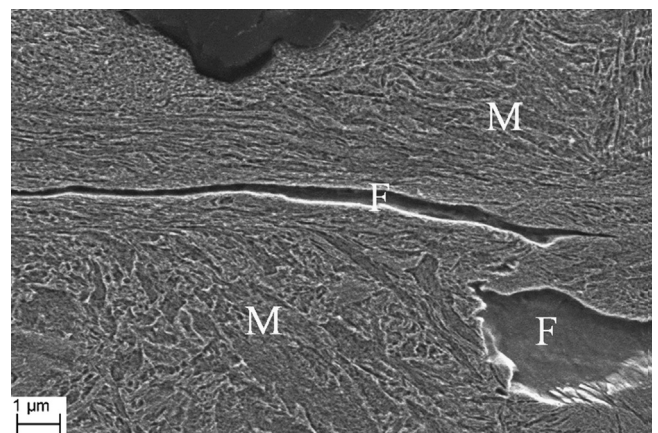


Fig. 13. FEG-SEM image of a deformed ferrite grain (F) in martensitic structure (M) in 650HB steel. Wear surface is at the top of the image.

depths from the micrographs in the 400HB and 500HB wear resistant steels were approximately 140 μm and 60 μm , respectively.

Fig. 12 presents a micrograph of the cross section of the wear surface of 650HB steel, which appeared deformed only to approximately 25 μm below the surface. Heavy deformation was observed only in the areas very close to the surface,

especially inside and around the ferrite grains. In the image, ferrite is shown as white. The used etching agent was Nital, which is good for outlining ferrite. However, Nital etching does not enable the distinguishing of martensite and finely distributed austenite from each other in the micrograph and they are both seen as darker phases [12]. Fig. 13 presents a FEG-SEM image of

such a deformed ferrite grain. Deformation of martensite close to the deformed ferrite grains was considerably more distinct than in other areas close to the surface. As in the 400HB and 500HB steels, mechanical fibering of the grains and martensite laths was observed also in 650HB steel. Compared to the 400HB and 500HB steels, the deformation was more uneven due to the easily deforming ferrite grains.

3.6. Wear surfaces

All samples were heavily worn during the tests, and craters from the impacts of the abrasives were visible in addition to scratches formed by plastic deformation. Fig. 14 presents an image of a worn surface with scratches in multiple directions. Moreover, lips formed by plastic deformation were frequently observed on the surfaces, as shown in Fig. 15. Some of them had a sharp edge, suggesting that they had probably fractured by a series of impacts. The overall wear seemed to occur largely by a mechanism where initially plastically deformed areas are removed by subsequent impacts. All wear surfaces contained embedded abrasives.

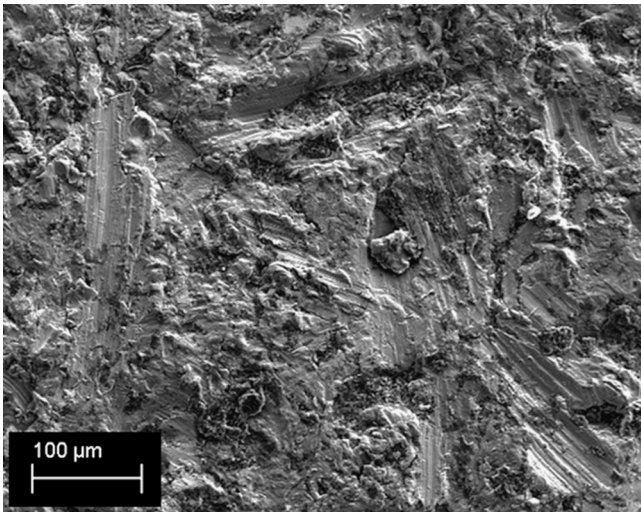


Fig. 14. FEG-SEM image of scratches on the wear surface of 650HB steel tested for 60 min at 60° angle.

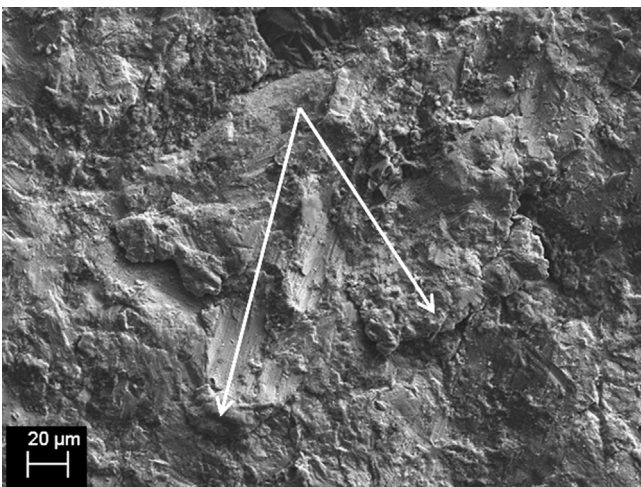


Fig. 15. FEG-SEM image of lips (marked with arrows) on the wear surface of 650 HB steel tested for 60 min at 90° angle.

Comparison of the 60 min sample wear surfaces to the 360 min test samples showed that the 360 min samples appeared slightly more heavily worn, containing more scratches, larger amounts of small debris and larger lip formations on the surface. Fig. 16 presents wear surfaces of 400HB steel tested for 60 and 360 min at 90° angle.

The differences between the two test angles were quite small in the 60 min tests. Even in the longer tests, the differences were not always quite obvious, but the 90° samples seemed to contain more craters and fewer scratches compared to 60° samples. However, the appearance of the wear surfaces varied locally markedly. In the hardest 650HB steel, 60° sample tested for 360 min appeared more uneven on its surface than the 90° sample. This was also detected by surface roughness measurements.

However, in the area at the tip of the sample the wear surfaces appeared substantially different already after 60 min. Fig. 17 presents the sample tips of 400HB steel tested at 60° and 90° angles for 60 min. The 90° sample had considerably more wear marks as opposed to the quite few marks on the 60° sample. Moreover, the wear scars consisted mostly of scratches in the 90° sample, whereas the 60° sample contained mostly impacting marks. In the 60° sample holder, the sample tip is at a tilted position, which is why the abrasives do not too often come into contact with this area. On the other hand, in the 90° sample holder the sample tip is parallel to the perimeter of the rotation, exposing the whole sample tip to contacts by the abrasives.

4. Discussion

This section discusses the obtained results considering the sample angle, test duration and differences in the wear behavior of the materials.

4.1. Sample angle

Overall the 90° angle led to higher wear in the samples. As for the mass loss relative to the 400HB reference, the difference between the 60° and 90° angles was largest in the softest S355 steel and, on the other hand, in the hardest 650HB steel. One possible explanation for this is that the conditions at the sample tip at 90° angle increase the total wear area by the area of the sample tip. However, the conditions in the sample tip are more scratching and less impacting than in the other actual areas of the wear surface. This, in turn, would emphasize the scratching abrasion resistance of the materials at 90° angle, which could lead to a difference in the relative mass loss between the sample angles in less scratch resistant materials.

There were surprisingly small differences between the wear surfaces in the center of the samples tested at 60° and 90° angles. The appearance of the surfaces was similar, and even in the longer tests the differences were not obvious. In addition, the surface roughness and microhardness results were almost similar for both 60° and 90° samples. However, the amount of craters was higher in the 90° samples but they had less distinct scratches than the 60° samples. This is also suggested by the smaller penetration depth of scars and abrasives in 90° samples.

The similarity of the wear surfaces especially in the center area suggests that the conditions in the 60° and 90° wear tests do not differ too much from each other in this test method. As the abrasives are loose and move at high speeds relative to the samples, they can be deflected from the sample or slide or roll on the surface. The process is almost similar at both angles and thus creates similar wear surfaces. The movement of the abrasive is affected by the sample angle to some extent, promoting the

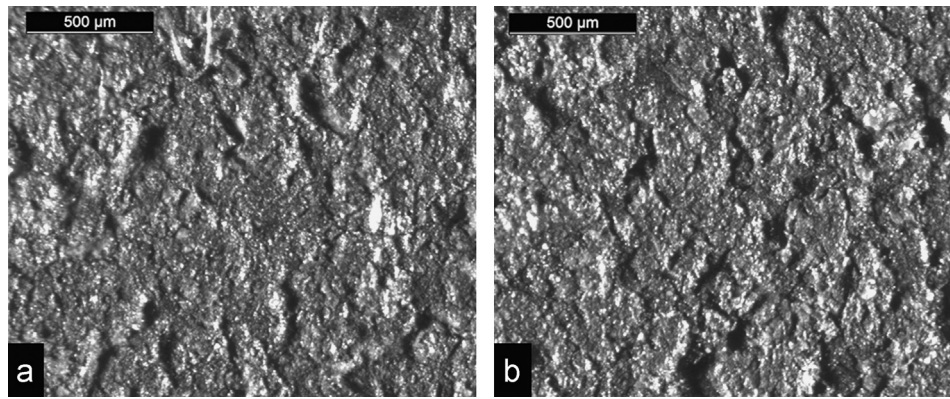


Fig. 16. Stereomicroscope image of wear surfaces of 400HB steel tested at 90° angle for (a) 60 and (b) 360 min.

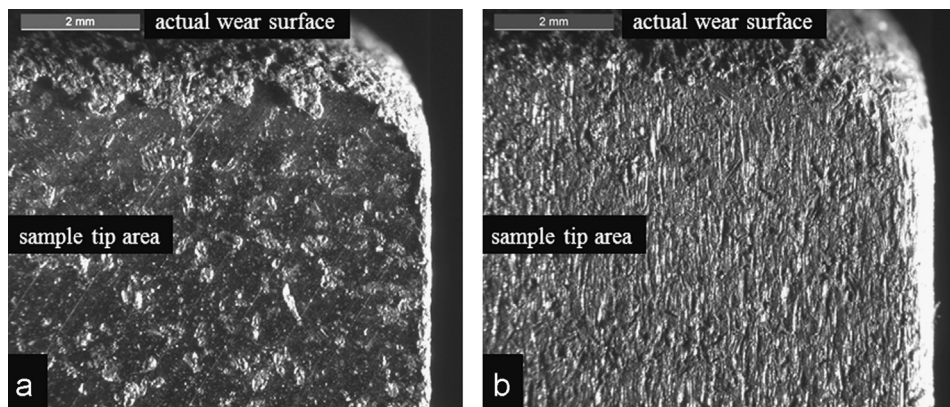


Fig. 17. Tip area of a 400HB sample tested for 60 min at (a) 60° and (b) 90° angle. The edge between the actual wear surface and the sample tip is at the top of the image.

movement towards the tip when the angle is decreased. This can be seen as long lip formations oriented towards the sample tip.

4.2. Test duration

The tested steels had clear differences in their properties, which could be seen in the wear test results as well. Hardness was the most dominant of the properties, higher hardness leading to smaller mass loss. Especially in the longer tests, the correlation between hardness and wear resistance was quite linear despite the differences in the microstructure. No definite findings have been reported on the effect of hardness on wear rate of steels in impeller-tumbler tests. Hardness has been reported to be of some benefit in reducing wear, but without major effect [3,6]. Tylczak et al. [4] and Hawk et al. [5] found no correlation between hardness and wear. On the other hand, Sundström et al. [2] reported that in their 60 min tests the correlation between hardness and wear resistance was linear, but the steels were divided into two separate sets with approximately same slope, one consisting of martensitic steels and the other of non-martensitic steels. Their study contained two martensitic steels and four non-martensitic ones. The 400HB and 500HB steels used in the current study showed a smaller effect of hardness on reducing wear during the 60 min tests when compared with the martensitic steel results of Sundström et al. [2].

The test duration had an effect on the wear of the materials. In the longer tests the effect of hardness on the reduction of wear was larger than in the short tests. The change in the effect of hardness is resulting from the dimensional changes in the sample combined with the role of ductility. At the beginning of the test, the sample edges are sharp. As the test proceeds, the edges are severely worn, and the rounded edges promote easier movement

of the abrasives over the edge, which decreases wear and sets it at a steadier rate. This is also what is happening in real-life components such as trucks' tail plates: at the early stage of their use, the tail plate edges are being rounded by wear. In ductile materials, plastic deformation can lead to a displacement of the material instead of its immediate removal. Especially in the tested softer steels, this was observed as heavy burring over the edges, which was not detected as a mass loss. However, the burrs were also worn out as the test was continued.

The conducted measurements did not reveal any distinct effects of the test duration on the wear surface. The surface roughness values were quite similar in the 60 and 360 min samples at both testing angles. The longer tests yielded slightly higher R_q values, but the differences were small. Also the penetration depth measurements gave quite similar results and no distinct differences could be detected.

However, when examining the wear surfaces with microscopes, the samples tested for 360 min appeared more heavily deformed. That could be determined, for example, from larger deformed lip formations on the surface. Also the amount of small debris, such as chips, was higher. In some cases the harder materials contained also more visible scratches. Such findings are not necessarily included in the numerical values of the surface roughness, or even in the penetration depths.

The microscopic investigations of the deformed subsurface microstructure suggested that there was a difference in the deformation depth between the samples tested for longer test durations compared to the shorter ones. The deformation depth was observed to increase when the test time was increased from 60 to 360 min. Some evidence of the larger work hardening in longer tests could also be observed in the microhardness measurements taken from the cross sections of the worn samples.

In general, there was a slight increase in the surface hardness of the samples tested for 360 min compared with those tested for 60 min. Similar observations have been made by Wilson and Hawk [6], who studied the evolution of work hardening during the 5 h tests by measuring the surface hardness of the worn steel samples hourly. They reported that most of the work hardening (approximately 71–96% of the total hardness increase) occurred during the first hour, but hardness kept increasing in most of the samples throughout the test.

The increase of the surface hardness can be a result of the increasing number of repetitive impacts. Already after the 60 min test, the samples are thoroughly worn on the surface exposed to wear, and the conditions remain the same in the 360 min tests. It should be noted that in the tests the force at which the abrasive particles hit the sample surface does not change in the course of the test.

4.3. Materials

The wear surfaces of all materials seemed heavily deformed. There were scratches, but mostly wear seemed to have occurred by impacts removing the formerly plastically deformed areas. Similar observations for steels have been made by Sundström et al. [2] and Wilson and Hawk [6]. The softer materials appeared more heavily deformed, which was also detected as higher surface roughness and penetration depth of scars.

Work hardening took place in all test materials, but the extent of it varied. Sundström et al. [2] reported that in their study, ferritic–pearlitic and bainitic steels work hardened to a higher extent compared with the martensitic steels. In the present study, the S355 with ferritic–pearlitic microstructure had the highest hardening depth and relative hardness increase, whereas for the 400HB and 500HB wear-resistant steels having fully martensitic microstructure the depth and amount of work hardening decreased as hardness increased. The 650HB steel containing ferrite, however, had slightly larger deformation depth than the 500HB wear resistant steel, possibly relating to the behavior of soft ferrite islands and finely distributed austenite amongst the hard martensite. The evident deformation depth determined from microstructure was only 25 μm , but microhardness measurements suggested the deformation depth to be larger. Nevertheless, it did not seem to notably affect the overall wear resistance of the material.

Elongation of grains and laths in the direction of metal flow during deformation was observed in the subsurfaces of the worn samples for all materials in all cases. The deformation caused by individual impacts led to wavy structures close to the surface. Of 400, 500 and 650 HB wear resistant steels, the most distinct difference between the microstructures was the presence of ferrite and austenite in the martensitic matrix of the 650HB steel. In the worn samples the effect of this difference could be seen as more distinct deformation of martensite in grains close to the ferrite grains. This could be resulting from the internal stresses between the phases. In the beginning of surface deformation, softer ferrite is more easily deformed. Small degree of deformation causes internal stresses between martensite and ferrite due to their un-relaxed plastic incompatibility. As the degree of deformation is increased, the internal stresses are leveled by the plastic deformation of martensite and plastic relaxation in ferrite [13]. However, it is still uncertain if the high local deformation of martensite is caused by the mismatch with ferrite, or if it is just caused by the inhomogeneous deformation. More tests with controlled deformation conditions should be conducted to verify this.

5. Conclusions

Changing of the sample angle resulted in surprisingly small differences in the wear surfaces and values of microhardness, penetration depth, and surface roughness of the samples. This suggests that the testing conditions at these sample angles are relatively similar to each other excluding the edge parts, where the 90° angle sample underwent larger dimensional changes.

The longer test duration decreased the relative amount of wear of the harder materials but increased that of the softest material when compared with the reference material. Based on these observations, the longer test yields more reliable information about the impact-abrasion wear resistance of the materials.

Despite the microstructural changes, the correlation between increasing hardness and decreased wear was quite linear in the steady-state wear. Work hardening occurred in all test materials, the softest material showing the highest deformation depth and amount of work-hardening. Ferrite in the microstructure of the 650HB steel with martensitic matrix seemed to promote deformation of the martensite around the ferrite grains, but this did not have a notable effect on the overall wear resistance of the material compared to fully martensitic wear resistant steels.

Acknowledgements

The work has been done within FIMECC Ltd and its DEMAPP program. We gratefully acknowledge the financial support from Tekes and the participating companies. The authors would like to express their gratitude for Lic. Tech. Kati Valtonen for help in preparing the manuscript and prof. Pentti Karjalainen for general advice in the physical metallurgy.

References

- [1] F.C. Bond, Lab equipment and tests help predict metal consumption in crushing and grinding units, *Engineering and Mining Journal* 165 (1964) 169–176.
- [2] A. Sundström, J. Rendón, M. Olsson, Wear behaviour of some low alloyed steels under combined impact/abrasion contact conditions, *Wear* 250 (2001) 744–754.
- [3] J. Rendón, M. Olsson, Abrasive wear resistance of some commercial abrasion resistant steels evaluated by laboratory test methods, *Wear* 267 (2009) 2055–2061.
- [4] J.H. Tylczak, J.A. Hawk, R.D. Wilson, A comparison of laboratory abrasion and field wear results, *Wear* 225–229 (1999) 1059–1069.
- [5] J.A. Hawk, R.D. Wilson, J.H. Tylczak, Ö.N. Doğan, Laboratory abrasive wear tests: investigation of test methods and alloy correlation, *Wear* 225–229 (1999) 1031–1042.
- [6] R.D. Wilson, J.A. Hawk, Impeller wear impact-abrasive wear test, *Wear* 225–229 (1999) 1248–1257.
- [7] E. Badisch, M. Kirchgaßner, F. Franek, Continuous impact/abrasion testing: influence of testing parameters on wear behaviour, *Proceedings of the Institution of Mechanical Engineers, Part J: Journal of Engineering Tribology* 223 (2009) 741–750.
- [8] V. Ratia, K. Valtonen, A. Kempainen, V.-T. Kuokkala, Impact–abrasion wear testing of wear resistant steels, in: *Proceedings of the Nordtrib 2012 Conference*, Trondheim, 2012.
- [9] P. Geiderer, Testing of Combined Impact–Abrasion Wear, Master of Science Thesis, Fachhochschule Wiener Neustadt für Wirtschaft und Technik, Wiener Neustadt (2005) 53–54.
- [10] A. Mein, G. Foularis, D. Crowther, P.J. Evans, The influence of aluminium on the ferrite formation and microstructural development in hot rolled dual-phase steel, *Materials Characterization* 64 (2012) 69–78.
- [11] M. Gomez, C.I. Garcia, D.M. Haezebrouck, A.J. DeArdo, Design of composition in (Al/Si)-alloyed TRIP steels, *ISIJ International* 49 (2009) 302–311.
- [12] A.O. Bencoter, Carbon and alloy steels: metallographic techniques and microstructures, in: *ASM Handbook vol. 9: Metallography and microstructures*, ninth ed., 8th Printing, ASM International, 1998, pp. 273–357.
- [13] T.S. Byun, I.S. Kim, Tensile properties and inhomogeneous deformation of ferrite-martensite dual-phase steels, *Journal of Materials Science* 28 (1993) 2923–2932.

Publication IV

Vilma Ratia, Vuokko Heino, Kati Valtonen, Minnamari Vippola, Anu Kemppainen,
Pekka Siitonen and Veli-Tapani Kuokkala

**Effect of abrasive properties on the high-stress three-body abrasion of steels and
hard metals**

Finnish Journal of Tribology 32 (2014) 3-18

© 2014 Finnish Tribology Society
Reprinted with permission

EFFECT OF ABRASIVE PROPERTIES ON THE HIGH-STRESS THREE-BODY ABRASION OF STEELS AND HARD METALS

VILMA RATIA^{1*}, VUOKKO HEINO¹, KATI VALTONEN¹, MINNAMARI VIPPOLA¹, ANU KEMPPAINEN², PEKKA SIITONEN³, VELI-TAPANI KUOKKALA¹

¹ Tampere University of Technology, Tampere Wear Center, Department of Materials Science, P.O.Box 589, FI-33101 Tampere

² SSAB Europe Oy, P.O.Box 93, FI-92101 Raahe, Finland

³ Metso Minerals Oy, P.O.Box 306, FI-33101 Tampere, Finland

*corresponding author: vilma.ratia@tut.fi

ABSTRACT

Especially in tunneling, the abrasiveness of rock is an important property, which can easily be determined by several methods developed for the purpose. With this in mind, it is rather surprising that the effects of different rock types on the wear mechanisms of engineering materials have not been too widely studied. In this paper, high stress three-body abrasive tests were conducted with four different abrasives with a relatively large (2-10 mm) particle size. As test materials, three different steels and three hard metals were used. The tests clearly showed that material type has an influence on how different abrasive and material properties affect the abrasive wear mechanisms and severity. For example with hard metals, the most important property of the abrasives is their crushability, as only small abrasive particles are able to properly attack the binder phase and cause high wear rates. On the other hand, it seems that the abrasiveness of rock is not the dominating property determining the severity of wear in the current test conditions for any of the tested materials. In fact, with steels no single abrasive property could be shown to clearly govern the abrasive wear processes. In any case, when using the determined abrasiveness values in wear estimations, the contact conditions in the method used for determining the abrasiveness values should be as similar as possible with the end application.

INTRODUCTION

Abrasive wear occurs widely in everyday life in both households and industry. The estimated annual cost of abrasive wear is 1-4 % of the GNP of the industrialized countries [1]. From the economical point of view, it has been estimated that in engineering abrasive wear is probably the most crucial type of wear [2].

A common way to study abrasive wear is to use the standard ASTM G65 dry sand rubber wheel test. However, the correlation of its conditions with real applications is not always

clear. For example, when screening materials for mineral crushing applications, Ala-Kleme et al. [3] concluded that the correspondence of the rubber wheel results with the field test results was very poor.

Since the conditions play an essential role in the wear processes, application-tailored wear tests have been of increasing interest in the industry. In order to obtain results, which are closely related to the application, one should try to simulate the true conditions as well as possible. In abrasive wear testing, a good way of increasing the degree of reality is to use abrasives that are likely to be present in the

intended application. Natural stones are therefore a good choice for abrasives when testing materials for earth moving and mining machinery.

Abrasive wear is a complex phenomenon and there are many variables to be taken into account, such as the wear environment, the type of motion, and the contact forces. Changing one variable can change the outcome of the tests substantially.

An essential variable in abrasive wear is the abrasive itself and its properties. The abrasive is in a big role largely determining the mechanisms with which the wear is happening. The effects of size [4–7] and shape of the abrasives [8–11] on wear have been discussed by several authors. The same abrasive properties may have different effects when conditions change, for example, from impacts to abrasion [12]. On the other hand, different wear mechanisms can be observed in systems where the conditions are similar and only the abrasive type is varied [12–14].

The abrasiveness of rock and soil and the methods of measuring it have been discussed widely in geology and tunneling [15–22]. Some methods used for determining the abrasiveness of rock are thin section analysis, Cerchar test, LCPC test, Schimazek index test, Sievers C-value test, Böhme grinding test [18], the brittleness value test, Sievers J-value test, and abrasion value and abrasion value cutter steel test [21]. The Cerchar abrasivity test is widely used for TBM tunneling and also for academic purposes [19,23]. On the other hand, it tests the properties of individual grains or blocks only [18] and is affected by the stress state of the rock [23]. The LCPC test is an abrasiveness test that enables the investigation of rock samples consisting of several grains with various sizes, and it has been reported to be one of the most used methods for determining the abrasiveness of rock materials in Europe [18].

There are only a limited number of papers, which take into consideration the properties of real rock materials in high stress abrasive wear conditions. Some researchers have investigated abrasive wear with larger size abrasives in impacting conditions [13,24–26]. On the other hand, in the abrasive wear tests, the particle size has often been restricted to less than a millimeter [4,5,12,26,27] even in the studies determining the size effect of abrasives or natural stones on wear.

The aims of this study are to compare different Finnish rock species and the wear type they produce in some typical mining and earth moving machinery materials under controlled compressive crushing conditions, and to find correlations between the rock properties and wear performance of selected steels and hard metals.

MATERIALS AND METHODS

Several different steel and WC-Co specimens were tested using the crushing pin-on-disc wear test procedure. Four different rock species were used as abrasives.

Metals and hard metals

The abrasive wear resistance of three steel and three hard metal grades were evaluated. Table 1 lists the steels along with their nominal mechanical properties and compositions. One of the steels was the commonly used structural steel grade S355 with a ferritic-pearlitic microstructure, and the two other steels were quenched wear resistant martensitic steels with different hardness, denoted as 400HB and 500HB according to their commercial hardness grade. Besides steels, three hard metal grades were also tested. Table 2 presents the hardness and nominal compositions of the hard metals. They all consisted of tungsten carbides (average carbide size 2.5 μm) with different amounts of cobalt as the binder phase.

Table 1. Nominal mechanical properties and compositions of the tested steels.

Material	S355	400HB	500HB
Hardness [HV]	172	423	505
Yield strength [N/mm ²]	355	1000	1250
Tensile strength [N/mm ²]	470-630	1250	1600
A5 [%]	20	10	8
Density [g/cm ³]	7.88	7.85	7.85
C [max%]	0.18	0.23	0.3
Si [max%]	0.5	0.8	0.8
Mn [max%]	1.6	1.7	1.7
P [max%]	0.025	0.025	0.025
S [max%]	0.02	0.015	0.015
Nb [max%]	0.05	-	-
Cr [max%]	-	1.5	1.5
Ni [max%]	-	1	1
Mo [max%]	-	0.5	0.5
B [max%]	-	0.005	0.005

Table 2. Hardness, density and nominal compositions of the tested hard metals.

Material	Hardness [HV]	Density [g/cm ³]	Composition [wt.-%]	
			WC	Co
WC-26Co	870	13.02	74	26
WC-20Co	1050	13.44	80	20
WC-15Co	1260	13.99	85	15

Abrasives

Table 3 lists the properties and nominal mineral contents of the used abrasives. As the abrasives are natural stones, their properties can vary locally and should be regarded only as approximates. The density, uniaxial compressive strength (UCS), and quartz content were obtained from the supplier of the rocks. The abrasiveness and crushability values were determined using the LCPC test, which is described in the French standard NF P18-579. The tests were conducted in the Metso Minerals Rock Laboratory in Tampere. The LCPC test gives the LCPC abrasion coefficient (LAC) and the LCPC breakability coefficient (LBC). In the test, a standardized steel block with hardness of 60-75 HRB is rotated in a 500 g batch of 4-6.3 mm rock in a container for 5 minutes [15]. The abrasiveness (LAC) is determined from the mass loss of the steel block and the crushability (LBC) from the rock sieving results using the following equations [19]:

$$LAC = \frac{m_0 - m}{M} \quad (1)$$

$$LBC = \frac{M_{1.6} \cdot 100}{M} \quad (2)$$

where m_0 and m are the steel block's mass before and after the test, respectively. M is the mass of the abrasive (500 g, i.e., 0.0005 t) and $M_{1.6}$ is the mass of the <1.6 mm fraction of the abrasives after the test.

The hardness values of the rocks were measured with Duramin A300 hardness tester. Several indentations were made, and the final average hardness was calculated by taking into account the relative fractions of the different phases and their hardness in the rock. The mineral compositions were determined with X-ray-diffraction.

Table 3. Properties and nominal mineral contents of the used abrasives.

Rock species	Tonalite	Granite	Gneiss	Quartzite
Abbreviation	T	GR	GN	Q
Quarry	Koskenkylä	Sorila, Tampere	Lakalaiva, Tampere	Nilsia, Haluna
Density (kg/m ³)	2660	2674	2747	2600
Uniaxial compressive strength (MPa)	308	194	64	90
Hardness (HV1)	960	800	700	1200
Quartz content (wt%)	40	25	24	98
Abrasiveness (g/t)	1460	1920	1430	1840
Crushability (%)	18	34	37	74
Nominal mineral contents (%)	quartz (40) plagioclase (40) biotite (17) amphibole (3)	plagioclase (45) quartz (25) orthoclase (13) biotite (10) amphibole (5)	plagioclase (36) biotite (25) quartz (24) orthoclase (7) amphibole (5) garnet(3)	quartz (98) sericite hematite

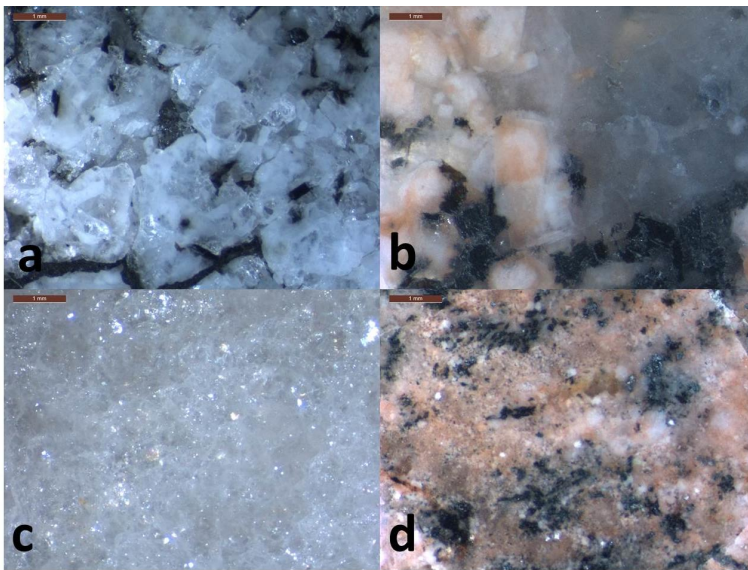


Figure 1. Images of the polished rock specimens used for wear testing a) gneiss, b) granite, c) quartzite and d) tonalite. Scale bar is 1 mm.

Figure 1 presents optical stereo microscope images of the polished surfaces of the abrasives. It can be observed that granite (1b) and gneiss (1a) have a similar and quite coarse grain structure. Tonalite (1d) consists of quite small size grains, and quartzite (1c) has the finest grain structure of the studied abrasives.

Figure 2 illustrates the appearance of the abrasive particles, revealing also the evident differences in their morphology. Gneiss (2a) has a quite heterogeneous structure including spherical, longitudinal and also flaky particles. Tonalite particles (2d), in turn, are quite round. Granite (2b) and quartzite particles (2c) have a quite similar morphology, consisting mainly of angular particles.

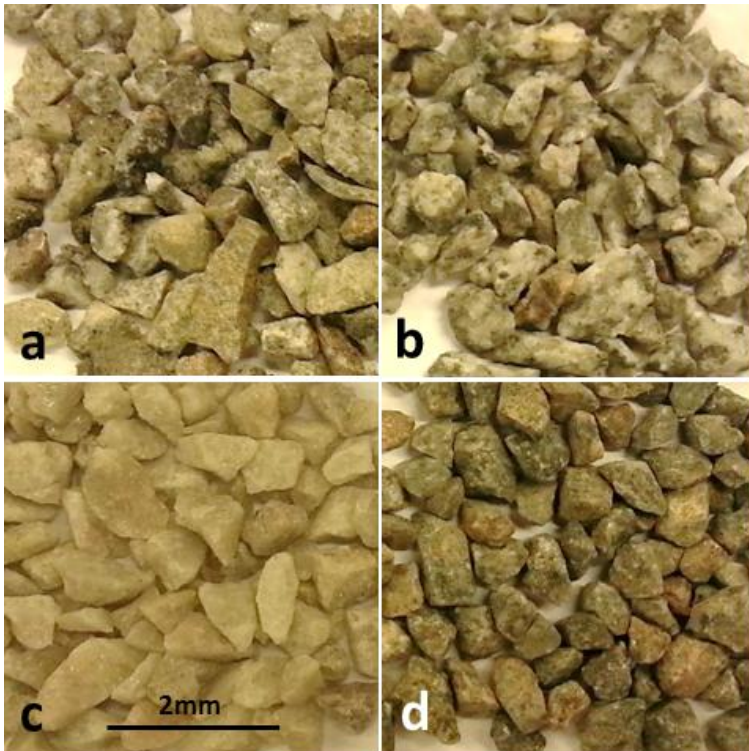


Figure 2. Images of the abrasive particles used for wear testing a) gneiss, b) granite, c) quartzite and d) tonalite.

Crushing pin-on-disc abrasive wear testing

The wear tests were conducted with a crushing pin-on-disc [14], which is a three-body high stress abrasive wear tester. It has a setup similar to the common pin-on-disc equipment, but it enables addition of 500 g of 2-10 mm abrasive between the pin and the disc. This helps to simulate heavy abrasive conditions better than, for example, the dry sand rubber wheel abrasion tester, where the size of the abrasive is 212-300 μm [28]. Figure 3 presents schematically the principle of the equipment.

Unlike in the common pin-on-disc setup, in the crushing pin-on-disc the pin and the disc are not in contact with each other during the test, and thus the wear is induced purely by the abrasives. In the test, the pin is pressed against the abrasive bed on the rotating disc with a force of 240 N for 5 seconds, followed by an idle time for the abrasive to replenish between the pin and the disc. The abrasive is maintained on the disc with a collar. The disc material was structural steel S355 (216 HV) for the steel samples and tool steel (690 HV) for the hard metal specimens.

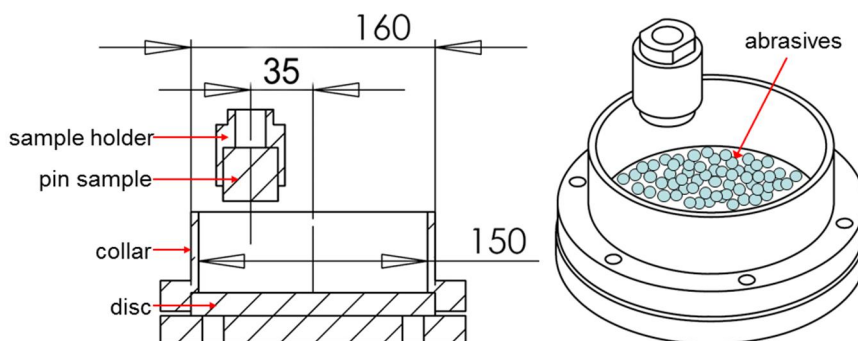


Figure 3. Schematic picture of the crushing pin-on-disc wear testing equipment.

Before the actual tests, the steel specimens were first subjected to a run-in period of 15 minutes, during which the steady-state wear was achieved. Also, in this way the effect of the embedded abrasive fragments on the mass loss was minimized. The total contact time when the pin was pressed against the abrasives was 20 minutes in each test. The wear was measured as mass loss, which was then converted to volume loss to enable better comparison of the wear in materials with different densities. Three repetitive tests were made on each specimen type.

After wear testing, the wear surfaces were characterized with Leica MZ 7.5 optical stereo microscope and Philips XL30 scanning electron microscope. Moreover, Wyko NT1100 optical profilometer was used to determine the wear surface profiles and to obtain numerical data of the roughness of the surface.

RESULTS

In this Chapter, the volume loss results are presented in relation to the properties of the abrasives. Also observations on the wear

surfaces and the abrasive sieving results are presented and discussed.

Volume loss results

Higher hardness is generally known to enhance the abrasive wear resistance of materials, which was also clear in the current tests. Figure 4 presents the volume loss results from the tests with different abrasives in relation to the hardness of the test materials. Figure 4a shows that for the steels (hardness 172-505 HV) the trend is very clear, while for hard metals (Figure 4b) the correlation is less pronounced. The role of the abrasive type is clearest with hard metals tested with quartzite, the results being distinctly different from the results obtained for hard metals with the other abrasives. Also in steel specimens quartzite produces relatively more wear in the hardest alloy, but in the case of softer steels granite and gneiss clearly rise above it. This may result from the formation of an embedded quartzite powder layer on the softer materials, protecting the surface from being penetrated with larger size abrasives thus decreasing the wear rate [29].

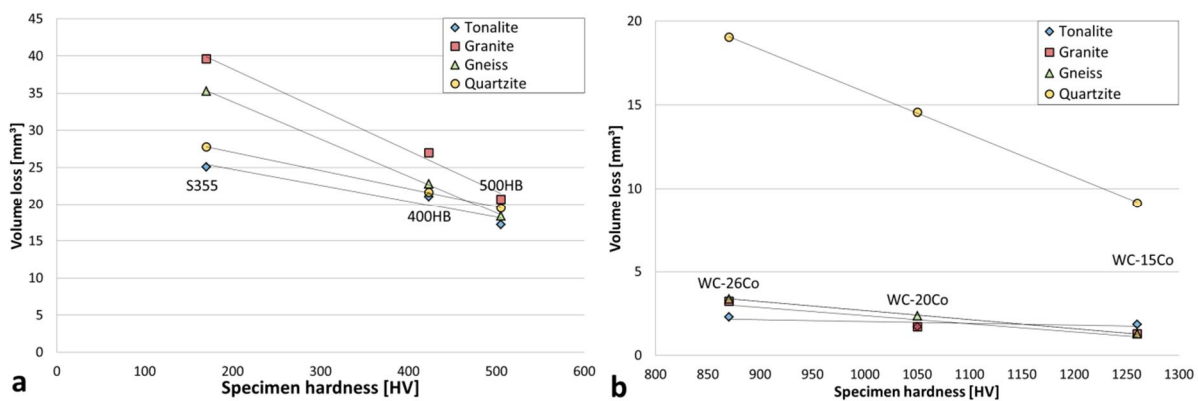


Figure 4. Volume loss of a) steel and b) hard metal specimens relative to their hardness.

Besides the volume loss of the pin, also the volume loss of the disc was monitored. For steels, the disc volume loss decreased as the pin hardness increased. This is probably because on harder materials the abrasive is more likely to pass the surface without embedding in it, and there is also less friction in the system.

Even though the pin and the disc are not in direct contact with each other during the test, the disc as the test counterpart has an effect on the moving of the abrasive in a three-body abrasion system [14,30,31]. The abrasive can move differently depending on whether the counterpart is softer or harder than the wearing part. For the tested steels, the pin/disc hardness ratio ranged from 0.8 to 2.3, while with the hard metals the ratio was 1.3-1.8. For both types of materials, the wear rate decreased as the ratio of the hardness of the pin and the disc increased, although no uniform dependence for both materials was found. It must also be kept in mind that in general the higher hardness of the specimen (pin) resulted in lower wear.

As there were distinct differences between the wear caused by different abrasives, the volume loss results were analyzed in view of the properties of the abrasives in order to find out, how they correlate with the wear test results and which properties have the largest effect. Figure 5 presents the wear results in relation to the crushability of the abrasives. It shows that there is a clear correlation between the wear of hard metals and the crushability of the abrasives, i.e., the amount of wear increases with increasing crushability. Moreover, the difference between the WC-Co grades is substantially larger when tested with quartzite compared to the other abrasives. For the steels, on the other hand, no such unambiguous trend can be observed. It is also worth noting that while the crushability seems to correlate with the wear rate of hard metals, for the uniaxial compressive strength (UCS) no such trend could be observed. This implies that while the uniaxial compressive strength is a measure of the overall rock strength,

crushability is only a measure of the rock's ability to produce fine size particles during crushing.

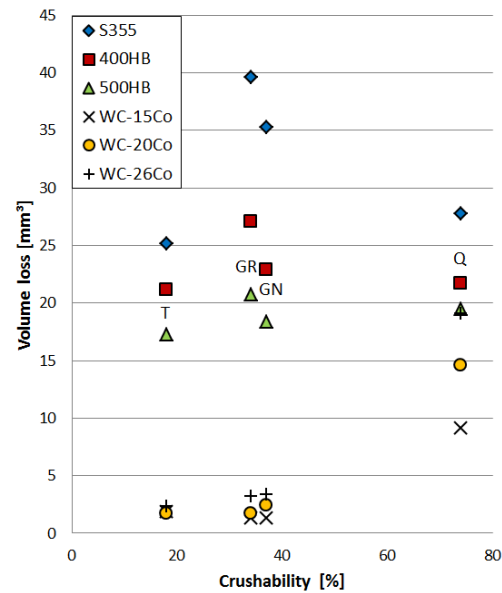


Figure 5. Volume loss of specimens in relation to the crushability of the abrasives.

Figure 6 presents the volume losses in relation to the abrasiveness of the abrasives. It is interesting to note that no clear linear correlation can be observed for either of the material groups. For example for steels, the abrasive with the highest abrasiveness value produces highest wear, but otherwise the results show only considerable scatter. This suggests that the contact conditions affect the abrasion process considerably and that the abrasiveness values determined with the LCPC test do not comply with the contact conditions prevalent in the crushing pin-on-disc test.

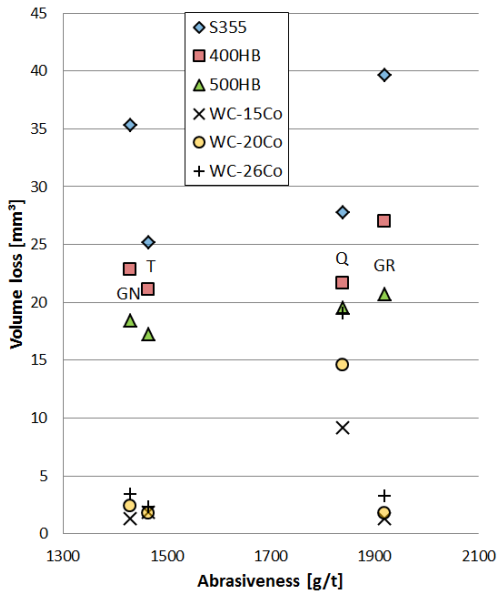


Figure 6. The volume loss of specimens in relation to the abrasiveness of the abrasives.

As hardness in any case plays a major role in the abrasive wear of materials and affects the choice of mechanisms by which it primarily happens, it is worthwhile to study also the effect of the hardness ratio of the test material and the abrasive on the wear process. It is generally taken that for a scratch to form the material hardness must be 80% or less of the abrasive hardness [32,33]. Figure 7 presents the volume loss as a function of the hardness ratio of the test materials and the abrasives. The trend is clear, showing that the higher is the hardness ratio, the lower is the wear rate. The value above which excess hardness does not anymore provide additional benefit seems to be around 0.9-1.1.

Abrasive sieving

Figure 8 presents the average sieving results of the abrasives after the tests with steels. The results are in good agreement with the crushability results presented in Table 3, where quartzite has a clearly higher and tonalite clearly lower crushability than granite

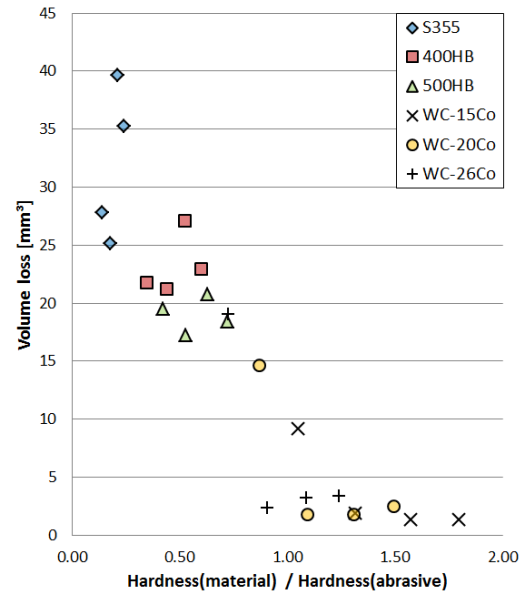


Figure 7. Volume loss dependence on the hardness ratio of the test material and the abrasive.

and gneiss, which again are very close to each other. The LBC crushability values show the percentage of particles smaller than 1.6 mm after the LCPC test. A direct comparison between the crushability and the sieving results after the crushing pin-on-disc cannot be made due to different initial size distribution and test time. However, an approximate assumption can be made by comparing the crushability value with the percentage of particles smaller than 2 mm after the crushing pin-on-disc. These percentage values are presented in Figure 8 above the sieving results. The values are overall higher than the crushability results of the LCPC test, which is to be expected because of the crushing motion during the test, along with the longer test duration. However, the observations about the effect of crushability on wear remain similar when using either LCPC or application-specific crushability values.

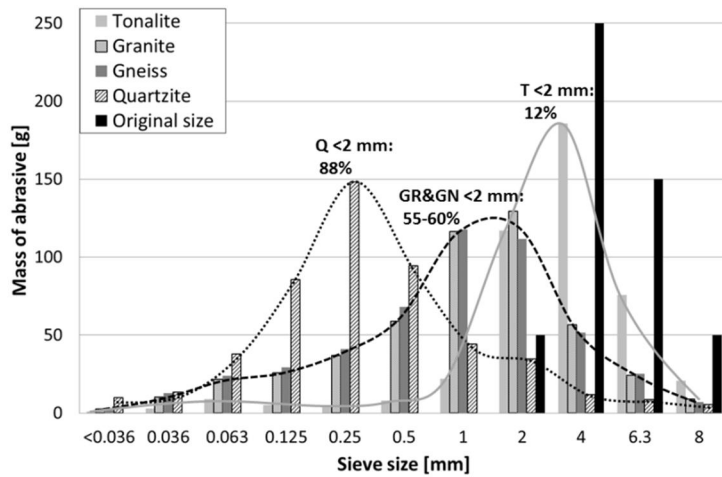


Figure 8. The average sieving results of the used abrasives after the tests with steels and the percentage of particles smaller than 2 mm. Also the original size distribution is shown.

Microscopy

The appearance of wear surfaces was investigated with a scanning electron microscope (SEM). Figure 9 presents the SEM images of 500HB specimens, where clear differences between the wear caused by different abrasive types can be observed. The specimen tested with granite (Figure 9b) contains wider and longer scratches compared to the specimen tested with gneiss (Figure 9a). Although granite and gneiss have approximately the same crushability and quartz content, their UCS are distinctly different, granite having values of about 194 MPa and gneiss about 64 MPa. As higher UCS transmits more effectively the crushing forces to the specimen, this leads to higher degree of deformation on the surface.

The specimen tested with quartzite (Figure 9c) shows the shortest and seemingly shallowest scratches. This is evidently associated with the high crushability value of quartzite, which means that quartzite breaks easily under high stress creating lots of small particles. This is also seen as the larger amount of very fine abrasive powder embedded on the surface, appearing as darker regions in the backscatter electron image.

Figure 9d shows the surface tested with tonalite, containing the highest amount of large scratches. The long scratches stem from the low crushability value of the mineral, enabling the particles to remain intact longer and thus to produce longer scratches.

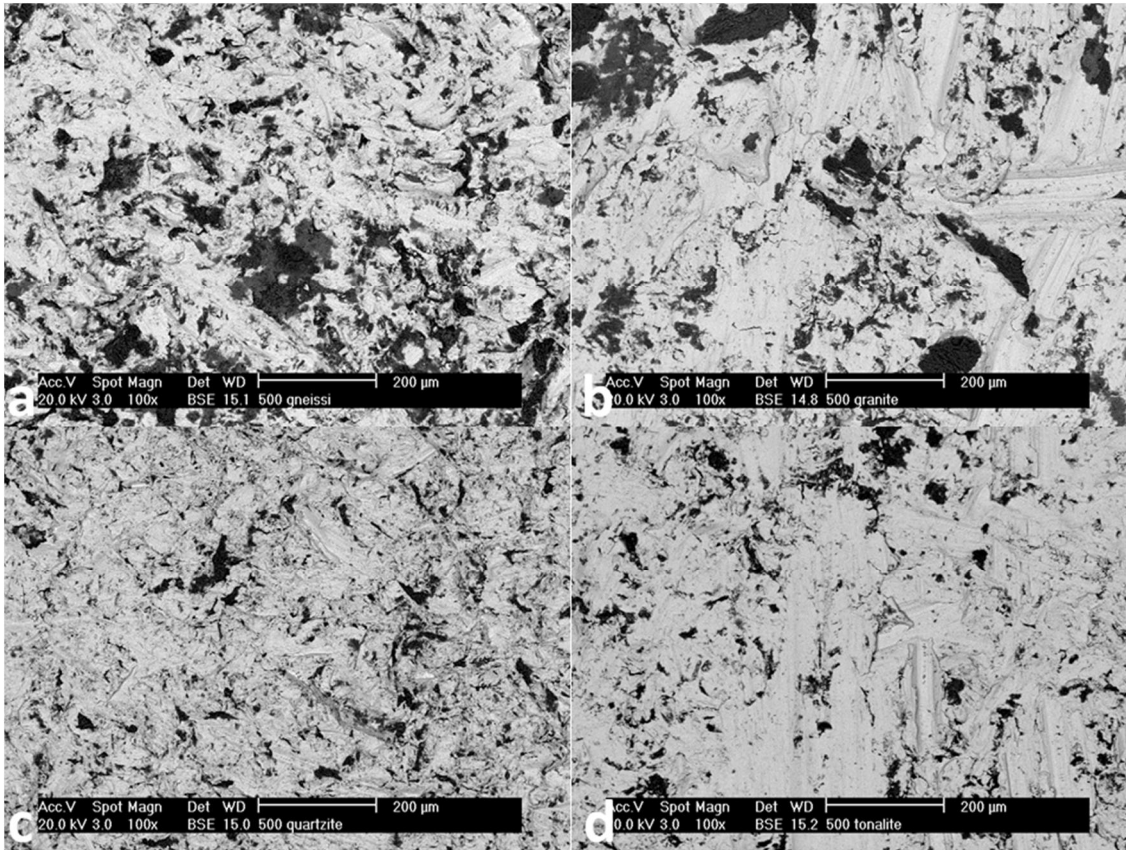


Figure 9. Backscatter scanning electron microscope image of 500HB steel tested with a) gneiss, b) granite, c) quartzite and d) tonalite. The metal is seen as light and the abrasives as dark areas.

Figure 10 shows the wear surfaces of the WC-Co specimens containing 26wt% of the soft binder phase, which is the reason for the relatively low hardness of the material. Although quartzite produced the highest wear rates in the hard metal specimens, the actual wear surface in Figure 10c has the least worn appearance. There are some scratches visible, but they are shorter and narrower than with the other abrasives. Gneiss (Figure 10a) has produced quite wide but shallow scratches, as could be expected due to the flakiness of the abrasive particles. Granite (Figure 10b), in

turn, has produced much deeper scratches than gneiss, but otherwise the wear surfaces look quite similar. The scratches produced by tonalite (Figure 10d) are long but quite narrow, and the harshness of the wear surface is lowest of all abraded WC-Co samples. Tonalite has a quite high compressive strength, and therefore it is able to scratch the surface longer before any fracture of the rock appears. Due to the bluntness of the tonalite particles, they are not able to produce deep scratches.

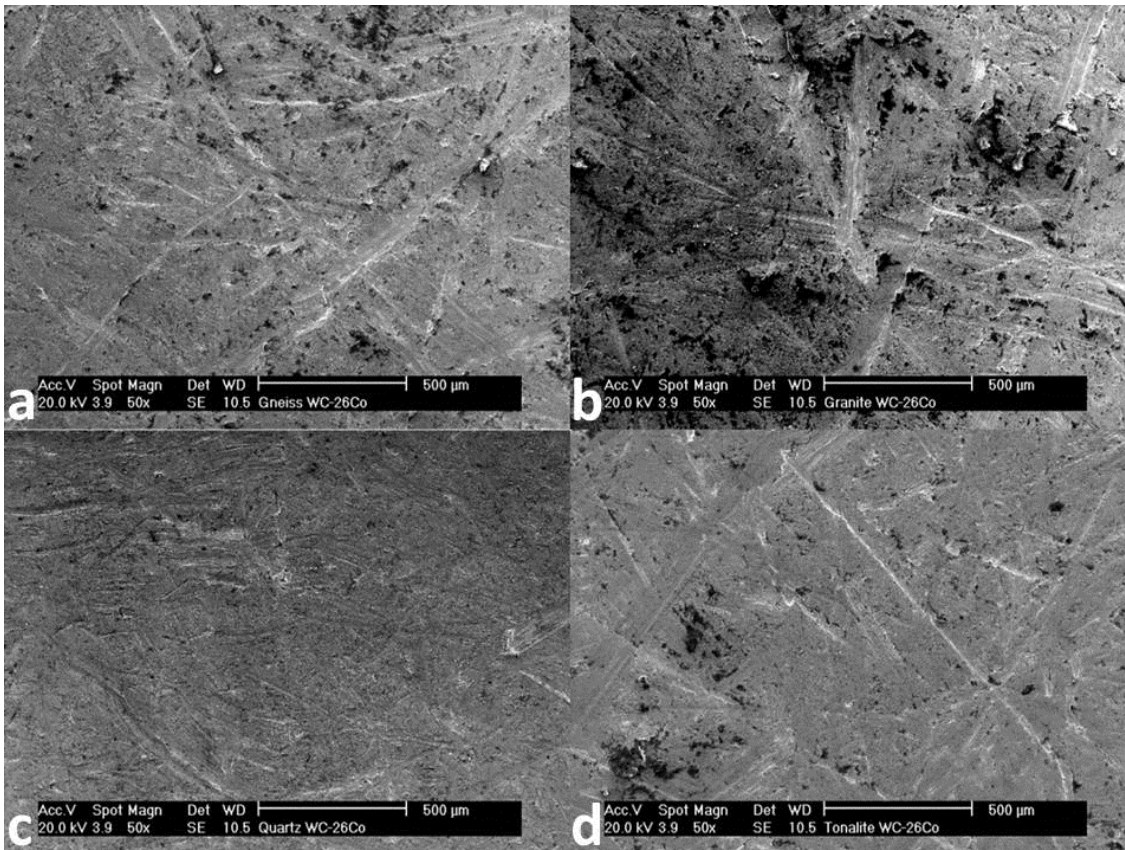


Figure 10. Scanning electron microscope images of WC-26Co hard metal tested with a) gneiss, b) granite, c) quartzite and d) tonalite.

Figure 11 gives a closer look at the wear surfaces of the WC-Co specimens. In all specimens, the carbides appear to be protruding from the surface, indicating that the binder matrix has worn more severely than the carbides. Also crushed carbides were found on every wear surface. The surfaces abraded with gneiss and granite look quite

similar with more local binder phase removal than with quartzite, where the binder phase removal seems to be more general. With quartzite also the amount of crushed carbides appears to be higher, while tonalite seems to be producing the least amount of crushed particles. Re-embedding of crushed carbides was also observed on the wear surfaces.

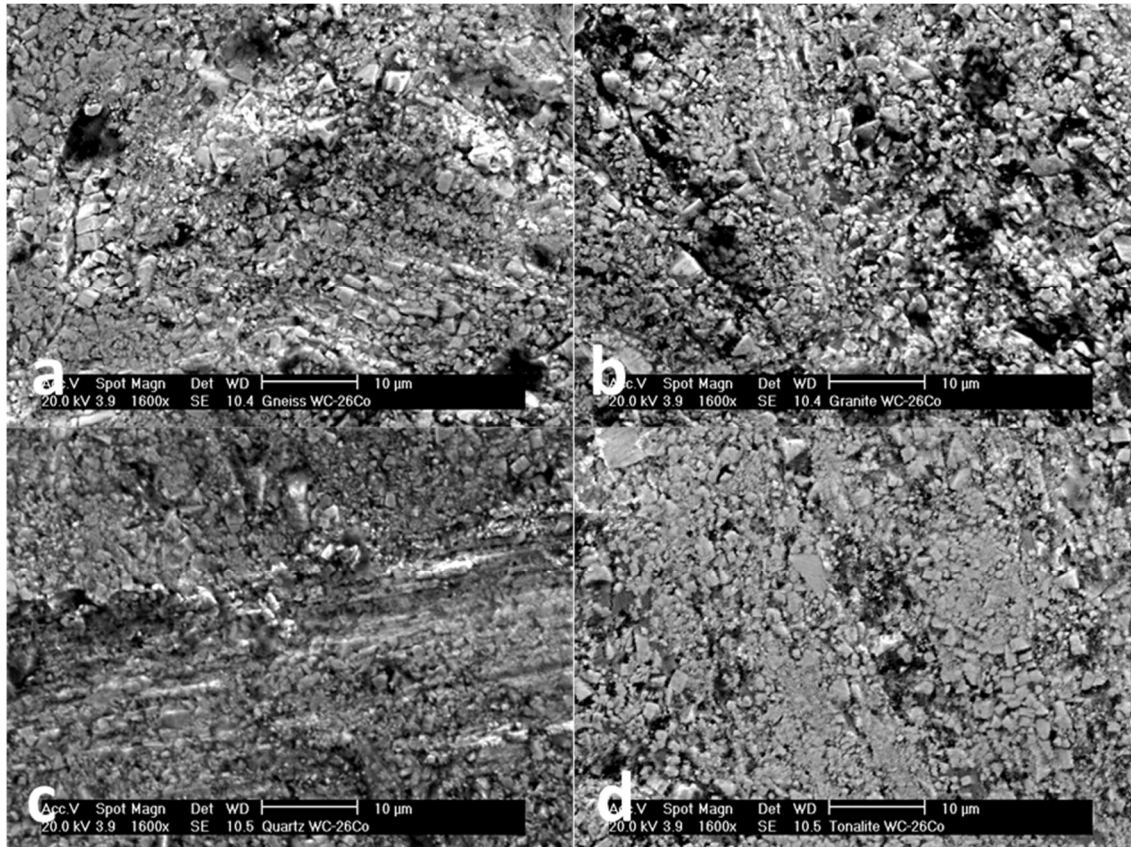


Figure 11. Higher magnification scanning electron microscope images of WC-26Co hard metal tested with a) gneiss, b) granite, c) quartzite and d) tonalite.

In addition to the SEM studies, also the surface roughness R_a values of the pin specimens were measured. As expected, the surface roughness was clearly smaller in the harder materials, but there were no distinct trends or differences observed between the different rock types.

The flat appearance of the steel surfaces observed with microscopy in specimens tested with quartzite could not be verified with optical profilometry. In fact, for the 500HB steel the surface roughness of quartzite worn specimens was to some extent higher than for the specimens tested with the other abrasives. This may be explained by the increased cutting caused by the presence of a large number of small and freshly ground sharp and very hard particles on the wear surface.

In the hard metals, quartzite produced clearly the roughest surfaces, as could be expected based on the volume loss results. On the whole, the R_a values of hard metals followed quite well the crushability values, the second roughest surface being produced by gneiss and tonalite leading to the smoothest surfaces.

DISCUSSION

In the current tests, quartzite produced wear in the studied materials in a clearly different manner than all the other tested abrasives. For steels, quartzite was relatively less abrasive than granite and gneiss. In hard metals, on the other hand, the wear produced by quartzite was 5-12 times higher than with any other abrasive. While the high bulk hardness enabled the hard metals to resist abrasive wear very well in general, the 500HB steel (505 HV) and the WC-26Co hard metal (870

HV) showed approximately the same mass loss when abraded with quartzite. Quartzite is clearly harder than the other used abrasives, and also its crushability is more than twice as high as that of any other of the investigated abrasives. The reason behind the observed differences in the wear test results regarding both the specimen materials and the used abrasives is likely due to the changes in the wear mechanism with changing material/abrasive combinations.

Hard metals consist of two phases: the carbides as the hard phase, and cobalt as the binder phase. In the current test materials, the binder content varied between 15 and 26 percent. Because the hardness of the cobalt matrix is relatively low (typically 140-210 HV), the bulk hardness of the hard metal decreases considerably with increasing binder phase content (see Table 2). Thus, if the hard abrasive particle is small enough to fit between the carbide particles, it can easily wear off the binder phase, leading to carbide pullout and breakage. This is why the high crushability of quartzite combined with high hardness is a more detrimental property to the hard metals than the high uniaxial compression strength or abrasiveness. As the abrasives are being crushed into smaller particles in a brittle manner, there are always fresh and hard angular particles available, which accelerates wear [9,11]. The same phenomenon has been reported also by Krahkmaliev [34]. Another property highlighting the wear potential of quartzite is its higher hardness in contrast to the other abrasives used in this study.

All of the tested abrasives had a different combination of properties, which made it challenging to study the effect of just one property at a time. Quite interestingly, the high hardness, high UCS, and high quartz content made tonalite only a moderate abrasive. Terva et al. [14], who also conducted tests with granite and tonalite, suggested that the cause for the difference is in the breakage mechanisms of these two rocks: granite fracturing produces sharper

contours that can penetrate the material deeper, thus causing more cutting damage.

On the steel wear surfaces, the differences in the wear behavior were clearly visible. The steels tested with quartzite and gneiss with lower UCS showed distinctly shorter scratches than the ones tested with abrasives with higher UCS. Petrica et al. [13] concluded that in a two-body contact the high-UCS abrasives produce cutting and ploughing, whereas the intermediate UCS abrasives produce more plastic deformation and abrasive grooves. This is in quite good agreement with the current findings, although the contact conditions in the tests were different.

In the high stress three-body abrasive conditions, crushability was found to be the key property of the abrasives in the wear of hard metals because of the wear mechanism based on the attack on the softer binder phase. In steels, a combination of moderate crushability and high enough abrasiveness produced the highest wear. In addition, for steels being relatively homogeneous in microstructure, the ability of the abrasives to transmit load without breaking and to maintain a reasonable portion of them sharp for easy penetration, are also important factors.

Abrasiveness of the rock is an important parameter when planning tunneling or excavations, but on the basis of the current results, attention must also be paid on the types of the materials used in the machinery and on the contact conditions existing on the site. The abrasiveness values are often determined using steels as the test material, like in the widely used Cerchar abrasiveness index or LCPC abrasiveness coefficient measurements. As observed in the current study, the wear behavior of steels and hard metals can be distinctly different when considering the wear mechanisms and the affecting abrasive properties, and therefore the abrasiveness values determined for steels do not necessarily apply to hard metals, which

are used in many tools such as rock drilling buttons. Moreover, the crushability (LBC) values should also be taken into consideration, especially with hard metals.

Another issue is the contact conditions. The abrasiveness value only states that a certain rock type is abrasive in certain type of conditions, and although different abrasiveness values may have a correlation with each other [18,20], their applicability in the situation to be simulated must be carefully assessed. For example in the LCPC abrasiveness test, wear is occurring to a great extent by open two-body abrasion in the edge parts of the blocks, whereas in the current high stress three-body abrasion tests wear mostly occurs in the center part of the specimen as three-body abrasion under the applied external force.

The effects of abrasive properties in the abrasive wear behavior are quite complex to study. There is no single abrasive property that determines the wear rates for both material types tested in this work, i.e., ferritic-pearlitic and martensitic steels and hard metals. It is also possible that the abrasive properties have combined effects on wear, which should be studied in greater details.

CONCLUSIONS

In three body high-stress abrasive wear, the increased crushability of the abrasive increases the wear of hard metals, because it changes the effective wear mechanism: the small and hard particles increase the wear of the soft binder phase between the load-bearing hard phases. On the other hand, in steels with a relatively homogeneous microstructure, no clear correlation between the wear and the studied abrasive properties was found. Thus, the potential of an abrasive type to cause wear depends not only on the abrasive type but also on the wearing material.

The different contact conditions explain the poor correlation between the wear test results obtained in this work and the LCPC abrasiveness values. As a consequence, it is essential that the contact conditions and the whole wear environment are properly taken into account when the effects of rock properties on the wear behavior are being determined. A better estimation of the wear behavior is obtained using test methods that simulate the true in-service conditions, such as high loads, large abrasive size, and the comminution behavior of the abrasive.

ACKNOWLEDGEMENTS

This study was a part of the FIMECC DEMAPP program funded by Tekes and the participating companies. The authors would like to express their gratitude to M.Sc. Ville Viberg for the LCPC results, and Mr. Ari Varttila and Mr. Terho Kaasalainen for constructing and maintaining the wear testing equipment.

REFERENCES

- [1] J. H. Tylczak, "Abrasive wear," in: ASM Handbook Volume 18. Friction, Lubrication, and Wear Technology, ASM International, 1992, pp. 184–190.
- [2] D. Scott, "Wear," in: Industrial tribology - The practical aspects of friction, lubrication and wear, 1983, pp. 12–30.
- [3] S. Ala-Kleme, P. Kivikytö-Reponen, J. Liimatainen, J. Hellman, and S.-P. Hannula, "Abrasive wear properties of tool steel matrix composites in rubber wheel abrasion test and laboratory cone crusher experiments," *Wear* 263 (2007) 180–187.
- [4] I. Sevim and I. B. Eryurek, "Effect of abrasive particle size on wear resistance in steels," *Mater. Des.* 27 (2006) 173–181.

- [5] A. A. Torrance, "The effect of grit size and asperity blunting on abrasive wear," *Wear* 253 (2002) 813–819.
- [6] M. Woldman, E. Van Der Heide, T. Tinga, and M. A. Masen, "The influence of abrasive body dimensions on single asperity wear," *Wear* 301 (2013) 76–81.
- [7] J. J. Coronado and A. Sinatora, "Effect of abrasive size on wear of metallic materials and its relationship with microchips morphology and wear micromechanisms: Part 1," *Wear* 271 (2011) 1794–1803.
- [8] D. A. Kelly and I. M. Hutchings, "A new method for measurement of particle abrasivity," *Wear* 250 (2001) 76–80.
- [9] G. B. Stachowiak and G. W. Stachowiak, "The effects of particle characteristics on three-body abrasive wear," *Wear* 249 (2001) 201–207.
- [10] D. V. De Pellegrin and G. W. Stachowiak, "Sharpness of abrasive particles and surfaces," *Wear* 256 (2004) 614–622.
- [11] G. W. Stachowiak, "Particle angularity and its relationship to abrasive and erosive wear," *Wear* 241 (2000) 214–219.
- [12] M. Petrica, E. Badisch, and T. Peinsitt, "Abrasive wear mechanisms and their relation to rock properties," *Wear* 308 (2013) 86–94.
- [13] M. Petrica, M. Painsi, E. Badisch, and T. Peinsitt, "Wear Mechanisms on Martensitic Steels Generated by Different Rock Types in Two-Body Conditions," *Tribol. Lett.* 53 (2014) 607–616.
- [14] J. Terva, T. Teeri, V.-T. Kuokkala, P. Siitonen, and J. Liimatainen, "Abrasive wear of steel against gravel with different rock–steel combinations," *Wear* 267 (2009) 1821–1831.
- [15] M. Köhler, U. Maidl, and L. Martak, "Abrasiveness and tool wear in shield tunnelling in soil / Abrasivität und Werkzeugverschleiß beim Schildvortrieb im Lockergestein," *Geomech. Tunn.* 4 (2011) 36–54.
- [16] R. Plinninger, H. Käsling, K. Thuro, and G. Spaun, "Testing conditions and geomechanical properties influencing the CERCHAR abrasiveness index (CAI) value," *Int. J. Rock Mech. Min. Sci.* 40 (2003) 259–263.
- [17] R. J. Plinninger and U. Restner, "Abrasiveness Testing, Quo Vadis? – A Commented Overview of Abrasiveness Testing Methods," *Geomech. und Tunnelbau* 1 (2008) 61–70.
- [18] K. Thuro and H. Käsling, "Classification of the abrasiveness of soil and rock," *Geomech. und Tunnelbau* 2 (2009) 179–188.
- [19] H. Käsling and K. Thuro, "Determining rock abrasivity in the laboratory," in: *ISRM International Symposium-EUROCK 2010, 2010*, 4 p.
- [20] R. Fowell and M. A. Bakar, "A review of the Cerchar and LCPC rock abrasivity measurement methods," in: *11th Congress of the International Society for Rock Mechanics, 2007*, pp. 155–160.
- [21] F. Dahl, A. Bruland, P. D. Jakobsen, B. Nilsen, and E. Grønv, "Classifications of properties influencing the drillability of rocks, based on the NTNU/SINTEF test method," *Tunn. Undergr. Sp. Technol.* 28 (2012) 150–158.
- [22] V. A. Golovanevskiy and R. A. Bearman, "Gouging abrasion test for rock abrasiveness testing," *Int. J. Miner. Process.* 85 (2008) 111–120.
- [23] M. Alber, "Stress dependency of the Cerchar abrasivity index (CAI) and its effects on wear of selected rock cutting tools," *Tunn. Undergr. Sp. Technol.* 23 (2008) 351–359.
- [24] P. Kulu, R. Tarbe, H. Käerdi, and D. Goljandin, "Abrasivity and grindability study of mineral ores," *Wear* 267 (2009) 1832–1837.

- [25] A. Sundström, J. Rendón, and M. Olsson, “Wear behaviour of some low alloyed steels under combined impact/abrasion contact conditions,” *Wear* 250 (2001) 744–754.
- [26] J. Rendón and M. Olsson, “Abrasive wear resistance of some commercial abrasion resistant steels evaluated by laboratory test methods,” *Wear* 267 (2009) 2055–2061.
- [27] M. Woldman, E. Van Der Heide, D. J. Schipper, E. van der Heide, T. Tinga, and M. A. Masen, “Investigating the influence of sand particle properties on abrasive wear behaviour,” *Wear* 294–295 (2012) 419–426.
- [28] “G65-04 Standard Test Method for Measuring Abrasion Using the Dry Sand / Rubber Wheel.” ASTM International, 2010, pp. 1–12.
- [29] M. Yao and N. W. Page, “Influence of comminution products on abrasive wear during high pressure crushing,” *Wear* 242 (2000) 105–113.
- [30] V. Ratia, K. Valtonen, A. Kemppainen, and V.-T. Kuokkala, “High-Stress Abrasion and Impact-Abrasion Testing of Wear Resistant Steels,” *Tribol. Online* 8 (2013) 152–161.
- [31] N. Axén, S. Jacobson, and S. Hogmark, “Influence of hardness of the counterbody in three-body abrasive wear—an overlooked hardness effect,” *Tribol. Int.* 27 (1994) 233–241.
- [32] A. Torrance, “An explanation of the hardness differential needed for abrasion,” *Wear* 68 (1981) 263–266.
- [33] I. M. Hutchings, “Abrasion processes in wear and manufacturing,” *Proc. Inst. Mech. Eng. Part J: J. Eng. Tribol.* 216 (2002) 55–62.
- [34] P. V. Krakhmalev, “Abrasion of ultrafine WC-Co by fine abrasive particles,” *Trans. Nonferrous Met. Soc. China* 17 (2007) 1287–1293.

Publication V

Vilma Ratia, Harald Rojacz, Juuso Terva, Kati Valtonen, Ewald Badisch and Veli-Tapani Kuokkala

Effect of multiple impacts on the deformation of wear-resistant steels

Tribology Letters 57 (2015) 15

<http://doi.org/10.1007/s11249-014-0460-7>

© 2015 Springer Science+Business Media
Reprinted with permission

Effect of Multiple Impacts on the Deformation of Wear-Resistant Steels

Vilma Ratia · Harald Rojacz · Juuso Terva ·
Kati Valtonen · Ewald Badisch · Veli-Tapani Kuokkala

Received: 13 October 2014 / Accepted: 22 December 2014 / Published online: 21 January 2015
© Springer Science+Business Media New York 2015

Abstract More durable materials enable reducing the downtime and maintenance costs by decreasing the number of replaced core components in various industrial applications. In this study, the behavior of three wear-resistant quenched martensitic steel grades and the S355 structural steel was examined in controlled impact conditions. The materials' impact behavior was investigated by several methods including residual stress measurements and electron backscatter diffraction. For all studied materials, the size and depth of the impact marks correlate via a logarithmic function to the number of impacts mostly due to work hardening. The underlying deformation behavior of the material depends on the mechanical properties and microstructure of the material. At high impact counts, softer martensitic steel was found to behave differently when compared to the other tested materials as it underwent severe changes in its microstructure and exhibited marked hardening.

Keywords Steel · Martensite · Impact · Deformation · Residual stresses · EBSD

1 Introduction

In many industrial applications, such as mining and other industries involving processing and transportation of minerals, the number of worn and replaced wear plates is high. Large savings could be obtained by using more durable materials that enable decreasing the downtime and maintenance costs, boosting the productivity of the manufacturing facilities.

The properties of materials do not remain the same throughout their life cycle. The harsh conditions, which the materials have to withstand in many machine components, often cause changes in the materials' microstructure and consequently in their mechanical properties. The changes can be detrimental, such as corrosion, but also beneficial, such as work hardening [1]. In some cases, the evolution of the properties can be beneficial at first but then lead into unwanted consequences, for example, when work hardening causes brittleness [2, 3]. In wear tests with longer duration, these factors can be taken into consideration by using proper test methods and test parameters. However, the testing conditions should correlate to a sufficient extent with the in-service conditions, as otherwise the changes may be neglected. The changes in the materials' behavior and the final outcome of such effects must be understood in greater detail for the benefit of different applications.

A good example of a material that undergoes distinct and positive changes is the high manganese steel, the surface hardness of which can be substantially increased by work hardening [4, 5]. This property is widely used in different industrial applications, such as mining [6]. However, to obtain its hardened state, the manganese steel requires a certain amount of stress. If the impact force is too low or the initial exposure is otherwise improper, the material will remain in its softer austenite state and the work hardening effect is not achieved [7].

V. Ratia (✉) · J. Terva · K. Valtonen · V.-T. Kuokkala
Tampere Wear Center, Department of Materials Science,
Tampere University of Technology, PO-Box 589,
33101 Tampere, Finland
e-mail: vilma.ratia@tut.fi

H. Rojacz · E. Badisch
AC2T research GmbH, Viktor-Kaplan-Straße 2,
2700 Wiener Neustadt, Austria

Work hardening due to impacts also occurs in other materials and steels. The increased dislocation density and grain refinement hinder the movement of dislocations in the microstructure, which leads to higher strength. This usually can be associated with better wear resistance. In real applications, the contact conditions can be complex and the components may be subjected to several different contact types, such as simultaneous impacts and abrasion. In impact-abrasive conditions, the hardness at and below the surface usually increases, implying work hardening of the materials due to the impacts [5, 8].

Wear-resistant plates are often used in applications subjected to heavy wear conditions. It is therefore of great scientific and industrial interest to study and understand the strain hardening effects in steels used in such applications. Usually these plates are steels with a mostly martensitic microstructure, but they may also contain other phases, such as austenite, and bainite [9].

In wear tests simulating real impact-abrasive conditions to a certain controlled extent, the sample materials are subjected to several impacts. Especially in tests containing more than one contact type, the controlling and observation of the exact impacting conditions can be difficult. For that purpose, tests with more controlled but simplified conditions are needed. In this study, the single and cyclic impact abrasion tests developed at AC²T research GmbH were used. These tests enable controlled impacts with predefined parameters, such as impact energy, momentum, and impact angle. The single impact test device has been previously used to study the influence of heat treatments and hard phases on the deformation behavior of steels and metal matrix composites, as well as to obtain knowledge about the influence of impact energy and momentum on the single impact behavior [10–12].

The actual effect of impacts on the properties of materials, such as hardness, usually depends on the number of impacts, as reported, for example, by Wilson et al. [5] and Ratia et al. [8]. In this study, both single and multiple impact tests were conducted on wear-resistant and structural steel samples to show the influence of impact energy and impact counts on the property changes of different wear-resistant steels.

The general aim of this study was to determine the influences of single and multiple impacts on the deformation and strain hardening behavior of different steels and thus gain deeper understanding on the deformation mechanisms active in impact dominated systems.

2 Experimental

2.1 Material Data

In the test series, four different steels were tested: two commercial wear-resistant steels (400HB and 500HB), one

laboratory rolled experimental steel (650HB), and a structural steel (S355) used for comparison. Table 1 presents the mechanical property data of the steels, their nominal alloying, and microstructures.

Figure 1 presents the initial microstructures of the tested steels. S355 has a ferritic–pearlitic microstructure, while 400HB and 500HB are martensitic with some retained austenite. The 650HB steel, which is a novel type of steel, has a martensitic microstructure with approximately 5 % of ferrite and 10 % of austenite.

The single impact test samples had the dimensions of 74 × 22 mm and thickness of 5 mm. The multiple impact test samples were approximately 22 × 20 × 5 mm in size. The sample surfaces were first machined, then ground with SiC papers, and finally polished with 1 μm diamond paste. One set of impacts was conducted on each multiple impact test sample.

2.2 Single Impact Test Rig (SIT)

The single impact tests were conducted with the SIT device, which was developed at the Austrian Center of Competence for Tribology (AC²T research GmbH). A detailed description of the test principle and different deformation mechanisms within the SIT can be found, for example, in previous literature [12, 13]. With the SIT, the impact behavior of materials can be determined at several impact energies (0.25–100 J) and momenta (1.11–44.72 Ns). The test rig comprises a dropping head with changeable weights and an impacting head. In the current tests, a cemented carbide ball with 6 mm diameter was used. The test principle, as seen in Fig. 2, is based on the potential energy turned into kinetic energy by a free fall. The energy spent on friction on the guide rails is minimized by using linear bearings. The used impact energy levels produce well-defined impact marks on the sample surfaces. The testing parameters can be chosen with predetermined potential energy E_p or predetermined momentum p , adjusted by the weight and the height of the dropping head as:

$$E_p = m \cdot g \cdot h \quad (1)$$

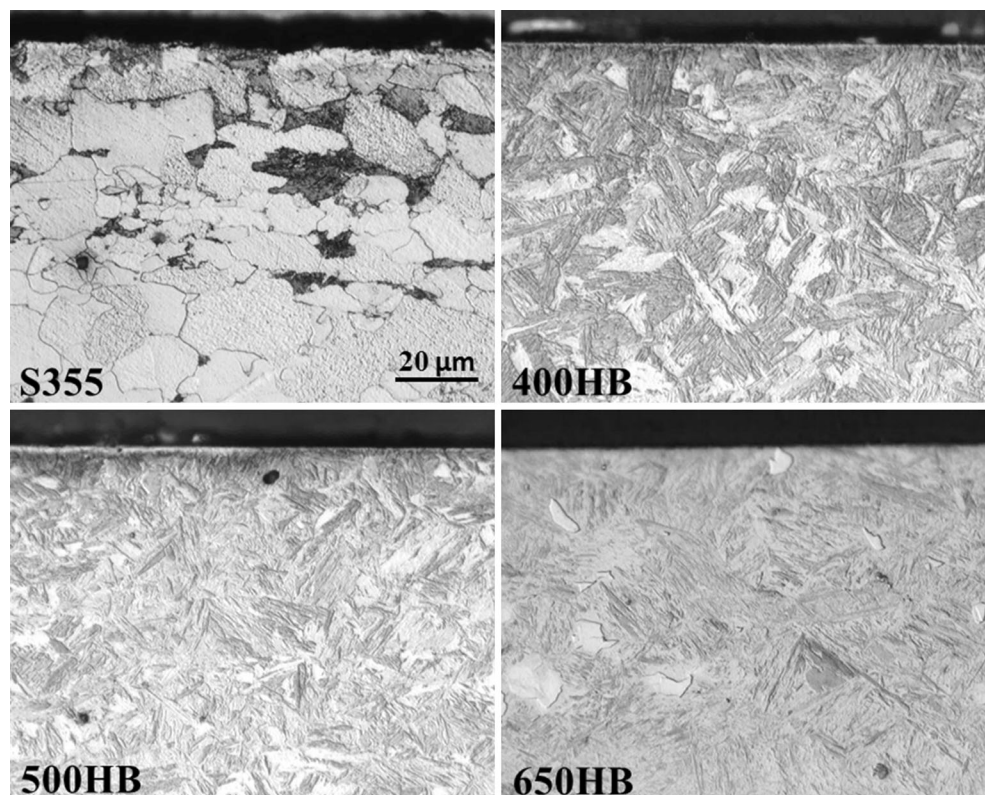
$$p = m \cdot v = m \sqrt{2 \cdot g \cdot h} \quad (2)$$

where m is the mass, g the gravitational acceleration, h the initial height (the dropping distance) and v the impact velocity. In the current tests, the momentum was chosen to be constant, while the impact energy was varied by changing the dropping mass and the dropping height.

After selecting the test parameters, the initial height and appropriate weight for the sledge can be adjusted and the sample fixed in the sample holder. The sledge is released by turning the trigger, after which the sledge impacts the

Table 1 Mechanical properties and nominal maximum compositions of the tested materials

Material	S355	400HB	500HB	650HB
Microstructure	Ferritic–pearlitic	Martensitic with some retained austenite	Martensitic with some retained austenite	Martensitic with 5 % ferrite and 10 % austenite
Rp0.2 (N/mm ²)	397 ± 4	1,117 ± 6	1,433 ± 9	–
Rm (N/mm ²)	485 ± 1	1,264 ± 5	1,637 ± 8	>1,800 ^a
A (%)	32 ± 0	13 ± 1	11 ± 0	–
Surface hardness (HV)	181 ± 8	400 ± 8	516 ± 7	680 ± 23
Impact toughness 20 °C (J)	198 ± 2	49 ± 2	29 ± 1	7
Impact toughness –40 °C (J)	183 ± 29	25 ± 3	16 ± 1	–
C (wt%)	0.12	0.23	0.30	0.47
Si (wt%)	0.03	0.80	0.80	0.53
Mn (wt%)	1.5	1.7	1.7	0.7
Cr (wt%)	–	1.5	1.5	0.2
Ni (wt%)	–	1.0	1.0	0.06
Mo (wt%)	–	0.5	0.5	0.03
B (wt%)	–	0.005	0.005	0.001
Al (wt%)	0.015 ^b	–	–	1.65

^a Estimated from hardness^b Minimum composition**Fig. 1** Initial microstructures of the tested steels. Scale bar is 20 μm

specimen and produces an impact mark on the sample surface. The test setup is also equipped with a sensor measuring the height of the impact sledge's rebound after

hitting the sample. Five impacts at every energy level were performed on each material for statistical considerations. The test parameters for the current tests are shown in

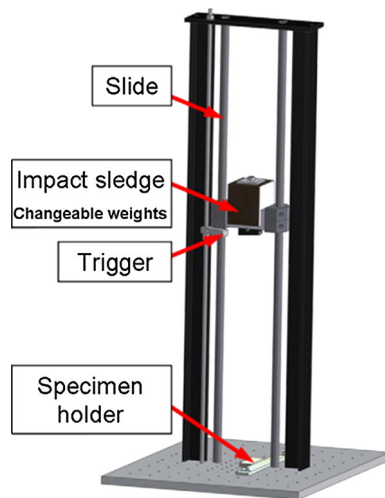


Fig. 2 Test setup for the single impact tests [modified from 11]

Table 2. In addition to single impacts, tests with ten impacts were conducted using the impact energy of 1 J.

2.3 High-Temperature Cyclic Impact Abrasion Test system (HT-CIAT)

The multiple impact experiments were conducted with the high-temperature cyclic impact abrasion tester (HT-CIAT), which also has been designed and built at AC²T research GmbH [13–15]. In the test, the impacting head is cyclically lifted to the predetermined height and dropped onto the specimen. The test system enables testing at elevated temperatures and the addition of abrasives, but the current tests were conducted only at room temperature. No abrasive was used in the tests, making the conditions purely impacting. The test setup is shown in Fig. 3.

In the current tests, the specimens were placed perpendicular to the impacting head, which was a similar 6-mm hard metal ball as used in the SIT tests. The total mass of the impacting head was 3 kg, the dropping height 34 mm, impact energy 1 J, frequency 0.94 Hz, and the momentum 2.45 Ns. Tests with 10, 100, and 1,000 impacts were conducted three times on each material.

2.4 Characterization

The impact marks were characterized with a Leica[®] MZ 7.5 optical stereo microscope and a Philips[®] XL30 scanning

Table 2 Testing parameters used in the single impact tests

E (J)	m (kg)	h (mm)	p (Ns)
1	3.032	33.6	2.46
2	1.538	132.5	2.48
3	1.089	281	2.56

electron microscope (SEM). The impact mark areas were determined by measuring their diameters with the stereo microscope. The volume losses were determined with a Veeco[®] Wyko NT1100 optical profilometer. From the data, also the cutting-to-plasticity ratios were determined as:

$$\phi = \frac{|V_{\text{neg}}| - |V_{\text{pos}}|}{|V_{\text{neg}}|} \quad (3)$$

where V_{neg} is the negative volume below the initial surface (zero level) and V_{pos} is the positive volume above the zero level [16, 17].

The residual stress and full width at half-maximum (FWHM) measurements were conducted with the X-ray diffraction method using a Stresstech Xtress 3000 X-ray stress analyzer. Cr-K α radiation at 30 kV acceleration voltage, 6.7 mA current, and a 1-mm-diameter collimator were used. The measurements were conducted at ten different tilt angles in two perpendicular directions across the impact mark. The penetration depth of the used Cr-K α radiation was 5–6 μm [18]. The measurements for intact samples were conducted on the polished surfaces described in Sect. 2.1. For the residual stress measurements in the bulk, the sample surface was electrolytically etched with Struers A2 electrolyte between the measurements until the desired depth was reached. Ferrite diffraction lines were used to determine the FWHM values.

Metallographic cross sections were prepared for the characterization of the subsurface cracks and the deformed microstructures after the impacts. The samples were cut, ground, and polished in the middle of the impact marks to investigate and compare the deformed zones. The etching was performed with 4 % nitric acid in alcoholic solution for 2–10 s to reveal the microstructures. Microscopical

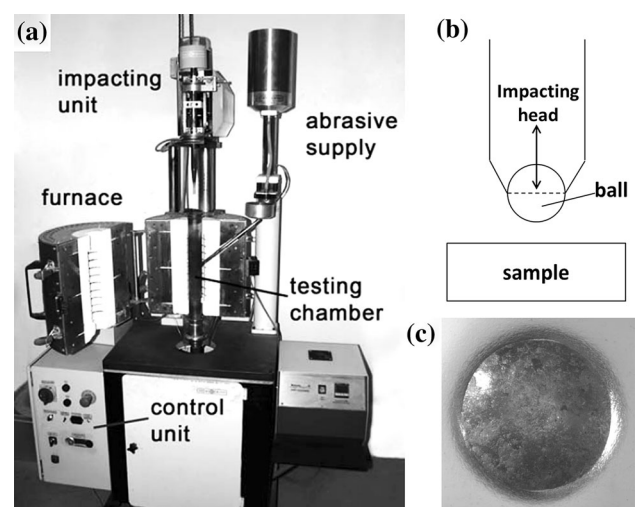


Fig. 3 High temperature cyclic impact abrasion tester: **a** setup, **b** schematic of the impacting section, and **c** an example of the resulting impact mark [modified from 13]

investigations were conducted with a Nikon® Eclipse MA100 optical microscope and Philips® XL30 SEM.

Siemens D5000 X-ray diffractometer was used for determining the amount of retained austenite. The amount of ferrite was determined with the point-counting method from the etched cross sections.

Electron backscatter diffraction (EBSD) imaging was performed with a Zeiss® Ultra field emission gun scanning electron microscope (FEG-SEM) with a beam step size of 0.1 μm . The metallographic cross sections were prepared by mechanical grinding and polishing and finished with a 40-nm polishing agent for optimal EBSD imaging.

Microhardness measurements were conducted from the cross sections. For multiple impact tests HV0.05 was used, whereas for single impacts the used method was HV0.01 to better reveal the hardening effects close to the surface. The indentations were performed using a Matsuzawa® MMT-X7 microhardness tester, and the indentation diameters were measured with either a Nikon® optical microscope (for HV0.05) or SEM (for HV0.01).

3 Results

In this section, the results of the single impact tests and their characterization are presented first, followed by the multiple impact results and an overview on the underlying deformation mechanisms and their influence on the impact behavior of the studied materials.

3.1 Single Impact Tests

3.1.1 Impact Mark Analysis

Figure 4a presents the impact mark diameters produced by single impacts with varying energies. The differences between the materials are clearly visible: The harder the steel, the smaller the impact mark. In general, higher impact energies cause larger impact marks. However, the dimensions of the wear marks did not always increase with the impact energy, which may be resulting from the chosen test parameters and relatively large scatter. For the 400HB and 500HB steels, the impact mark diameter increased slightly with the increasing impact energy, while for the S355 and 650HB steels, the 3 J impact marks were on average somewhat smaller than the 2 J impact marks. That being said, all differences are small—in the range of a few percent—and often fit within the scatter. In an earlier study [11], it was found that the changes in impact marks between the impact energies can be small, especially for ferritic–pearlitic steels impacted with low impact energies.

In the current tests, the momentum of the impact was practically constant (2.46–2.56 Ns) and the change in

energy was realized by changing the load and the dropping height, as presented in Table 2. It may be that the decrease in the impacting mass, in addition to the impact energy, has a large role in transferring the load to the sample material. Moreover, the ratio of elastic and plastic deformation can change at different energies and loading situations. For the comparison of single and multiple impacts with the same energy, as seen in Fig. 4b, multiple impacts increase the diameter of the impact marks, as expected.

3.1.2 Cross-Sectional Analysis and the Correlation of Hardness and Rebound Measurements

The single impact samples were investigated with optical microscopy, revealing that all samples had undergone plastic deformation. S355 was the softest of the investigated steels and consequently showed the highest plastic deformation due to the impacts. Its microstructure had transformed into pearlite and ferrite lamellae oriented along the direction of the surface. Figure 5a shows a comparison of the ferritic–pearlitic microstructure of the S355 in the deformed and initial states. The changes extend to the depth of several hundreds of micrometers below the surface of the samples.

In martensitic steels, the changes in the microstructures were not that evident. Figure 5b presents a cross-sectional image of a 400HB sample impacted for ten times, as well as of the bulk material for comparison. Microstructural changes were largest close to the surface, where refinement and reorientation of the microstructures were observed, but the changes did not extend very deep into the material. No tribologically induced white-etching layers were observed in the samples either after one or ten impacts. Some cracks were observed in the samples of the 500HB and 650HB steels tested at 1 J, but not in all cross sections. At higher impact energies, no cracks could be observed, which can be ascribed to crack closing mechanisms at higher impact energies.

A large number of microhardness measurements were conducted on the samples to distinguish between the effects of different energies at a constant value of momentum. As expected, work hardening occurred, especially in softer steels, but the current method indicated no clear difference between of applied energies. However, there were obvious changes in the microstructure, as can be deduced from the height measurements of the bouncing impacting head. The increasing rebound height usually correlates with higher hardness and increasing storage of elastic energy [19, 20]. Figure 6 presents the average height values for the multiple impact tests. For S355, the height increases throughout the test, whereas the martensitic steels tend to stabilize the rebound heights after a few impacts. In practice, the impacting head bounced about three times after the initial impact on the sample, but the height measurements were made only for the first bounces.

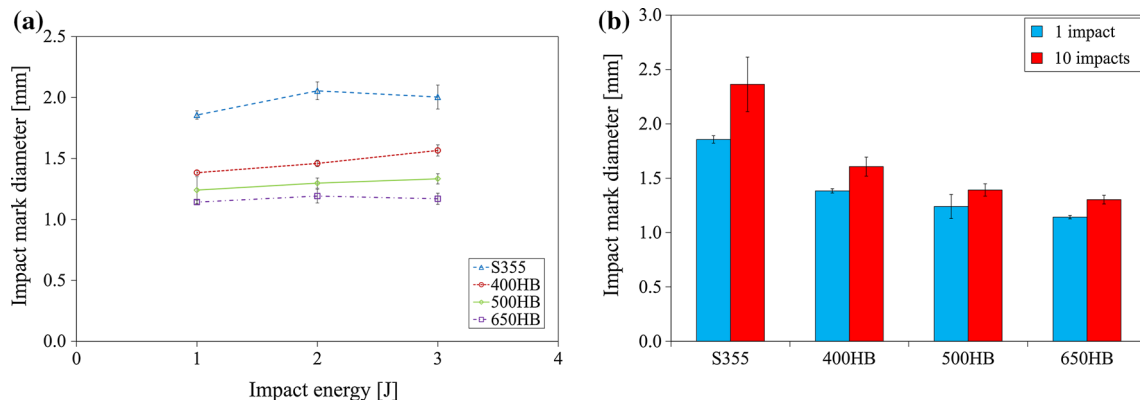
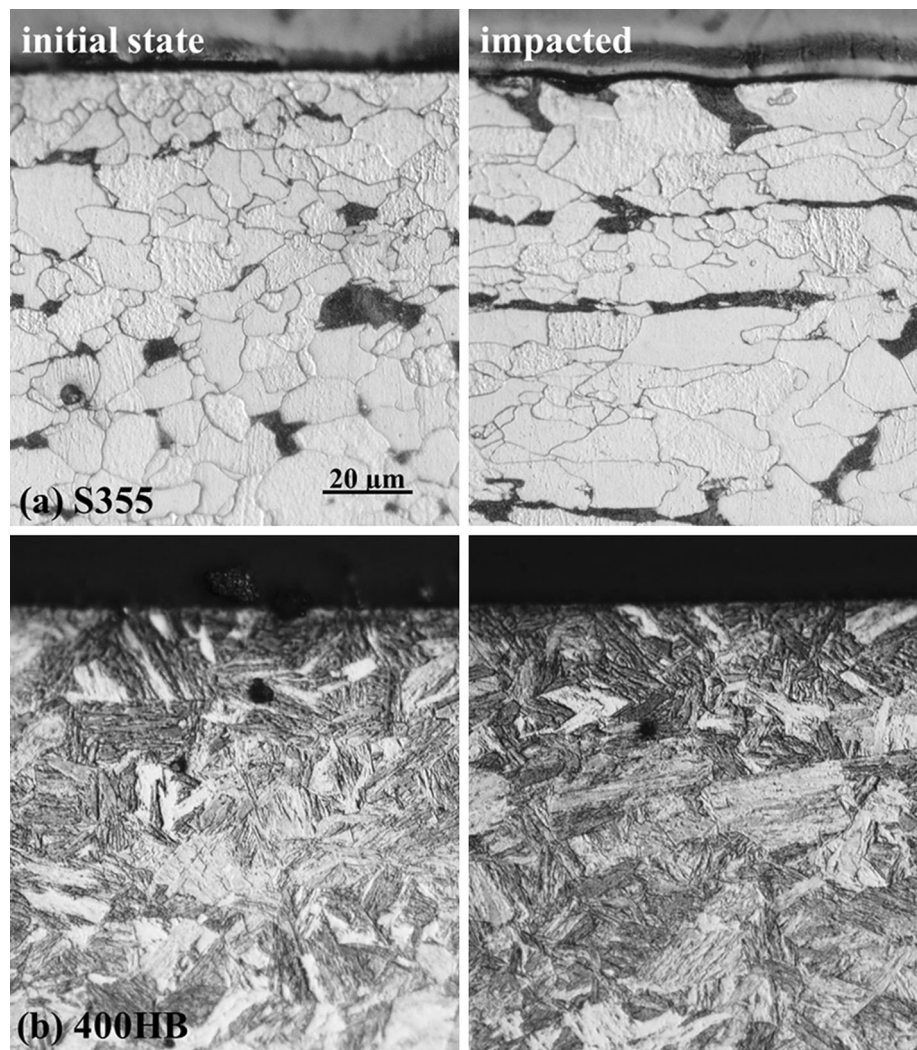


Fig. 4 Impact mark diameters produced **a** by single impacts with different energies and **b** by single and ten impacts with 1 J impact energy

Fig. 5 Cross-sectional analysis of **a** S355 and **b** 400HB steels impacted for ten times in comparison with the initial state. Scale bar is 20 μ m



3.2 Multiple Impact Tests

3.2.1 Impact Mark Analysis

Figure 7a shows the diameters of the multiple impact marks for all studied materials and Fig. 7b the depths of

impact marks. The effect is quite linear on the logarithmic scale. In the wear-resistant steels, impact mark diameters correlate well with the hardness.

Figure 8 presents the impact marks in the S355 steel after 10, 100, and 1,000 impacts. Increasing the number of impacts results in an expansion of the diameter, but it also

affects the surface of the impact mark. After ten impacts, the steel surface is still shiny, while 100 impacts result in a heavily deformed and worn appearance. The deformation extends also beyond the crater marks, as the material is pushed to the sides of the crater.

Figure 9 presents the impact marks in the wear-resistant steels after 10 and 1,000 impacts. It can be seen that the ten impact marks consist of several distinctly different impacts. When comparing the theoretical diameters of the impact marks calculated with the assumption of the ball hitting the exactly same location with every impact with the measured diameters, it was observed that the measured diameters were approximately 1 mm larger for all materials. This suggests that the clearance of the impacting head was in the range of 0.5 mm in all directions. In the 1,000 impact samples, the larger number of impacts has merged the distinct marks into a single larger crater. In the 400HB steel after 1,000 impacts, a partially detached layer can also be observed within the impact mark.

The removal of material was induced by adhesion to the impacting ball and, on the other hand, by cutting of the deformed areas in the ridges of the impact marks. The small dark spots in Figs. 8 and 9 are quartzite, which is frequently used in the HT-CIAT with abrasive testing. Some remnants from the previous tests have obviously remained in the testing chamber and transferred to the impacting area. However, these scarce remnants are not believed to affect the outcome of these tests.

The optical profilometer measurements were conducted on one sample per material of each test type. The optical profilometer data help to determine the amount of plastic deformation in the samples, as well as the cutting ratio, which is the ratio between the amounts of cutting and plastic deformation. Figure 10 presents the cross-sectional profile of the impact marks in the steels after ten impacts. As expected, the softest of the steels, S355, has clearly the deepest impact mark. The depth of the impact mark, as well as the overall volume loss, decreases steadily with

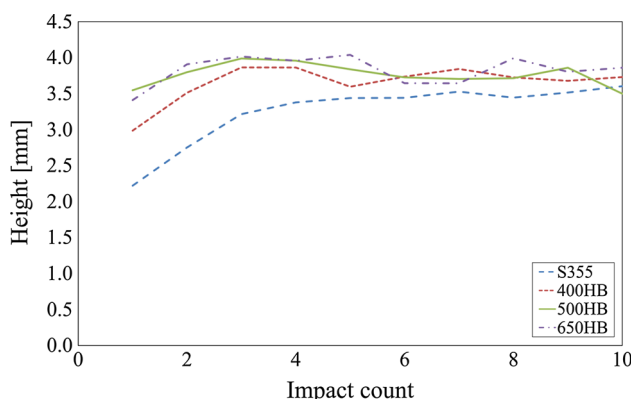


Fig. 6 Average height values of the impacting head after bouncing back from the specimen in the SIT tests

hardness just like the impact mark diameters presented in Fig. 7a. The steep slopes of the impact marks cause challenges in the data collection, which is why the volume loss data should be treated only as an approximation.

The cutting-to-plasticity ratios were generally higher in the harder steels that are more susceptible to cutting than to pure plastic deformation. For the wear-resistant steels, the ratio after ten impacts varied between 0.6 and 0.7, whereas for S355 the ratio was as low as 0.3. The cutting ratios generally decreased with increasing impact count. This indicates that there was more plastic deformation than material removal by cutting in the impact mark ridges in the later stages of the tests.

Figure 11 presents the results of the residual stress measurements from the impact mark bottoms. The S355, 400HB, and 500HB steels all behaved basically in the same way: During the first ten impacts, the compressive stress first increases slightly, after which the stress starts to decrease with the increasing number of impacts.

In all samples, the initial stress state after cutting, grinding, and polishing is quite high in the compressive direction. Moreover, the initial stresses are the higher the harder the steel, i.e., the higher the yield strength of the material. It is evident that the high compressive stresses are largely caused by the preparation of the samples. The measured stresses of the samples are in the same range as observed in some other studies using steel samples prepared by grinding or polishing [21–23]. The scatter of the measurements is quite large, which is probably due to the rather uneven bottom of the impact marks and the possible presence of remaining flakes. To get statistically more reliable results, all three samples for each material were measured and their average residual stress values used.

Figure 12 presents the overall residual stresses at different depths for the polished 400HB steel samples in both impacted and initial states, showing that the distance from the surface has an effect on the magnitude of the residual stresses.

In general, the compressive stresses decrease with increasing number of impacts. On the other hand, as the impact crater becomes deeper, the measurement will be made further away from the original surface, which may have an effect on the obtained stress values. To study this effect, a sample of 400HB without compressive residual stresses was prepared and impacted. It was found that the stresses induced by the impacts in the sample were clearly compressive up to a few hundred MPas. To verify this, residual stress measurements in the impact mark fringe of a 400HB sample with 1,000 impacts were conducted. The compressive stress was usually higher than the value obtained from the impact mark bottom. This indicates that the stress state is affected by both the impacts and the stress gradient close to the surface.

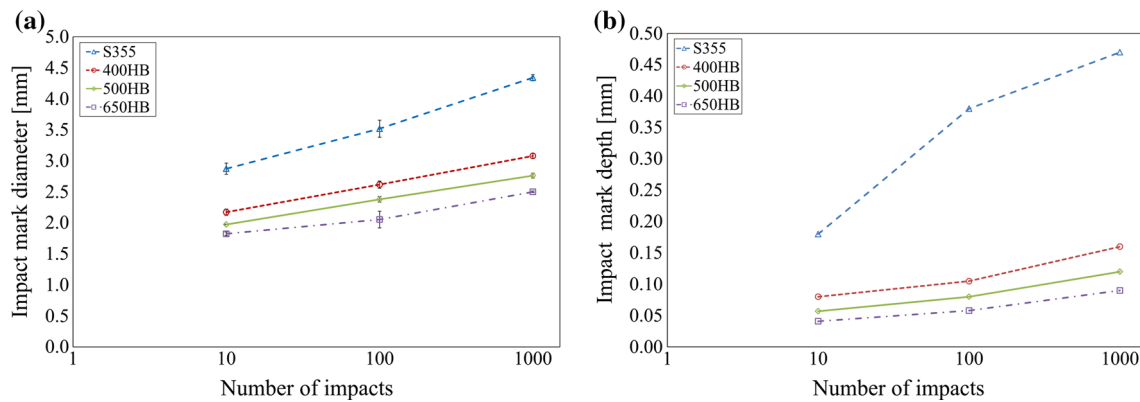


Fig. 7 Impact mark characteristics of the materials after multiple impacts at 1 J: **a** impact mark diameters and **b** approximate maximum depths

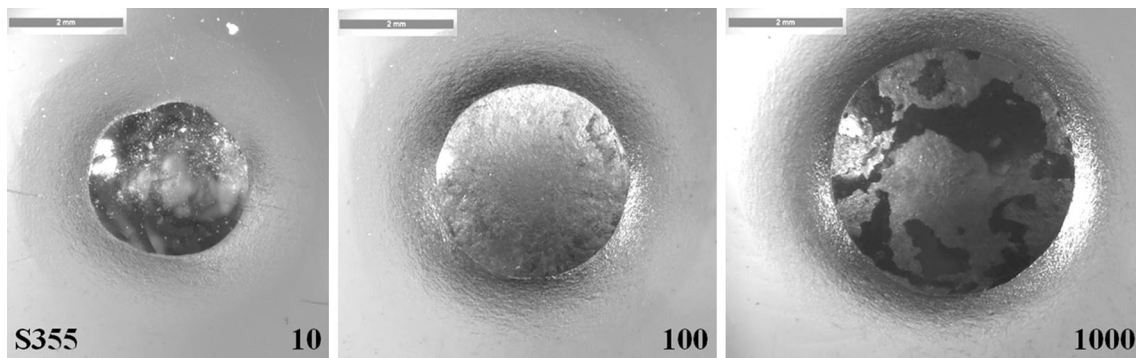


Fig. 8 Stereo images of S355 HT-CIAT tested samples after 10, 100, and 1,000 impacts. Scale bar is 2 mm

The 650HB steel residual stress measurement results show clear deviations from the results obtained for the other materials. Its compressive stress state seems to be less after ten impacts than in the initial state, and the stress level after 100 impacts is more in compression than in the less impacted samples. After 1,000 impacts, however, the results appear again in line with the other test materials. All in all, the scatter of the residual stress measurements of the 650HB steels is very large and the variance in the results after 10 and 100 impacts is within the scatter.

Figure 13 presents the full width at half-maximum values of the X-ray peaks used in the residual stress determinations of the impacted samples. As for the residual stress determinations, averages of three separate samples were used. The higher FWHM values in steels usually correlate with work hardening [24] and changes in hardness due to fatigue [25]. In the present case, the FWHM values tend to increase as the number of impacts increase, indicating increasing work hardening and distortion of the microstructure. Like the residual stresses, also the FWHM values are affected by the sample preparation, and thus the values obtained from the surface do not correlate with the values determined deeper in the material. For the 400HB steel, the FWHM shows much higher values for the

samples after 1,000 impacts than could be expected on the basis of the 10- and 100-impact samples. On the other hand, the 500HB steel samples after 1,000 impacts show a significantly large scatter in their FWHM values compared to the other measurements, which indicates that there are some differences in the deformed structures between the samples.

3.2.2 Cross-Sectional Analysis

Figure 14 presents the microhardness measurements conducted on the 400HB steel samples impacted for 10, 100 and 1,000 times. Due to continuing strain hardening, in the sample impacted for 1,000 times the hardness is significantly higher than in the samples impacted for 10 or 100 times. The hardened depth extends to approximately 400 μm , after which the hardness is approximately on the same level as in the bulk. The difference between the 10- and 100-impact samples is only small, and the hardness values are close to those of the bulk material. Similar behavior was also seen in the FWHM results. As shown in Fig. 14, the microhardness values of the 500HB steel after 1,000 impacts are typically in the same range with the 400HB sample impacted for 1,000 times.

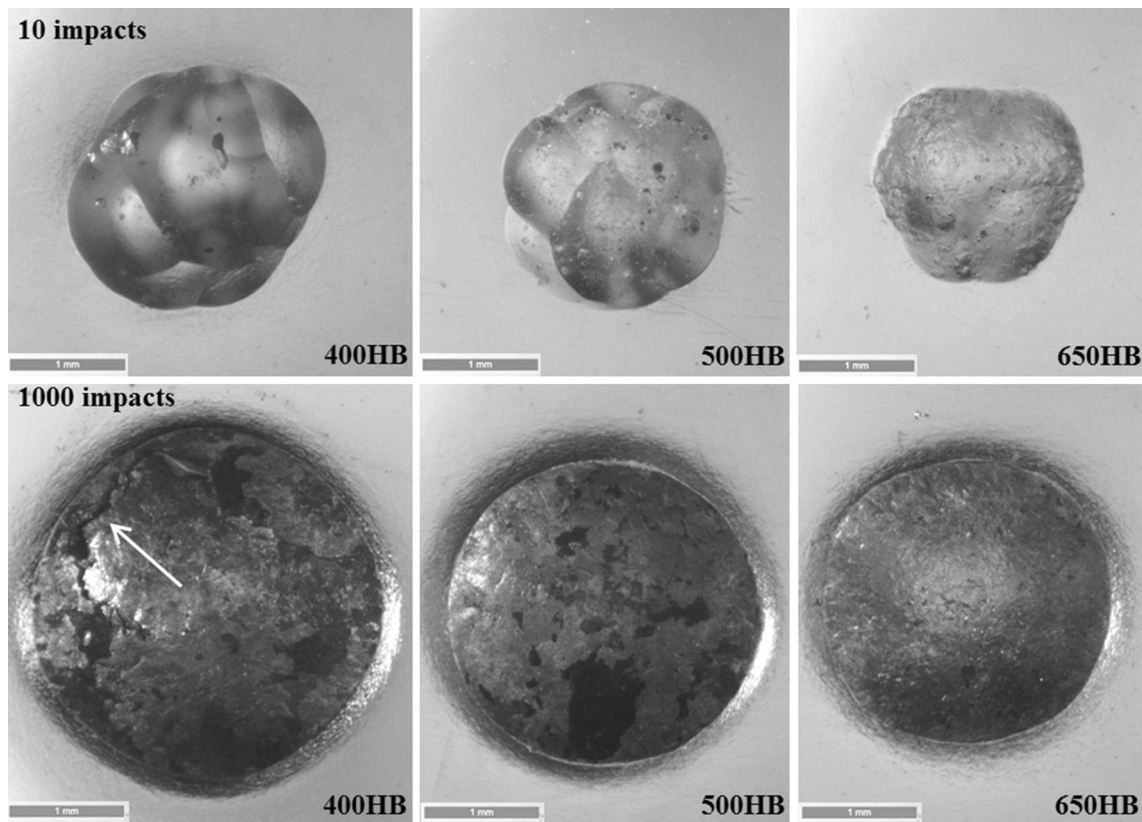


Fig. 9 Stereo images of HT-CIAT tested samples after 10 and 1,000 impacts. The *arrow* points to a partially detached area. *Scale bar* is 1 mm

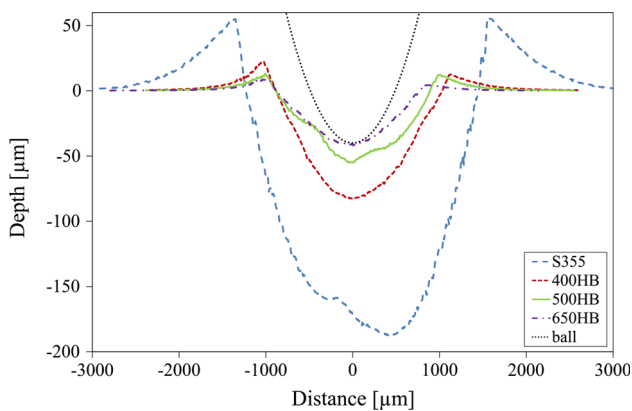


Fig. 10 Depth profiles of the wear-resistant steel samples after ten impacts and the profile of the ball in relation to the impact marks

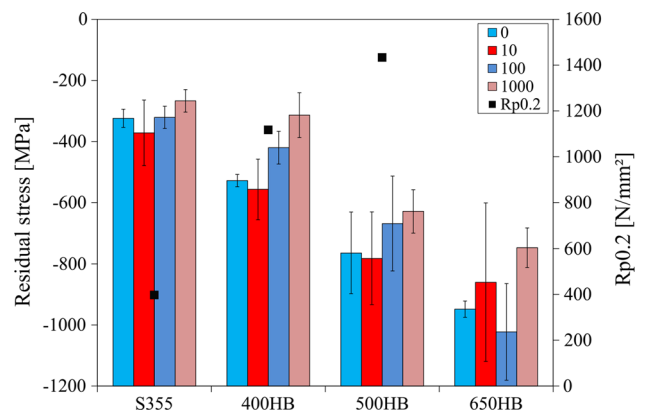


Fig. 11 Residual stress measurement results for all materials. The presented values are averages of three measurements

The etched cross sections of the impacted samples were examined to reveal the possible changes in their microstructures. In the samples impacted for ten times, there were no visible changes or cracks in the microstructures of any of the studied materials.

Figure 15 presents the etched optical microscope images of the samples impacted for 1,000 times. The difference in the degree of deformation has led to uneven etching of the

samples, and the most heavily deformed areas resemble white layers, which are more resistant to etching [26].

All steels contained some cracks after 1,000 impacts, but the nature of the observed cracks was different. The wear-resistant martensitic steels showed mostly lateral and quite straight subsurface cracks, whereas the S355 steel could contain wavy vertical cracks reaching from the surface down to the depth of several hundreds of micrometers.

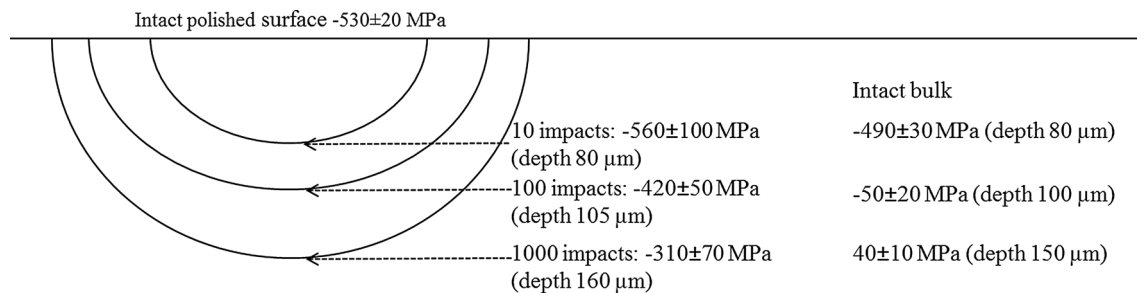


Fig. 12 Residual stress measurements of 400HB steel samples

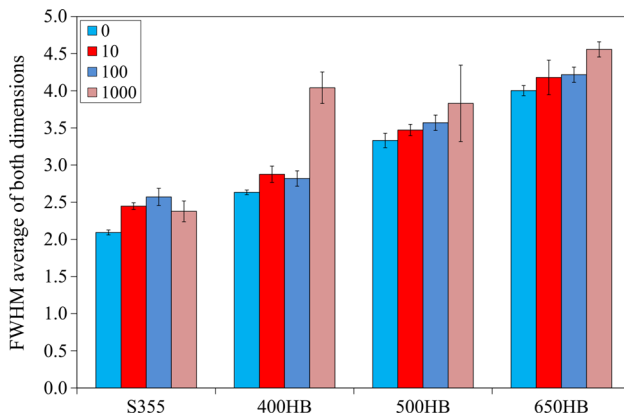


Fig. 13 Average full width at half-maximum values of the diffraction peaks in the initial state and in the impacted samples

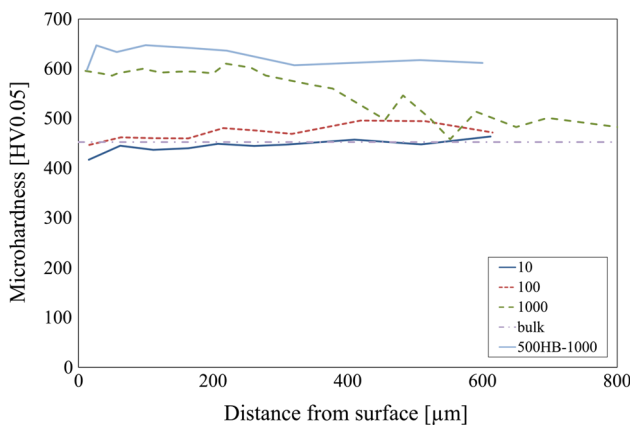


Fig. 14 Microhardness measurements of the cross sections of 400HB steel samples and 500HB steel after 1,000 impacts

Harder materials contained shorter cracks and their typical location with respect to the center of the impact mark was different. The harder the material, the more deviated from the impact mark center the cracks appear to be.

To investigate closer the microstructural changes, the microstructure of 400HB in the samples impacted for 1,000 times was studied by SEM. Figure 16 presents the sub-surface microstructure of the 400HB steel compared with

the bulk microstructure. The images clearly show that there is very little left of the initial martensitic microstructure in the heavily deformed area right below the surface. The martensitic laths and packages have rearranged perpendicularly to the surface and form a fibrous, refined structure, which is harder than the initial martensite structure.

To examine the effect of impacts on the microstructures in a greater detail, electron backscatter diffraction studies were performed on the 400HB bulk material and samples impacted for 10 and 1,000 times. Figure 17 presents the band contrast and inverse pole figure colored images of a sample impacted for ten times and of the bulk material close to the surface. From Fig. 17, it is evident that the grains in the impacted sample are slightly smaller and rearranged.

Figure 18 presents the band contrast and inverse pole figure colored images of a 400HB sample after 1,000 impacts. The images were taken from the depth of 300–400 µm below the surface, next to an area containing cracks. Unfortunately the degree of deformation in the material is so high that it weakens the quality of the images, which was to be expected. The original confidence indexing rate was 39.7 %, which means that over 60 % of the data points could not be crystallographically identified. Nevertheless, it is quite evident that the microstructure is much more heavily deformed and the grain structure much more refined into long formations compared to the initial microstructure.

Figure 19a, b, c presents the changes in of the crystallographic orientation of the grains due to impacting in the 400HB steel. The {100}, {110}, and {111} pole figures show that in the undeformed and ten time-impacted samples the pole distributions are quite random, but after 1,000 impacts very strong clustering of the poles can be observed. The pole figures in Fig. 19c show that the texture developed in the material is close to {111} plane texture, i.e., in most of the grains the $\langle 111 \rangle$ direction is parallel to the wear surface normal. Figure 19d shows the pole figures of 500HB steel after 1,000 impacts. A similar texture development, although with a slightly lower intensity can be observed.

Fig. 15 Optical micrographs of the etched cross sections of samples after 1,000 impacts. The *arrows* pinpoint some of the cracks. *Scale bar* is 0.5 mm

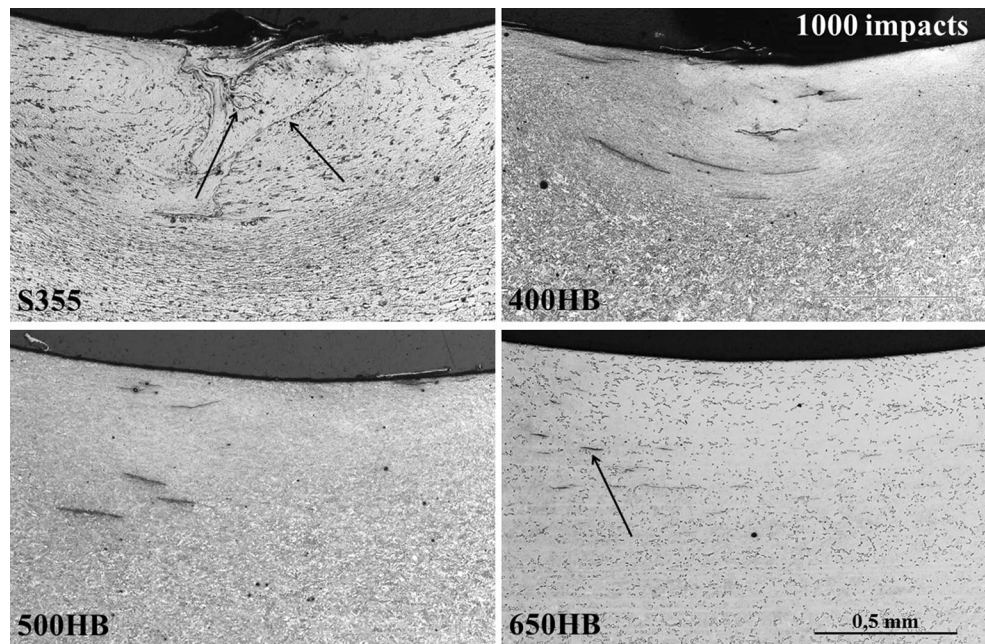
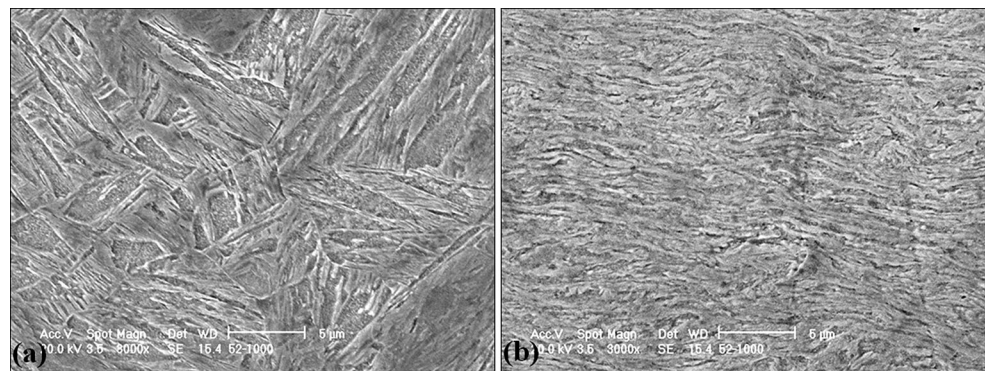


Fig. 16 A 400HB sample impacted for 1,000 times, **a** the bulk microstructure and **b** the microstructure close to the surface. *Scale bar* is 5 μm



4 Discussion

In this study, the effects of impact counts in impact dominated wear regimes on different steels have been examined and characterized by several methods. It was revealed that in single impacts the energy of the impact is not necessarily the only governing factor when assessing the size of the impact mark. Rojacz et al. [11, 12] found that the increased momentum leads to higher deformation in terms of impact mark size and deformation depth. In the current tests, the momentum was kept constant by varying the mass and the dropping height of the impacting head. The higher impact energy, however, did not cause larger impact marks in all materials, but the differences were small and often within the statistical scatter. It is likely that the ratio of elastic and plastic deformation can vary with different impact parameters, causing different outcomes for different steels. Besides the various phases present in the investigated steels, also differences in the substructures of certain

phases, such as martensite, may cause differences in the impact deformation behavior. Unfortunately, the dependences between the impacting parameters and the impact mark diameter do not seem to be straightforward and cannot be exhaustively explained on the basis of the three parameter settings used in the testing in this work. Moreover, in the harder steels some cracks were observed at the 1 J impact sites, but not at the 2 J and 3 J sites. This may be caused by the experimental scatter, but it may also suggest that with impacts of the same momentum the higher impacting head mass could induce more damage in this type of steels.

In the cyclic impact tests, the only variable was the number of impacts. The effect of multiple impacts on the deformation of the tested materials was studied with several methods, revealing many similarities but also differences in their behavior. The impact mark size and depth increased as a logarithmic function of the number of impacts for all tested steels, as previously pointed out. The

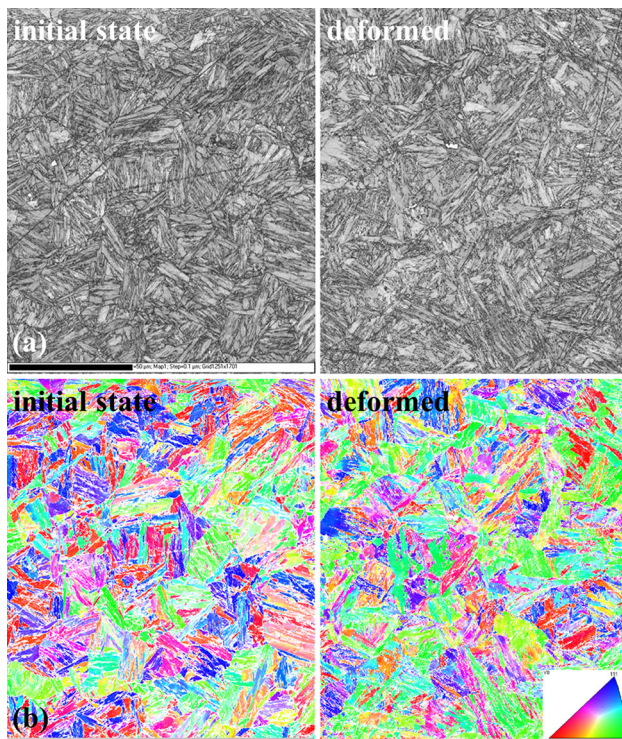


Fig. 17 Images of a 400HB sample with ten impacts and of the bulk material as **a** a band contrast image (data extrapolated for easier interpretation) and **b** an inverse pole figure colored image (original data). The top of the image is approximately 20 μm below the surface of the sample. Scale bar is 50 μm . The color codes indicate the orientation of each grain toward the wear surface of the sample

impact mark diameters were found to be affected by several factors, such as the material properties and their development in the course of testing, the clearance of the impacting head, and the change in the surface pressure as discussed in the following.

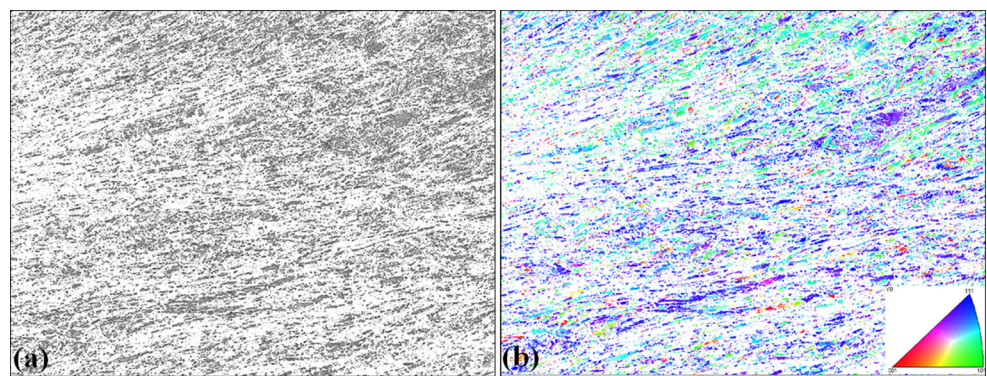
The contact area between the impacting ball and the sample surface changes as the impact mark widens and deepens, which leads to a change in the effective surface pressure caused by the impact. This effect is probably not this distinct during the first impacts, where the area of impacts scatter and the impacting head land partly on the

ridges of the existing impact marks, which minimizes the initial contact area between the ball and the already impacted sample. After several impacts, as the lateral clearance limits of the impacting head have been reached, the impacts are landing on the surface that has been previously impacted and the contact area widens, decreasing the surface pressure. The clearance may also have an effect on how the impact marks develop. For a smaller number of impacts, the impact mark is relatively wider in diameter than the impact mark after a larger number of impacts. As the impacts land on the same area repeatedly, the ratio between the depth and the diameter of the impact mark gets larger. The shape of the impact mark can also affect the surface pressure: When the impact mark is wider and shallower, it has a less curved surface and thus there is a smaller initial contact area between the ball and the sample than there would be for a more curved surface, i.e., with a deeper impact mark with a similar diameter.

There is also a difference in the surface pressure between the materials: Harder materials have smaller and shallower impact marks, which have to withstand higher surface pressures than the softer materials. Moreover, the effect of the clearance in the impacting head is relatively larger in harder steels, and the impacts lead to relatively wider impact marks and thus higher surface pressures. It is difficult to determine how much exactly the change in the surface pressure decreases the severity of the impact in each case, as it depends on the clearance of the impacting head and the development of the impact mark, which is different for each material. However, by comparing the change in the ratios between the possible maximum contact area of the impacting ball and the impact mark area at a certain depth, it seems that the effect is relatively small and is not likely to be a governing factor in the development of the impact marks.

The difference in the observed crack formation below the impacted areas suggested a difference in the studied steels' impact behavior. The crack formation varied with the properties of the steel, even though it seemed that the stress maximum was at the depth of a few hundred micrometers in all steels. The wear-resistant martensitic

Fig. 18 Band contrast (a) and inverse pole figure colored (b) images of a 400HB sample after 1,000 impacts determined 300–400 μm below the surface. Scale bar is 50 μm . The color codes indicate the orientation of each grain toward the wear surface of the sample



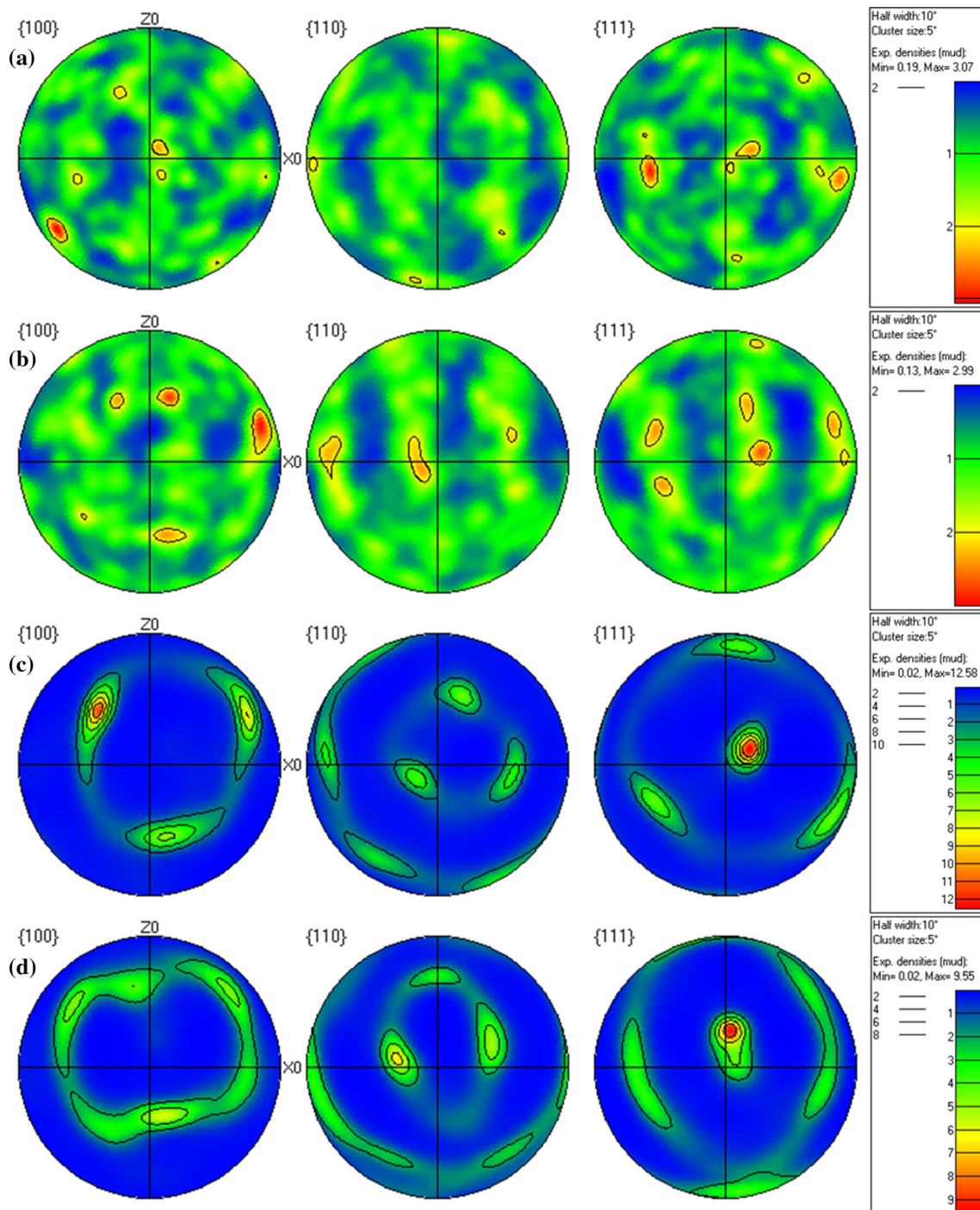


Fig. 19 {100}, {110}, and {111} pole figures of **a** the initial microstructure, **b** after 10 impacts and **c** after 1,000 impacts for 400HB steel and **d** after 1,000 impacts for 500HB steel. Z0 is perpendicular to the cross section and Y0 points toward the impact surface

steels showed lateral and quite straight subsurface cracks, whereas the structural steel S355 contained wavy vertical cracks extending to the surface. This is probably originating from the distinctly different strength and ductility properties of the materials. S355, being a softer and more ductile steel, has a stronger tendency to adhesion, and it is possible that some of the material has been attached to the

impacting counterpart leading to further asperities on the surface. Through the subsequent impacts, some of the removed material may also have re-attached onto the surface, producing a layered structure on it. This kind of behavior was observed more frequently in the softer S355 and 400HB steels, as seen in the impact marks in Figs. 8 and 9. The harder steels did not seem to experience this

kind of detachment and layering, at least not to such an extent. Another thing that may have an effect on the material removal and adhesion during multiple impact tests is the assumed temperature increase at the impact site. As the material is subjected to several repeated impacts, the temperature at the impact site tends to increase due to accumulating plastic deformation, further increasing the adhesion tendency between the sample and the impact head.

In the end, the ability to endure stresses dictates the ability of the steel to resist impact wear. It is also clear that both the stresses generated by external conditions and the internal residual stresses affect the behavior of the material and should therefore be accounted for. In the current study, the internal stresses in the samples are mostly caused by the sample preparation processes, such as cutting, grinding, and polishing. However, such stresses affect also the functional properties of real components and are in practice always generated by the machining processes [27]. The residual stresses produced, for example, by grinding depend quite much on the properties of the material [23]. On the other hand, similar stresses may also have been generated during the running-in stage of the component, if the conditions are somewhat abrasive. Similar to the case of fatigue, the compressive stresses have been found to be beneficial for the abrasive wear resistance [23, 28]. This effect only takes place close to the immediate surface and does not prevent the formation of subsurface cracks deeper in the material. The depth of the impact craters was found to have a distinct effect on the residual stresses in the current study as well. Compared with impact wear, the role of residual stresses is larger in abrasive wear, for which Garbar [23] found a stronger correlation between the compressive residual stress and abrasive wear resistance than between the wear resistance and the initial hardness.

While the residual stresses showed quite similar trends for the S355, 400HB, and 500HB steels, i.e., first a slight increase and then a gradual decrease with increasing number of impacts, the 650HB steel behaved distinctly different from the other materials. After an initial slight decrease in residual stresses, 650HB showed a substantial increase in compressive residual stresses after 100 impacts. One possible explanation for this kind of behavior is the different microstructure: Compared with the other tested steel grades, the 650HB steel contains more retained austenite and also some ferrite. The initial decrease in residual stresses may originate from the lack of deformation after the first ten impacts, i.e., the deformation has not been large enough to cause marked stress induced martensite formation. After 100 impacts, the austenite has, at least to some extent, transformed to martensite, which raises the compressive stress levels in the material by local distortion of the microstructure. This possibly also creates the very large

scatter in the 650HB residual stress measurements after 100 and 100 impacts. After the transformation has taken place, the structure is more stable and the impact mark continues to deepen, showing lowering compressive stresses in the same way as in the other materials. The verification of this explanation, however, would require more precise retained austenite measurements. Also, taking into consideration the large scatter in the obtained stress values, this result could be just coincidental and should therefore be considered with caution.

Another material showing distinctly different behavior compared with the other materials under impacts was 400HB in terms of its hardening due to microstructural evolution. While the other materials showed quite steady increase in the FWHM values of the X-ray diffraction peaks with increasing number of impacts, the FWHM value of 400HB jumped after 1,000 impacts to a very high level. As the change was so noticeable, all possibilities of material mix-ups and measurement errors were carefully excluded. Moreover, the microhardness measurements indicated similar behavior: In the 400HB steel, the surface was markedly hardened and the 400HB and 500HB steels reached microhardness of the same range after 1,000 impacts. These numerical measurements support the observations made from the micrographs, which show extremely heavy deformation to the depth of several hundreds of micrometers in 400HB. The microstructure next to the surface is not typical martensitic: A more fibrous and rearranged structure can be detected. This transformation cannot properly be seen yet after 100 impacts, although the deformation is already distinct.

Figure 16b shows long fiber-like formations in the 400HB steel oriented parallel to the surface. Similar deformation was observed in a previous study [8] in impact-abrasive conditions with much higher number of impacts but smaller impact energies. Compression of the bcc structure tends to develop textures with $\langle 111 \rangle$ or $\langle 100 \rangle$ directions perpendicular to the direction of compression [29], which according to Fig. 19 seems to be the case in the current samples as well. Both 400HB and 500HB steels showed similar development of textures after 1,000 impacts, but the extent of hardening indicated by the FWHM and microhardness measurements is typically higher in the 400HB steel. However, although the 400HB surface has higher hardness and strength due to work hardening, the textured structure does not prevent the formation of cracks parallel to the surface, of which the 400HB sample suffered. A study on the deformation of steels by Wetscher et al. [30] also concluded that crack propagation depends on the alignment of the formed microstructure.

The reason why work hardening occurs to such extent in the 400HB steel can be considered by comparing the 400HB and 500HB steels, which both have a nominally

similar microstructure and tendency of texturing after 1,000 impacts. Also, the amount of retained austenite is in the same level for both 400HB and 500HB, so it does not explain the difference. On the other hand, the martensite substructure size can be expected to have an effect on the deformation, and the lower amount of boundaries hindering the dislocation movement would enable easier deformation and rearrangement of the microstructure. This behavior shows that the characteristics of the materials can depend quite much on the generated stress. Moreover, it is not known how the materials would respond to further impacts. The large scatter of the FWHM values in the 500HB samples after 1,000 impacts indicates that there are differences in the behavior between the samples and suggests that extended hardening has taken place in some of the specimens. However, the trend is not as clear as in the 400HB samples after 1,000 impacts, which all underwent similar changes.

The microstructure of 400HB after 1,000 impacts was markedly refined, which enhances its hardness and possibly also other mechanical properties. However, after 1,000 impacts, the 400HB steel contained also numerous visible cracks, which could be detrimental to its impact properties if the amount of impacts was much higher. Thus, the benefits or disadvantages of this behavior could be revealed only in further testing, which shows that the sufficient duration of tests is very important. Even if the behavior of a material is seemingly constant or stabilized, some of the mechanisms causing increased wear may occur only in tests with longer duration.

5 Conclusions

Based on the performed measurements and interpretation of the obtained results, the following concluding remarks can be drawn:

- In single impacts, besides the impact energy also other parameters have a definite role in the deformation.
- In multiple impact tests, the impact mark sizes increase as a logarithmic function of the number of impacts mostly due to work hardening.
- Softer martensitic steels deform and work harden during 1,000 impacts to a much higher extent than the initially harder martensitic steels. This can be partially ascribed to the higher tendency for grain refinement and reorientation of the microstructure compared to harder martensitic structures.
- Sufficient test durations are necessary to determine the behavior and suitability of materials resisting certain impact wear-dominated conditions in industrial applications. Some of the essential processes occurring in

materials may take place only after a sufficient number of repetitions or time in specific loading conditions.

Acknowledgments This study was a part of the FIMECC DEMAPP program funded by Tekes and the participating companies. The authors want to express their gratitude to Tuomo Saarinen, M.Sc., for helpful discussions, Matti Lindroos, M.Sc., for his help in determining the volume loss of the samples, Dr. Suvi Santa-aho for her help with the residual stress measurements, Kauko Östman, M.Sc., for the EBSD measurements of 500HB steel, and Ilkka Miettunen, M.Sc., for providing the austenite and ferrite content information. Also the support by the Association of Finnish Steel and Metal Producers and Emil Aaltonen foundation is gratefully acknowledged. AC²T research GmbH is grateful to the “Austrian Comet-Program” (governmental funding program for pre-competitive research) for the funding via the Austrian Research Promotion Agency (FFG) and the TecNet Capital GmbH (Province of Lower Austria).

References

1. Yan, W., Fang, L., Sun, K., Xu, Y.: Effect of surface work hardening on wear behavior of Hadfield steel. *Mater. Sci. Eng. A* **460–461**, 542–549 (2007)
2. Zum Gahr, K.-H.: *Microstructure and Wear of Materials*, p. 406. Elsevier, Amsterdam (1987)
3. Tianfu, J., Fucheng, Z.: The work-hardening behavior of medium manganese steel under impact abrasive wear condition. *Mater. Lett.* **31**, 275–279 (1997)
4. Xiaoyun, L., Wei, W., Fangqiu, Z., Lanjun, L., Xianfeng, Z.: Influence of impact energy on work hardening ability of austenitic manganese steel and its mechanism. *Foundry Journal Agency China Foundry*. <http://www.foundryworld.com/upload/file/2012082747991625.pdf> (2012). Accessed 29 May 2014
5. Wilson, R.D., Hawk, J.A.: Impeller wear impact-abrasive wear test. *Wear* **225–229**, 1248–1257 (1999)
6. Wen, Y.H., Peng, H.B., Si, H.T., Xiong, R.L., Raabe, D.: A novel high manganese austenitic steel with higher work hardening capacity and much lower impact deformation than Hadfield manganese steel. *Mater. Des.* **55**, 798–804 (2014)
7. Abbasi, M., Kheirandish, S., Kharrazi, Y., Hejazi, J.: On the comparison of the abrasive wear behavior of aluminum alloyed and standard Hadfield steels. *Wear* **268**, 202–207 (2010)
8. Ratia, V., Miettunen, I., Kuokkala, V.-T.: Surface deformation of steels in impact-abrasion: the effect of sample angle and test duration. *Wear* **301**, 94–101 (2013)
9. Sundström, A., Rendón, J., Olsson, M.: Wear behaviour of some low alloyed steels under combined impact/abrasion contact conditions. *Wear* **250**, 744–754 (2001)
10. Rojacz, H., Varga, M., Winkelmann, H.: Deformation mechanisms at elevated temperatures: Influence of momenta and energy in the single impact test. *World Academy of Science, Engineering and Technology*. <http://waset.org/publications/5880/deformation-mechanisms-at-elevated-temperatures-influence-of-momenta-and-energy-in-the-single-impact-test> (2013). Accessed 27 Sept 2014
11. Rojacz, H., Mozden, G., Winkelmann, H., Modzen, G.: Deformation and strain hardening of different steels in impact dominated systems. *Mater. Charact.* **90**, 151–163 (2014)
12. Rojacz, H., Hutterer, M., Winkelmann, H.: High temperature single impact studies on material deformation and fracture behaviour of metal matrix composites and steels. *Mater. Sci. Eng. A* **562**, 39–45 (2013)

13. Winkelmann, H., Badisch, E., Kirchgaßner, M., Danninger, H.: Wear mechanisms at high temperatures. Part 1: wear mechanisms of different Fe-based alloys at elevated temperatures. *Tribol. Lett.* **34**, 155–166 (2009)
14. Badisch, E., Winkelmann, H., Franek, F.: High-temperature cyclic impact abrasion testing: wear behaviour of single and multiphase materials up to 750 °C. *Est. J. Eng.* **15**, 359–366 (2009)
15. Badisch, E., Katsich, C., Winkelmann, H., Franek, F., Roy, M.: Wear behaviour of hardfaced Fe–Cr–C alloy and austenitic steel under 2-body and 3-body conditions at elevated temperature. *Tribol. Int.* **43**, 1234–1244 (2010)
16. Zum Gahr, K.-H.: *Microstructure and Wear of Materials*, p. 137. Elsevier, Amsterdam (1987)
17. Kato, K., Adachi, K.: *Wear Mechanisms*. In: Bhushan, B. (ed.) *Modern Tribology Handbook*, p. 28. CRC Press, Boca Raton (2001)
18. Hauk, V.: *Structural and Residual Stress Analysis by Nondestructive Methods*. Elsevier, Amsterdam (1997)
19. ASTM E 448-82(1997) Practice for scleroscopic hardness testing of metallic materials. *Annual book of ASTM standards*. ASTM (2001)
20. ASTM E 140-97 Standard hardness conversion tables for metals: relationship among Brinell hardness, Vickers hardness, Rockwell hardness, superficial hardness, Knoop hardness, and scleroscope hardness. *Annual book of ASTM standards*, pp. 282–302. ASTM (2001)
21. Hayashi, M., Enomoto, K.: Effect of preliminary surface working on fatigue strength of type 304 stainless steel at ambient temperature and 288°C in air and pure water environment. *Int. J. Fatigue* **28**, 1626–1632 (2006)
22. James, M.R., Lu, J.: Introduction. In: Lu, J. (ed.) *Handbook of Measurement of Residual Stresses*, p. 3. Fairmont Press, Lilburn (1996)
23. Garbar, I.I.: Correlation between abrasive wear resistance and changes in structure and residual stresses of steels. *Tribol. Lett.* **5**, 223–229 (1998)
24. Fernández Pariente, I., Guagliano, M.: About the role of residual stresses and surface work hardening on fatigue ΔK_{th} of a nitrated and shot peened low-alloy steel. *Surf. Coat. Technol.* **202**, 3072–3080 (2008)
25. Zhang, Z., Qi, Y., Delagnes, D., Bernhart, G.: Microstructure variation and hardness diminution during low cycle fatigue of 55NiCrMoV7 steel. *J. Iron. Steel Res. Int.* **14**, 68–73 (2007)
26. Bulpett, R.: *The Characterisation of White-Etching Layers Formed on Engineering Steels*. Brunel University, London (1991)
27. Leppert, T., Peng, R.: Surface residual stresses in dry turning of 0.45 % C steel. JCPDS-International Centre for Diffraction Data *Advances in X-ray Analysis*. http://www.icdd.com/resources/axa/vol52/V52_39.pdf (2008). Accessed 10 April 2014
28. Astashkevich, B.M., Vershinina, N.I., Eparkhin, O.M., Maznova, G.A.: Influence of surface layer residual stresses on wear resistance of cylinder liners. *Met. Sci. Heat Treat.* **35**, 92–94 (1993)
29. Engler, O., Randle, V.: *Introduction to Texture Analysis*, p. 156. CRC Press, Boca Raton (2010)
30. Wetscher, F., Stock, R., Pippan, R.: Changes in the mechanical properties of a pearlitic steel due to large shear deformation. *Mater. Sci. Eng. A* **445–446**, 237–243 (2007)

Tampereen teknillinen yliopisto
PL 527
33101 Tampere

Tampere University of Technology
P.O.B. 527
FI-33101 Tampere, Finland

ISBN 978-952-15-3610-6
ISSN 1459-2045